

An Investigation of Radiofrequency Fields Associated with the Itron Smart Meter



An Investigation of Radiofrequency Fields Associated with the Itron Smart Meter

EPRI Project Manager
G. Mezei



3420 Hillview Avenue
Palo Alto, CA 94304-1338
USA

PO Box 10412
Palo Alto, CA 94303-0813
USA

800.313.3774
650.855.2121

askepri@epri.com

www.epri.com

1021126

Final Report, December 2010

DISCLAIMER OF WARRANTIES AND LIMITATION OF LIABILITIES

THIS DOCUMENT WAS PREPARED BY THE ORGANIZATION(S) NAMED BELOW AS AN ACCOUNT OF WORK SPONSORED OR COSPONSORED BY THE ELECTRIC POWER RESEARCH INSTITUTE, INC. (EPRI). NEITHER EPRI, ANY MEMBER OF EPRI, ANY COSPONSOR, THE ORGANIZATION(S) BELOW, NOR ANY PERSON ACTING ON BEHALF OF ANY OF THEM:

(A) MAKES ANY WARRANTY OR REPRESENTATION WHATSOEVER, EXPRESS OR IMPLIED, (I) WITH RESPECT TO THE USE OF ANY INFORMATION, APPARATUS, METHOD, PROCESS, OR SIMILAR ITEM DISCLOSED IN THIS DOCUMENT, INCLUDING MERCHANTABILITY AND FITNESS FOR A PARTICULAR PURPOSE, OR (II) THAT SUCH USE DOES NOT INFRINGE ON OR INTERFERE WITH PRIVATELY OWNED RIGHTS, INCLUDING ANY PARTY'S INTELLECTUAL PROPERTY, OR (III) THAT THIS DOCUMENT IS SUITABLE TO ANY PARTICULAR USER'S CIRCUMSTANCE; OR

(B) ASSUMES RESPONSIBILITY FOR ANY DAMAGES OR OTHER LIABILITY WHATSOEVER (INCLUDING ANY CONSEQUENTIAL DAMAGES, EVEN IF EPRI OR ANY EPRI REPRESENTATIVE HAS BEEN ADVISED OF THE POSSIBILITY OF SUCH DAMAGES) RESULTING FROM YOUR SELECTION OR USE OF THIS DOCUMENT OR ANY INFORMATION, APPARATUS, METHOD, PROCESS, OR SIMILAR ITEM DISCLOSED IN THIS DOCUMENT.

The following organization, under contract to EPRI, prepared this report:

Richard Tell Associates, Inc.

NOTE

For further information about EPRI, call the EPRI Customer Assistance Center at 800.313.3774 or e-mail askepri@epri.com.

Electric Power Research Institute, EPRI, and TOGETHER...SHAPING THE FUTURE OF ELECTRICITY are registered service marks of the Electric Power Research Institute, Inc.

Copyright © 2010 Electric Power Research Institute, Inc. All rights reserved.

Acknowledgments

The following organization, under contract to the Electric Power Research Institute (EPRI), prepared this report:

Richard Tell Associates, Inc.
1872 E. Hawthorne Avenue
Colville, WA 99114

Principal Investigator
R. Tell

This report describes research sponsored by EPRI and overseen by Gabor Mezei, MD, Ph.D, EPRI's Program Manager for the EMF and RF Health Assessment and Safety Program. Expertise, review and comment were provided by a cross-functional team at EPRI including Rob Kavet, D.Sc., Senior Technical Executive; Chris Melhorn, Program Manager; Kermit Phipps, Project Engineer/Scientist and Brian Seal, Senior Project Manager, EPRI.

Numerous individuals from Southern California Edison (SCE) Electric Company conducted and supported the measurement work reported here in both South Carolina and California: Glenn Sias, Manager, SCE EMF and Energy Group; Al Vazquez, Enterprise Network Architect, SmartGrid Engineering; Kevin Nesby, Project Manager in the Edison SmartConnect™ Deployment Program; Brian Thorson, EMF Specialist in the Operations Support Business Unit; Jack Sahl, Director of Operations Support in the SCE Operations Support Business Unit; and John Bubb, Manager of Product Management for SCE SmartConnect.

Background information on operational characteristics of smart meters was provided by Vijay Lakkasetty, System Engineering & Operations - Smart Meter Project, Jay Xu, Principal Engineer, and Jim Turman, Program Manager, Department & Employee Readiness, Safety and Emergency Services, all of San Diego Gas and Electric Company.

As further described within the report, testing support, facility access and cooperation was provided by Itron, which facilitated this work, particularly by Dan Lakich, Design & Development Manager, Electricity Metering; Mike Belanger, Product Line Manager, Itron OpenWay Network Communications; Sudhir Thumaty, R&D Manager; Suresh Kumar Yada, Design Engineer; Ben Smith, Engineer; Ken Prevatte, Project Director; and Matthew DeCubellis, Application Engineer.

This publication is a corporate document that should be cited in the literature in the following manner:

*An Investigation of Radiofrequency Fields
Associated with the Itron Smart Meter*
EPRI, Palo Alto, CA: 2010. 1021126

Product Description

Smart meters represent one component of the advanced metering infrastructure (AMI). Although data to and from smart meters may be transmitted through wired connections, many smart meters make use of miniature, low power radio transceivers to wirelessly communicate with the electric utility and with the Home Area Network (HAN) that provides home owners with the ability to interact with electrical appliances and systems within the home. Deployment of smart meters has raised concerns by members of the public about possible adverse health effects that could be related to exposure to the radiofrequency (RF) emissions of the meters. As part of on-going efforts to address public concerns on this issue, this report documents the collection of information on RF exposure related to the operation of two particular models of Smart Meter produced by Itron Inc.

Results & Findings

The smart meters studied in this report are currently being deployed by two electric utilities in California. The meters are part of wireless mesh networks in which one meter is configured as a collector point, referred to as a “cell relay” by Itron, for each of approximately 500 to 750 “end point meters.” The cell relay collects data from the various end point meters and conveys these data onto the cellular wireless wide area network (WWAN) for communication back to the electric utility company’s data management system. Mesh network communication among the many meters is provided by the 900 MHz band transceiver RF LAN (local area network). A HAN feature is supported by a 2.4 GHz transceiver.

Data collection was carried out in a laboratory setting and at residences and in neighborhoods in southern California and Colville, Washington, supplemented with theoretical modeling studies. The results indicate that RF field from the investigated smart meter are well below the maximum permitted exposure (MPE) established by the Federal Communications Commission (FCC). For instance, at one foot, the RF field from an end point meter would be expected to not exceed 0.8% of the MPE established by the Federal Communications Commission (FCC). For the cell relay, the RF field would not exceed 0.2% of the MPE. Even at very close distances, such as one foot directly in front of the meter, with an unrealistic assumption that the transmitters operate at 100% duty cycle, the resulting exposure is less than the FCC MPE. When viewed in the context of a typical, realistic exposure distance of 10 feet, the RF fields are much smaller, about 0.008% for the end point meter and about 0.002% of MPE for the cell relay. For occupants of a home equipped with a Smart Meter, interior RF fields would be expected to be at least ten times less intense simply due to the directional properties of the meter. When the attenuation afforded by a stucco home’s construction is included, a realistic

value of the interior RF field would be about 0.023% of the MPE for an end point meter and about 0.065% for a cell relay. Regardless of duty cycle values for end point and cell relay meters, typical exposures that result from the operation of smart meters are very low and comply with scientifically based human exposure limits by a wide margin.

Challenges & Objective(s)

This report is focused on the RF aspects of smart meters and in particular, the strength of the transmitted RF fields that may be produced by the meters from a human exposure perspective. The greatest difficulty in arriving in determining realistic time-averaged exposure from smart meters is associated with determining transmitter duty cycles since the meters only emit RF radiation at intervals

Applications, Values & Use

This report documents an investigation of the characteristics of RF fields associated with Itron Smart Meter. The project was undertaken to improve understanding of public exposure to the RF emissions produced by smart meters and to respond to public concerns about potential health effects.

EPRI Perspective

Measuring electric energy consumption with so-called smart meters in residential and commercial environments is becoming more commonplace as part of the development of Advanced Metering Infrastructure (AMI) in the electric utility industry. With the deployment of smart meters public concern was raised about potential health effects associated with RF emissions from smart meters EPRI is responding to these concerns with research efforts to provide objective information on RF emissions related to smart meters.

Approach

The project team conducted laboratory and field measurements of the RF emissions of Itron smart meters. A key objective was to determine realistic estimates of the operational duty cycle of meter transmitters. The team also investigated the effectiveness of metal meshes and stucco walls in shielding smart meters.

Keywords

Smart meters
Radiofrequency emissions
EMF health assessment
Environmental issues

Table of Contents

Section 1: Summary	1-1
Section 2: Introduction and Background.....	2-1
Smart Meters as RF Sources.....	2-1
How Smart Meters are Deployed	2-2
Section 3: Objective of Investigation	3-1
Section 4: Technical Approach to Investigation	4-1
Measurements at Itron	4-1
Measurements in residential locations.....	4-1
Measurements in Colville, WA	4-2
Section 5: Transmitter Powers.....	5-1
Section 6: The Measurement Challenge Presented by Smart Meters.....	6-1
Section 7: Measurement Methods and Instrumentation	7-1
Section 8: Laboratory Pattern Measurements	8-1
Section 9: Smart Meter Field Measurements	9-1
Meter farm measurements	9-1
Individual meters	9-2
Groups of meters	9-8
Residential settings	9-15
Homes.....	9-15
Residential apartment setting	9-25
Neighborhoods with and without Smart Meters	9-29
Section 10: Shielding Effectiveness Measurements... 	10-1
Shielding effectiveness of different metal meshes.....	10-1
Shielding effectiveness of a simulated stucco wall	10-4
Section 11: Spatial Variation of RF Fields	11-1
Section 12: Operational Duty Cycle of Meter Transmitters	12-1
SRM-3006 measurements of peak and average values.....	12-1
Wi-Spy spectrum analyzer measurements	12-3
SCE Smart Meter Network Management System.....	12-7
SDG&E Smart Meter Network Management System	12-9

Section 13: Ancillary Measurements	13-1
Microwave Oven	13-1
Cordless telephone.....	13-2
Wireless router	13-3
Measurement comparison (Model B8742D probe and SRM-3006).....	13-4
Section 14: Theoretical Analysis of RF Fields.....	14-1
Section 15: RF Exposure Limits.....	15-1
FCC	15-1
IEEE.....	15-2
ICNIRP.....	15-3
Section 16: Discussion of Results and Insights	16-1
Section 17: Conclusions	17-1
Appendix A: Instrument Calibration Certificates	A-1
Appendix B: SRM-3006 900 MHz Spectrum Measurement Scans (meter farm)	B-1
Appendix C: SRM-3006 900 MHz Spectrum Measurements Scans (rear of meters)	C-1
Appendix D: SRM-3006 2.4 GHz Spectrum Measurement Scans (meter farm)	D-1
Appendix E: SRM-3006 2.4 GHz Spectrum Measurement Scans (rear of meters).....	E-1
Appendix F: Photos of Simulated Stucco Wall During Construction.....	F-1
Appendix G: Modeling of RF fields of a 915 MHz Dipole for Spatial Averaging	G-1
Appendix H: Glossary of Terms	H-1

List of Figures

Figure 1-1 Calculated RF fields near Itron end point and cell relay meters based on 99th percentile transmitter power values, main beam exposure (point of maximum RF field), inclusion of the possibility of ground reflected fields and an assumed 99th and 99.9th percentile duty cycles.	1-4
Figure 2-1 Photo of Itron Smart Meter.	2-2
Figure 2-2 Simplistic illustrative diagram of an RF mesh network. Each end point also provides a Home Area Network (HAN) feature. The cell relay acts as a collector point for multiple meters distributed in a neighborhood and transmits received data onto a cellular wireless wide area network (WWAN).	2-3
Figure 2-3 Cell relay meter with flexible, dual band (850 MHz and 1900 MHz) antenna affixed to interior surface of the meter cover.	2-4
Figure 5-1 Accumulative fraction of 900 MHz RF LAN transmitter output power vs. transmitter power for a sample of 200,000 units. The median transmitter power is approximately 24.1 dBm (257 mW).	5-1
Figure 5-2 Number of 900 MHz RF LAN transmitters with powers within selected ranges. The transmitter power mode is approximately 24.5 dBm (282 mW).	5-2
Figure 5-3 Accumulative fraction of 2.4 GHz Zigbee transmitter output power vs. transmitter power for a sample of 200,000 units. The median transmitter power is approximately 18.2 dBm (66.1 mW).	5-3
Figure 5-4 Number of 2.4 GHz Zigbee transmitters with powers within selected ranges. The transmitter power mode is approximately 18.5 dBm (70.8 mW mW).	5-4
Figure 7-1 Close up view of dual axis antenna positioner system used to obtain antenna patterns of Smart Meter transmitters.	7-1
Figure 7-2 Interior of anechoic chamber showing reception horn antenna with Smart Meter on antenna positioner in background. During pattern measurements, the spectrum analyzer shown below the Smart Meter is removed.	7-2
Figure 7-3 Instrumentation system for acquiring antenna pattern data.	7-3

Figure 7-4 Frequency shaped, isotropic, electric field probe and meter (Narda B8742D and Narda 8715 meter).	7-4
Figure 7-5 Selective radiation meter (Narda Model SRM-3006).	7-5
Figure 7-6 Wi-Spy USB spectrum analyzer connected to a notebook computer running software to operate the analyzer (Chanalyzer version 3.4) and an external yagi antenna.....	7-6
Figure 8-1 Azimuth plane pattern of the 900 MHz RF LAN transmitter configured in an end point meter showing the horizontal, vertical and total pattern as viewed from bottom of meter. The scale is in dB with the maximum field at the outer edge of the pattern circle.	8-2
Figure 8-2 Azimuth plane view of the total EIRP of the 900 MHz RF LAN transmitter configured in an end point meter.	8-3
Figure 8-3 Elevation plane pattern of the 900 MHz RF LAN transmitter in an end point meter showing the horizontal, vertical and total pattern. The scale is in dB with the maximum field at the outer edge of the pattern circle.....	8-3
Figure 8-4 Elevation plane view of the total EIRP of the 900 MHz RF LAN transmitter in an end point meter.....	8-4
Figure 8-5 Azimuth plane pattern of the 900 MHz RF LAN transmitter in a cell relay showing the horizontal, vertical and total pattern as viewed from bottom of meter. The scale is in dB with the maximum field at the outer edge of the pattern circle.....	8-5
Figure 8-6 Azimuth plane view of the total EIRP of the 900 MHz RF LAN transmitter configured in a cell relay.	8-5
Figure 8-7 Elevation plane pattern of the 900 MHz RF LAN transmitter in a cell relay meter showing the horizontal, vertical and total pattern. The scale is in dB with the maximum field at the outer edge of the pattern circle.....	8-6
Figure 8-8 Elevation plane view of the total EIRP of the 900 MHz RF LAN transmitter in a cell relay meter.....	8-6
Figure 8-9 Azimuth plane pattern of the 2.4 GHz Zigbee transmitter configured in an end point meter showing the horizontal, vertical and total pattern as viewed from bottom of meter. The scale is in dB with the maximum field at the outer edge of the pattern circle.	8-7
Figure 8-10 Azimuth plane view of the total EIRP of the 2.4 GHz Zigbee transmitter configured in an end point meter.	8-7
Figure 8-11 Elevation plane pattern of the 2.4 GHz Zigbee radio in an end point meter showing the horizontal, vertical and total pattern. The scale is in dB with the maximum field at the outer edge of the pattern circle.	8-8

Figure 8-12 Elevation plane view of the total EIRP of the 2.4 GHz Zigbee radio in an end point meter.8-8

Figure 8-13 Azimuth plane pattern of the 2.4 GHz Zigbee transmitter configured in a cell relay meter showing the horizontal, vertical and total pattern as viewed from bottom of meter. The scale is in dB with the maximum field at the outer edge of the pattern circle.8-9

Figure 8-14 Azimuth plane view of the total EIRP of the 2.4 GHz Zigbee transmitter configured in a cell relay meter.....8-9

Figure 8-15 Elevation plane pattern of the 2.4 GHz Zigbee radio in a cell relay meter showing the horizontal, vertical and total pattern. The scale is in dB with the maximum field at the outer edge of the pattern circle.8-10

Figure 8-16 Elevation plane view of the total EIRP of the 2.4 GHz Zigbee radio in a cell relay meter.....8-10

Figure 8-17 Azimuth plane pattern of the 836.6 MHz GSM cellular transmitter in a cell relay meter showing the horizontal, vertical and total pattern as viewed from bottom of meter. The scale is in dB with the maximum field at the outer edge of the pattern circle.8-11

Figure 8-18 Azimuth plane view of the total EIRP of a GSM 836.6 MHz cellular radio in a cell relay meter.8-11

Figure 8-19 Elevation plane pattern of the 836.6 MHz GSM cellular transmitter in a cell relay meter showing the horizontal, vertical and total pattern as viewed from bottom of meter. The scale is in dB with the maximum field at the outer edge of the pattern circle.8-12

Figure 8-20 Elevation plane view of the total EIRP of a GSM 836.6 MHz cellular radio in a cell relay meter.8-12

Figure 8-21 Azimuth plane pattern of the 1880 MHz GSM PCS transmitter in a cell relay meter showing the horizontal, vertical and total pattern as viewed from bottom of meter. The scale is in dB with the maximum field at the outer edge of the pattern circle.....8-13

Figure 8-22 Azimuth plane view of the total EIRP of a GSM 1880 MHz PCS radio in a cell relay meter.8-13

Figure 8-23 Elevation plane pattern of the 1880 MHz GSM PCS transmitter in a cell relay meter showing the horizontal, vertical and total pattern as viewed from bottom of meter. The scale is in dB with the maximum field at the outer edge of the pattern circle.....8-14

Figure 8-24 Elevation plane view of the total EIRP of a GSM 1880 MHz PCS radio in a cell relay meter.8-14

Figure 9-1 Aerial view of the Itron meter farm in West Union, SC. Yellow lines represent rows of Smart Meters grouped, generally, as racks of ten meters each. Photo courtesy of Itron.	9-1
Figure 9-2 Typical rack of ten meters shown in the western part of the Itron meter farm.	9-2
Figure 9-3 Layout of Smart Meter rack showing designated meter locations and frequency of various meters (L, M and H - see text) for the 900 MHz RF LAN and 2.4 GHz Zigbee transmitters.	9-3
Figure 9-4 Use of the broadband field probe with a cardboard spacer attached to the probe near meters in a rack of ten meters.	9-4
Figure 9-5 Corrected broadband probe RF field readings of the 900 MHz RF LAN transmitters from ten Smart Meters at the surface and at 20 cm and 30 cm from the meter.	9-5
Figure 9-6 Corrected broadband probe RF field readings of the 2.4 GHz Zigbee transmitters from ten Smart Meters at the surface and at 20 cm from the meter.	9-8
Figure 9-7 Using the Narda SRM-3006 to measure aggregate RF fields near a rack of ten meters programmed for fixed frequency, continuous transmission in the meter farm.....	9-9
Figure 9-8 900 MHz band composite RF field from rack of 10 SmartMeters at 1 foot.	9-10
Figure 9-9 Field measurements at successively greater distances behind the subject meter rack resulted in closer proximity to other meter racks with the probability of detecting stronger, but intermittent, signals due to the ambient background.....	9-11
Figure 9-10 Spectrum measurement of 2.4 GHz RF fields from ten simultaneously transmitting Smart Meters.	9-12
Figure 9-11 Integrated, total composite RF field obtained in meter farm for emissions from the 900 MHz RF LAN and 2.4 GHz Zigbee transmitters operating simultaneously in the vicinity of a meter rack (linear plot).....	9-14
Figure 9-12 Integrated, total composite RF field obtained in meter farm for emissions from the 900 MHz RF LAN and 2.4 GHz Zigbee transmitters operating simultaneously in the vicinity of a meter rack (logarithmic plot).....	9-14
Figure 9-13 SCE meter technician replacing existing Smart Meter with specially programmed meter for residential measurements.	9-16
Figure 9-14 Planar scans were performed at several distances in front of a residential Smart Meter by slowly moving the SRM-3006 within a plane at a fixed distance.....	9-17

Figure 9-15 Interior residential measurements included measurements on the opposite side of the wall where the Smart Meter was installed at the home.....	9-19
Figure 9-16 Residential measurements at residence A included both outdoors and indoors measurements of RF fields in both the 900 MHz and 2.4 GHz bands.....	9-20
Figure 9-17 Measurements at residence A included exterior locations in the backyard.	9-21
Figure 9-18 Residence B in Downey, CA where indoor and outdoor measurements were made with specially programmed Smart Meters installed to facilitate measurements.	9-22
Figure 9-19 Performing a planar scan of RF fields adjacent to a Smart Meter at residence B.	9-23
Figure 9-20 Measured RF fields inside residence B, similar to residence A, tended to be predominated by signals produced by wireless routers used for Internet connectivity throughout the home.	9-24
Figure 9-21 A nine-meter bank at an apartment house in Downey, CA.	9-26
Figure 9-22 An eleven-meter bank at an apartment house in Downey, CA.	9-27
Figure 9-23 Measured maximum (peak) and average RF fields in the 900 MHz band at one foot in front of a nine-meter bank of Smart Meters.	9-28
Figure 9-24 Measured maximum (peak) and average RF fields in the 900 MHz band at one foot in front of an eleven-meter bank of Smart Meters.	9-28
Figure 9-25 Route in Downey, CA neighborhood with SCE deployed Smart Meters over which a driving survey was conducted to test the ability to detect RF signals associated with residential meter installations.	9-29
Figure 9-26 Conducting a “driving survey” of a Smart Meter deployed neighborhood.....	9-30
Figure 9-27 Measured peak spectrum of RF fields detected with the SRM-3006 during traveling the route mapped in Figure 9-25. Fields were monitored for a total of approximately 34 minutes.	9-31
Figure 9-28 Route in Santa Monica, CA neighborhood where SCE Smart Meters have not been deployed over which a driving survey was conducted to test the ability to detect RF signals that might exist in the 900 MHz band.	9-32

Figure 9-29 Spectrum scan in residential neighborhood of Santa Monica, CA consisting of an approximately 20 minute drive. The single peak near 912 MHz is an apparent internal spurious signal due to the SRM-3006 electronics and not caused by external RF fields.....	9-32
Figure 9-30 Spectrum scan in residential neighborhood of Santa Monica, CA showing weak signals, apparently caused by 900 MHz cordless telephones.....	9-33
Figure 9-31 Spectrum scan in a commercial district of Santa Monica, CA showing noticeable activity from devices other than Smart Meters.	9-33
Figure 9-32 Spectrum scan of the FM radio broadcast band in Santa Monica, CA with a band integrated RF field equivalent to 0.013% of the FCC MPE for the public.....	9-34
Figure 9-33 Spectrum scan of the 800 MHz to 900 MHz band in Santa Monica, CA, with a band integrated RF field equivalent to 0.012% of the FCC MPE for the public.....	9-35
Figure 9-34 Spectrum scan of the 1.9 GHz to 2.0 GHz band in Santa Monica, CA, with a band integrated RF field equivalent to 0.103% of the FCC MPE for the public.....	9-35
Figure 9-35 Spectrum scan of the 50 MHz to 216 MHz band in Santa Monica, CA, with a band integrated RF field equivalent to 0.036% of the FCC MPE for the public.....	9-36
Figure 9-36 Spectrum scan of the 2.4 GHz to 2.5 GHz band in Santa Monica, CA, with a band integrated RF field equivalent to 0.0026% of the FCC MPE for the public.....	9-36
Figure 10-1 Measurement setup to determine the insertion loss presented by a conductive mesh (chicken wire in this case).....	10-2
Figure 10-2 Measurement setup to determine the insertion loss presented by a conductive mesh (chicken wire in this case).....	10-3
Figure 10-3 Insertion loss of three different metal mesh sizes. ...	10-3
Figure 10-4 Measurement setup for determining insertion loss of simulate stucco wall shown with the 900 MHz yagi antenna.....	10-5
Figure 10-5 Measurement setup for determining insertion loss of simulate stucco wall shown with the 2.4 GHz yagi antenna.....	10-6
Figure 10-6 Illustrative display of the Wi-Spy spectrum analyzer display showing the captured average signal measured over a period of 81 seconds from a 900 MHz RF LAN Smart Meter transmitter. In this measurement, the simulated wall was not present. Marker readout data are shown on the right side of the display.....	10-7

Figure 11-1 Vertical spatial variation in Smart Meter 900 MHz RF LAN field from 0 to 6 feet above the floor at a lateral distance from the Smart Meter of approximately 1 foot.....	11-1
Figure 11-2 Vertical spatial variation in Smart Meter 2.4 GHz Zigbee transmitter field from 0 to 6 feet above the floor at a lateral distance from the Smart Meter of approximately 0.5 feet.....	11-2
Figure 12-1 Measurements of aggregate maximum and average RF fields found along two rows of Smart Meters in the Itron meter farm during normal operation of the meters.....	12-2
Figure 12-2 Spectrum analysis measurement of RF fields during walk through section of the Itron meter farm in which both the maximum (peak) field and the average field was measured.	12-3
Figure 12-3 Wi-Spy display of Smart Meter RF fields observed during 66 minute monitoring period beginning at 10:56 P.M. local time. The blue spectrum is the “max hold” spectrum showing the maximum received signal power detected during the entire monitoring period. The four peaks that stand out from all of the rest of the detected signals, because of close proximity of the Wi-Spy to the meter, represent the momentary emissions detected from the Smart Meter being studied. Lower level signal peaks (typically 20 to 30 dB lower) are from other smart meters in the neighborhood.	12-4
Figure 12-4 Wi-Spy display of Smart Meter RF fields observed during 115 minute monitoring period beginning at 9:25 P.M. local time.	12-5
Figure 12-5 Processed signal power values obtained with the Wi-Spy spectrum analyzer on November 4, 2010, in the Itron meter farm. The average values of the peak and average spectra were -51.8 dBm and the -88.1 dBm respectively.....	12-6
Figure 12-6 Analysis of SCE daily average duty cycle distribution for different percentiles based on 4,156,164 readings of transmitter activity from an average of 46,696 Itron Smart Meters over a period of 89 consecutive days. Analysis based on estimated transmitter activity during a day (see text).	12-8
Figure 12-7 Results of an analysis of duty cycles for a sample of 6865 Itron Smart Meters deployed by SDG&E based on transmit duration during a single day of observation.....	12-9
Figure 13-1 Measurement of microwave oven leakage at 1 foot from oven door seal.	13-1
Figure 13-2 Microwave oven leakage vs. distance.	13-2

Figure 13-3 900 MHz cordless telephone RF fields from the base unit near the upper end of the spectrum and from the portable receiver unit near the lower end of the spectrum, measured at 1 foot from the base and receiver. 13-3

Figure 13-4 Measured RF emission spectrum of a wireless router at one foot from the router. The router was set to operate on Wi-Fi channel 10. 13-3

Figure 14-1 Relative EIRP of a 900 MHz RF LAN transmitter as observed along a six foot vertical line located one foot adjacent to the Smart Meter..... 14-3

Figure 14-2 Calculated RF fields up to 100 feet at point of maximum intensity in main beam expressed as percentage of FCC general public MPE as function of distance in maximum beam for Itron Smart Meter components investigated in this study. No ground reflections have been included in this analysis, the field values are relevant to the peak value of field during the time that the transmitter is actually transmitting (no duty cycle correction) and spatial averaging has not been applied to the values. Normal operation of the Smart Meter will significantly reduce the actual field found in practice near operating meters. 14-4

Figure 14-3 Calculated RF fields up to 1000 feet associated with Smart Meters included in this study with the assumption that the transmitters operate continuously (not possible in actual operation in a mesh network) and no ground reflections occur that might add constructively to enhance the field at the point of interest. 14-5

Figure 14-4 Calculated RF field produced by Smart Meter 900 MHz RF LAN transmitter using most likely transmitter power (solid curve) and 99th percentile transmitter power (bars above solid curve). Calculated maximum possible values are based on the 99th percentile transmitter power but assume the possibility of ground reflections ($\Gamma = 2.56$) that would enhance the RF field at the calculation point (point of maximum RF field emission near the meter). Such ground reflections are not realistic but follow guidance in FCC OET 65..... 14-7

Figure 14-5 Calculated RF field produced by Smart Meter 2.4 GHz Zigbee transmitter using most likely transmitter power (solid curve) and 99th percentile transmitter power (bars above solid curve). Calculated maximum possible values are based on the 99th percentile transmitter power but assume the possibility of ground reflections ($\Gamma = 2.56$) that would enhance the RF field at the calculation point (point of maximum RF field emission near the meter). Such ground reflections are not realistic but follow guidance in FCC OET 65..... 14-8

Figure 14-6 Relative calculated plane wave equivalent power density along a six-foot vertical path, one foot adjacent from a 900 MHz half-wave dipole positioned at five feet above the ground. Power density values are compared with and without ground reflections.....	14-10
Figure 14-7 Impact of ground reflections on six-foot spatial average of power density for different distances lateral to a 900 MHz dipole antenna mounted at five feet above ground. Vertical axis is represents the percentage that the spatially averaged power density that includes any ground reflected fields is greater than the spatially averaged power density in free space (without any ground reflected fields).....	14-11
Figure 14-8 Ratio of magnitude of measured RF fields of group of ten meters to magnitude of calculated RF field of a single meter from 1 to 100 feet.	14-12
Figure 15-1 Chart of FCC MPEs applicable to members of the general public.	15-1
Figure 15-2 Summary of the IEEE C95.1-2005 action levels or MPEs for the lower tier (applicable to members of the general public if uninformed about RF exposure and not able to reduce their exposure if necessary).	15-3
Figure 15-3 Summary of ICNIRP guidelines on RF exposure limits for the general public.....	15-4
Figure 16-1 Estimated maximum likely time-averaged RF fields near Itron end point and cell relay Smart Meters included in this study. The plotted values are based on the 99th percentile values of transmitter powers, duty cycles given in Table 14-3 based on the conservative estimates from SCE data, main beam exposure and inclusion of realistic ground reflected fields ($\Gamma = 1.344$) that might add constructively to the resultant field. An assumption is made that the maximum RF field from all transmitters occurs at the same point in space. The graph pertains to a single end point meter and a single cell relay meter.	16-4
Figure A-1 Calibration certificate for the Narda Model 8715 digital meter for use with the Model B8742D probe.	A-1
Figure A-2 Calibration certificate for the Narda Model B8742D broadband probe.....	A-2
Figure A-3 Calibration certificate sheet 1 for the Narda Model SRM-3006 SN A-0077.	A-3
Figure A-4 Calibration certificate sheet 1 for the Narda Model SRM-3006 SN H-0100.	A-9
Figure A-5 Calibration certificate sheet 1 for the Narda Model SRM-3006 SN H-0100.	A-14
Figure A-6 Calibration certificate sheet 1 for the Narda Model SRM-3006 SN H-0100.	A-20

Figure B-1 900 MHz band composite RF field from rack of 10 SmartMeters at 1 foot.	B-1
Figure B-2 900 MHz band composite RF field from rack of 10 SmartMeters at 2 feet.....	B-2
Figure B-3 900 MHz band composite RF field from rack of 10 SmartMeters at 3 feet.....	B-2
Figure B-4 900 MHz band composite RF field from rack of 10 SmartMeters at 4 feet.....	B-3
Figure B-5 900 MHz band composite RF field from rack of 10 SmartMeters at 5 feet.....	B-3
Figure B-6 900 MHz band composite RF field from rack of 10 SmartMeters at 6 feet.....	B-4
Figure B-7 900 MHz band composite RF field from rack of 10 SmartMeters at 7 feet.....	B-4
Figure B-8 900 MHz band composite RF field from rack of 10 SmartMeters at 8 feet.....	B-5
Figure B-9 900 MHz band composite RF field from rack of 10 SmartMeters at 9 feet.....	B-5
Figure B-10 900 MHz band composite RF field from rack of 10 SmartMeters at 10 feet.....	B-6
Figure B-11 900 MHz band composite RF field from rack of 10 SmartMeters at 15 feet.....	B-6
Figure B-12 900 MHz band composite RF field from rack of 10 SmartMeters at 20 feet.....	B-7
Figure B-13 900 MHz band composite RF field from rack of 10 SmartMeters at 25 feet.....	B-7
Figure B-14 900 MHz band composite RF field from rack of 10 SmartMeters at 30 feet.....	B-8
Figure B-15 900 MHz band composite RF field from rack of 10 SmartMeters at 40 feet.....	B-8
Figure B-16 900 MHz band composite RF field from rack of 10 SmartMeters at 50 feet.....	B-9
Figure B-17 900 MHz band composite RF field from rack of 10 SmartMeters at 75 feet.....	B-9
Figure B-18 900 MHz band composite RF field from rack of 10 SmartMeters at 100 feet.....	B-10
Figure C-1 900 MHz band composite RF field from rack of 10 SmartMeters at 20 cm behind meters.....	C-1
Figure C-2 900 MHz band composite RF field from rack of 10 SmartMeters at 5 feet behind meters.....	C-2
Figure C-3 900 MHz band composite RF field from rack of 10 SmartMeters at 10 feet behind meters.....	C-2

Figure D-1 2.4 GHz band composite RF field from rack of 10 SmartMeters at 1 foot.	D-1
Figure D-2 2.4 GHz band composite RF field from rack of 10 SmartMeters at 2 feet.....	D-2
Figure D-3 2.4 GHz band composite RF field from rack of 10 SmartMeters at 3 feet.....	D-2
Figure D-4 2.4 GHz band composite RF field from rack of 10 SmartMeters at 4 feet.....	D-3
Figure D-5 2.4 GHz band composite RF field from rack of 10 SmartMeters at 5 feet.....	D-3
Figure D-6 2.4 GHz band composite RF field from rack of 10 SmartMeters at 6 feet.....	D-4
Figure D-7 2.4 GHz band composite RF field from rack of 10 SmartMeters at 7 feet.....	D-4
Figure D-8 2.4 GHz band composite RF field from rack of 10 SmartMeters at 8 feet.....	D-5
Figure D-9 2.4 GHz band composite RF field from rack of 10 SmartMeters at 9 feet.....	D-5
Figure D-10 2.4 GHz band composite RF field from rack of 10 SmartMeters at 10 feet.....	D-6
Figure D-11 2.4 GHz band composite RF field from rack of 10 SmartMeters at 15 feet.....	D-6
Figure D-12 2.4 GHz band composite RF field from rack of 10 SmartMeters at 20 feet.....	D-7
Figure D-13 2.4 GHz band composite RF field from rack of 10 SmartMeters at 25 feet.....	D-7
Figure D-14 2.4 GHz band composite RF field from rack of 10 SmartMeters at 30 feet.....	D-8
Figure D-15 2.4 GHz band composite RF field from rack of 10 SmartMeters at 40 feet.....	D-8
Figure D-16 2.4 GHz band composite RF field from rack of 10 SmartMeters at 50 feet.....	D-9
Figure D-17 2.4 GHz band composite RF field from rack of 10 SmartMeters at 75 feet.....	D-9
Figure D-18 2.4 GHz band composite RF field from rack of 10 SmartMeters at 100 feet.....	D-10
Figure E-1 2.4 GHz band composite RF field at 20 cm behind rack of 10 SmartMeters.....	E-1
Figure E-2 2.4 GHz band composite RF field at 5 feet behind rack of 10 SmartMeters.....	E-2
Figure E-3 2.4 GHz band composite RF field at 10 feet behind rack of 10 SmartMeters.....	E-2

Figure E-4 2.4 GHz band composite RF field obtained with lateral walk at 3 feet in front of rack of 10 SmartMeters from well beyond each side of rack. E-3

Figure F-1 Simulated wall section prior to installation of insulation, sheetrock and stucco lath (netting)..... F-1

Figure F-2 Simulated wall section showing initial installation of stucco scratch coat of stucco during construction with underlying 1.5 inch stucco netting. F-2

Figure G-1 Plane wave equivalent power density with and without ground reflections along a six-foot vertical line at 1 foot adjacent to a 900 MHz horizontally polarized dipole located at 5 feet above ground. Ratio of spatial average with reflections to spatial average without reflections is 1.032. G-1

Figure G-2 Plane wave equivalent power density with and without ground reflections along a six-foot vertical line at 3 feet adjacent to a 900 MHz horizontally polarized dipole located at 5 feet above ground. Ratio of spatial average with reflections to spatial average without reflections is 1.103. G-2

Figure G-3 Plane wave equivalent power density with and without ground reflections along a six-foot vertical line at 6 feet adjacent to a 900 MHz horizontally polarized dipole located at 5 feet above ground. Ratio of spatial average with reflections to spatial average without reflections is 1.190. G-2

Figure G-4 Plane wave equivalent power density with and without ground reflections along a six-foot vertical line at 10 feet adjacent to a 900 MHz horizontally polarized dipole located at 5 feet above ground. Ratio of spatial average with reflections to spatial average without reflections is 1.344. G-3

Figure G-5 Plane wave equivalent power density with and without ground reflections along a six-foot vertical line at 15 feet adjacent to a 900 MHz horizontally polarized dipole located at 5 feet above ground. Ratio of spatial average with reflections to spatial average without reflections is 1.432. G-3

Figure G-6 Plane wave equivalent power density with and without ground reflections along a six-foot vertical line at 20 feet adjacent to a 900 MHz horizontally polarized dipole located at 5 feet above ground. Ratio of spatial average with reflections to spatial average without reflections is 1.650. G-4

List of Tables

Table 5-1 Sierra Wireless Transceivers Operation Maximum Powers	5-4
Table 8-1 Summary of antenna measurement data	8-15
Table 9-1 Measurements of 900 MHz RF LAN emissions of individual Smart Meters installed in meter position A in the meter rack with the broadband field probe.....	9-4
Table 9-2 Summary of measurements of the 900 MHz composite RF field produced by an increasing number of closely spaced, collocated Smart Meters (meters A - J).	9-6
Table 9-3 Summary of corrected measurement data on RF fields of individual 2.4 GHz Zigbee transmitters installed in meter position A and of the collection of all ten meters.....	9-7
Table 9-4 Summary of composite RF field values (% general public MPE) determined with the SRM-3006 at various distances in front of a meter rack of 10 simultaneously operating Smart Meters.....	9-13
Table 9-5 Summary of planar area scans performed with the SRM-3006 in front of residential meter installation at residence A, Downey, CA.	9-15
Table 9-6 Spectrum scan measurements of Smart Meter fields in the 900 MHz and 2.4 GHz bands in residence A, Downey, CA. RF field is peak value obtained from a spatial scan of the room interior or area in percent of FCC general public MPE.	9-18
Table 9-7 Summary of planar area scans performed with the SRM-3006 in front of residential meter installation at residence B, Downey, CA.	9-24
Table 9-8 Spectrum scan measurements of Smart Meter fields in the 900 MHz and 2.4 GHz bands in residence B, Downey, CA. RF field is peak value obtained from a spatial scan of the room interior or area in percent of FCC general public MPE.	9-25
Table 10-1 Insertion loss measurement results for three different types of metal lath expressed as a reduction factor (F) and in decibels (dB).	10-3
Table 10-2 Insertion loss measurement data for simulated wall in 900 MHz and 2.4 GHz bands.....	10-8
Table 13-1 Comparison of RF field probe readings at 902.25 MHz and 2405 MHz	13-4

Table 14-1 Approximate RF field reductions (dB) caused by Smart Meter elevation plane patterns in the 60° to 90° range below a horizontal to the meter.	14-2
Table 14-2 Summary of nominal transmitter peak powers and 99 th percentile powers for Itron Smart Meters studied in this investigation. °	14-6
Table 14-3 Calculated worst case maximum possible RF fields associated with the 900 MHz RF LAN, 2.4 GHz Zigbee and cellular cell relay Smart Meter transmitters. The 99 th percentile powers for the RF LAN and Zigbee transmitters, main beam exposure, 100% duty cycle and presence of ground reflections (using a ground reflection factor of 2.56) to enhance fields was assumed. However, no spatial averaging was assumed.....	14-9
Table 16-1 Estimated maximum likely RF fields as a percentage of the FCC MPE for the public associated with Itron end point meters and cell relay meters including all RF components (900 MHz RF LAN, 2.4 GHz Zigbee and 850 MHz cellular transmitters). The 99 th percentile powers for the RF LAN and Zigbee transmitters, main beam exposure and possibility of ground reflections to enhance fields was assumed.....	16-3
Table 16-2 Summary of interior residential RF field measurements on two residences equipped with Smart Meters operating in continuous transmit mode.	16-5

Section 1: Summary

Measuring electric energy consumption with so-called Smart Meters in residential and commercial environments is becoming more commonplace. Smart Meters represent one component of what is referred to as Advanced Metering Infrastructure (AMI) in the electric utility industry. AMI systems comprise both wired and wireless technologies with each exhibiting their own advantages. Electric utility companies, thus, have options to implementing AMI systems. Even within the wireless category of AMI system, equipment can operate over a wide range of frequencies and powers and levels of activity. The Smart Meters, based on wireless technology, make use of miniature, low power radio transceivers, typically inside the meter, to wirelessly communicate with the electric utility. Two-way radio communication provided by Smart Meters allows for transmission of energy consumption data from a residence or business to the utility company and reception of data pertaining to time-of-day pricing of electric energy.

As wireless AMI technology is projected to become widely distributed, it becomes prudent to quantitatively assess the levels of RF emissions from meters to which the public may be exposed. Nearly two dozen communities have placed moratoria on further deployment of Smart Meters in northern California and more than 2000 health-related complaints have been received by the California Public Utilities Commission¹. This report documents the collection of information related to the operation of two particular models of Smart Meters² produced by Itron Inc. for purposes of supporting exposure assessment exercises that can address public concerns about exposure. The Itron products are currently being deployed by Southern California Edison Electric Company (SCE) and San Diego Gas and Electric Company (SDG&E) and both companies provided support to EPRI (the Electric Power Research

Institute) for this activity. A number of companies currently manufacture different forms of Smart Meters and, most commonly, these meters employ radio transmitters that operate in Federal Communications Commission (FCC) designated license free bands³. The Itron meters in this study use transmitters that operate in the license free bands of 902 MHz to 928 MHz (the “900 MHz band”) and 2400 MHz to 2500 MHz (the “2.4 GHz band”).

The Smart Meters studied here act as nodes in wireless mesh networks consisting of approximately 500 residences (for SCE) or 750 residences (for SDG&E); these are referred to as “end point meters.” Within each mesh network, one residence, designated as a “collection point,” is equipped with a Smart Meter having an additional internal transmitter (referred to as a “cell relay” for communicating data to the utility over a wireless wide area network (WWAN). The cell relay collects data from the various end point meters and conveys these data onto the cellular wireless wide area network (WWAN) for communication back to the electric utility company’s data management system. Mesh network communications among the many meters is provided by the 900 MHz band transceiver RF LAN (local area network). A HAN feature is supported by the 2.4 GHz transceiver. A data protocol used by the HAN called Zigbee is used to refer to the 2.4 GHz transceiver as in “the 2.4 GHz Zigbee radio”.

The data collection effort included gathering of information and working with the manufacturer at their facility in West Union, South Carolina, measurements at residences and in neighborhoods in southern California and some more limited measurements in Colville, Washington. Itron graciously provided technical support and access to its facilities and personnel to assist in this effort. Data included transmitter power levels, radiation patterns, RF field strengths or power densities of individual meters and groups of meters, spatial variations of RF fields in a vertical plane near Smart Meters, attenuation of Smart

¹See, for example, “Smart Meters - They’re Smart, But Are They Safe?”. <http://www.publicnewsservice.org/index.php?/content/article/16846-1> (November 8, 2010).

² Itron model CL200 (end point meter) and model C2SORD (cell relay).

³ Some Smart Meters are designed to operate in FCC licensed bands and may operate with higher powers.

Meter RF fields by building materials, and information potentially useful for assessing transmitter duty cycles. To characterize the systems currently operating, parallel efforts included modeling of RF fields based on measured values of maximum equivalent isotropic radiated power (EIRP) of both end point and cell relay meters and analysis of end point meter transmission statistics for estimating duty cycles. Antenna patterns were determined for the 900 MHz RF LAN and 2.4 GHz Zigbee transmitter in both end point and cell relay meter configurations. Patterns were also measured for both the 850 MHz and 1900 MHz cellular bands from a cell relay.

Antenna pattern measurements revealed that RF fields are emitted preferentially toward the frontal region of the meters; the direction of maximum EIRP, however, might not be directly normal to the front of the meter. Apparent antenna gain values were modest, ranging between 0.88 dBi and 5.08 dBi, depending on the frequency band and the configuration (end point vs. cell relay). Patterns typically exhibited a reduced RF field behind the meter of approximately 10 dB down from the maximum frontal value of field with relatively narrow notches in the pattern directly behind the meter of as much as 20-30 dB less than in front.

Transmitter power data were obtained on 200,000 RF LAN 900 MHz transmitters with a most likely value of approximately 24.5 dBm (282 mW) with a 99th percentile power of 26.0 dBm (298 mW). Based on a sample size of 200,000 2.4 GHz radios, the most likely power was found to be 18.5 dBm (70.8 mW) with a 99th percentile power of 20.8 dBm (114.8 mW). Cellular transmitters were specified as 31.8 dBm in the 850 MHz band and 28.7 dBm in the 1900 MHz band.

Because of the very intermittent nature of transmissions from Smart Meters and their frequency hopping spread spectrum transmitters, accurate measurement of RF fields can be challenging. To facilitate the measurements, Smart Meters were programmed to transmit continuously on a single frequency. RF field measurements were performed on a single meter inside the Itron anechoic chamber and on ten individual meters installed in the Itron meter farm. These measurements were obtained with two different instruments including an isotropic, broadband, frequency conformal electric field probe (Narda Model B8742D) and a spectrum analyzer based selective radiation meter (Narda Model SRM-3006). Measurement data for the 900 MHz RF LAN

transmitters showed RF fields in the range of a few percent of the FCC MPE for the general public at 30 cm (approximately 1 foot) in front of the meters (0.7 to 5.5%) with the broadband probe depending on frequency. Similar measurements for the 2.4 GHz Zigbee radios at a distance of 20 cm showed 0.75% to 1.7% of the MPE, again depending on the frequency of the transmitter.

Using the SRM-3006 instrument, RF fields were measured as a function of distance from the rack of ten meters in both the 900 MHz and 2.4 GHz bands. These measurements produced readings ranging between approximately 8% at 1 foot to less than 0.1% at 75 feet from the meters in the 900 MHz band and approximately 4.5% at 1 foot to less than 0.01% at 75 feet in the 2.4 GHz band. 900 MHz field measurements showed that the emissions associated with the ten meters dropped into the background produced by other meters in the meter farm at a distance of approximately 50 feet.

By using the maximum hold and average measurement feature of the SRM-3006, a measurement in the meter farm obtained by walking along two rows of meter racks resulted in an integrated peak RF field equivalent to 0.114% of MPE and an average value of 0.00023% of MPE. The ratio of average to peak readings corresponds to an apparent duty cycle of about 0.2%. In measurements taken at two apartment houses in Downey, California, ratios of average to peak values of RF field obtained over five-minute monitoring periods resulted in estimated duty cycles of approximately 0.001%. Using a tiny USB spectrum analyzer designed specifically for just the 900 MHz band in the Itron meter farm, spectral measurements were captured for approximately one hour. This measurement resulted in an apparent duty cycle of approximately 0.02%.

Interior residential measurements were performed in two homes in Downey, California after temporarily replacing the existing Smart Meter with specially programmed units that would transmit continuously in the 900 MHz and 2.4 GHz bands. Inside measurements ranged from approximately 0.006% to 22% of MPE, the highest value associated with operation of a microwave oven in the kitchen at 2 feet from the oven. The greatest value immediately behind the Smart Meter, inside the home, was 0.009% of MPE. Wireless routers found in both homes resulted in RF fields in the range of 0.02 to 0.03% of MPE.

Residential neighborhood surveys were performed in areas with and without deployed Smart Meters while driving the streets of two communities, one in Downey, CA and one in Santa Monica, CA respectively. The exercise demonstrated that the emissions of randomly emitting Smart Meters could be detected in the Downey neighborhood but virtually no signals were detected in Santa Monica with the exception that when driving through a commercial district, the 900 MHz band came alive with noticeable activity, presumably caused by various 900 MHz sources, such as cordless telephones, etc. Spectrum measurements in several other band were also performed including the FM radio broadcast band, two cellular telephone bands and the 2.4 GHz Wi-Fi band.

The insertion loss of three different metal meshes was evaluated in California at one of the residences in which RF measurements were obtained. Three different sizes of mesh were used in the tests by inserting the mesh between a specially prepared, portable Smart Meter as a source, and the SRM-3006 meter. These measurements were performed at close range with the Smart Meter approximately six inches behind the mesh and the SRM-3006 probe approximately the same distance on the other side of the mesh. These measurements resulted in values for insertion loss ranging from 4.1 dB to 19.1 dB in the 900 MHz band and from 1.2 dB to 11.4 dB in the 2.4 GHz band, depending on mesh opening size. Additional insertion loss measurements were performed on a simulated stucco wall in Colville, WA resulting in values of 6.1 dB and 2.5 dB for the 900 MHz and 2.4 GHz bands respectively.

Since human RF exposure standards are based on spatial averages, spatially averaged values of RF fields were obtained along a vertical line at approximately one foot in front of a Smart Meter. It was found that over a six-foot vertical span, the spatially averaged RF field in the 900 MHz band corresponded to a value 23% of the measured peak value found near the height of the meter. In the 2.4 GHz band, the spatially averaged field was 18% of the spatial peak.

Using the detailed pattern measurement data described earlier, theoretical calculations of RF fields that could be associated with each of the transmitters in either end point meters or cell relays were made. A detailed analysis was developed to investigate the effect that ground reflected fields could have on the resultant field and what factors would be appropriate for including the

effect of ground reflections in theoretical RF field calculations.

Human exposure to RF fields is judged by comparison to applicable exposure limits or standards. For the United States, and in regard to Smart Meters, the most applicable limits are those promulgated by the FCC, a spatially averaged and time averaged value of 610 microwatts per square centimeter ($\mu\text{W}/\text{cm}^2$) in the 900 MHz band and 1000 $\mu\text{W}/\text{cm}^2$ in the 2.4 GHz band. A proper comparison of Smart Meter produced RF fields to these limits should involve a determination of the time-averaged value where the averaging time is specified as any 30-minute period. To arrive at time-averaged values, the measurements or calculated fields reported above must be corrected for the operational duty cycle of the transmitters. This is the most complex issue connected with Smart Meter RF evaluations since transmitter activity is semi-random in nature, with only brief transmissions occurring throughout a day. The maximum value of duty cycle for end point meters has been estimated by Itron to be in the range of 5%. Actual measurements, however, tend to result in substantially smaller values, typically less than 1%. Because of the variable nature of transmitter activity, even accurate measurements of a specific meter or meters need to be repeated for some days and, possibly, weeks to obtain reliable estimates of typical duty cycles. Rather than measurements, Itron developed special software implemented by the two companies to collect transmit data gathered and reported on in this report. Such an approach represents a practical way for bracketing realistic values of meter duty cycles since it can be implemented in software and extended to a very large sample size, something that would be impractical to do via physical measurements of RF fields at the meters. Using this approach, SCE generated data were examined to identify what fraction of meters in the sample exhibited transmit durations over a range of times which are related directly to the transmitter duty cycle. This exercise, for example, supported 99th and 99.9th percentile duty cycles of 0.11% and 4.7% for the RF LAN component of end point meters. A complimentary analysis conducted by SDG&E but using a more accurate determination of transmitter activity revealed smaller duty cycles. Similarly small duty cycle values are associated with the HAN and cellular transmitters. Figure 1-1 illustrates the estimated maximum likely time-averaged RF fields that would be produced by both end point and cell relay meters.

Estimated Maximum Likely Time-Averaged RF Field Near an Itron Smart Meter (Not including spatial averaging)

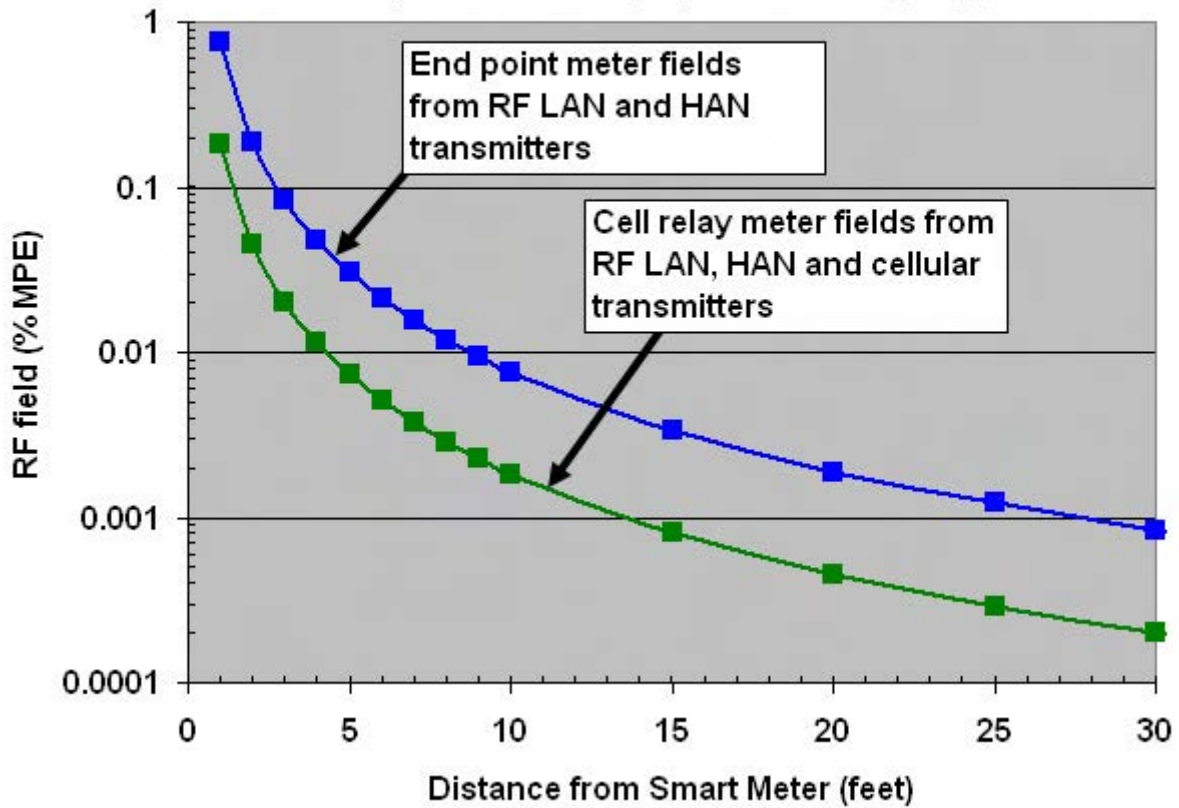


Figure 1-1
 Calculated RF fields near Itron end point and cell relay meters based on 99th percentile transmitter power values, main beam exposure (point of maximum RF field), inclusion of the possibility of ground reflected fields and assumed 99th percentile duty cycles.

These data, when taken collectively, indicate that the RF emissions produced by the Itron Smart Meters evaluated in this study result in RF fields <0.06 mW/cm² (at least 10-fold below the FCC limit at 900 MHz). For instance, at one foot, the RF field from an end point meter would be expected to not exceed 0.8% of the MPE. For the cell relay, the RF field would not exceed 0.2% of the MPE. Even at very close distances, such as one foot directly in front of the meter, with an unrealistic assumption that the transmitters operate at 100% duty cycle (at which point the mesh network would not function) the resulting exposure is less than the FCC MPE. When viewed in the context of a typical, realistic exposure distance of 10 feet, the RF fields are much smaller, about 0.008% for the end point meter and about 0.002% of MPE for the cell relay. Spatial averaging of these “spatial maximum” fields brings the estimated values down to approximately one-fourth of these magnitudes.

For potential exposure of occupants of a home equipped with a Smart Meter, interior RF fields would be expected to be at least ten times less intense simply due to the directional properties of the meter. When the attenuation afforded by a stucco home’s construction is included, a realistic value of the interior RF field would be about 0.023% of the MPE for an end point meter and about 0.065% for a cell relay meter. The WWAN operates at a far greater data throughput than the RF LAN within the mesh. Therefore, the duty cycle is correspondingly less for the cellular modem within the cell relay, despite the fact that it transmits all of the data collected from the relevant meters of its mesh network.

The most uncertainty in determining realistic time-averaged exposure from Smart Meters is associated with transmitter duty cycles. Hence, the most potentially useful avenue of future RF exposure assessment would include extensive statistical analyses of Smart Meter transmitter activity.

A detailed evaluation of possible RF fields produced by the Itron meters included in this study shows that regardless of duty cycle values for end point and cell relay meters, typical exposures that result from the operation of Smart Meters are very low and comply with scientifically based human exposure limits by a wide margin.

Section 2: Introduction and Background

As the electric utility industry in the United States moves toward implementing a “smart grid”, one of the key components consists of so-called Smart Meters. These new technology electric power meters represent a part of the advanced metering infrastructure (AMI) that provides for automatic meter reading (AMR) and sophisticated control over the use of electric energy by consumers in their homes and businesses. When AMI technology is fully implemented, an enhanced balancing of power distribution throughout the various electrical grids of the country will exist and utility customers will be able to, among other things, determine when certain electrically operated appliances may operate, based on time-of-day pricing of electricity. Such advanced capability requires close to real-time data acquisition on electric energy usage and such data requirements mean that the existing, traditional electric power meters that employ manual energy consumption readings, for example, once a month, can’t provide such timely data.

The modern technology of Smart Meters provides for an ability to almost instantly interrogate specific power meters as to electric energy usage. For the Smart Meters investigated in this study, this capability is accomplished via the use of data communications between the electric

utility company and individual power meters through the medium of radio signals. This report is focused on the radiofrequency (RF) aspects of Smart Meters and in particular, the strength of the transmitted RF fields that may be produced by the meters from a human exposure perspective.

Smart Meters as RF Sources

A wireless Smart Meter makes use of miniature, low power (typically less than one watt) radio transceivers inside the meter to wirelessly communicate with the electric utility company. The transceivers (transmitter and receiver) allow both transmission of data as well as reception of data and instructions from the utility. These transmitters are contained within the housing of the electric meter but are not necessarily visually obvious to an observer. Antennas used for the transmitters are commonly created as slots on the various printed circuit boards that constitute the electronic makeup of the meter. A common transmitter configuration of Smart Meters includes two or three transmitters in the meter. Figure 2-1 shows a Smart Meter with its digital display that is used to indicate electric energy usage.



Figure 2-1
Photo of Itron Smart Meter.

How Smart Meters are Deployed

Radio communication by Smart Meters makes use of wireless networks whereby each Smart Meter can both transmit and receive data to and from the electric utility company. The wireless network is configured as a so-called mesh network. Mesh networks are characterized by providing a means for routing data and instructions between nodes. A mesh network allows for continuous connections and reconfiguration around broken or blocked data paths by “hopping” from node to node until the destination is reached. In the context of how Smart Meters are deployed, end-point meters are installed throughout neighborhoods, replacing existing electromechanical meters. The transceivers⁴ within the

Smart Meters act as wireless routers, identifying and, then, connecting with available transmission paths between themselves and a cell relay meter that collects data from the many, various meters in the region.⁵ If communication between a given end-point meter and the associated cell relay cannot be achieved due to inadequate signal strength, an alternative end-point meter is used to establish communications onward toward the cell relay meter. In this sense, the mesh network is said to be self-healing in that should a particular transmission path becomes blocked, the network finds another way to get its data through the system. A simple example of this process could be that at some particular moment, a moving van travels down a street and temporarily blocks the previously preferred path from an end-point meter to the cell relay meter. In

⁴ The RF devices inside the Smart Meter function as transceivers since they both transmit and receive radio signals. In this report, the term transmitter is often used in place of transceiver since the primary characteristic of the meters of interest in this study is the meter’s ability to transmit radio signals.

this case, the data is rerouted via other end-point meters that act as alternative paths for the meter to initiate the data communications. This very powerful networking approach provides for good data communication reliability and can even allow communications for end-point meters that are outside the line-of-sight range to their cell relay meter. Additional end-point meters,

therefore, have the ability to expand the geographical extent of a network. Figure 2-2 illustrates the concept behind a wireless mesh network implemented for a Smart Meter equipped neighborhood. Each meter communicates either directly with the cell relay meter or via multiple “hops” of the signals through other meters.

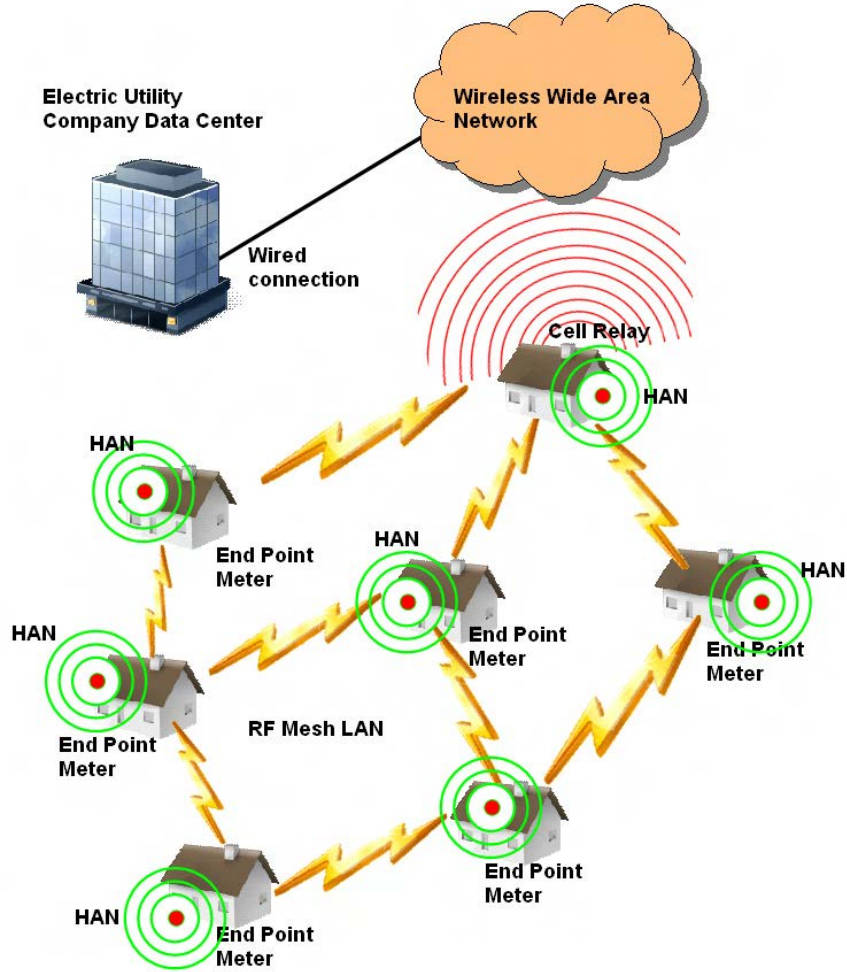


Figure 2-2
Simplistic illustrative diagram of an RF mesh network. Each end point also provides a Home Area Network (HAN) feature. The cell relay acts as a collector point for multiple meters distributed in a neighborhood and transmits received data onto a cellular wireless wide area network (WWAN).

⁵ Southern California Edison Electric Company is deploying Smart Meters as part of their SmartConnect™ program with one access point for approximately every 500 end-point meters on residences. In the case of San Diego Gas and Electric Company, each access point serves for data collection from approximately every 750 end-point meters.

For the Itron equipment that was the subject of this investigation, two separate transmitters are contained in the end-point meters. The wireless mesh network can be referred to as an RF LAN (radio frequency local area network). The Itron RF LAN operates in the 902-928 MHz license free band using spread spectrum transmitting technology. A second, separate transmitter that operates in the 2.4 GHz frequency range (2405 MHz to 2483 MHz) uses direct sequence spread spectrum technology that is referred to as a Zigbee radio⁶. This second transmitter is included for use with Home Area Networks (HANs) allowing customers, for example, to control certain electric appliances or systems within the home. When fully implemented, the customers will be able to connect wirelessly with the HAN radio and set times at which various appliances and/or electrical systems may operate, thereby taking

advantage of those times during which electricity rates are lowest.

The RF LAN provides data communications among the various end-point meters and an associated cell relay meter. Cell relays are end-point meters that contain yet a third transceiver that is designed for wireless connection to the cellular WWAN, i.e., relaying of the data received from the various end-point meters over a private connection to the electric utility company. The transceivers use the same frequency bands used by cell phones. Two different frequency bands are used by these cell-relay transceivers, either the 850 MHz band or the 1900 MHz band.⁷ Figure 2-3 shows a cell relay with the flexible dual band antenna located on the inside surface of the meter cover.



Figure 2-3
Cell relay meter with flexible, dual band (850 MHz and 1900 MHz) antenna affixed to interior surface of the meter cover.

⁶Zigbee is a name for a particular data communications protocol used in the HAN system.

⁷These frequency designations indicate the nominal frequencies used for the wireless WAN for Internet connectivity.

An important characteristic of this wireless mesh network technology is the fact that the RF emissions produced by Smart Meters, i.e., the signals that represent the data being transmitted, are not continuous but very intermittent in nature. For example, an electric utility company may interrogate the Smart Meters multiple number of times a day to acquire electric energy usage by the customer. While the Smart Meter may remain in stand-by in terms of transmissions at other times of the day, when an instruction is received to transmit energy consumption data, the meter transmits and proceeds to deliver the requested data to the cell relay meter. Hence, for the most part, Smart Meter transmissions are relatively infrequent during the day and may only consist of emissions for a few milliseconds during each of the interrogations throughout the day. This means that while the transceivers stand ready to transmit, there may be very little or no activity during most of the time. In addition to those periods during which data on electricity usage has been requested, however, Smart Meters must insure that they have a mesh network connection with at least one other Smart Meter so that, when necessary, it can deliver the data requested. Maintaining this connectivity within the mesh network requires periodic transmissions to alert the cell relay meter and other meters to its availability to be interrogated for data. So, Smart Meters spend part of their time in a so-called stand-by mode in which they issue beacon signals⁸ to signify their identity to other nodes of the network with the objective of establishing a connection with the network. These beacon signals last for very brief periods of, nominally, 7.5 milliseconds and occur at various intervals. Finally, there are other instances during which certain network maintenance activities are accomplished and during which, again, various, very short duration and intermittent emissions exist. The cumulative effect of these transmissions is that while the total time spent transmitting signals from a Smart Meter is generally very modest within a day, the signals are very intermittent. They are not continuous in the same sense as the signal received from an FM radio broadcast station but, rather, exist as very short duration signals scattered throughout the day. This intermittency contributes to the difficulty in accurately measuring the strength of the emissions.

In practice, homes in a Smart Meter equipped neighborhood will have end-point Smart Meters installed that communicate with a cell relay meter either directly or through the medium of multiple end-point meter radio signal hops. Approximately every 500th (in

the case of SCE) or 750th (in the case of SDG&E) residence may be equipped with a cell relay that not only handles the normal RF LAN communications but, also, relays these data onward, wirelessly, to the electric utility. All of these data communications proceed intermittently throughout each day.

The fact that the Itron Smart Meters studied here contain RF transmitters, albeit low power transmitters, means that relatively weak ambient RF fields exist in the vicinity of the meters. At the surface of the meter, the RF field strengths will be greatest with rapidly decreasing field strengths with increasing distance from the meter. While these low power transmitters cannot produce extremely intense RF fields, nonetheless, the issue of potential human exposure to these RF fields has, in some areas, become a question by the public.⁹ A concern expressed by some has been the potential for adverse health effects that might be caused by exposure to the weak RF fields produced by Smart Meters. This report documents an investigation of the characteristics of RF fields associated with the Itron wireless Smart Meter that can assist in a better understanding of possible public exposure to the RF emissions produced by Smart Meters. Throughout this report, the term Smart Meter is intended to refer to the wireless type represented by the Itron meters discussed in this report.

⁸ During the initial installation of an Itron Smart Meter, the meter enters a “discovery phase” in which it seeks to establish a link with the mesh network. During this discovery phase, beacon signals are emitted during approximately 3.5 second intervals until the meter becomes synchronized with the network or until a total time of about 6 minutes is reached after which beacons are emitted once about every 34 seconds until linked with the network or for up to 1½ hours. After this period, if a meter does not establish a link, it issues beacons once every hour during which it attempts to connect with the network. After 104 attempts, if still not linked with the network, the meter resets itself and begins the discovery sequence again. Once the meter becomes synchronized with the network, a beacon signal is emitted once every 94 seconds to 30 minutes depending on the level of other data traffic.

⁹ Newspaper accounts of public reaction to Smart Meters



Section 3: Objective of Investigation

The work described in this report was focused on understanding the physical characteristics of the RF fields that are produced by Smart Meters such that an informed conclusion can be made as to the magnitude of possible human RF exposure caused by the meters. In

this context, the objective of the work was to develop insight to the magnitude and spatial characteristics of Smart Meter RF fields including temporal aspects of the emissions that would allow a meaningful evaluation of possible exposures by reference to applicable RF human exposure limits.

Section 4: Technical Approach to Investigation

Characterizing RF fields produced by Smart Meters can be difficult. The intermittent nature of the emissions, addressed above, means that it is not a simple matter to simply bring instrumentation to an installed meter and be able to instantly detect the presence of the various emissions. The meter may or may not be in a transmit mode at the time when measurements are sought. Further, the spread spectrum characteristic of the emissions of the RF LAN and HAN transmitters leads to a further complication. For example, with the 900 MHz RF LAN transmitter, the emitted signal, at any particular instant in time, may be on any specific frequency within the 902 to 928 MHz band. When using narrow-band instrumentation, such as a frequency swept spectrum analyzer, the challenge is to have the analyzer on the specific frequency at the very instant in time that the emission is occurring to be able to measure its strength. Since the emissions are highly intermittent, this may take considerable time to insure that any such emissions have been captured by the instrumentation.

After careful consideration of the complexities associated with these kinds of measurements, it was decided that direct support of the testing by Itron, the manufacturer of the Smart Meter, could prove to be the most expedient approach to collecting the data useful to a complete exposure assessment study. As the manufacturer, Itron would have the knowledge and ability to control the Smart Meter to allow for meaningful measurements, avoiding the complications and uncertainties associated with working with already deployed meters.

Measurements at Itron

During the week of July 27, 2010, an extensive series of measurements was accomplished by the Principal Investigator at the Itron facility.

While at the Itron facility, detailed antenna pattern measurements were performed by the Principal Investigator on end point (Model CL200) and cell relay (Model C2SORD) meters. This included pattern measurements for the 900 MHz RF LAN transmitters in both the end point meter and as installed in a cell relay meter, pattern measurements of the 2.4 GHz

Zigbee transmitter in both an end point meter and a cell relay meter and pattern measurements of the cell relay cellular transceiver operating in both the 850 MHz and 1900 MHz bands.

In addition to pattern measurements, Itron provided access to their Smart Meter farm, an area of some 20 acres in which approximately 7000 Smart Meters are installed. The ability to access this field provided insight to the cumulative RF field environment of multiple Smart Meters in close proximity with one another, and whether aggregate exposure produced by a multiplicity of Smart Meters concentrated in one area raises exposure risks.

Measurements in residential locations

Beyond the on-site measurements performed at the Itron facility, additional Smart Meter measurements were performed in a variety of residential environments. Using two Smart Meters that had been specifically programmed by Itron to operate continuously, to facilitate the measurements of field strength, measurements were performed at two residences in Downey, CA. These specially programmed meters were temporarily installed in the electrical service panel at each home and RF measurements were accomplished in the near vicinity of the meter and throughout the interior of each home. This procedure allowed for characterizing the RF fields that might exist inside of residences equipped with a Smart Meter. As a part of the residential measurements, a brief evaluation of the insertion loss afforded by three different metallic meshes, similar to what might be used in the construction of residential stucco walls, was conducted.

In addition to residence specific measurements with pre-programmed meters, RF fields were also measured adjacent to two separate apartment buildings wherein groups of 9 and 11 Smart Meters were grouped tightly together. Finally, a general area survey was conducted by driving throughout an established route within Downey, CA representative of a Smart Meter deployed neighborhood to form general observations of the ability to detect the presence of Smart Meter emissions. The residential measurements aspect of the work reported

here was concluded with a driving survey through Santa Monica, CA within which, at the time, there had been no deployment of Smart Meters.

Measurements in Colville, WA

Separate from the measurements at the Itron facility and the residential measurements in Downey, California, some limited measurements were conducted at the author's location in Colville, WA. These measurements included an evaluation of the comparative readings of RF field obtained by both the broadband field probe and the spectrum analyzer (selective radiation meter) used in the project measurements as well as an evaluation of the attenuation effect on Smart Meter signal propagation through a simulated, residential stucco wall.

Section 5: Transmitter Powers

A crucial aspect of any RF source, relative to its ability to produce RF fields, is the power of the transmitter. At the beginning of interactions with Itron, measurement data were sought on transmitter power levels. Historically, Itron has determined the power level of every transmitter used for the 900 MHz RF LAN and the 2.4 GHz Zigbee radios. These are transmitter devices on Itron manufactured printed circuit boards. All of the transmitters used in the Itron Smart Meters

operate with low power, regardless of the frequency band used, nominally one watt or less. The 900 MHz RF LAN transmitter operates at a nominal power of 24 dBm (251 mW). Using Itron test data obtained from power measurements on a sample of 200,000 RF LAN transmitters, Figure 5-1 illustrates the accumulative fraction of transmitters having output powers across a range of power.

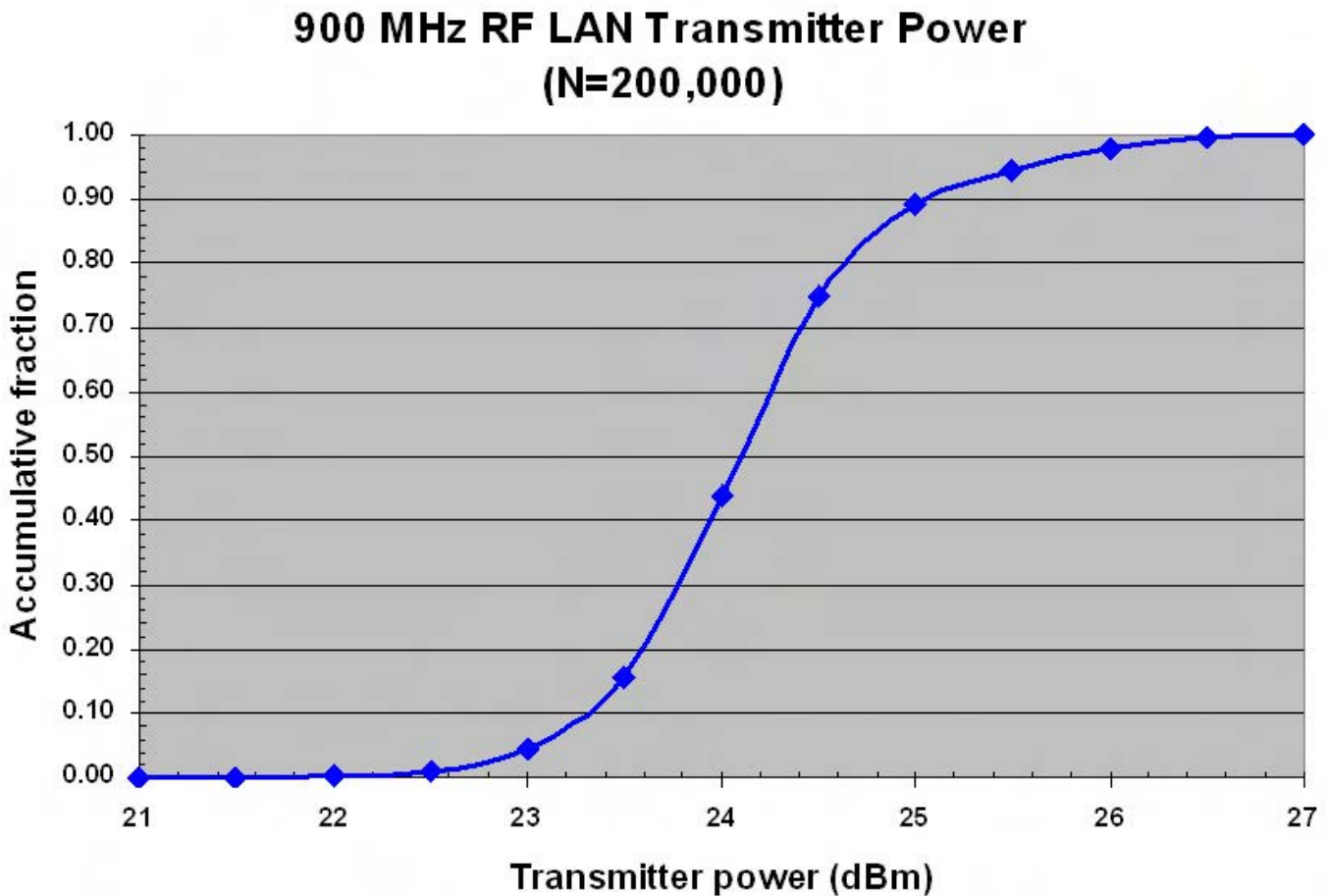


Figure 5-1
Accumulative fraction of 900 MHz RF LAN transmitter output power vs. transmitter power for a sample of 200,000 units. The median transmitter power is approximately 24.1 dBm (257 mW).

Based on a separate sample of 65,536 transmitters, used in end point meters, an average power output of 23.95 dBm (248 mW) was obtained with a standard deviation of 0.695 dBm. Using these data, the 95% confidence interval would correspond to a range of transmitter power from 22.6 dBm (182 mW) to 25.3 dBm (339 mW) and the 99% confidence interval would correspond to a power range from 22.2 dBm (166 mW) to 25.7 dBm (372 mW).

Using the 200,000 transmitter sample, the median power level corresponds to approximately 24.1 dBm (257). The number of transmitters with power values in selected ranges is shown in Figure 5-2. The mode of transmitter power is approximately 24.5 dBm (282 mW).

Number of 900 MHz RF LAN Transmitters with Powers in Selected Ranges (N=200,000)

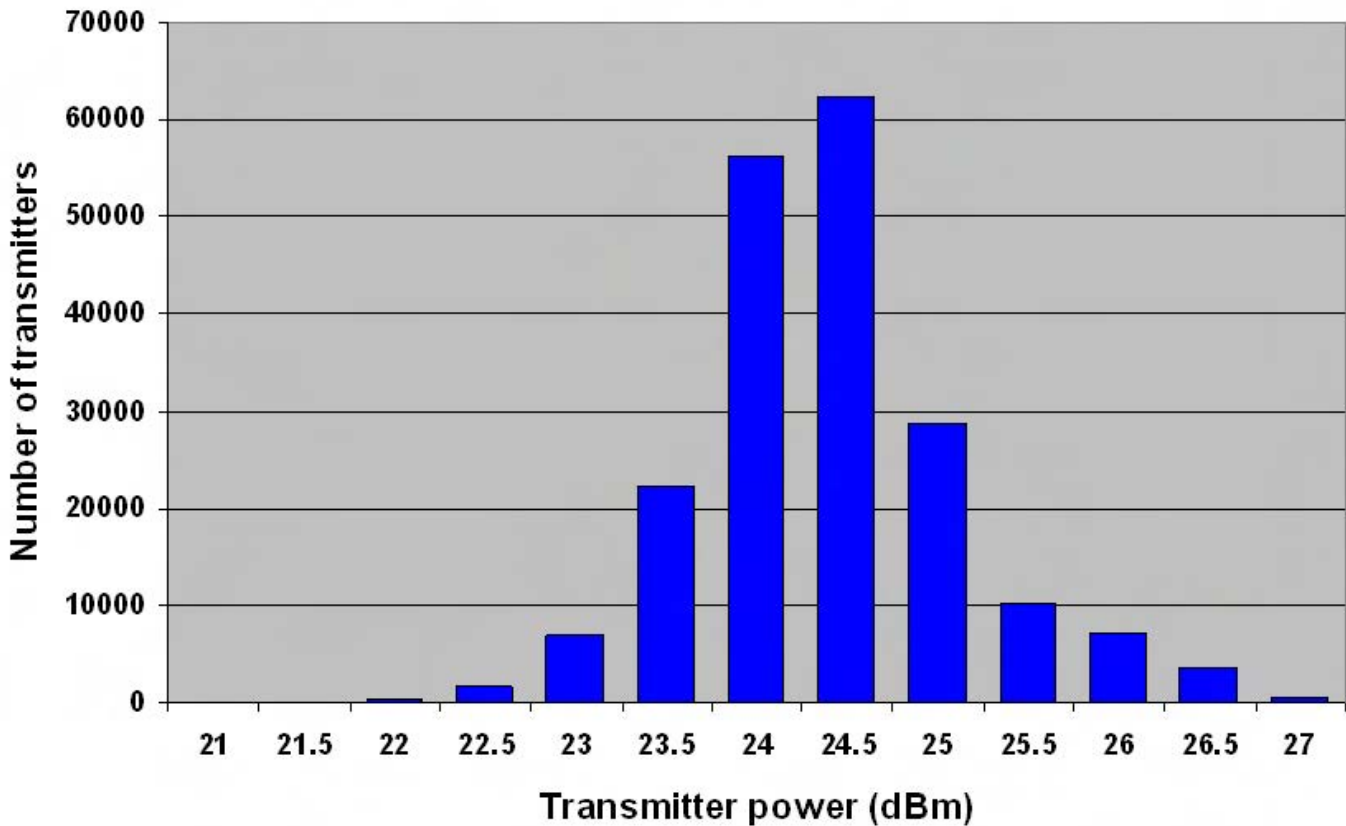


Figure 5-2
Number of 900 MHz RF LAN transmitters with powers within selected ranges. The transmitter power mode is approximately 24.5 dBm (282 mW).

These statistical data on the 900 MHz RF LAN transmitter powers indicate that the most likely power is 24.5 dBm (282 mW); an upper value of 26.0 dBm (398 mW), a value 41% greater than the most likely power, would include 99% of all transmitters.

mean value was found to be 18.31 dBm (67.6 mW) with a standard deviation of 0.76 dBm. This distribution would represent a 95% confidence interval of transmitter power from 16.8 dBm (47.9 mW) to 19.8 dBm (95.5 mW) and the 99% confidence interval would correspond to a power range from 16.4 dBm (43.7 mW) to 20.3 dBm (107.2 mW).

In the case of the 2.4 GHz Zigbee transmitters, in a sample of 65,535 units used in end point meters, the

Figure 5-3 shows the accumulative fraction of transmitters having output powers across a range of power. Figure 8 illustrates the number of 2.4 GHz

transmitters with powers within selected ranges. The transmitter power mode is approximately 18.5 dBm (70.8 mW).

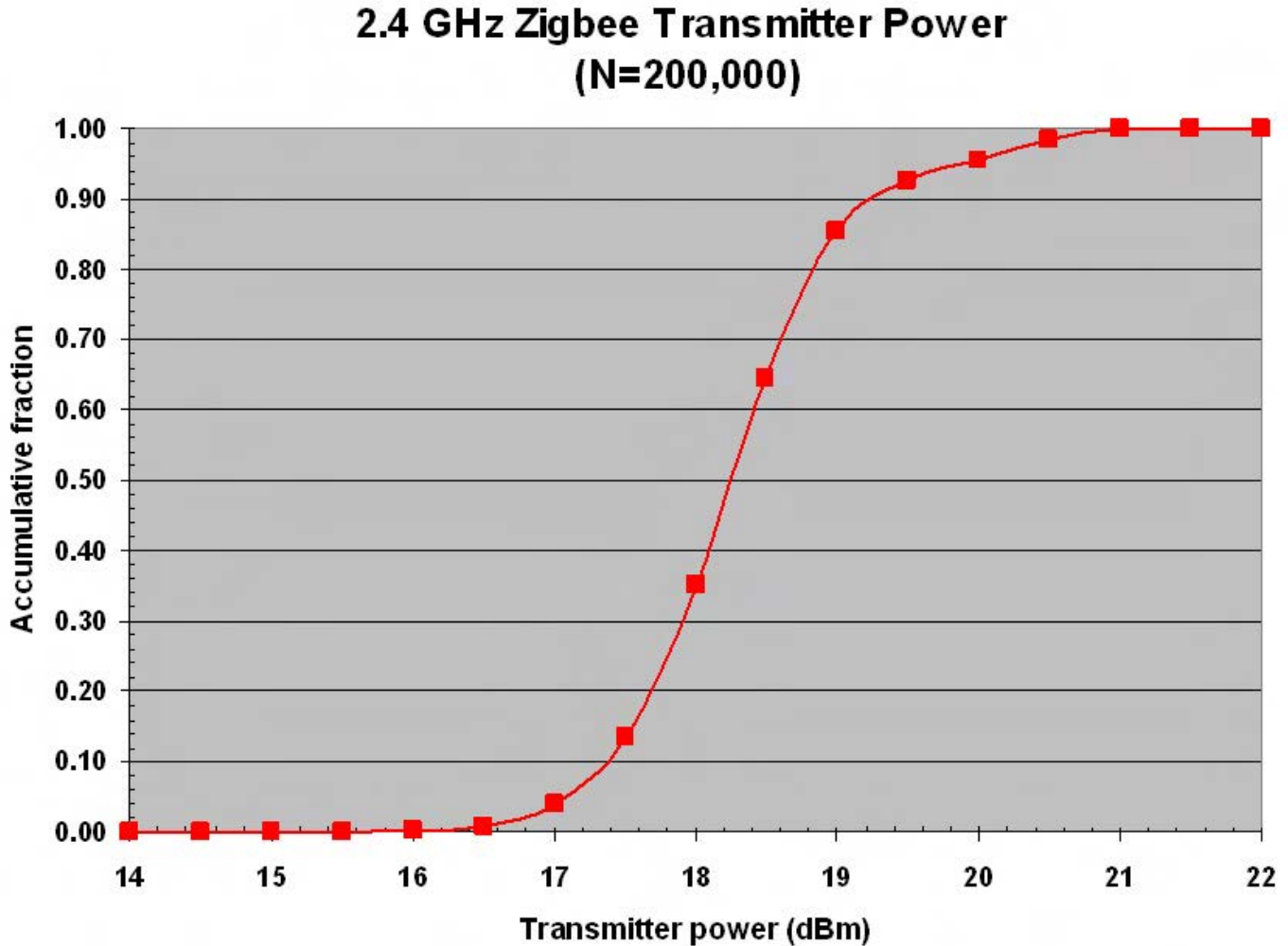


Figure 5-3
Accumulative fraction of 2.4 GHz Zigbee transmitter output power vs. transmitter power for a sample of 200,000 units. The median transmitter power is approximately 18.2 dBm (66.1 mW).

These statistical data on the 2.4 GHz Zigbee transmitter powers indicate that the most likely power is 18.5 dBm (70.8 mW); an upper value of 20.6 dBm (114.8 mW), a value 62% greater than the most likely power, would include 99% of all transmitters.

Cell relay meters contain the additional transceiver used for cellular WWAN connectivity in either the 850 MHz cellular band or 1900 MHz PCS band (personal

communications service). Because these transceiver boards are produced by a different company and the units are specified to operate with specific powers and the fact that these units are separately certified by independent test labs for compliance with those specifications, Itron does not carry out additional power measurements. The transceivers, produced by Sierra Wireless operate with the following maximum powers:

Table 5-1
Sierra Wireless Transceivers Operation Maximum Powers

	GSM Modem Model MC8790 FCC ID: N7NMC8790	CDMA Modem Model MC5725 FCC ID: N7N- MC5725
Frequency Band (MHz)	Maximum power output (dBm) (mW)	
850	31.8 (1,514)	25.13 (326)
1900	28.7 (741)	24.84 (305)

Cell relays operate at the highest power of any of the meters due to their cellular/PCS modems but, similar to cellular telephones, the output power of the cellular modem is dynamically controlled by the applicable WWAN base station. This means that the actual operating power of the cellular radio in a cell relay will, generally, be less than the maximum power but will be

determined by the signal strength it produces at whatever base station it is communicating with. Only one of the two modems would be active in a given deployment of Smart Meters in a neighborhood; the modem of choice is determined by the cellular wireless network service available and selected by the electric utility company.

Number of 2.4 GHz Zigbee Transmitters with Powers in Selected Ranges (N=200,000)

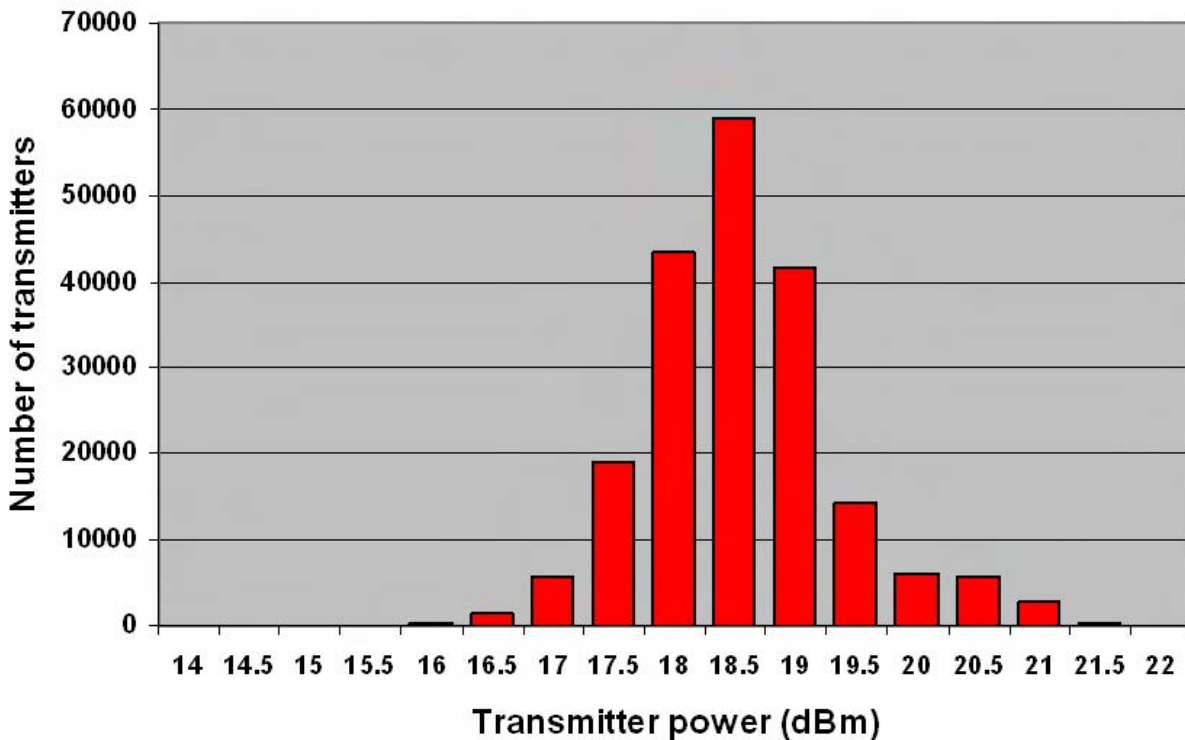


Figure 5-4
Number of 2.4 GHz Zigbee transmitters with powers within selected ranges. The transmitter power mode is approximately 18.5 dBm (70.8 mW).



Section 6: The Measurement Challenge Presented by Smart Meters

The difficulty of accurate RF field measurements near Smart Meters was discussed earlier. Low transmitted power levels in conjunction with intermittent emissions place considerable constraints on the measurement process. While a broadband measurement probe can eliminate the problem of the RF emissions occurring randomly on many different frequencies within the band, the relatively low sensitivity of broadband instruments places considerable restrictions on performing field strength measurements except within extremely close proximity of the meter. Intermittent emissions with very short duration, even if detectable, mean that it is difficult to observe when a transmission occurred. Generally, the desired measure of RF fields, from a human exposure perspective, is a measure of the average (root mean square - rms) value of the field strength or incident power density. The ratio of the average power density to the peak power density, for most Smart Meters is such that trying to measure the average field magnitude for a normally operating meter is very challenging. This can change if there exists a large aggregation of Smart Meters such that with their random on-off transmissions, much greater opportunity to “see” the emissions is possible.

Because of the rapid changes of frequency associated with the spread spectrum nature of the RF LAN and Zigbee radios in the Itron Smart Meters, an alternative

approach is used to facilitate any antenna pattern and field measurements. This approach involves programming the relevant radios to transmit continuously, rather than their normal intermittent operation, and to transmit on a specific frequency within the relevant band as opposed to hopping across more than 50 channels within the 900 MHz band. Through this programming of the radios, the average signal level is now at its maximum, making it much easier to detect the RF field, and the fact that the emitted signal is now fixed on a specific and known frequency allows for ready confirmation that the measurement is of the intended signal. Since measurements under this scenario will indicate the peak value of RF field, other information is required to translate the peak field into what the equivalent average field would be. This requires a knowledge of the duty cycle of the emissions from the Smart Meter. The duty cycle can be thought of as the ratio of the amount of time that the transmitter is transmitting its signal to the total observation period. For example, if the Smart Meter were to typically transmit as much as 10 seconds during an hour (3600 seconds), the duty cycle would be 0.28%. In other words, the time-averaged power density of the RF field would be just 0.28% of the peak power density measured. The issue of Smart Meter duty cycles will be addressed later in this report.

Section 7: Measurement Methods and Instrumentation

Several different methods were applied during the course of this investigation to measure Smart Meter RF fields. These included detailed antenna radiation pattern measurements of both end point and cell relay Smart Meters in the Itron anechoic chamber facility, survey type measurements used at close and far distances from single meters and groups of meters, such as in the Itron meter farm and at residences in California, drive-through type surveys in neighborhoods in which Smart Meters had been deployed, instrumentation comparison measurements using special Smart Meters programmed for the occasion and measurements of the attenuation provided by various forms of metal lath (commonly used in construction of stucco homes).

In the Itron facility, pattern measurements were

accomplished using a sophisticated system that permits orientation of a Smart Meter in 15 degree increments in all possible directions using a dual axis rotating system as shown in Figure 7-1. Associated instrumentation included a spectrum analyzer (Agilent Model E4405B (SN US40240612)) as the detector connected to a sense antenna (ETS Model 3115 double ridge guide horn (SN 0005-6166)) inside the anechoic chamber with instrumentation interfaced with a systems controller (Sunol Sciences Model SC104V). Data acquisition and analysis software provided for analysis and graphic display of measured antenna patterns (MI-Technologies Model MI-3000 workstation). Figure 7-2 shows the interior of the anechoic chamber with the reception horn antenna used to receive the signal emitted by the meter.

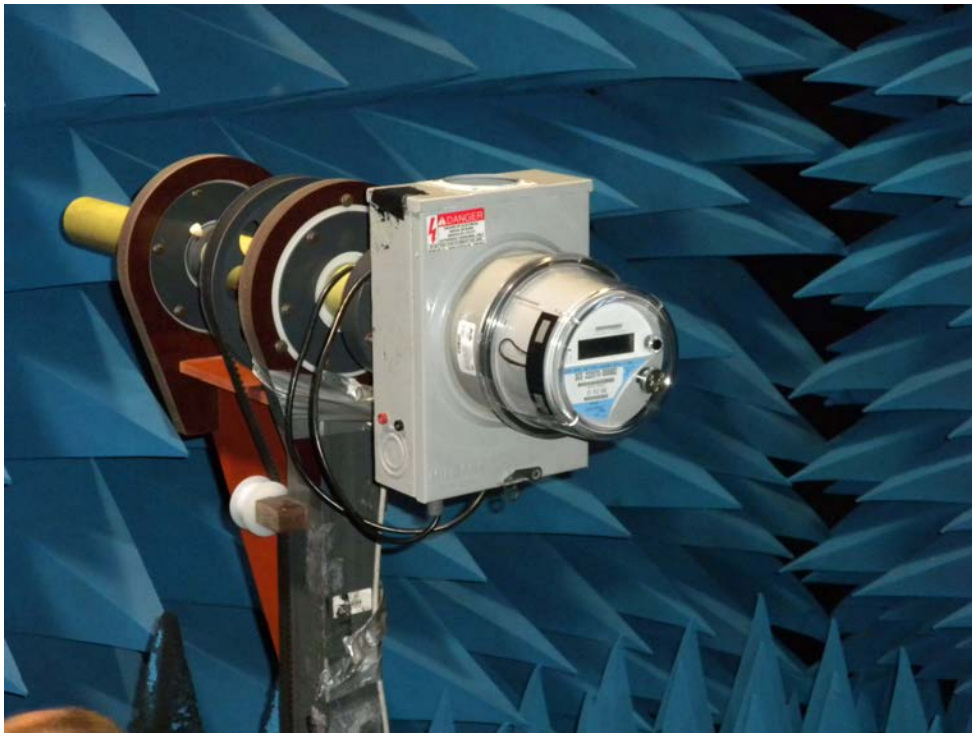
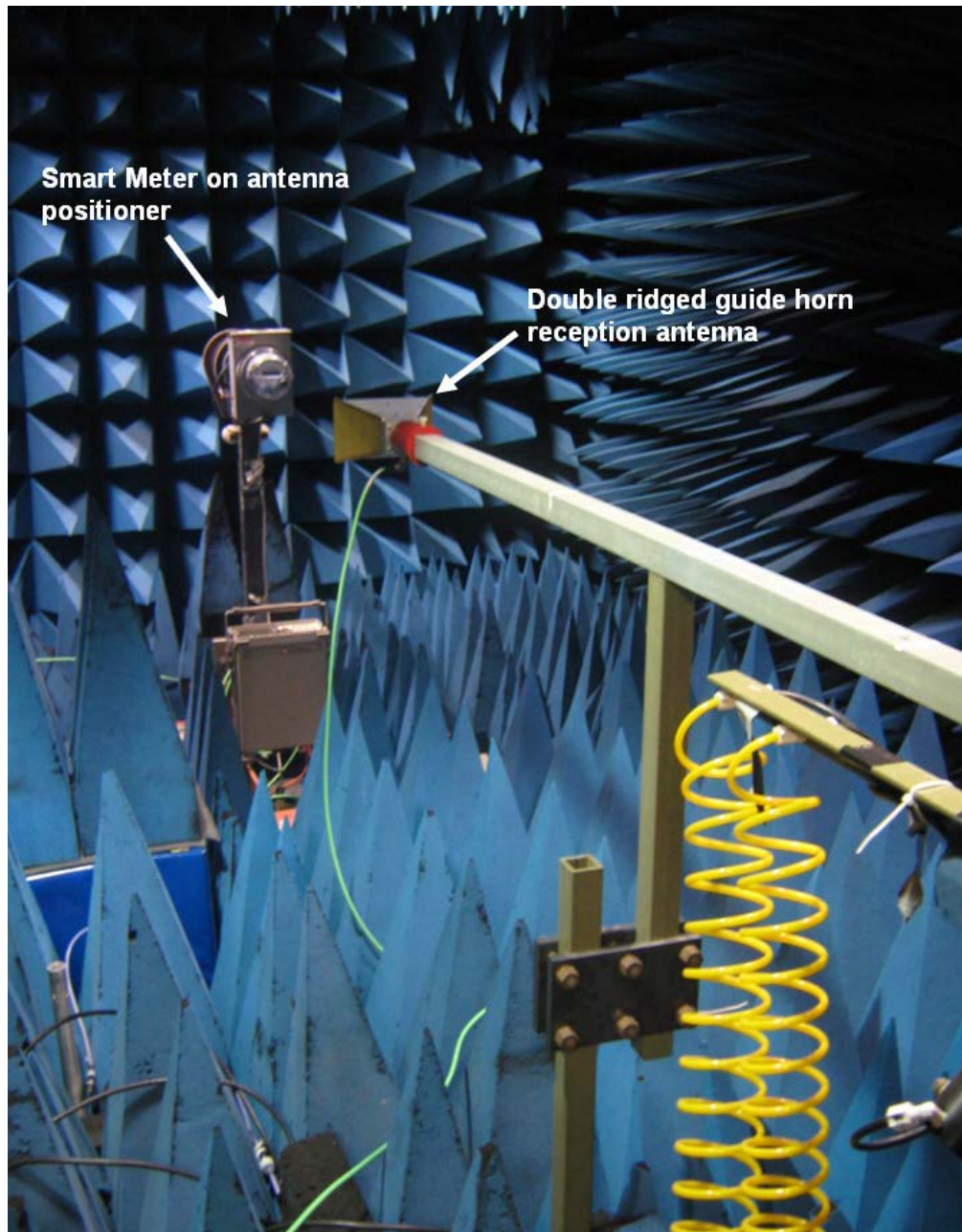


Figure 7-1
Close up view of dual axis antenna positioner system used to obtain antenna patterns of Smart Meter transmitters.



*Figure 7-2
Interior of anechoic chamber showing reception horn antenna with Smart Meter on antenna positioner in background.
During pattern measurements, the spectrum analyzer shown below the Smart Meter is removed.*

Figure 7-3 shows the measurement instrumentation used for collecting and analyzing antenna pattern data. Smart Meters, when measured in the anechoic chamber, were installed in a metal meter box (Milbank Type 3R meter enclosure) supported on a dual axis rotator system

(see Figure 7-1 for a close-up photo of the dual axis rotator system and meter box). Calibration signals could be injected into the spectrum analyzer with a separate signal generator (Agilent Model E4432B).

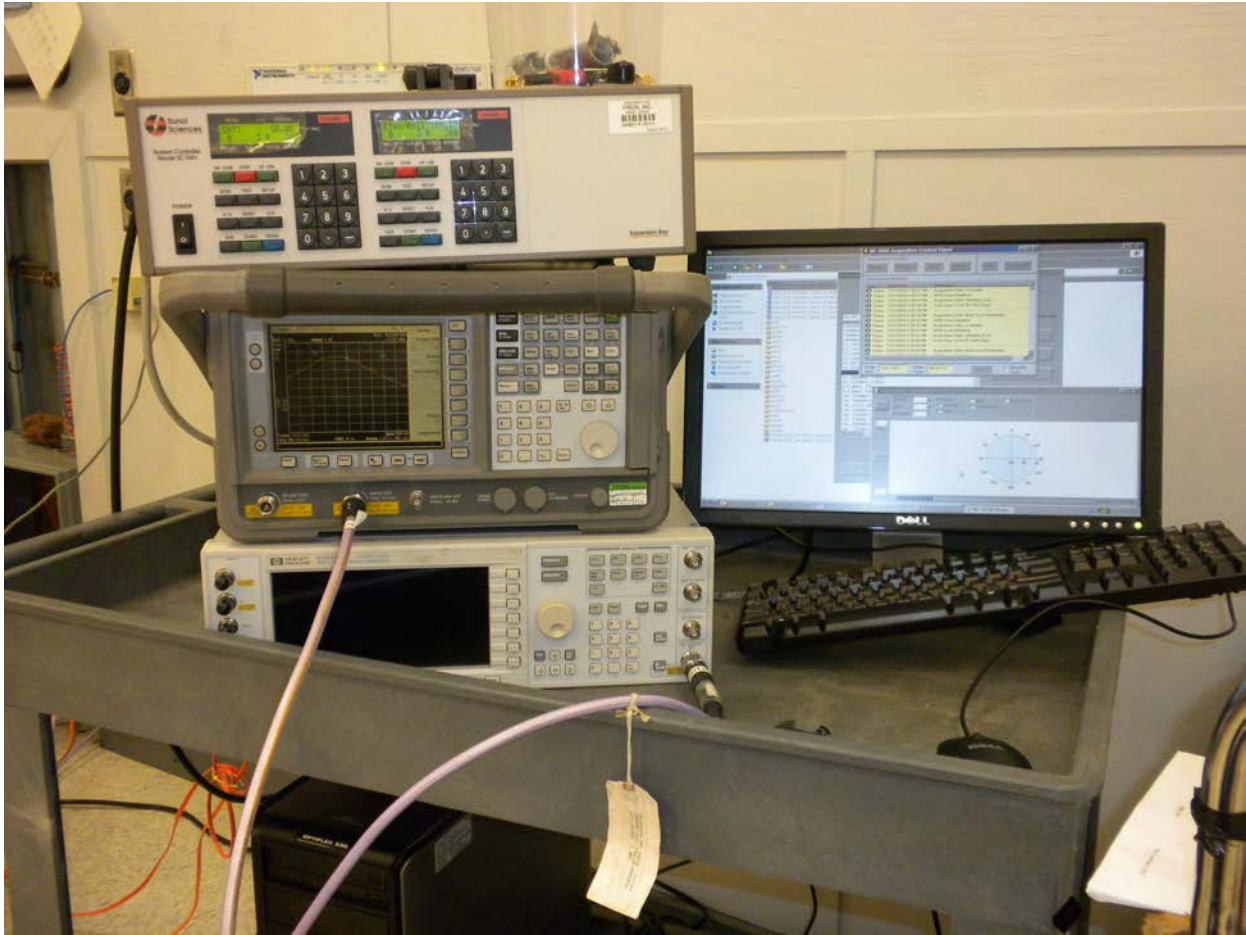


Figure 7-3
Instrumentation system for acquiring antenna pattern data.

All Smart Meter pattern measurements were performed in the Itron anechoic chamber. The interior of the shielded (0.2" metal) chamber measures 16 feet wide, 25 feet long and 12 feet high and is lined with anechoic material. The anechoic nature of the chamber provides for a very low level of reflection of RF fields from the floor, walls and ceiling, minimizing any perturbation that such reflections could have on the measured pattern of the Smart Meter transmitter.

Other instrumentation used in field measurements included use of a broadband, frequency conformal, isotropic, electric field probe (Narda Model B8742D, SN 03002) used with a readout meter (Narda Model 8715, SN 01028). This probe exhibits a frequency shaped response that follows the shape of the maximum permissible exposure (MPE) limit established by the Federal Communications Commission (FCC).¹⁰ Such a

shaped response allows the meter to read out directly in terms of a percentage of the MPE, regardless of the frequency or frequencies of the incident RF field(s). The B8742D is designed for response across the spectrum from 300 kHz to 3 GHz and is specified to yield reliable readings as low as 0.6% of the FCC general public MPE. Under optimum conditions (low ambient RF noise and a thermally stable environment), the meter can be used to read even lower RF field levels. The broadband probe consists of three, small mutually orthogonal elements combined electrically to yield an output on the meter that represents the resultant RF field magnitude. The isotropic nature of the probe

¹⁰ FCC rules

produces an output that is independent of the orientation of the probe within the field being measured, thereby accounting for all field components of any polarization. The meter and probe, shown in Figure 7-4, had been calibrated at the factory within the

previous twelve months of its application in this project as recommended by the manufacturer. Appendix A provides the calibration certificates for the meter and probe.



Figure 7-4
Frequency shaped, isotropic, electric field probe and meter (Narda B8742D and Narda 8715 meter).

Besides the use of the broadband meter, a special spectrum analyzer system was also used. This instrument (Narda Model SRM-3006 selective radiation meter, SN A-0077) combines a spectrum analyzer with an isotropic antenna (Narda three-axis-antenna, E-Field, SN H-0100) such that spectral scans may be performed with the resultant RF field value displayed on the analyzer's screen. The resultant field value is represented as the vector sum of the three orthogonal polarization components of the field, similar to how the broadband probe works. Built into the spectrum analyzer is a digital representation of the frequency dependence of the FCC MPE values. The

system automatically corrects the measured fields for this frequency dependence so that the indicated spectrum observed on its screen is expressed, again, as a percentage of the FCC MPE. Further, the instrument can be instructed to integrate across a desired frequency range so that the overall, equivalent RF field as a percentage of the MPE can be displayed. Since this instrument can also display both the peak and average value of the RF fields being measured, it can provide insight to the duty cycle of the Smart Meter emissions. The SRM-3006 is shown in Figure 7-5. Calibration certificates for the SRM-3006 are provided in Appendix A.



Figure 7-5
Selective radiation meter (Narda Model SRM-3006).

One other piece of equipment used in the project is a tiny band-specific spectrum analyzer designed for the 902-928 MHz band. This analyzer (Metageek Model Wi-Spy 900X) is a USB based instrument that is connected to a portable computer such as a laptop or notebook computer.¹¹ The instrument, shown in Figure 7-6, is designed for investigating RF signals in the 900 MHz range from an interference perspective. A similar instrument is available for measurements in the 2.4 GHz wireless network band. The use of this device was aimed at exploring its potential utility in measurement of Smart Meter emissions in view of its low cost. An associated software program (Chanalyzer version 3.4) creates displays of the measured spectrum and provides for analysis of the measured RF signals. Using the

¹¹ Metageek, LLC, 423 N. Ancestor Place, Suite 180, Boise, ID 83704 www.metageek.net.

software, for example, allows for retention of the maximum detected field at any given moment as well as the average value over whatever observation period is desired. A unique aspect of this spectrum analyzer is that, in conjunction with the connected computer, it records the result of each individual spectrum scan on the computer's hard disc drive. These recorded spectra can then be "replayed" at a later time to observe what the spectrum looked like at any previous point in time. Further, the stored, accumulated scans can be converted to a spreadsheet format for subsequent, custom analysis of the measurement data. Figure 7-6 shows a yagi antenna that was used with the Wi-Spy analyzer to achieve a higher level of system sensitivity and provide directionality for identifying the location of specific RF sources. The spectrum displayed on the notebook computer in Figure 7-6 is that acquired in the Itron laboratory with a Smart Meter operating on a fixed

frequency with lower level 900 MHz signals in the background from other meters in the vicinity.

The Wi-Spy unit was used for measurements of the insertion loss of a simulated wall in the Colville measurements. It was also employed in measurements

of Smart Meter transmission activity in California. The Wi-Spy 900X has a detection sensitivity of approximately -105 dBm in the 900 MHz band, an amazing achievement for a device costing less than \$200US.

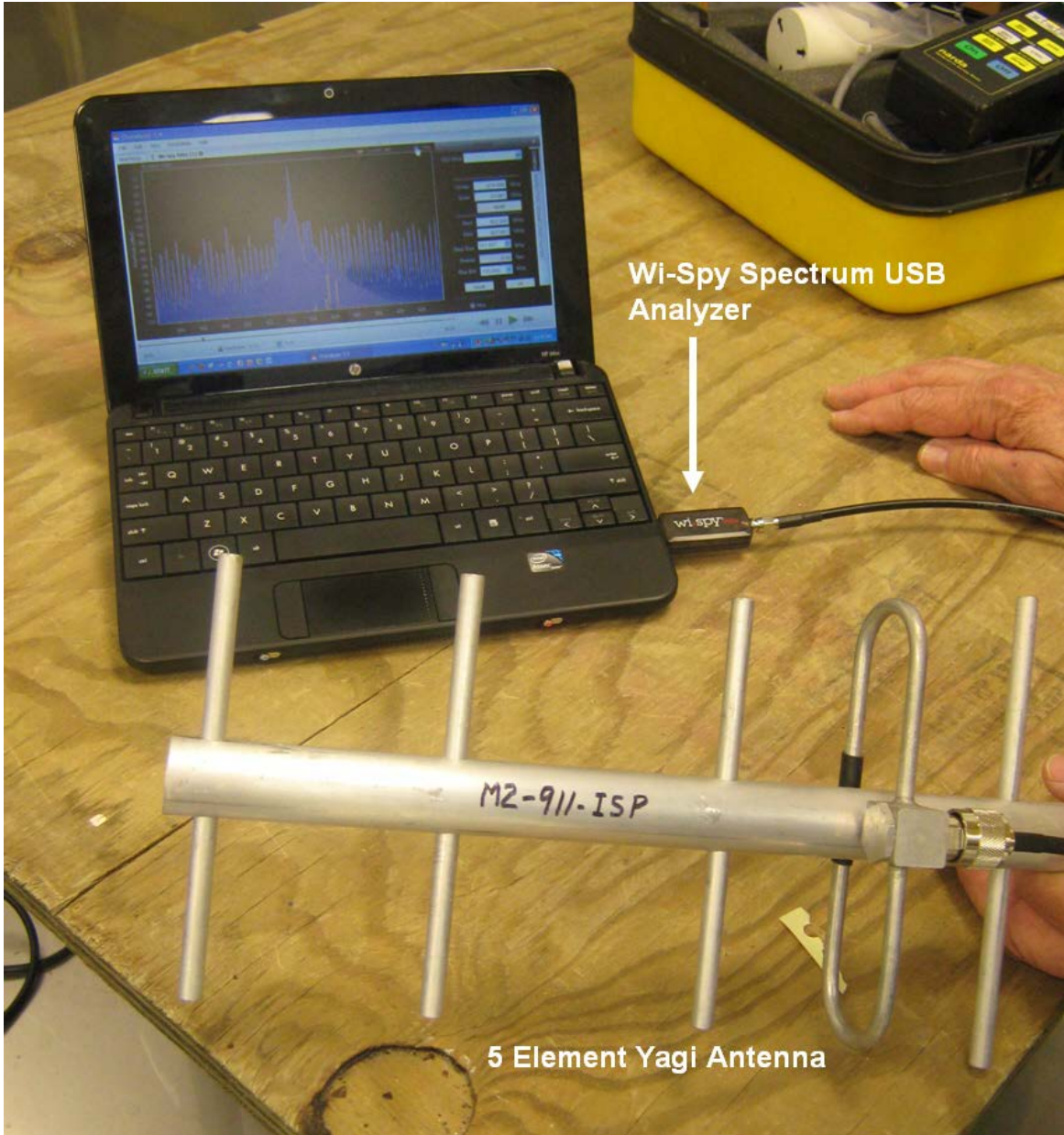


Figure 7-6
Wi-Spy USB spectrum analyzer connected to a notebook computer running software to operate the analyzer (Chanalyzer version 3.4) and an external yagi antenna.

Section 8: Laboratory Pattern Measurements

The radiation patterns for each antenna contained in the end point and access point Smart Meters were measured in the Itron anechoic chamber. This represented a total of six sets of patterns including: 900 MHz RF LAN in an end point meter and in a cell relay meter (access point), 2.4 GHz Zigbee radio in an end point meter and in a cell relay meter and the pattern of a cell relay meter using the GSM band (850 MHz) or the PCS band (1900 MHz). The 900 MHz RF LAN and 2.4 GHz Zigbee radios each have their own quarter-wave slot antennas that are etched on printed circuit boards inside the meter. The 900 MHz antenna is horizontal and located approximately 2.1 cm behind the front surface of the meter enclosure. When contained in a cell relay, the 900 MHz antenna is located approximately 15.1 cm from the front surface of the metal meter box in which it may be installed. The 2.4 GHz antenna is vertically oriented on its circuit board and is located approximately 2.5 cm behind the front surface of the meter enclosure; when installed in a cell relay, the antenna is approximately 14.7 cm in front of the metal meter box. A flexible dual band antenna is used for the cell relay function and it is adhered to the interior surface of the clear meter enclosure at a nominal nine o'clock position. The dual band antenna (AMR Under Glass Mount Antenna produced by WP Wireless)¹², shown in Figure 2-3, is approximately 2.5 cm wide with the front edge located approximately 0.4 cm from the front surface of the meter enclosure.

A feature of the Itron antenna pattern analysis system is the determination of the maximum isotropic effective radiated power (EIRP) for a particular amount of power being delivered to the antenna by the relevant transmitter. Because the Itron 900 MHz and 2.4 GHz transmitters are not designed for continuous operation (normal application in the Itron Smart Meters corresponds to a rather low duty cycle), all pattern measurements were obtained with the transmitters programmed to operate at a power level lower than their normal, maximum average power. This methodology

helped avoid a slight decrease in transmitter output power after prolonged periods of transmitter activity during which the transmitters can heat up, insuring that the measured data was representative of the peak power that is achieved under normal operating conditions. Knowing the EIRP of each transmitter system in a meter, relative to the particular transmitter output power during the test, allowed subsequent RF field calculations to be scaled to actual maximum transmitter power levels. Acquiring a complete three dimensional antenna pattern requires almost two hours of measurement. The meter is repositioned every 15 degrees in both azimuth and elevation and measurements are made of both the horizontal and vertical polarization components of the emitted field. Through examination of the entire data set after the pattern has been measured, the single maximum value of field is converted to EIRP. This single value was used in most of the subsequent analyses in this report since it represents the EIRP that is associated with the strongest RF fields in the vicinity of the Smart Meter.

Measured radiation patterns for the 900 MHz RF LAN transmitter configured in an end point meter, Model CL200 (Itron #62_305_199, SCE #222010-273721) are shown in Figures 8-1 – 8-4. In these figures, a drawing representing the Smart Meter as mounted in a meter box is shown for reference to the meter orientation. These patterns were determined at near-mid-band frequency of 914.8 MHz. Figure 8-1 represents the azimuth plane pattern of the 900 MHz emissions. This particular pattern is for a horizontal plane running through the meter and as viewed from the bottom of the meter. The pattern data are referenced to 0 dB at the point of maximum field, close to 0°, with each dotted line, in this particular pattern, representing a 20 dB variation in signal level. Three curves are shown in the figure; one representing the pattern for the horizontally polarized component of the field (the black curve), one representing the vertical polarization component of the field (the blue curve) and one representing the total field produced by the composite sum of both the horizontal and vertical components (the red curve). From an exposure

¹² WP Wireless - A Division of World Products Inc., 19654 Eight Street East, Sonoma, CA 95476 www.wp-wireless.com.

assessment perspective, the total pattern is of more relevance for evaluating RF fields relative to human exposure limits. The pattern shows a reduction of radiated field, generally, to the rear of the meter being between 10 and 20 dB less than the values to the front of the meter. A colorized picture in Figure 8-4 illustrates the azimuth plane representation of total EIRP of the 900 MHz RF LAN transmitter.

Elevation plane patterns for the 900 MHz RF LAN transmitter are shown in Figures 8-3 and 8-4 with

Figure 8-3 representing the patterns of the horizontal and vertical polarization components and the composite field (total), similar to the figure for the azimuth plane. Figure 8-4 illustrates the elevation plane representation of total EIRP of the 900 MHz RF LAN transmitter in an end point meter. In the elevation plane pattern, it can be seen that the maximum field is directed slightly upwards at about 30° rather than perfectly straight out toward the front of the meter.

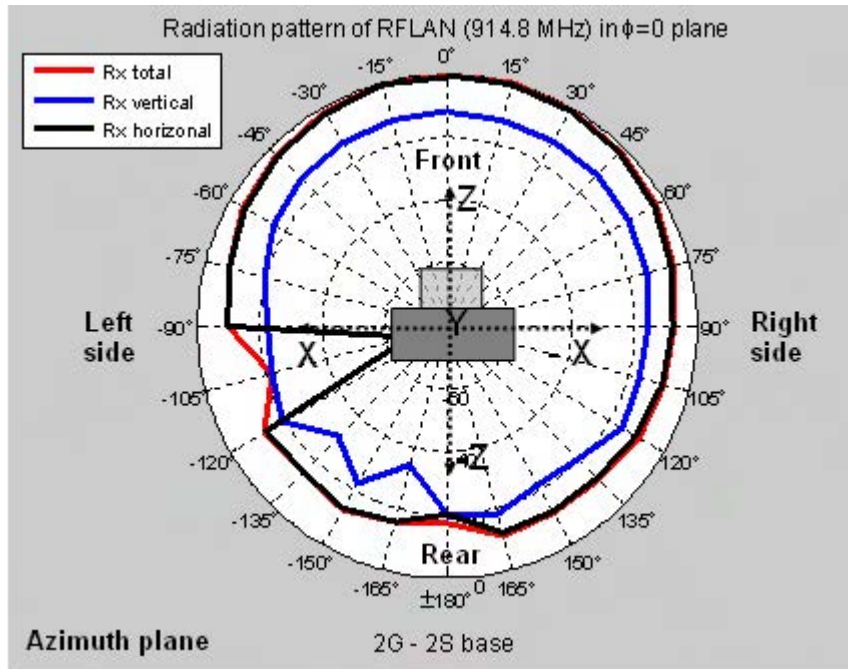


Figure 8-1
 Azimuth plane pattern of the 900 MHz RF LAN transmitter configured in an end point meter showing the horizontal, vertical and total pattern as viewed from bottom of meter. The scale is in dB with the maximum field at the outer edge of the pattern circle.

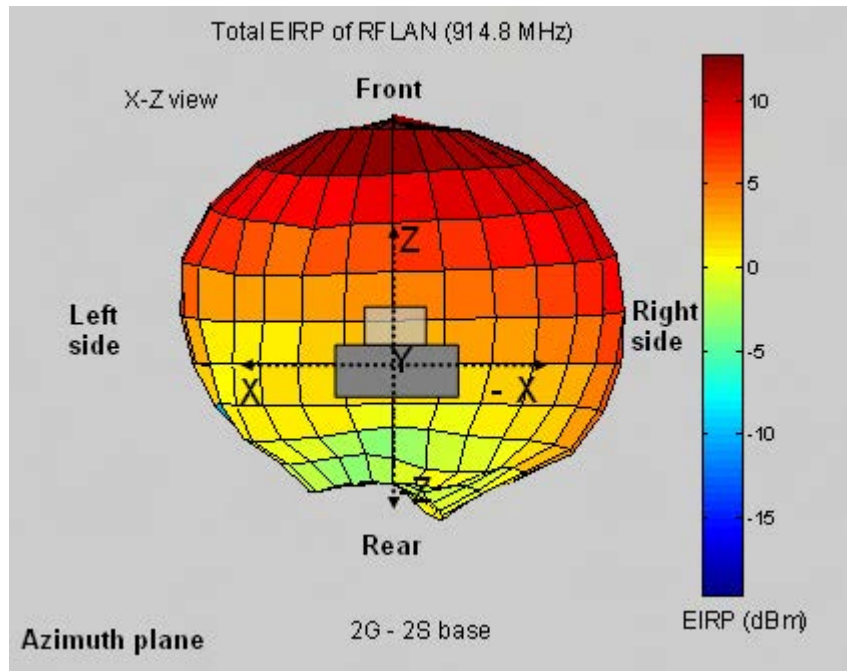


Figure 8-2
Azimuth plane view of the total EIRP of the 900 MHz RF LAN transmitter configured in an end point meter.

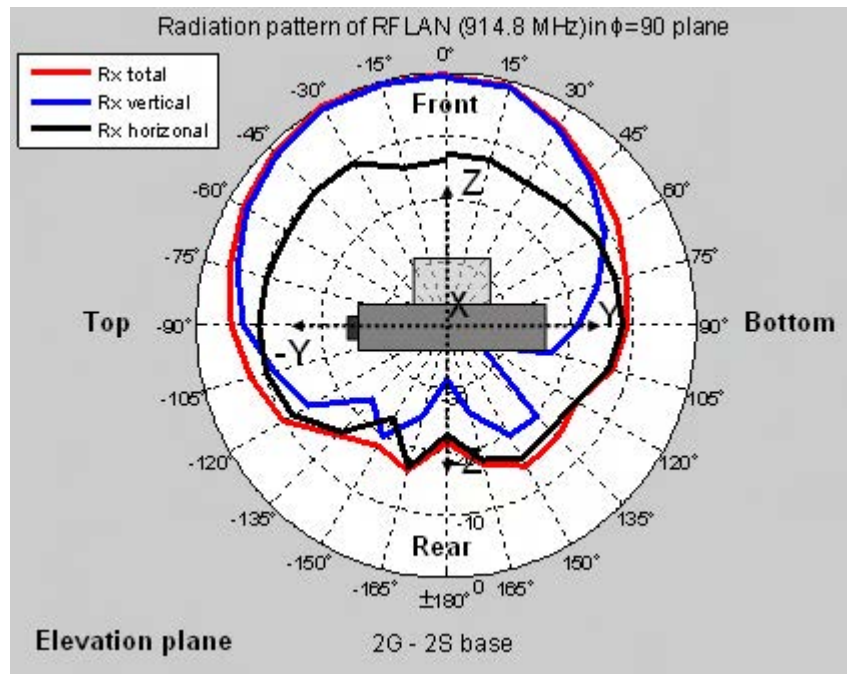


Figure 8-3
Elevation plane pattern of the 900 MHz RF LAN transmitter in an end point meter showing the horizontal, vertical and total pattern. The scale is in dB with the maximum field at the outer edge of the pattern circle.

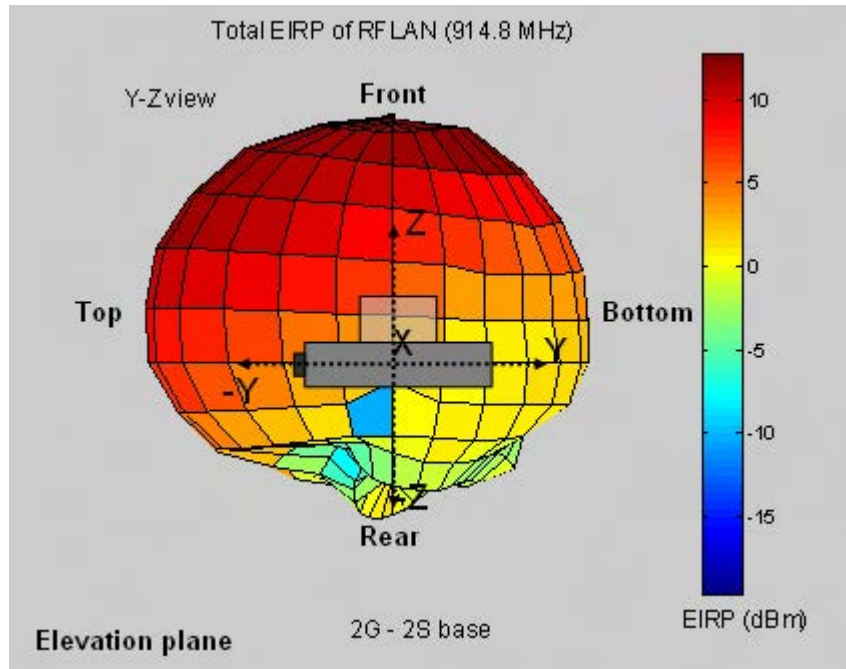


Figure 8-4
Elevation plane view of the total EIRP of the 900 MHz RF LAN transmitter in an end point meter.

Similar to the pattern measurements for the 900 MHz RF LAN transmitter in an end point meter, measured radiation patterns for the 900 MHz RF LAN transmitter configured in a cell relay meter, Model C2SORD, (Itron #661_912_646, SCE #222070-000082) are shown in Figures 8-5 – 8-8. The rationale behind documenting the pattern of the same transmitter and antenna type, but when installed in a cell relay, was to examine any differences that might be apparent that could be caused by the slightly different distance that the antenna would be relative to the front of the metal meter box.

Figures 8-5 and 8-6 represent the azimuth plane patterns of the 900 MHz cell relay emissions and total EIRP respectively. The pattern in Figure 8-5 shows a reduction of radiated field, generally, to the rear of the meter being between 10 and 20 dB less than the values to the front of the meter, similar to the 900 MHz RF LAN transmitter in an end point meter. A colored

picture in Figure 8-6 illustrates the azimuth plane representation of total EIRP of the 900 MHz RF LAN transmitter.

Elevation plane patterns for the 900 MHz RF LAN transmitter in a cell relay are shown in Figures 8-7 and 8-8 with Figure 8-7 representing the patterns of the horizontal and vertical polarization components and the composite field (total), similar to the figure for the azimuth plane. Figure 8-8 illustrates the elevation plane representation of total EIRP of the 900 MHz RF LAN transmitter in a cell relay. Similar to the upward maximum radiation direction for the end point 900 MHz RF LAN transmitter, it can be seen that the maximum field is directed slightly upwards at about 30° rather than perfectly straight out toward the front of the meter.

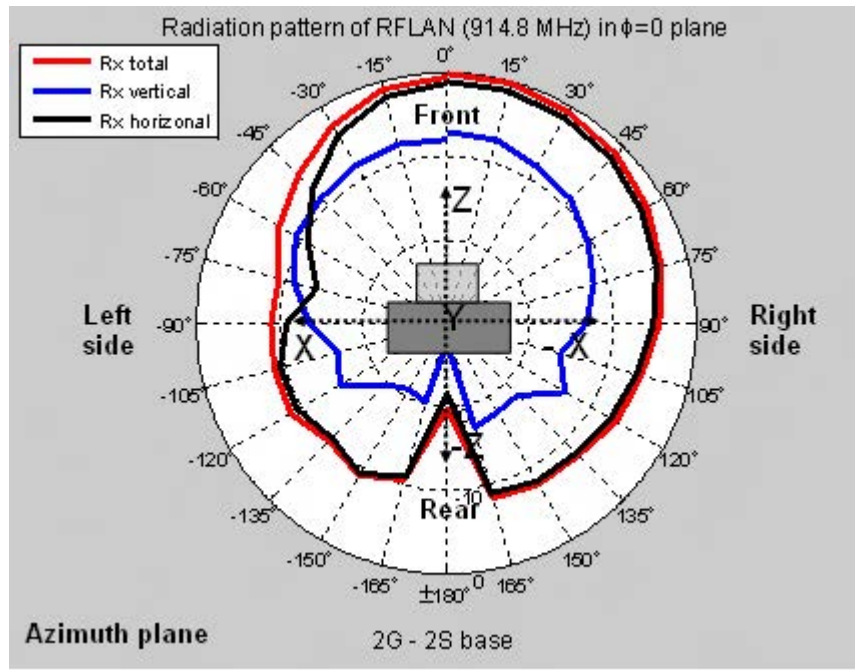


Figure 8-5
 Azimuth plane pattern of the 900 MHz RF LAN transmitter in a cell relay showing the horizontal, vertical and total pattern as viewed from bottom of meter. The scale is in dB with the maximum field at the outer edge of the pattern circle.

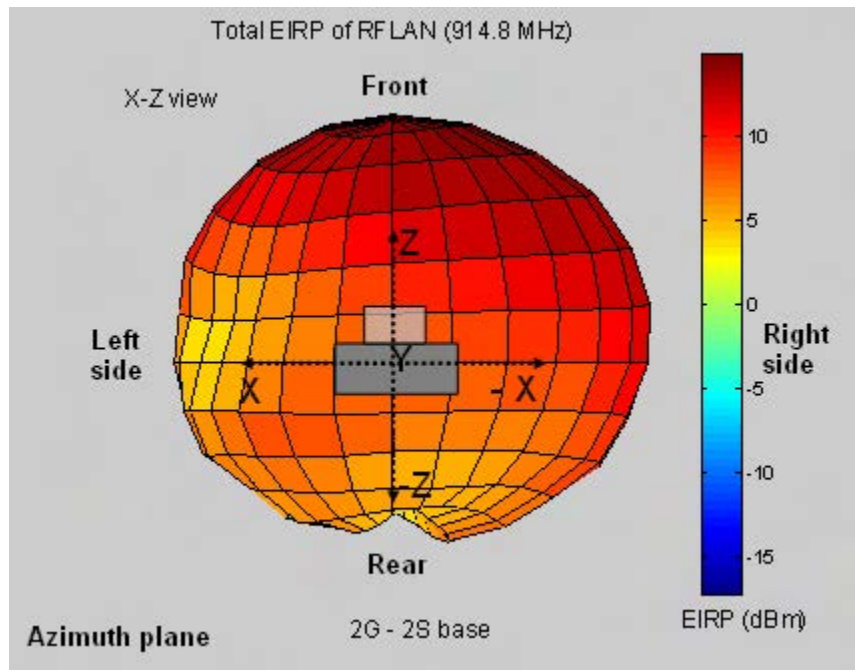


Figure 8-6
 Azimuth plane view of the total EIRP of the 900 MHz RF LAN transmitter configured in a cell relay.

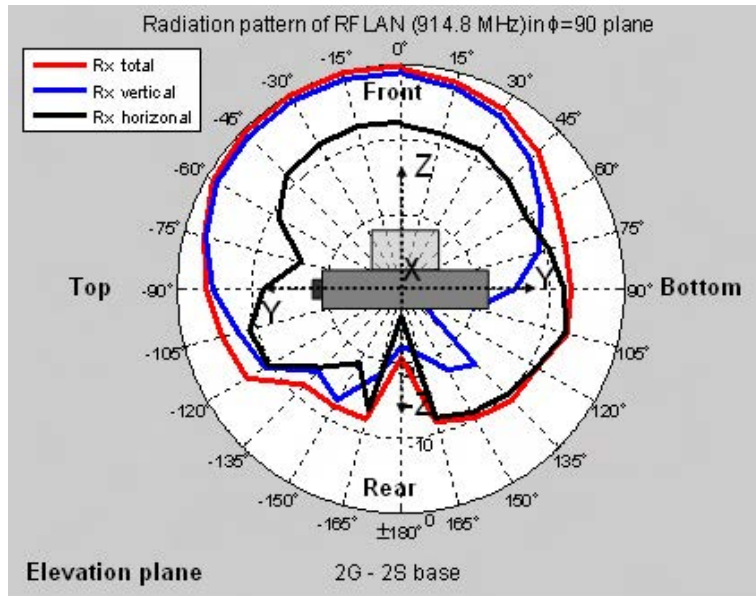


Figure 8-7
 Elevation plane pattern of the 900 MHz RF LAN transmitter in a cell relay meter showing the horizontal, vertical and total pattern. The scale is in dB with the maximum field at the outer edge of the pattern circle.

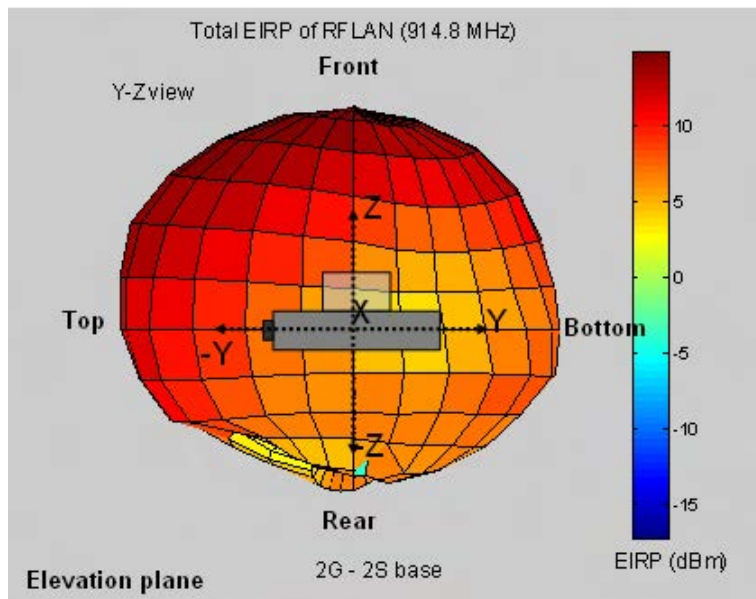


Figure 8-8
 Elevation plane view of the total EIRP of the 900 MHz RF LAN transmitter in a cell relay meter.

A series of similar pattern measurements of the 2.4 GHz Zigbee radio configured in an end point meter, Model CL200 (Itron #62_305_199, SCE #222010-273721) are shown in Figures 8-9 – 8-12. Figure 8-9 shows the azimuth plane pattern; the azimuth plane

pattern total EIRP is shown in Figure 8-10. Figure 8-9 shows that the direction of the maximum radiated field is very slightly canted to the right side of the meter, as viewed from the front, at about 15°.

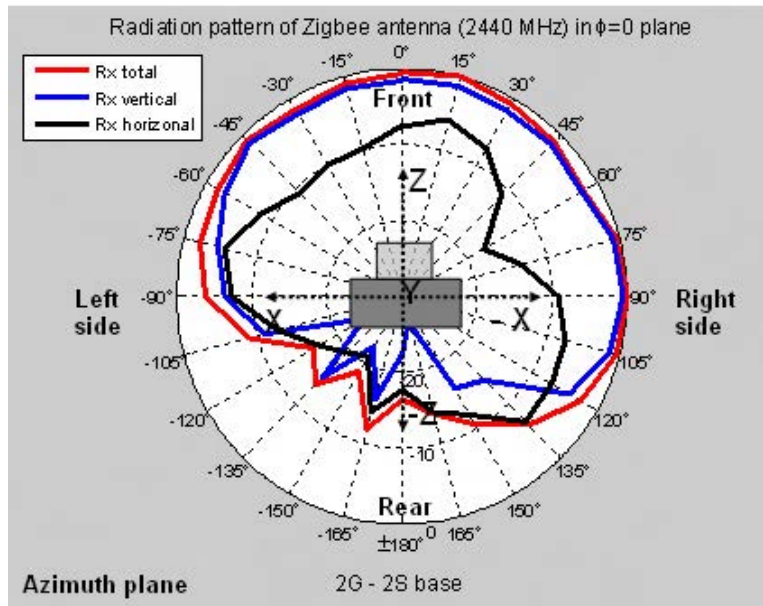


Figure 8-9

Azimuth plane pattern of the 2.4 GHz Zigbee transmitter configured in an end point meter showing the horizontal, vertical and total pattern as viewed from bottom of meter. The scale is in dB with the maximum field at the outer edge of the pattern circle.

The elevation plane pattern seen in Figure 8-11 reveals a tendency for the 2.4 GHz emission in the end point meter to be directed upwards, above the midline of the meter with a maximum field at approximately 45 to 60°.

Similar patterns were measured for the 2.4 GHz Zigbee radio in a cell relay meter (Model C2SORD, Itron #

61_912_646, SEC # 222070-000082). These patterns are shown in Figures 8-13 – 8-16 for the azimuth and elevation planes for relative field and total EIRP respectively. Figure 8-15 shows the tendency for an upward direction for emitted fields at approximately 45°.

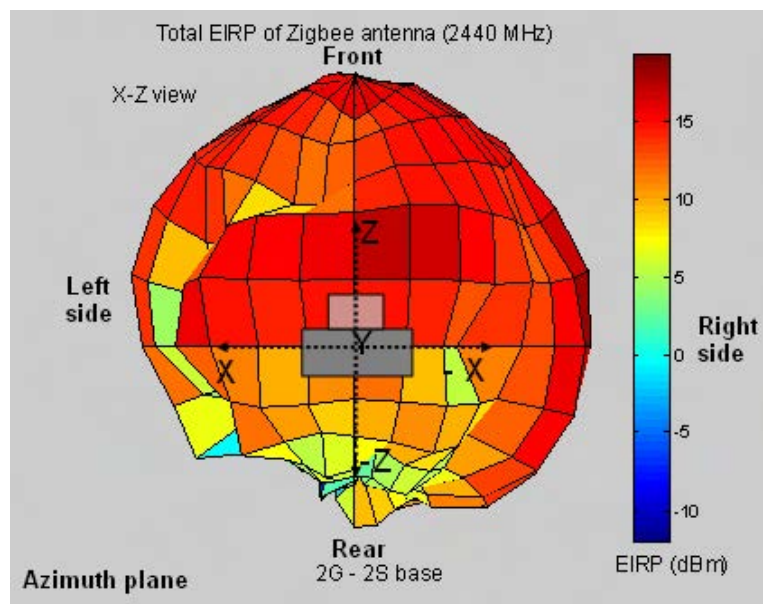


Figure 8-10

Azimuth plane view of the total EIRP of the 2.4 GHz Zigbee transmitter configured in an end point meter.

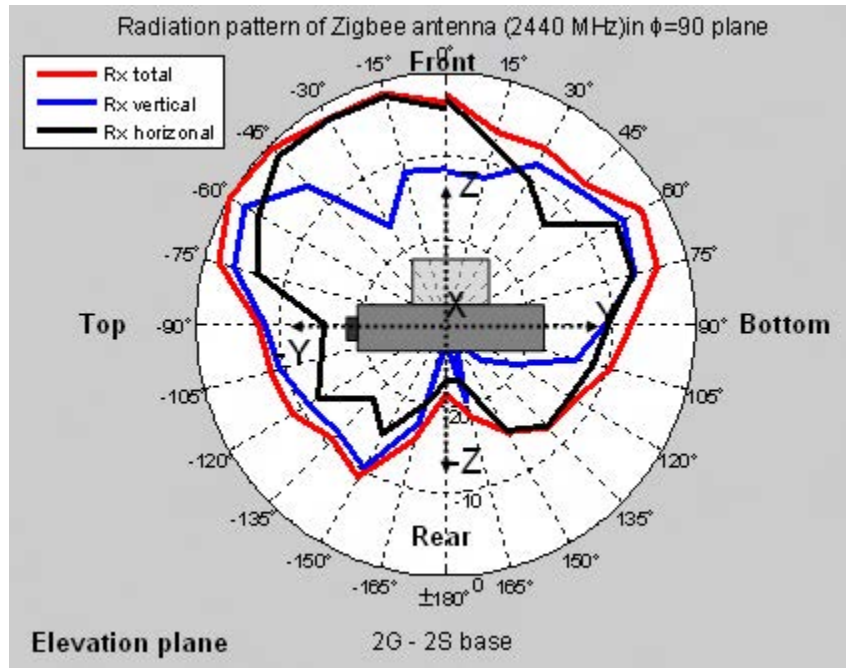


Figure 8-11
 Elevation plane pattern of the 2.4 GHz Zigbee radio in an end point meter showing the horizontal, vertical and total pattern. The scale is in dB with the maximum field at the outer edge of the pattern circle.

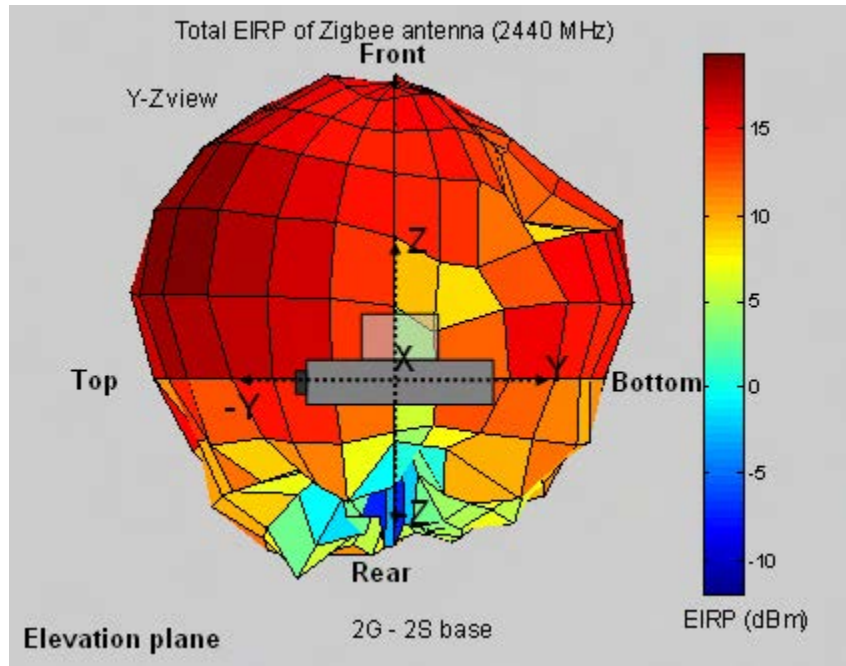


Figure 8-12
 Elevation plane view of the total EIRP of the 2.4 GHz Zigbee radio in an end point meter.

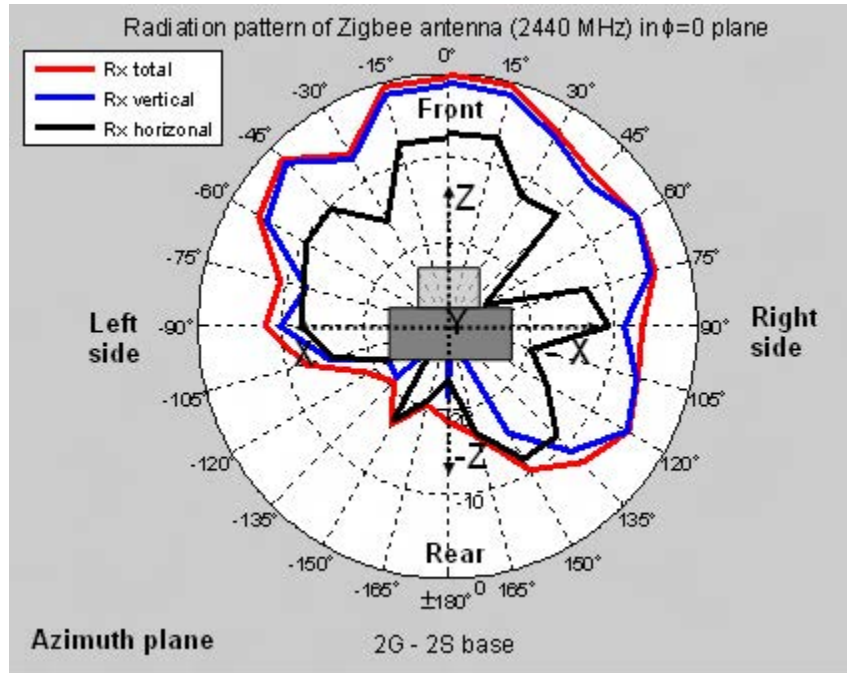


Figure 8-13
 Azimuth plane pattern of the 2.4 GHz Zigbee transmitter configured in a cell relay meter showing the horizontal, vertical and total pattern as viewed from bottom of meter. The scale is in dB with the maximum field at the outer edge of the pattern circle.

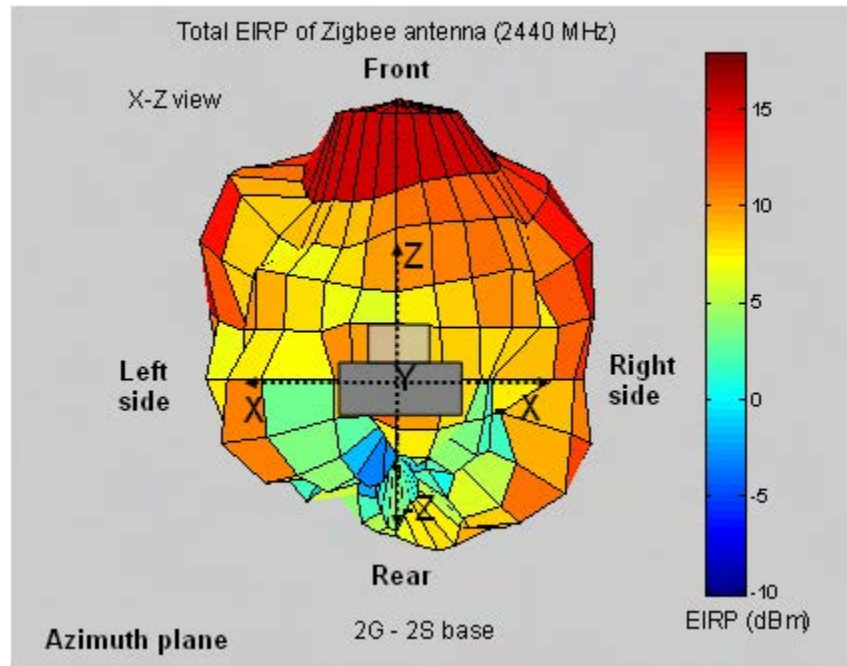


Figure 8-14
 Azimuth plane view of the total EIRP of the 2.4 GHz Zigbee transmitter configured in a cell relay meter.

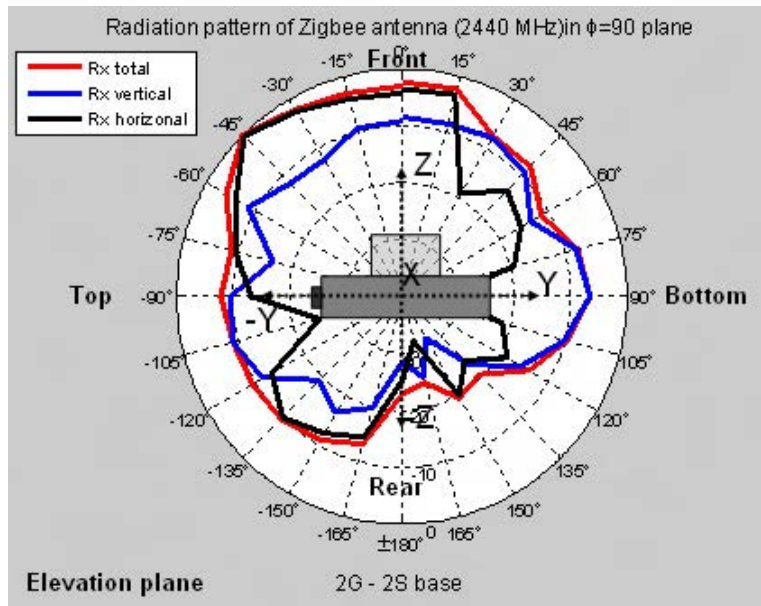


Figure 8-15
 Elevation plane pattern of the 2.4 GHz Zigbee radio in a cell relay meter showing the horizontal, vertical and total pattern. The scale is in dB with the maximum field at the outer edge of the pattern circle.

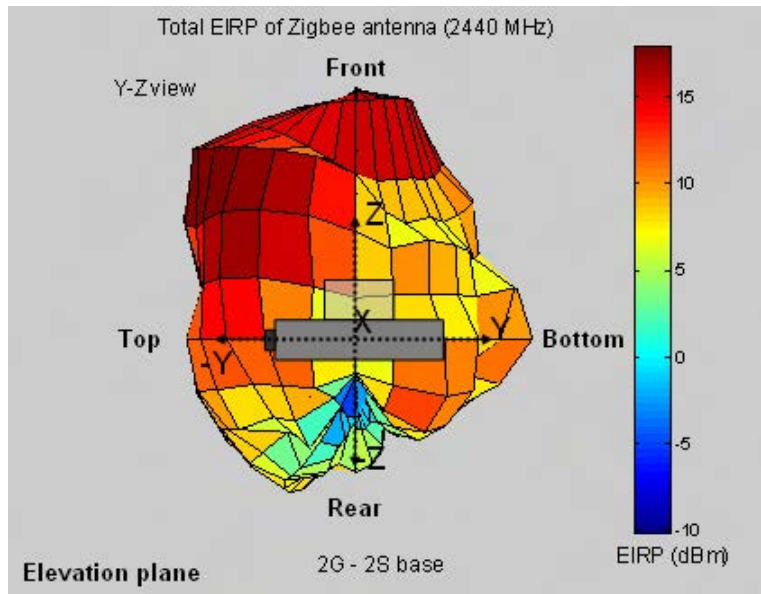


Figure 8-16
 Elevation plane view of the total EIRP of the 2.4 GHz Zigbee radio in a cell relay meter.

For completeness, patterns of the cell relay cellular and PCS band antennas were also determined during this documentation. Figures 8-17 and 8-18, based on measurements at a frequency of 836.6 MHz for the cell relay Model C2SORD (Itron # 61_912_646, SCE # 222070-00082, GSM # 12460), show azimuth patterns for the relative field and total EIRP. Elevation patterns

for the 836.6 MHz GSM transmitter are shown in Figure 8-19 and 8-20.

Antenna patterns were measured for the GSM radio operated in the 1900 MHz band as well. Figures 8-21 and 8-22 represent the azimuth patterns and Figures 8-23 and 8-24, the elevation patterns. The patterns were measured with the transmitter operating on a frequency of 1880 MHz.

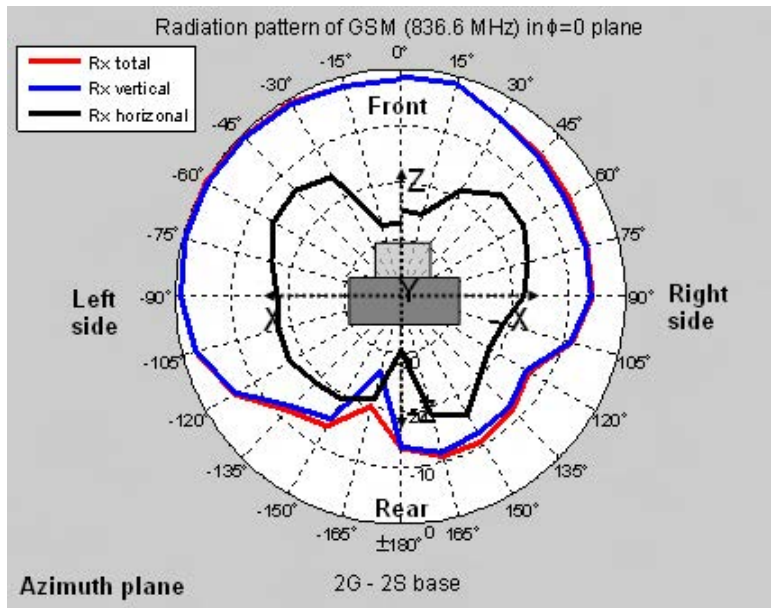


Figure 8-17
 Azimuth plane pattern of the 836.6 MHz GSM cellular transmitter in a cell relay meter showing the horizontal, vertical and total pattern as viewed from bottom of meter. The scale is in dB with the maximum field at the outer edge of the pattern circle.

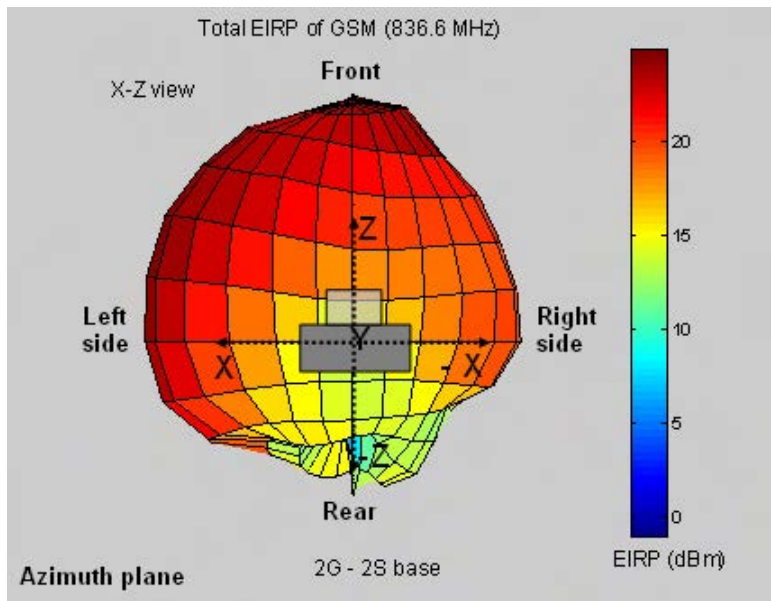


Figure 8-18
 Azimuth plane view of the total EIRP of a GSM 836.6 MHz cellular radio in a cell relay meter.

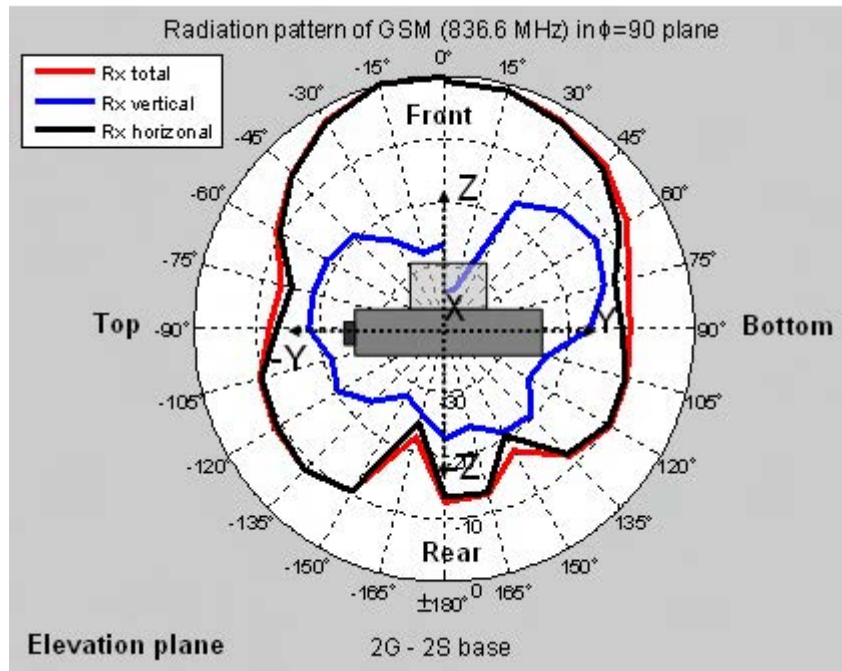


Figure 8-19
 Elevation plane pattern of the 836.6 MHz GSM cellular transmitter in a cell relay meter showing the horizontal, vertical and total pattern as viewed from bottom of meter. The scale is in dB with the maximum field at the outer edge of the pattern circle.

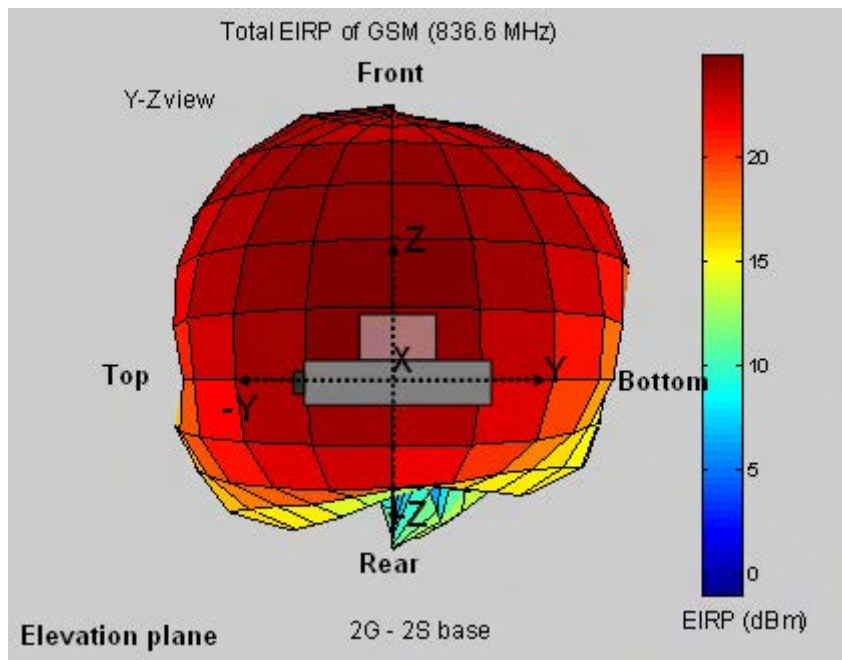


Figure 8-20
 Elevation plane view of the total EIRP of a GSM 836.6 MHz cellular radio in a cell relay meter.

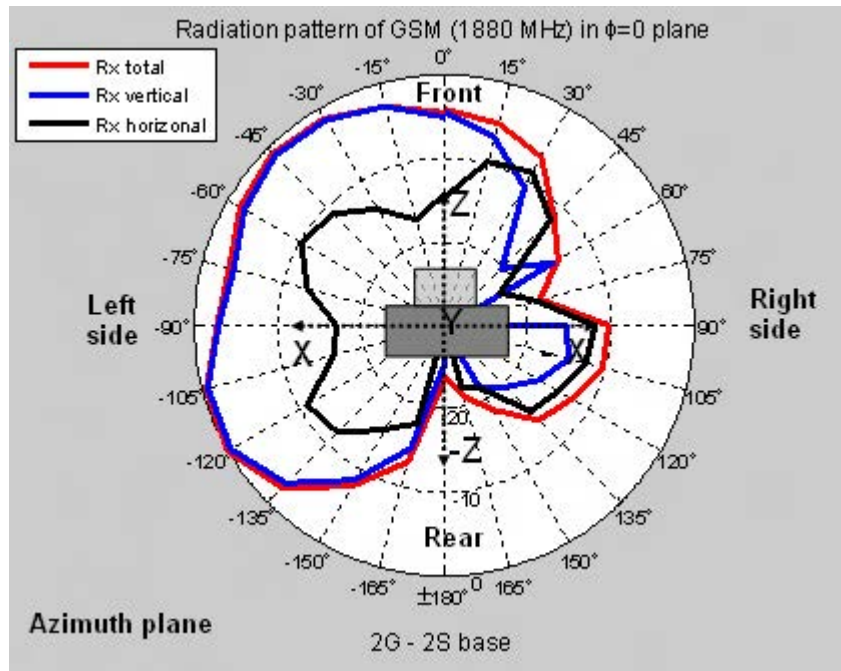


Figure 8-21
Azimuth plane pattern of the 1880 MHz GSM PCS transmitter in a cell relay meter showing the horizontal, vertical and total pattern as viewed from bottom of meter. The scale is in dB with the maximum field at the outer edge of the pattern circle.

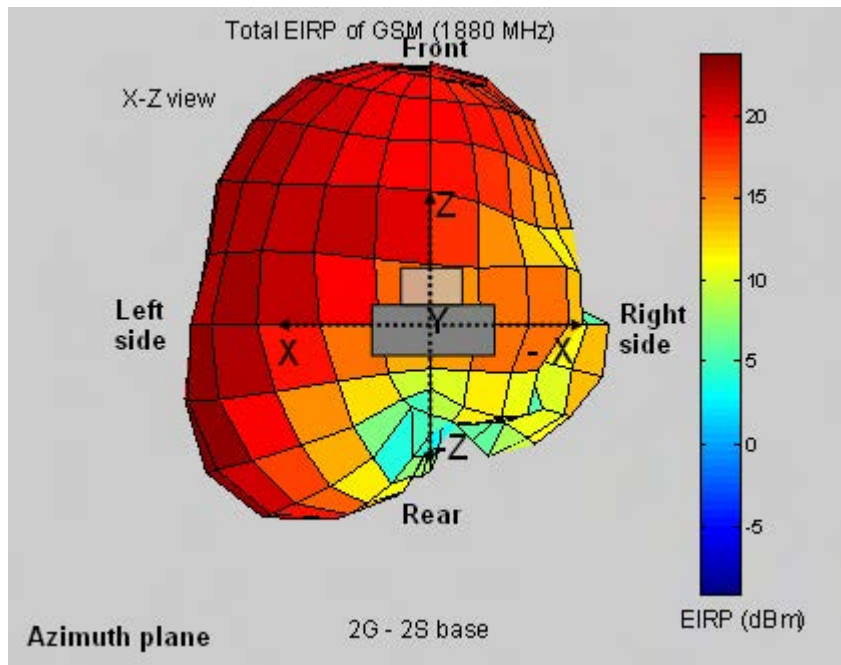


Figure 8-22
Azimuth plane view of the total EIRP of a GSM 1880 MHz PCS radio in a cell relay meter.

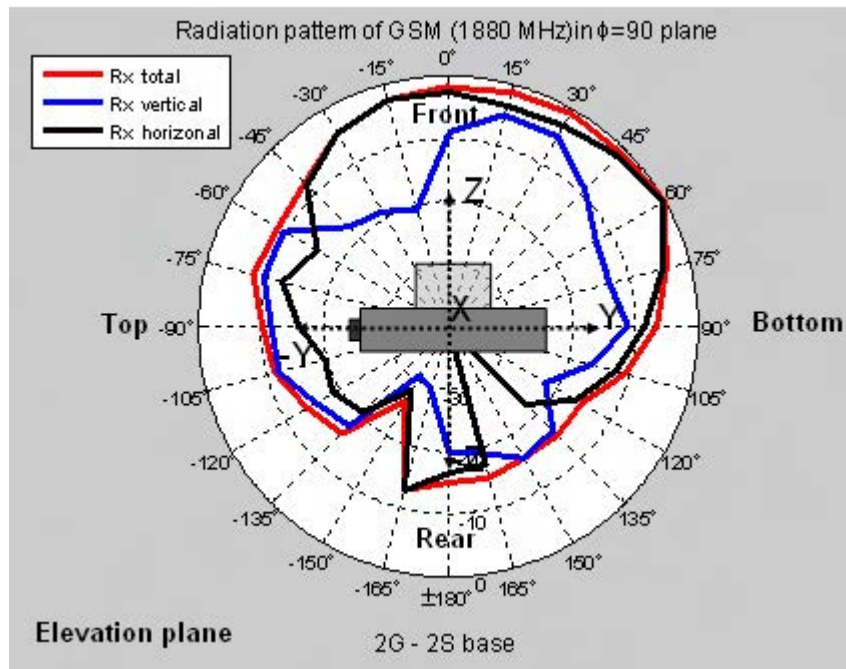


Figure 8-23
 Elevation plane pattern of the 1880 MHz GSM PCS transmitter in a cell relay meter showing the horizontal, vertical and total pattern as viewed from bottom of meter. The scale is in dB with the maximum field at the outer edge of the pattern circle.

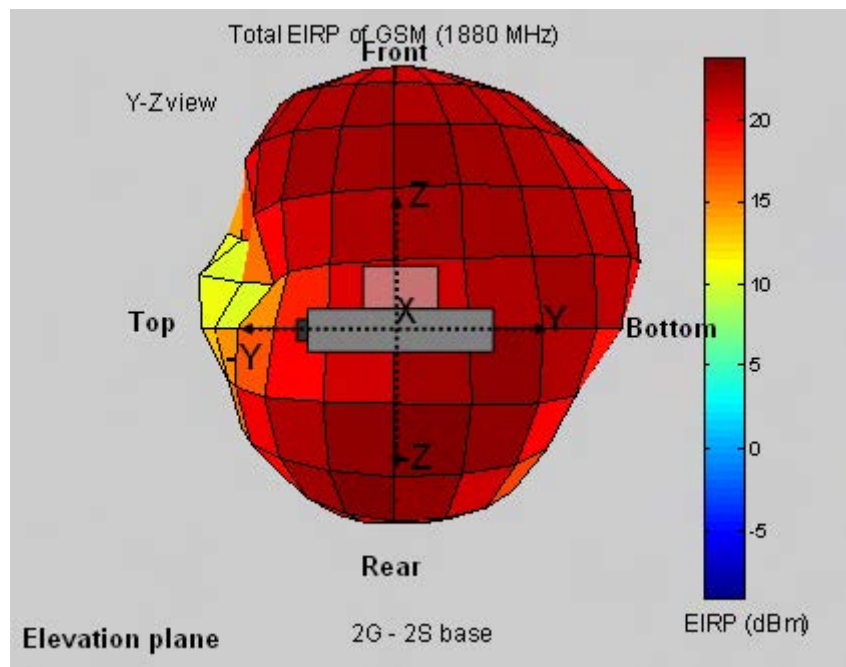


Figure 8-24
 Elevation plane view of the total EIRP of a GSM 1880 MHz PCS radio in a cell relay meter.

From analysis of each set of pattern measurement data, the EIRP was determined for a given transmitter output power delivered to the antenna. Table 8-1 summarizes the maximum EIRP found for each of the different measurement conditions described above. Maximum EIRP is the absolute greatest value of EIRP found from all of the pattern measurements at any angle. As observed from the pattern data shown above, the maximum EIRP may not be aligned with a line directly normal to the face of the Smart Meter. In each case, the

maximum EIRP has been referenced to one milliwatt. Hence, subsequent analyses making use of the maximum EIRP simply require adjusting the EIRP value for the actual transmitter power expected under normal operating conditions. In Table 8-1, the nominal specified transmitter power values are given in the next to last column and the maximum transmitter EIRP, referencing the nominal specified transmitter power, is given in the last column.

*Table 8-1
Summary of antenna measurement data*

Transmitter description	Max test EIRP (dBm)	Test power (dBm)	Gain (dBi)	Max TX P^a (dBm)	Max TX EIRP^b (dBm)
End point RF LAN, 914.8 MHz	12.8	9.9	2.9	24.0	26.9
Cell Relay RF LAN, 914.8 MHz	15.0	14.1	0.9	24.0	24.9
End point Zigbee, 2440 MHz	19.4	15.2	4.2	18.3	22.5
Cell Relay Zigbee, 2440 MHz	17.9	12.8	5.1	18.3	23.4
Cell Relay GSM, 836.6 MHz	24.9	23.1	1.8	31.8	33.6
Cell Relay GSM, 1880 MHz	23.9	22.3	1.6	28.7	30.3

^aNominal specified transmitter power

^bThe maximum transmitter EIRP assumes the nominal specified transmitter power.

Section 9: Smart Meter Field Measurements

The following narrative describes measurements of RF fields produced by Smart Meters that were obtained at the Itron meter farm in West Union, South Carolina, at residential settings in California and instrumentation comparisons and attenuation measurements for some selected materials including a simulated residential wall.

Meter farm measurements

A major feature of the Itron facility is a large “Smart Meter farm”. An aerial view of the geographic layout of the meter farm is seen in Figure 9-1. Approximately 20 acres comprise the installation of some 7000 Smart Meters for evaluating the performance of Itron’s meters in mesh networks. For the most part, Smart Meters are

organized in groups of ten meters on wooden racks as shown in Figure 9-2. The meters are arranged in two rows of five meters each, one above the other. The rack is 48 inches wide with the meters mounted so that there is a 16 inch vertical spacing of the two rows of meters, center to center. The bottom row of meters is nominally 48 inches above the ground. In one area in which area survey measurements were performed, the meter racks were found to be 16 feet apart, side to side, with the rows of racks 20.5 feet apart. Broadband probe and spectrum analyzer field measurements were performed on both individual Smart Meters and groups of ten meters comprising a rack.

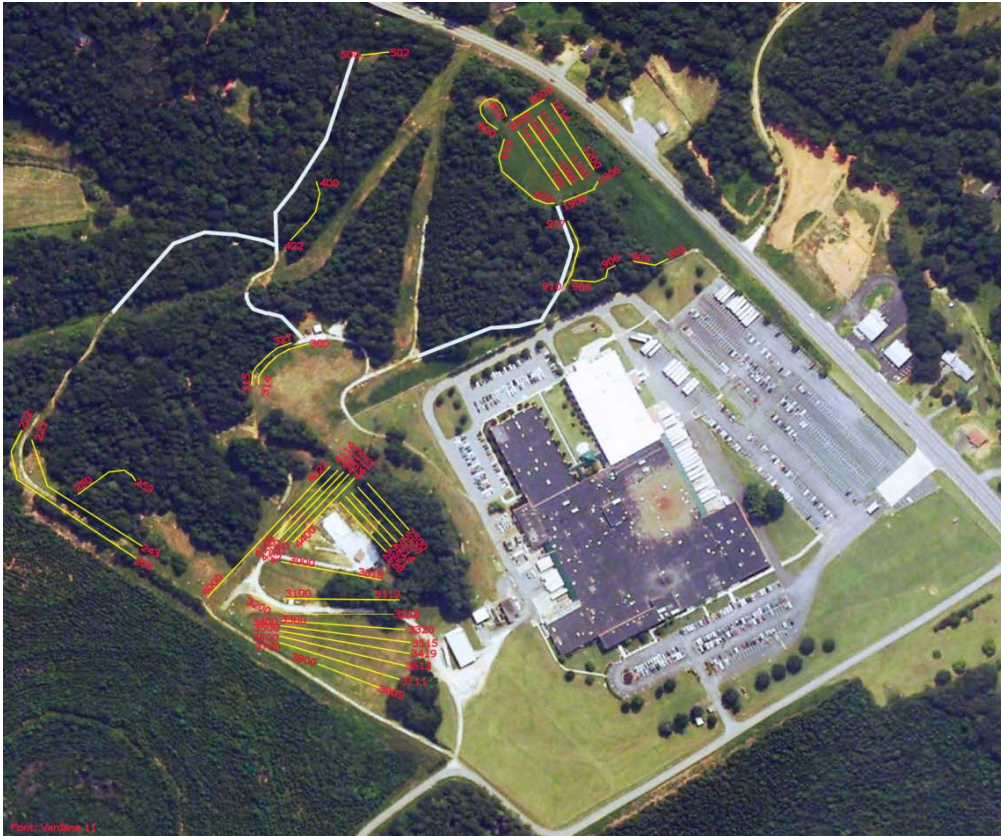


Figure 9-1
Aerial view of the Itron meter farm in West Union, SC. Yellow lines represent rows of Smart Meters grouped, generally, as racks of ten meters each. Photo courtesy of Itron.



Figure 9-2
Typical rack of ten meters shown in the western part of the Itron meter farm.

Individual meters

Initial field measurements in the meter farm were made using the broadband field probe (Narda Model B8742D). An objective of the broadband measurements was to assess what effect multiple Smart Meters might have on the measured RF field magnitude. The measurement approach sought to, first, examine the uniformity of measured field strengths among ten end point meters. To accomplish this, Itron programmed each of the ten meters to enter the continuous transmit mode of operation with three of the ten meters programmed to operate on the lowest frequency (L) in the 900 MHz RF LAN band (902.25 MHz), three meters to operate at the mid-band (M) frequency (914.75 MHz) and the remaining four meters to operate at the upper most channel (H) in the band (927.75 MHz). Measurements were performed over a

period of time during which the transmitter power was not expected to diminish due to transmitter heating. RF sources on precisely the same frequency and physically coincident with one another could lead to the possibility of phase addition or phase cancellation of the resultant RF field at specific points. In the measurement method used, the ten meters were physically distributed over a distance of up to 48 inches (this being equivalent to approximately four wavelengths in the 900 MHz band and approximately ten wavelengths in the 2.4 GHz band). Further, while individual meter frequencies on specific channels are very close to one another, they are not exactly the same due to crystal drift in the oscillator circuitry. Hence, the likelihood of RF fields from various meters actually being perfectly coherent is extremely small. Further, because of the measurement technique of scanning a planar area for the maximum,

peak RF field at each distance from the rack of meters, whether constructive or destructive phase addition may have existed, become irrelevant.

Each of the ten Smart Meter locations within a rack were identified with a letter from A to J and a location for each of these meters was determined as shown in Figure 9-3. The rationale behind this arrangement was to try to group meters in such a way as to enhance the potential for RF field contribution from adjacent meters

to the extent feasible when all ten meters were installed in the rack and actively transmitting. Initially, however, measurements were started with one meter only in the A position and successively replacing it with each of the other meters so that, ultimately, each of the ten meters had been installed in the A meter socket and the RF field was measured with the broadband probe. Each of the meter positions is also labeled as to the frequency of the associated meter as L, M or H, designating its frequency.

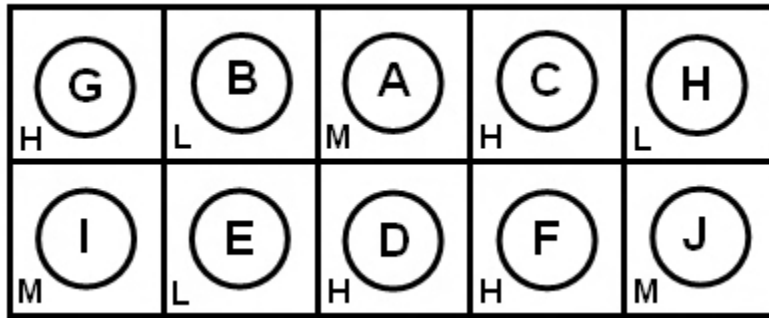


Figure 9-3
Layout of Smart Meter rack showing designated meter locations and frequency of various meters (L, M and H - see text) for the 900 MHz RF LAN and 2.4 GHz Zigbee transmitters.

Broadband field probe measurements were taken with the probe touching the surface of the meter face, with the probe at 20 cm from the meter face, with the probe at 30 cm from the meter face and, finally, with the probe behind the meter rack with the probe in contact with the rear of the rack, immediately behind meter position A. Use of the broadband field probe with a cardboard spacer affixed to the probe at the rack of ten meters is illustrated in Figure 9-4. These measurement results are given in Table 9-1. Each of the indicated

values was obtained by multiplying the meter reading by the manufacturer's calibration correction factor applicable at 915 MHz of 0.67. Surface field measurements with an isotropic probe must be interpreted with care due to the potential for erroneous readings. Nonetheless, because others may apply such probes in this fashion, it was deemed relevant to examine what kind of response would be exhibited when contacting the probe to the Smart Meter.



Figure 9-4
Use of the broadband field probe with a cardboard spacer attached to the probe near meters in a rack of ten meters.

Table 9-1
Measurements of 900 MHz RF LAN emissions of individual Smart Meters installed in meter position A in the meter rack with the broadband field probe.

Meter	Frequency	RF field measured (% of FCC public MPE)			
		Surface	20 cm	30 cm	Rear surface
A	M	45.9	4.2	2.2	0.0
B	L	65.3	6.9	5.5	0.0
C	H	18.5	1.6	1.1	0.0
D	H	16.8	2.3	1.6	0.0
E	L	53.7	5.6	4.2	0.0
F	H	19.1	2.1	0.7	0.0
G	H	20.5	1.9	0.7	0.0
H	L	48.6	4.9	3.5	0.0
I	M	45.7	4.6	2.8	0.0
J	M	29.6	3.1	1.9	0.0

In examining the results, two issues are immediately apparent. First the instrument readings appear to be related to the channel to which the 900 MHz RF LAN transmitter was programmed. This can be more easily seen in Figure 9-5. Clearly, the indicated field magnitude is related to the frequency of the 900 MHz RF LAN transmitter; the highest readings are correlated with the lowest frequency and the lowest

readings are correlated with the highest transmitter frequency. From data in Table 9-1 at 20 cm, the mean value of readings of the L meters is 5.8% while the mean value of the readings of the H meters is 2.0%; this corresponds to a ratio of 2.9 or a total range of about 4.6 dB from the lowest to the highest readings, i.e., a variation of ± 2.3 dB relative to the band center frequency.

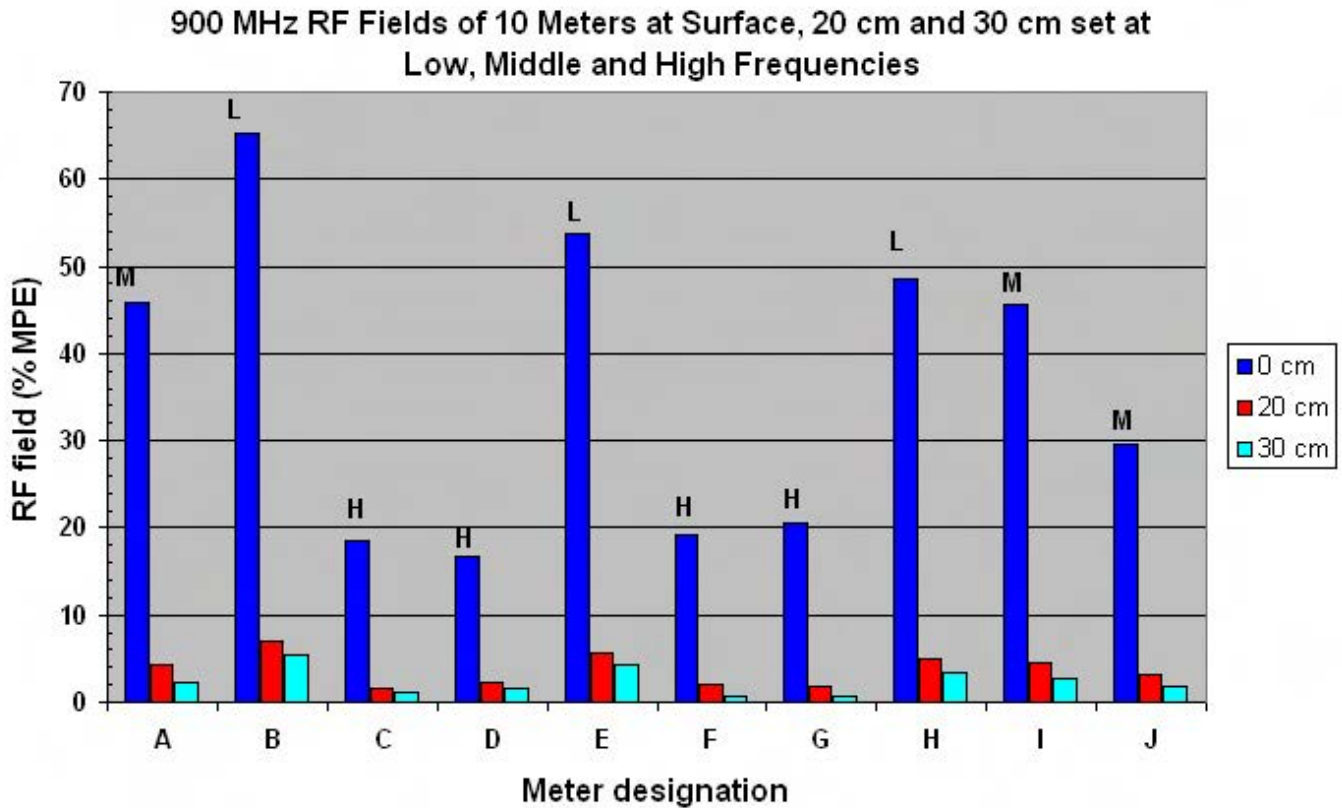


Figure 9-5
Corrected broadband probe RF field readings of the 900 MHz RF LAN transmitters from ten Smart Meters at the surface and at 20 cm and 30 cm from the meter.

A second observation is that the surface field strength readings are significantly greater than those at 20 cm. Why might this be the case? The probe protective shell surface is being placed in contact with the face of the Smart Meter, bringing the probe elements very significantly closer such that the probe is within the reactive near field region of the source antenna. The 900 MHz RF LAN antenna is only about 2.1 cm behind the meter envelope face; this is comparable to about only

0.06 wavelengths. Under these conditions, the probe may couple to the field source leading to erroneously high readings. Generally, field probes should not be used in such close proximity to the source because of this very issue. For example, IEEE Standard C95.3-2002¹³ recommends a minimum measurement distance

¹³ IEEE Standard C95.3-2002. IEEE Recommended Practice for Measurements and Computations of Radio Frequency

of 20 cm to minimize nearfield coupling and field gradient effects when using common broadband field probes. Measurement data can also be distorted when using an isotropic probe to measure steep spatial gradients close to a radiating element of the Smart Meter. These gradients can lead to considerable variation of the indicated amplitude of the field being measured over the volume of space occupied by the measurement probe elements. This is particularly true when employing field probes in the reactive near field that are comparable to the size of the source antenna. It should be noted that the elements inside the Narda B8742D probe are approximately 8 cm long; this is approximately the same length as the slot antenna of the 900 MHz RF LAN antenna that is approximately 6.3 cm long. Based on the potential for significant probe coupling with the Smart Meter internal transmitting antenna, the measured values indicated for surface contact of the probe with the Smart Meter should be considered suspect and, likely, substantial over estimates of the true field. Measurements at 20 cm and 30 cm,

however, are deemed to be reliable since they are substantial fractions of the 900 MHz wavelength (20 cm is equivalent to 0.6 wavelengths and 30 cm is equivalent to 0.9 wavelengths).

Following measurement of the fields produced by the ten individual meters, measurements of the maximum indicated RF field were conducted in front of and behind the rack as individual meters were successively installed into their respective meter sockets. The objective was to observe for any increase in cumulative RF field caused by the contribution of an increasing aggregate of actively transmitting Smart Meters. These measurement results are summarized in Table 9-2. Due to technical problems associated with programming of two of the meters at the time (meters D and F), not all meters were included in each collection of active meters. However, at the end of the process, all meters were included when all ten meters were active.

*Table 9-2
Summary of measurements of the 900 MHz composite RF field produced by an increasing number of closely spaced, collocated Smart Meters (meters A - J).¹⁴*

Meters active	RF field at 20 cm	RF field at 30 cm	RF field behind rack
A	4.2	3.3	0.0
AB	7.9	5.0	0.0
ABC	7.4	5.3	0.1
ABCE	7.9	5.9	0.1
ABCEG	8.6	6.1	0.1
ABCEGH	9.0	6.2	0.3
ABCEGHI	8.7	6.8	0.7
ABCEGHIJ	9.2	6.7	0.9
ABCDEGHIJ	9.1	7.2	0.7
ABCDEFGHIJ	8.1	7.5	0.8

¹⁴ During the testing, meter D exhibited a problem that was subsequently fixed but was left out of some of the test rows in Table 3.

In each case of added meters, the entire surface of the meter rack was scanned with the broadband probe with 20 and 30 cm spacers attached to the probe to search for the greatest meter reading. The location of maximum reading was not necessarily the same in each case and the data strongly suggest that for a given distance from the front of the meter rack, a finite maximum value of field is developed that will not be exceeded with the addition of more meters. Beyond three or four meters, the aggregate field does not materially increase with additional meters. The data indicate a maximum observed, composite field of 9.2% of the general public MPE at 20 cm and a maximum of 7.5% of the MPE at 30 cm (almost one foot). Immediately behind the meter rack, a maximum composite field equivalent to 0.9% of the MPE was measured.

A somewhat similar approach was used to measure the collective composite RF field produced by multiple

Smart Meters with the 2.4 GHz Zigbee transmitters activated for transmission. Itron programmed each of the ten meters to enter the continuous transmit mode of operation with three of the ten meters programmed to operate on the lowest frequency (L) in the 2.4 GHz band (2405 MHz), three meters to operate at the mid-band (M) frequency (2440 MHz) and the remaining four meters to operate at the upper most channel (H) in the band (2475 MHz). In this case, the individual meters were measured with each meter being placed in position A but the overall composite field, with all meters active, was performed by inserting all meters into their designated positions without sequentially adding active meters as was done with the 900 MHz RF LAN tests. Table 9-3 summarizes the results of these measurements. All readings of the 2.4 GHz emissions were corrected by applying the manufacturer's determined correction factor for 2.45 GHz of 0.97.

*Table 9-3
Summary of corrected measurement data on RF fields of individual 2.4 GHz Zigbee transmitters installed in meter position A and of the collection of all ten meters.*

A	M	10.2		
B	L	11.8	1.7	0.0
C	H	5.1	1.4	0.0
D	H	5.5	1.0	0.0
E	L	11.8	0.9	0.0
F	H	6.3	1.5	0.0
G	H	5.4	0.9	0.0
H	L	8.8	1.0	0.0
I	M	7.0	1.0	0.0
J	M	5.1	0.7	0.0
All on		14.3	1.0	0.0
A	M	10.2	2.5	0.0

These data support the contention that the Zigbee transmitters operating at the lowest frequency within the 2.4 GHz band tended to produced the greatest

measured field strength, similar to the finding for the 900 MHz RF LAN transmitters. Figure 9-6 illustrates the data in Table 9-3 graphically.

2.4 GHz RF Fields of 10 Meters at Surface and 20 cm set at Low, Middle and High Frequencies

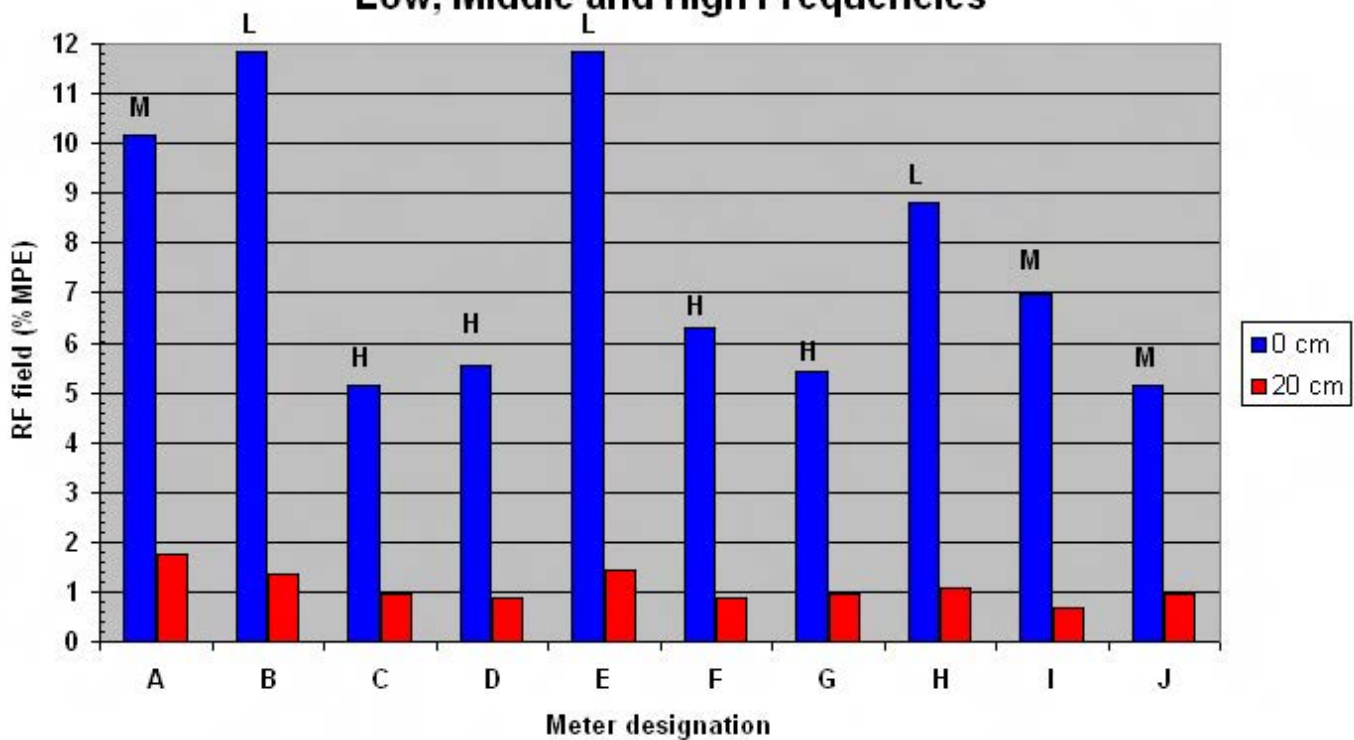


Figure 9-6
Corrected broadband probe RF field readings of the 2.4 GHz Zigbee transmitters from ten Smart Meters at the surface and at 20 cm from the meter.

Table 9-3 also indicates that the composite RF field associated with simultaneous operation of all ten Smart Meters with their Zigbee radios active provided a maximum reading of 14.3% of the FCC general public MPE with the probe in surface contact with the meters and a maximum of 2.5% of the MPE at 20 cm from the surface. The surface readings must also be considered suspect as is the case with the 900 MHz band measurements. The RF field behind the rack of ten active meters was not detectable with the broadband field probe.

Groups of meters

Through use of the Narda SRM-3006 instrument, measurements of RF fields could be made at much

greater distances from the meter rack due to the significantly greater sensitivity of the narrowband device when compared to the broadband field probe. The aggregate RF field produced by a meter rack of ten Smart Meters was examined with the SRM-3006 by making measurements at successively greater distances from the front of the rack and observing the spectral display of the measurement result. The measurement process consisted of holding the SRM-3006 at the approximate mid-height of the rack at different distances from the frontal plane of the meters in the rack as shown in Figure 9-7



*Figure 9-7
Using the Narda SRM-3006 to measure aggregate RF fields near a rack of ten meters programmed for fixed frequency, continuous transmission in the meter farm.*

The instrument was used to acquire a “max hold” spectrum over a period of approximately one minute while slowly moving the probe in a planar area measuring approximately 2 feet by 2 feet. Figure 9-8 shows the result of the measurement with the SRM-3006 probe/antenna positioned at 1 foot from the front of the meter rack. In this display, the continuously operating 900 MHz RF LAN transmitters are clearly

seen on their respective frequencies (902.25 MHz, 914.75 MHz and 927.95 MHz). A resolution bandwidth of 100 kHz was used in these spectral measurements within the frequency band of 902 MHz to 928 MHz. The SRM-3006 was set to display the maximum measured field at each distance directly as a percentage of the FCC general public MPE as seen on the vertical axis of the display.

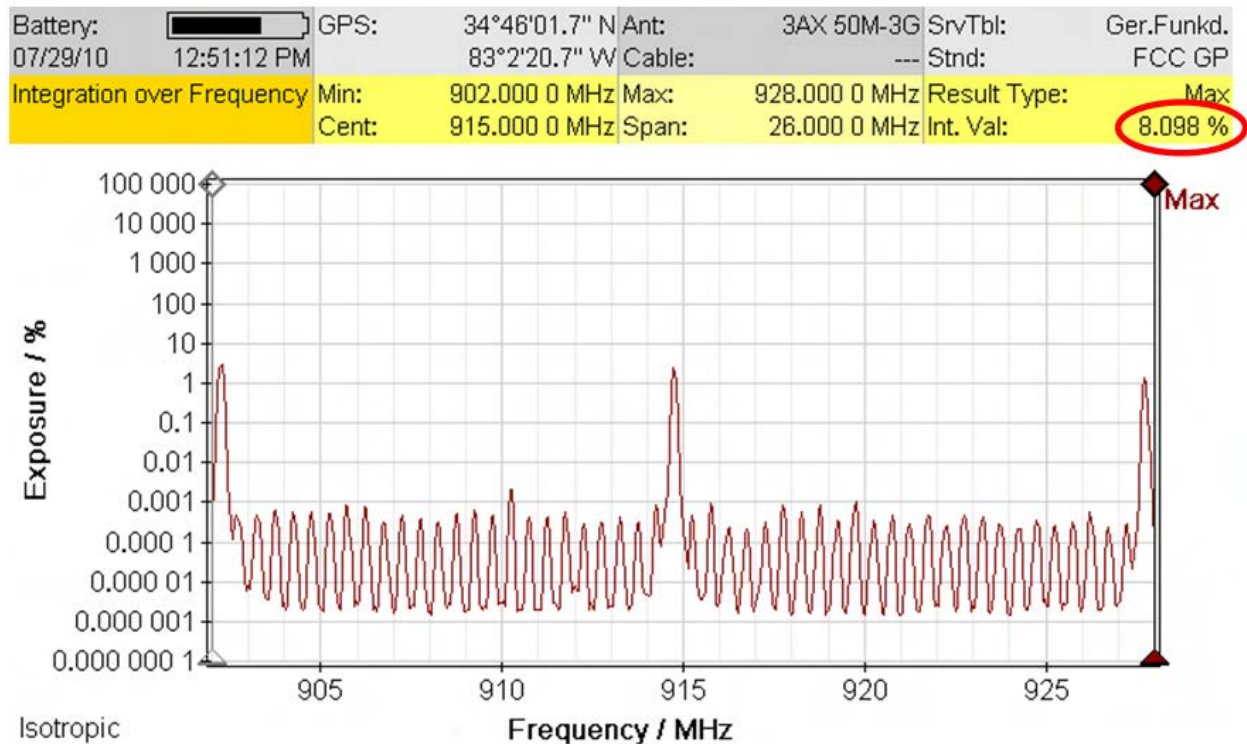


Figure 9-8
900 MHz band composite RF field from rack of 10 SmartMeters at 1 foot.

The many lower level spectral peaks were caused by the multiplicity of Smart Meters within the meter farm; in practice, it was not possible to completely remove oneself from the ambient background of RF fields present in the meter farm since moving away from one rack of meters meant that one was getting closer to another rack in some location. While the signals from the other thousands of Smart Meters were randomly occurring across the band, because of the number of meters simultaneously operating, the presence of signals on each frequency was evident. Had only one Smart Meter been operating, this would not have been the case, as discussed earlier. Using the internal integration feature of the SRM-3006, the total equivalent RF field power density was reported by the instrument as a percentage of the general public MPE in the upper right region of the spectral plot (see circled area). For the measurement at 1 foot in front of the meter rack, a total integrated RF field equivalent to 8.1% of the MPE was determined.

Using the spectrum analysis method describe above, measurements were made at successively greater distances from 1 foot to 100 feet from the Smart Meter

rack. These spectrum scans obtained from the SRM-3006 are shown in Appendix B. Referring to Appendix B, it can be seen that as the distance between the rack and the measuring instrument was increased, the signal level of the programmed meters decreased until, at approximately 50 feet from the rack, the signal levels of the meter rack being investigated blended into the background of all of the other ambient RF fields from other meters within that area of the meter farm. In other words, the emitted signals became indistinguishable from the ambient environment of RF fields and could not be identified as being contributed by a specific meter rack or collection of Smart Meters. Field measurements taken to the rear of the meter rack are provided in Appendix C. Figure 9-9 shows measurements being performed behind the rack of specially programmed Smart Meters. The presence of other racks of active meters are evident in the background. As distance from the back side of the subject rack was increased, the distance to the other meter racks located behind the subject rack decreased meaning that the ambient, but intermittent, RF fields of other meters in the farm could be detected.



Figure 9-9

Field measurements at successively greater distances behind the subject meter rack resulted in closer proximity to other meter racks with the probability of detecting stronger, but intermittent, signals due to the ambient background.

Another set of field measurements in front of the meter rack was performed with the Zigbee radios in the meters programmed for continuous transmit operation on 2405 MHz, 2440 MHz and 2475 MHz. The SRM-3006 was set for a resolution bandwidth of 200 kHz over the band of 2400 to 2483 MHz for these measurements. A similar pattern of decreasing field magnitude with increasing distance was observed for the Zigbee radio emissions. Figure 9-10 shows the spectrum plot obtained at 1 foot from the front of the meter rack with all ten radios operating with an

integrated RF field equivalent to 4.5% of the general public MPE. Appendix D provides each of the spectrum measurements of the ten Zigbee transmitters at distances from 1 foot to 100 feet from the front of the meter rack. Appendix E provides similar spectrum plots taken behind the meter rack as well as the result of a lateral walk at three feet in front of and across the face of the meter rack extending from a few feet beyond the edge of the rack to an equivalent distance beyond the opposite edge.

Battery: 07/29/10 02:29:42 PM	GPS: 34°46'01.2" N 83°2'20.3" W	Ant: 3AX 50M-3G	SrvTbl: ---	Ger.Funkd. FCC GP
Integration over Frequency	Min: 2 400.000 MHz Cent: 2 441.500 MHz	Max: 2 483.000 MHz Span: 83.000 MHz	Result Type: Max	Int. Val: 4.499 %

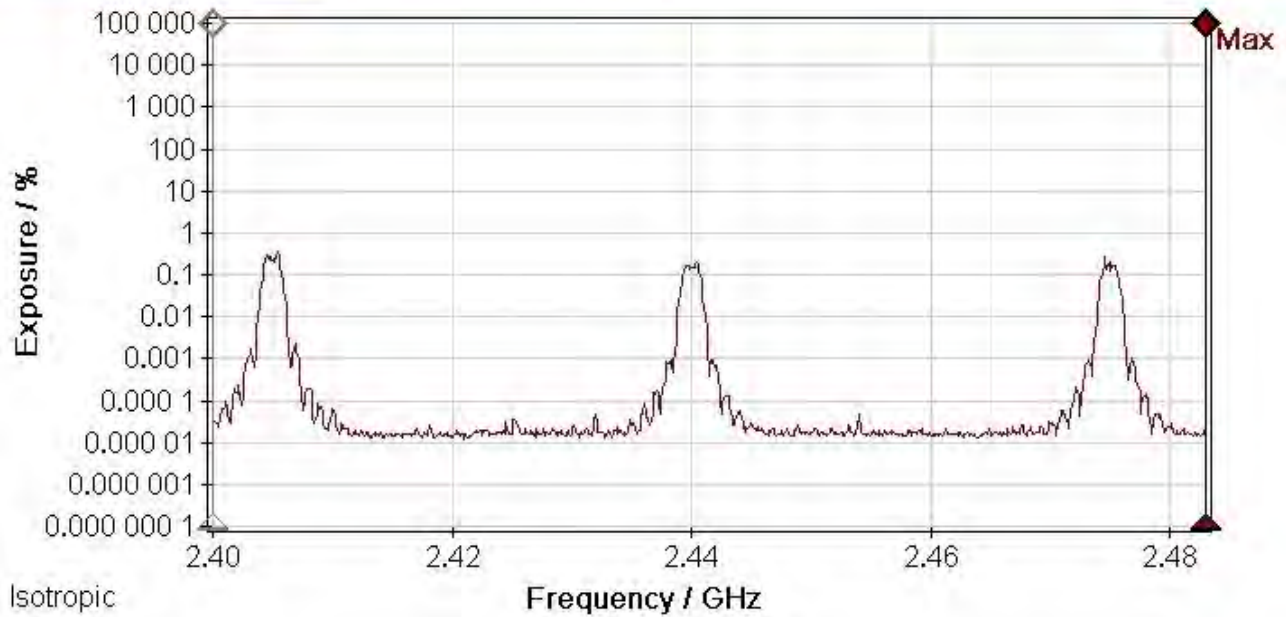


Figure 9-10
Spectrum measurement of 2.4 GHz RF fields from ten simultaneously transmitting Smart Meters.

Table 9-4 lists the integrated RF fields determined for both the 900 MHz RF LAN and 2.4 GHz Zigbee transmitters over the range of distances used. The data in Table 9-4 are plotted in both linear (Figure 9-11)

and logarithmic (Figure 9-12) formats to illustrate graphically the decrease in RF field with distance from the meter farm rack of ten meters.

Table 9-4

Summary of composite RF field values (% general public MPE) determined with the SRM-3006 at various distances in front of a meter rack of 10 simultaneously operating Smart Meters.

Distance (ft)	900 MHz	2.4 GHz
1	8.098	4.499
2	3.898	2.459
3	2.471	1.021
4	1.827	0.587
5	1.382	0.457
6	1.157	0.348
7	0.722	0.258
8	0.655	0.187
9	0.681	0.163
10	0.536	0.134
15	0.356	0.076
20	0.177	0.044
25	0.152	0.033
30	0.144	0.02
40	0.113	0.014
50	0.107	0.013
75	0.073	0.0091
100	0.092	0.00852
Distance (ft)	900 MHz	2.4 GHz

From Table 9-4 and Figures 9-11 and 9-12, it is evident that the peak RF field measured for the group of ten active Smart Meters drops to less than 1% of the FCC general public MPE at a distance of approximately seven feet where the combined RF field from both frequency bands are summed. This peak value is not

representative of the time averaged field that would be present during normal operation of the Smart Meter since the typical duty cycle of the meters would cause the composite time-averaged field to be substantially less.

**RF Fields vs Distance in Meter Farm
with 10 Meters Operating Continuously**

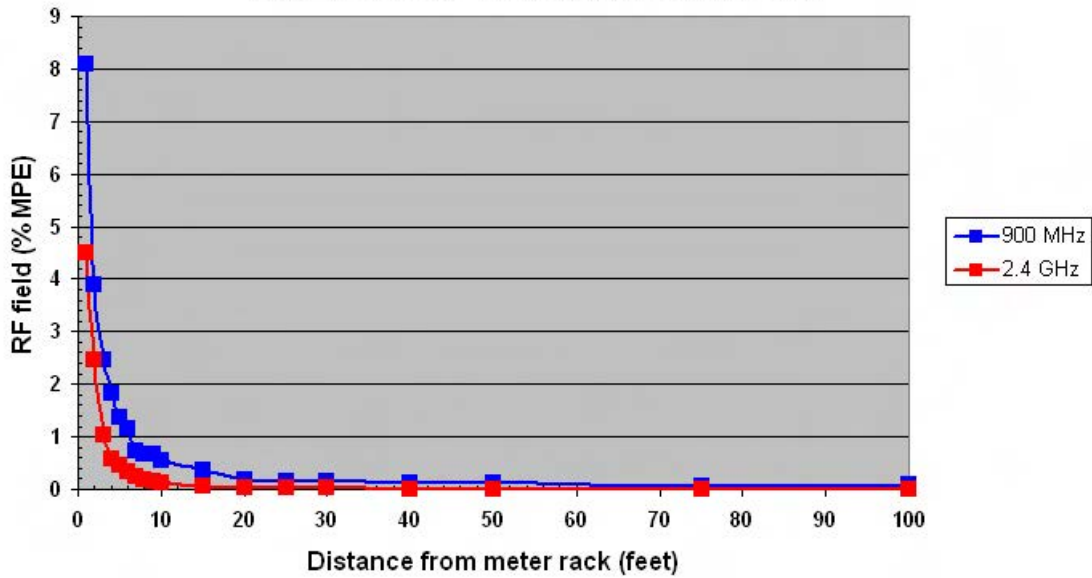


Figure 9-11
Integrated, total composite RF field obtained in meter farm for emissions from the 900 MHz RF LAN and 2.4 GHz Zigbee transmitters operating simultaneously in the vicinity of a meter rack (linear plot).

**RF Fields vs Distance in Meter Farm
with 10 Meters Operating Continuously**

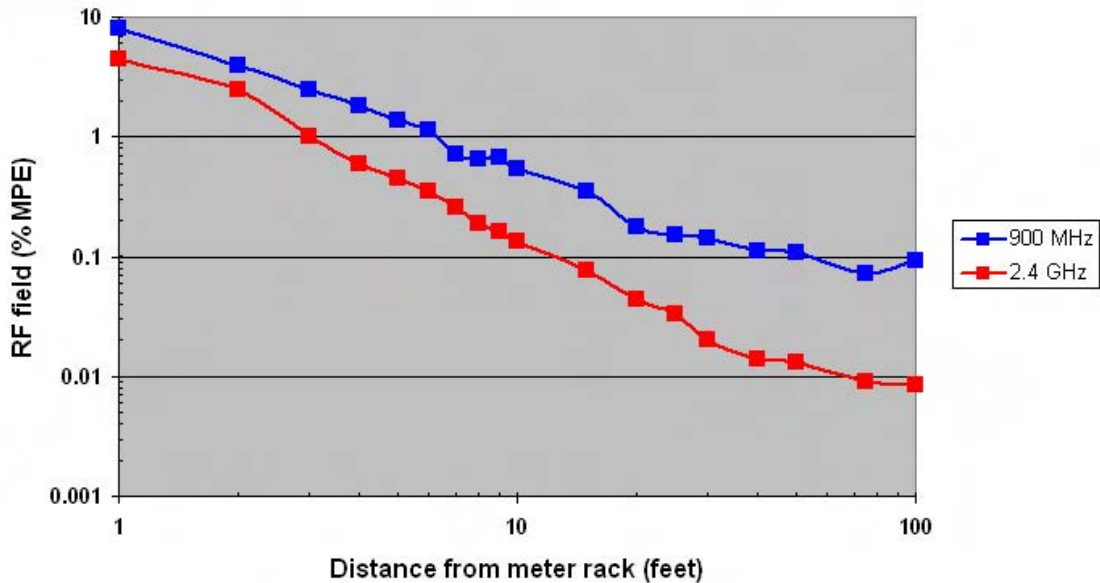


Figure 9-12
Integrated, total composite RF field obtained in meter farm for emissions from the 900 MHz RF LAN and 2.4 GHz Zigbee transmitters operating simultaneously in the vicinity of a meter rack (logarithmic plot).

**Residential settings
Homes**

In the interest of gathering data on RF fields from Smart Meters in a realistic residential environment, additional measurements were performed in a Downey, California neighborhood. On August 19, 2010, measurements were conducted at two different residences at which SCE Smart Meters had been previously deployed. Two different Smart Meters were used to facilitate the measurements, one that had been programmed to operate in continuous transmit mode on the lowest frequency in the 900 MHz band and the other programmed to operate in continuous transmit mode on the lowest frequency in the 2.4 GHz band. Each meter was temporarily installed at each of the two

homes during which a series of RF measurements were taken at the meter service box on the home, within the front, side and backyards, and throughout the home in all rooms of the home. Figure 9-13 shows an SCE meter technician in the process of installing one of the special “test” meters in place of the meter normally present.

At the first residence, designated residence A, measurements of the maximum, instantaneous peak RF field were conducted by scanning a planar region at 1, 2, 3, and 5 feet in front of the meter. The measurements are summarized in Table 9-5. The region near the service box for residence A was somewhat cramped and measurements were not possible beyond five feet from the face of the Smart Meter.

Table 9-5

Summary of planar area scans performed with the SRM-3006 in front of residential meter installation at residence A, Downey, CA, with transmitters operating continuously.

Location relative to meter (feet)	900 MHz RF LAN		2.4 GHz Zigbee	
	RF field (% public MPE)	Time of measurement (PDT)	RF field (% public MPE)	Time of measurement (PDT)
Surface	9.67	9:49	7.93	11:19
1	0.875	9:54	0.615	11:22
2	0.361	9:56	0.258	11:22
3	0.186	9:58	0.142	11:23
5	0.096	10:00	0.071	11:25

With each of the two specially programmed Smart Meters installed in the home’s service box meter socket, spectrum measurements were performed throughout the home including some outside areas. Figure 9-14 shows the measurement of a planar scan at the residence. Procedurally, the 900 MHz band measurements were performed first, followed by the 2.4 GHz measurements. Table 9-6 summarizes the measurements taken at residence A including a few outdoor measurements. The RF field reading recorded

for each room or area represents the overall peak value of field obtained through a spatial scan of the room or area. It is noted that directly behind the service box with the Smart Meter, inside bedroom 1, the greatest field detected corresponded to 0.01% of the FCC general public MPE. Overall, the greatest RF fields found were in the home office area, where a wireless router was installed for Internet connectivity and in the kitchen when the microwave oven was operating.



Figure 9-13
SCE meter technician replacing existing Smart Meter with specially programmed meter for residential measurements.



Figure 9-14
Planar scans were performed at several distances in front of a residential Smart Meter by slowly moving the SRM-3006 within a plane at a fixed distance.

Table 9-6

Spectrum scan measurements of Smart Meter fields in the 900 MHz and 2.4 GHz bands in residence A, Downey, CA. RF field is peak value obtained from a spatial scan of the room interior or area in percent of FCC general public MPE.

Location at residence	RF field (% MPE)	
	900 MHz	2.4 GHz
Front yard	0.00014	0.00611
Bedroom 1	0.00355	0.00876
Bedroom 1 (directly behind meter)	0.010	
Bath	0.009	0.00941
Bedroom 2	0.00909	0.00637
Master bedroom	0.00056	0.00644
Family room	0.00055	0.00627
Dining room/Living room	0.00057	0.00651
Kitchen	0.00057	0.00616
Kitchen (microwave at 6.5 feet)		0.016
Kitchen (microwave at 2 feet)		22.04
Laundry room	0.00053	0.00588
Bath	0.00054	0.00723
Office (Wi-Fi on)	0.00052	0.0288
Garage	0.00055	0.00622
Back side yard	0.00053	0.00653
Backyard	0.00059	0.00658
Pool	0.00058	0.00647

Figure 9-15 shows an interior measurement taken at residence A in a bedroom directly opposite to the mounting location of the Smart Meter on the outside of the house. Outdoor measurements at residence A are shown in Figures 9-16 and 9-17.



Figure 9-15
Interior residential measurements included measurements on the opposite side of the wall where the Smart Meter was installed at the home.



*Figure 9-16
Residential measurements at residence A included both outdoors and indoors measurements of RF fields in both the 900 MHz and 2.4 GHz bands.*



Figure 9-17
Measurements at residence A included exterior locations in the backyard.

At the second residence (Figure 9-18), designated residence B, also in the same neighborhood of Downey, CA as residence A, the measurement process again included scanning a planar region at 1, 2, 3, 4, 5, 6 and 10 feet in front of the meter. The measurements for residence B are summarized in Table 9-7. The specially programmed Smart Meters were used to facilitate

measurements throughout the property. Figure 9-19 shows the Smart Meter installed at residence B and a planar scan being performed. Within residence B, similar to residence A, a wireless router for Internet connectivity was found in a home office (Figure 9-20). Field measurements acquired within and around the residence are listed in Table 9-8.



*Figure 9-18
Residence B in Downey, CA where indoor and outdoor measurements were made with specially programmed Smart Meters installed to facilitate measurements.*



*Figure 9-19
Performing a planar scan of RF fields adjacent to a Smart Meter at residence B.*



Figure 9-20
 Measured RF fields inside residence B, similar to residence A, tended to be predominated by signals produced by wireless routers used for Internet connectivity throughout the home.

Table 9-7
 Summary of planar area scans performed with the SRM-3006 in front of residential meter installation at residence B, Downey, CA.

Location relative to meter	900 MHz RF LAN		2.4 GHz Zigbee	
	RF field (% public MPE)	Time of measurement (PDT)	RF field (% public MPE)	Time of measurement (PDT)
Surface	10.84	1:34	10.02	1:34
1	1.386	1:35	0.985	1:35
2	0.351	1:36	0.290	1:36
3	0.159	1:37	0.160	1:37
4	0.104	1:38	0.117	1:38
6	0.048	1:40	0.053	1:40
10	0.020	1:41	0.026	1:41

Table 9-8

Spectrum scan measurements of Smart Meter fields in the 900 MHz and 2.4 GHz bands in residence B, Downey, CA. RF field is peak value obtained from a spatial scan of the room interior or area in percent of FCC general public MPE.

Location at residence	RF field (% MPE)	
	900 MHz	2.4 GHz
Front yard	0.00056	0.00659
Bedroom 1	0.00053	0.0063
Bath	0.00056	0.00597
Bedroom 2	0.00052	0.00618
Bedroom 3	0.0015	0.00638
Bedroom 3 (closet behind meter)	0.00872	0.00755
Master bedroom	0.00060	0.00643
Family room	0.00057	0.00753
Dining room/Living room	0.00063	0.00641
Kitchen	0.00056	0.012
Study (with Wi-Fi)	0.00055	0.015
Bath	0.0011	0.00596
Backyard	0.0051	0.015

Residential apartment setting

The use of the specially programmed Smart Meters allowed for relatively quick and definitive measurements of the peak RF fields produced by the internal 900 MHz and 2.45 GHz transmitters. In an effort to acquire data on neighborhood RF fields that might be produced by existing in-place meters, a Downey, CA neighborhood was explored to identify apartment complexes that had obvious groups of meters installed in easily accessible areas for measurement. Measurements with the SRM-3006 instrument were subsequently accomplished in front of meter banks at two apartment buildings on August 20, 2010. Figures 9-21 and 9-22 show the two apartment meter banks with nine and eleven Smart Meters respectively.

At each of the two meter banks, the SRM-3006 was held at a distance of 1 foot from the frontal plane of the meters and moved back and forth and up and down in this plane to maximize the probability of capturing the peak value of any meter emissions. This process was continued for a period of five minutes at each of the two meter banks. Captured spectra were integrated to obtain the composite RF fields in terms of the instantaneous peak values and average values over the five minute monitoring period. Figure 9-23 shows the resulting observed spectrum of peak values at the nine meter bank with the integrated value of 4.6% of the public MPE. The corresponding integral of the average field was 0.00105% of the MPE.



Figure 9-21
A nine-meter bank at an apartment house in Downey, CA.



Figure 9-22
An eleven-meter bank at an apartment house in Downey, CA.

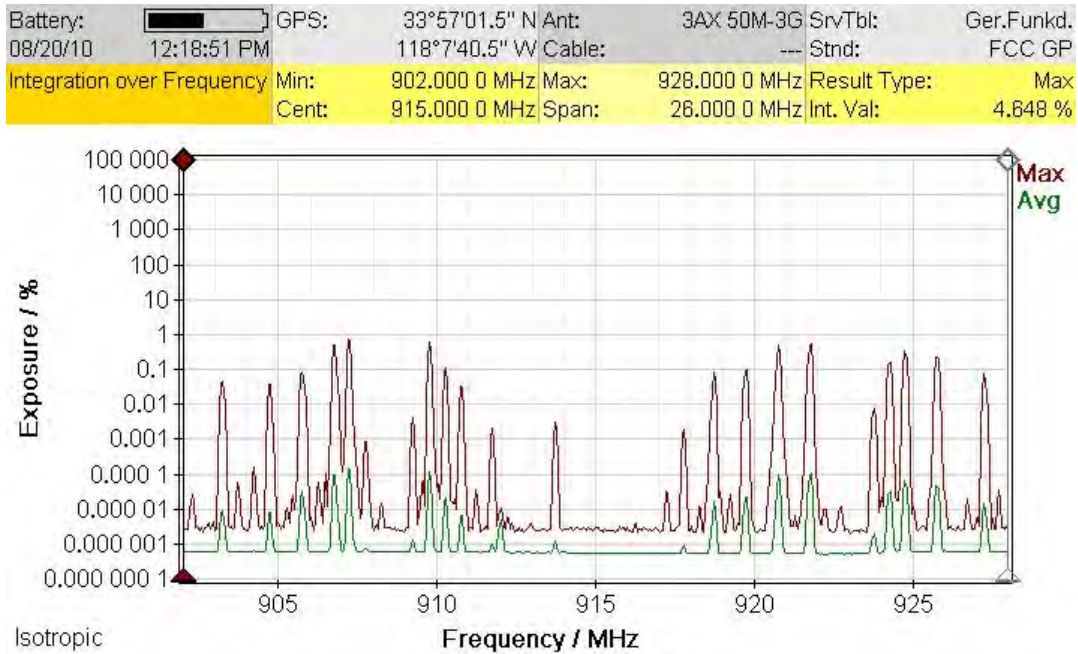


Figure 9-23
 Measured maximum (peak) and average RF fields in the 900 MHz band at one foot in front of a nine-meter bank of Smart Meters.

Figure 9-24 provides the measured spectrum of fields at the second meter bank consisting of eleven meters. In this case the integrated composite peak field was 4.9% of the MPE with an integrated composite average field of 0.00124% of MPE.

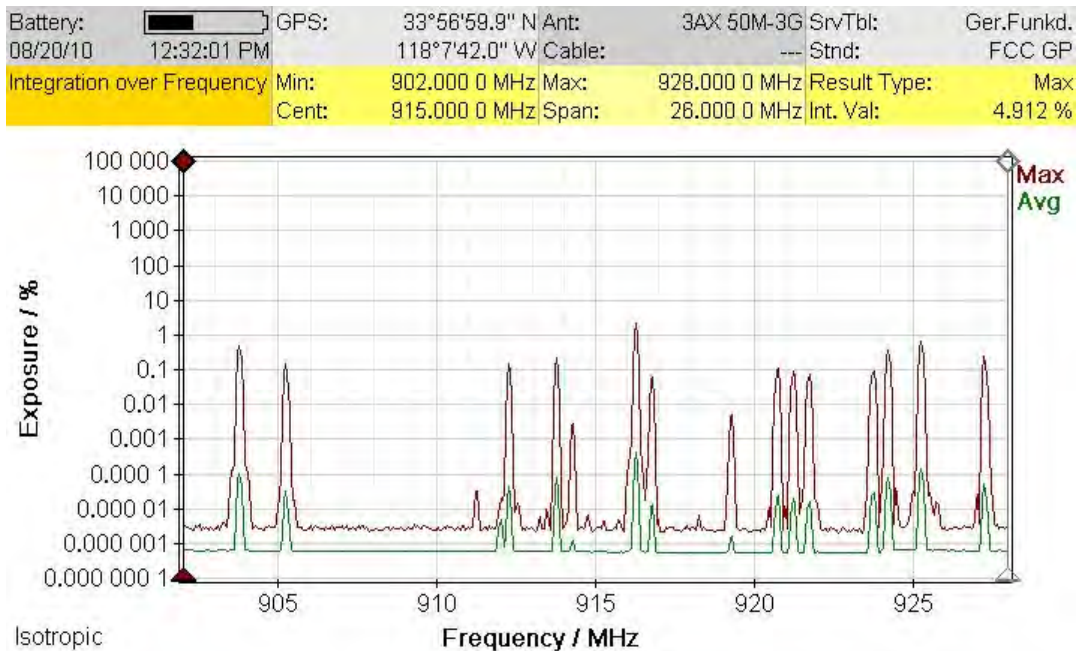


Figure 9-24
 Measured maximum (peak) and average RF fields in the 900 MHz band at one foot in front of an eleven-meter bank of Smart Meters.

Neighborhoods with and without Smart Meters

A driving survey of a Downey neighborhood where SCE had deployed Smart Meters was also conducted. Figure 9-25 illustrates the route followed by slowly driving in an automobile with the SRM-3006 probe held out of the front passenger window (see Figure 9-26). The objective of this exercise was to see if Smart Meter RF fields could be detected with the instrumentation used under these conditions and to see if a neighborhood with installed Smart Meters could be distinguished from another neighborhood in which Smart Meters had not been deployed. The resulting accumulative spectrum of peak fields is shown in Figure 9-27. It must be noted that these integrated values of RF field represent the instantaneous peak values of RF fields that were observed on the spectrum analyzer, even

if the field existed for a fraction of a second; for proper comparison to RF exposure standards, time-averaged values of RF fields must be used. Hence, the indicated integrated values are extremely conservative estimates of actual time-averaged exposure. A peak value corresponding to 0.00686% of the FCC MPE was found from the 34 minute drive. Because of the intermittent nature of the Smart Meter signals, peaks would appear from time to time but quickly vanished. While a large number of apparent Smart Meter signals could be observed, the average value of these signals is nearly vanishingly small. This activity was somewhat similar to walking through the Itron meter farm in that signals from the many meters occur randomly, making it difficult to definitely identify any particular meter's emission but relatively easy to observe signals when originating from many different meters.



Figure 9-25
Route in Downey, CA neighborhood with SCE deployed Smart Meters over which a driving survey was conducted to test the ability to detect RF signals associated with residential meter installations.



Figure 9-26
Conducting a "driving survey" of a Smart Meter deployed neighborhood.

Battery: 08/20/10 11:54:17 AM	GPS: 33°56'38.9" N 118°7'50.9" W	Ant: 3AX 50M-3G Cable: ---	SrvTbl: Ger.Funkd. Stnd: FCC GP
Integration over Frequency	Min: 902.000 0 MHz Cent: 915.000 0 MHz	Max: 928.000 0 MHz Span: 26.000 0 MHz	Result Type: Max Int. Val: 0.006 86 %

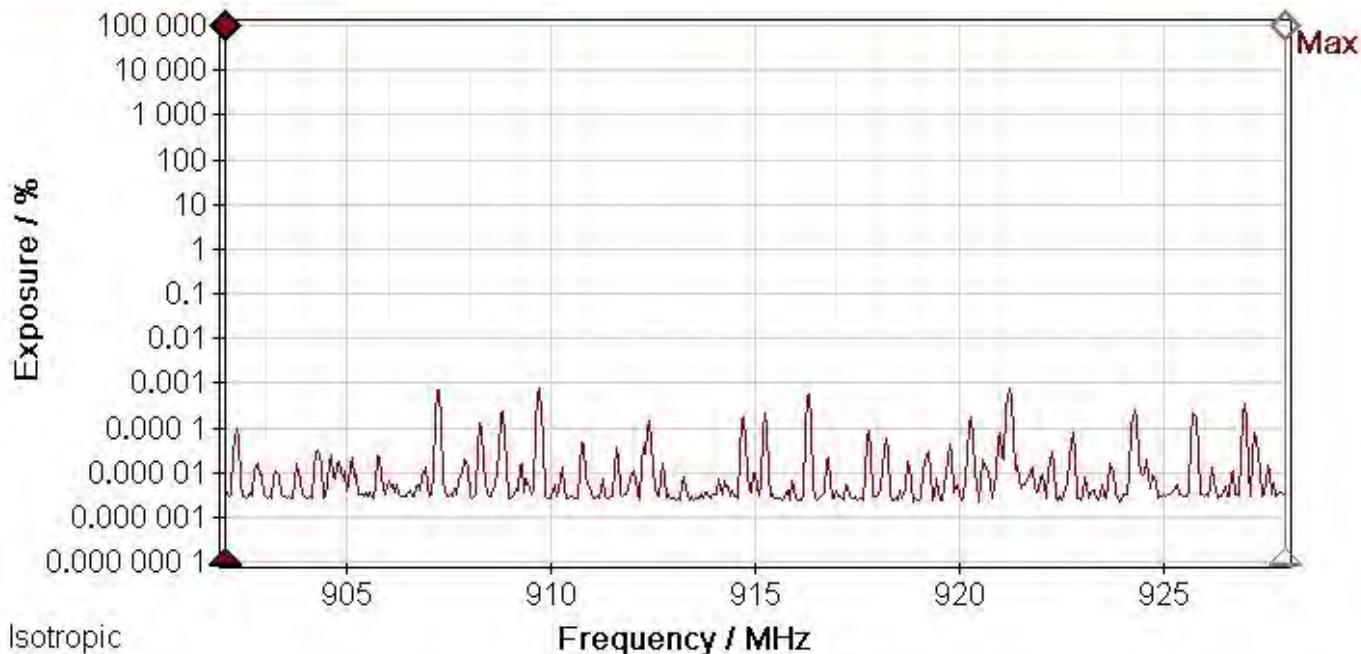


Figure 9-27
Measured peak spectrum of RF fields detected with the SRM-3006 during traveling the route mapped in Figure 9-25. Fields were monitored for a total of approximately 34 minutes.

To develop a comparative view of neighborhood ambient RF fields in the 900 MHz band, a driving survey through a portion of Santa Monica was conducted in the afternoon of August 20, 2010 (see route map in Figure 9-28). SCE had not yet deployed Smart Meters in Santa Monica at that time. The results of two spectrum scans in which the instantaneous peak fields were monitored are shown in Figures 9-29 and 9-30. These scans reveal a lack of 900 MHz signal activity other than for an occasional emission, perhaps related to

cordless telephones. While the residential neighborhood areas were essentially absent of 900 MHz activity, such was not the case for a commercial district in Santa Monica, as shown in Figure 9-31. As the survey vehicle turned onto a main street in the commercial district, signals were almost immediately noted to appear on the spectrum analyzer. None of these signals were exceptionally strong but they were plentiful during the few minutes spent within the commercial district.

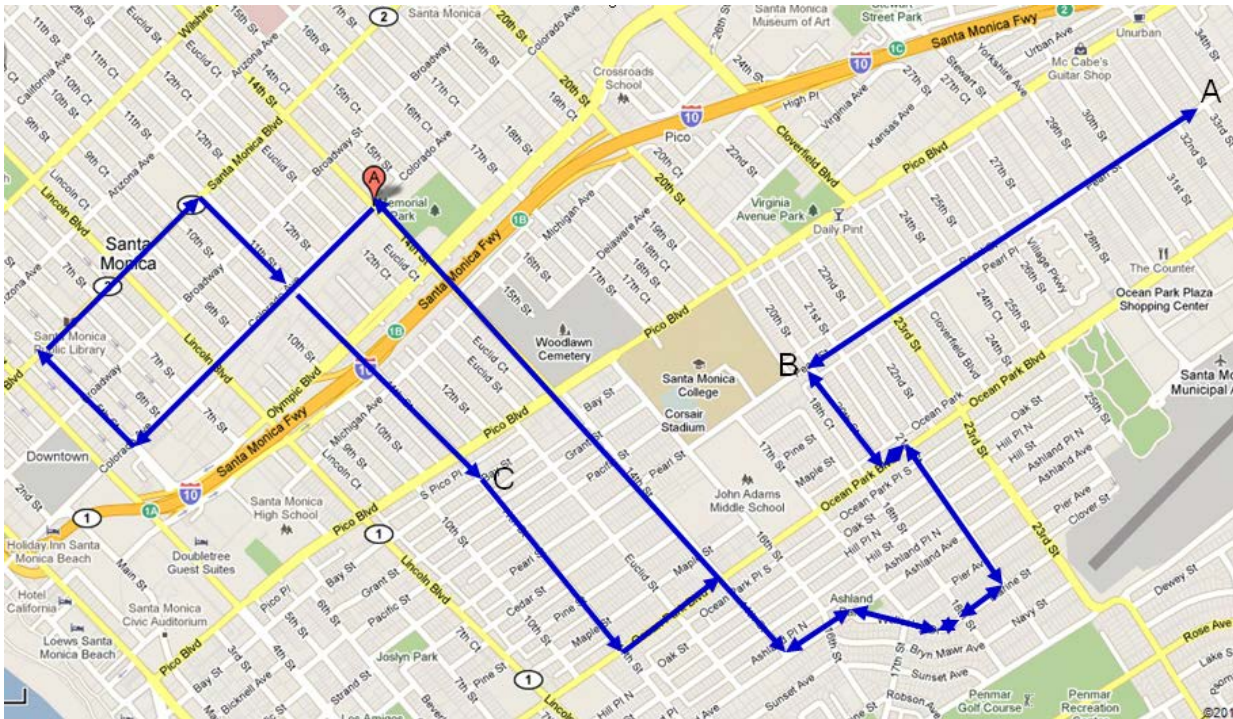


Figure 9-28
Route in Santa Monica, CA neighborhood where SCE Smart Meters have not been deployed over which a driving survey was conducted to test the ability to detect RF signals that might exist in the 900 MHz band.

Battery:	08/20/10	12:41:37 PM	GPS:	33°56'29.2" N	118°6'54.4" W	Ant:	3AX 50M-3G	SrvTbl:	---	Std:	Ger.Funkd.	FCC GP
Integration over Frequency	Min:	902.000 0 MHz	Max:	928.000 0 MHz	Result Type:	Max	Cent:	915.000 0 MHz	Span:	26.000 0 MHz	Int. Val:	0.000 60 %

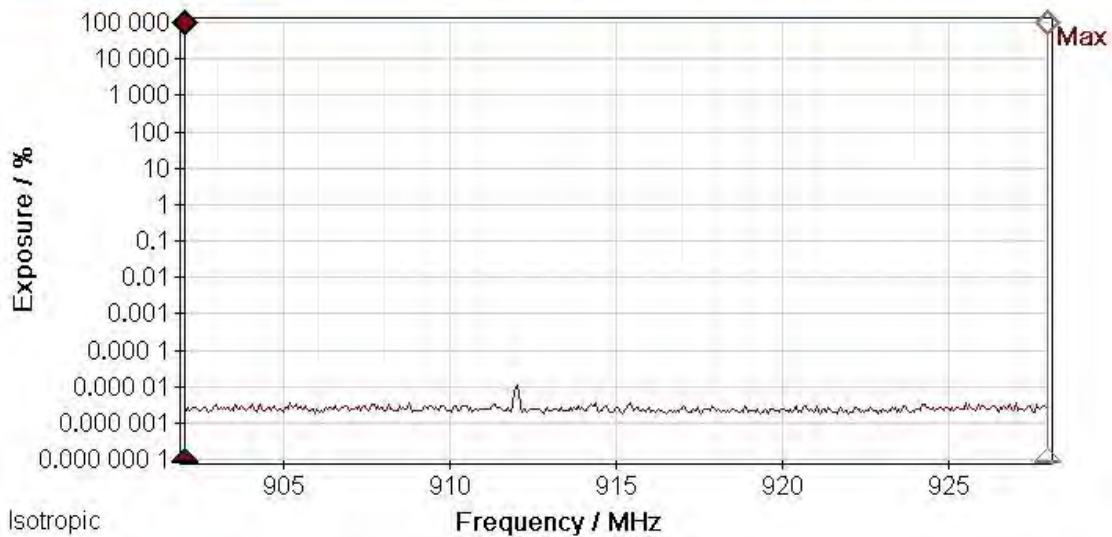


Figure 9-29
Spectrum scan in residential neighborhood of Santa Monica, CA consisting of an approximately 20 minute drive.

Battery:	Ext. Power	GPS:	34°0'37.6" N	Ant:	3AX 50M-3G	SrvTbl:	Ger.Funkd.
08/20/10	03:14:22 PM		118°27'37.0" W	Cable:	---	Stnd:	FCC GP
Integration over Frequency		Min:	902.000 0 MHz	Max:	928.000 0 MHz	Result Type:	Max
		Cent:	915.000 0 MHz	Span:	26.000 0 MHz	Int. Val:	0.000 93 %

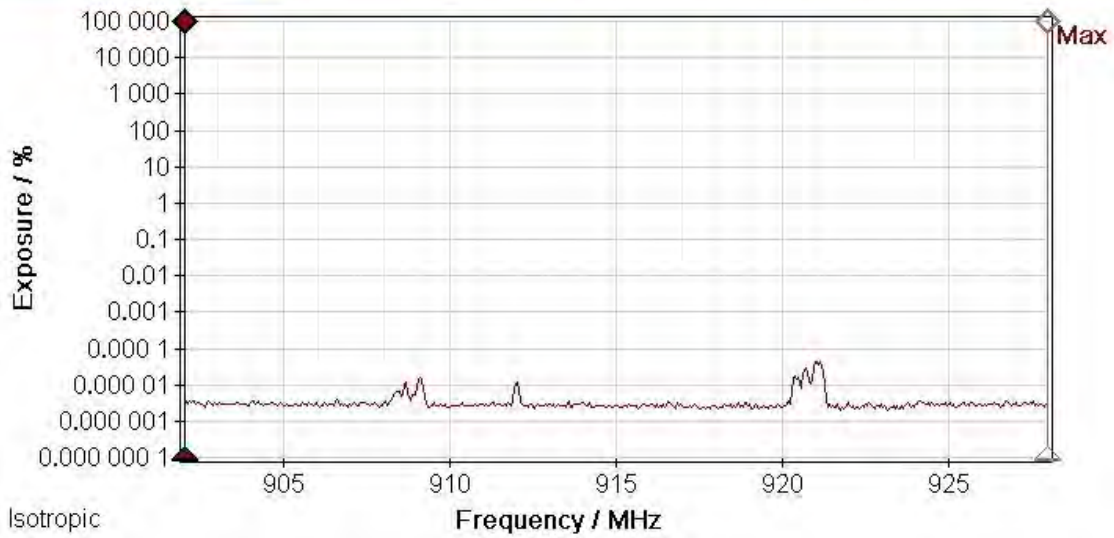


Figure 9-30
Spectrum scan in residential neighborhood of Santa Monica, CA showing weak signals, apparently caused by 900 MHz cordless telephones.

Battery:	Ext. Power	GPS:	34°0'48.8" N	Ant:	3AX 50M-3G	SrvTbl:	Ger.Funkd.
08/20/10	02:53:02 PM		118°28'44.4" W	Cable:	---	Stnd:	FCC GP
Integration over Frequency		Min:	902.000 0 MHz	Max:	928.000 0 MHz	Result Type:	Max
		Cent:	915.000 0 MHz	Span:	26.000 0 MHz	Int. Val:	0.001 96 %

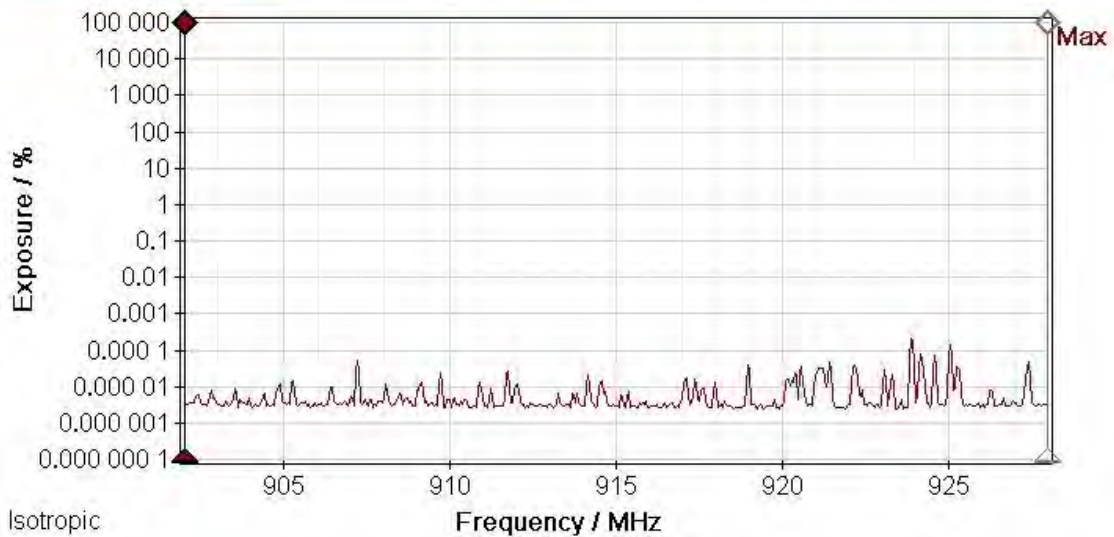


Figure 9-31
Spectrum scan in a commercial district of Santa Monica, CA showing noticeable activity from devices other than Smart Meters.

A second SRM-3006 was used to measure RF fields in several other frequency bands in Santa Monica, CA (The calibration certificates are contained in Appendix A). Measurements included the:

- FM radio broadcast band of 88-108 MHz (Figure 9-32),
- spectrum of 800 to 900 MHz band (Figure 9-33),
- PCS band from 1.9 to 2.0 GHz (Figure 9-34).
- VHF spectrum of 50 MHz to 216 MHz (Figure 9-35), and
- 2.4 to 2.5 GHz band which includes Wi-Fi and microwave ovens (Figure 9-36)

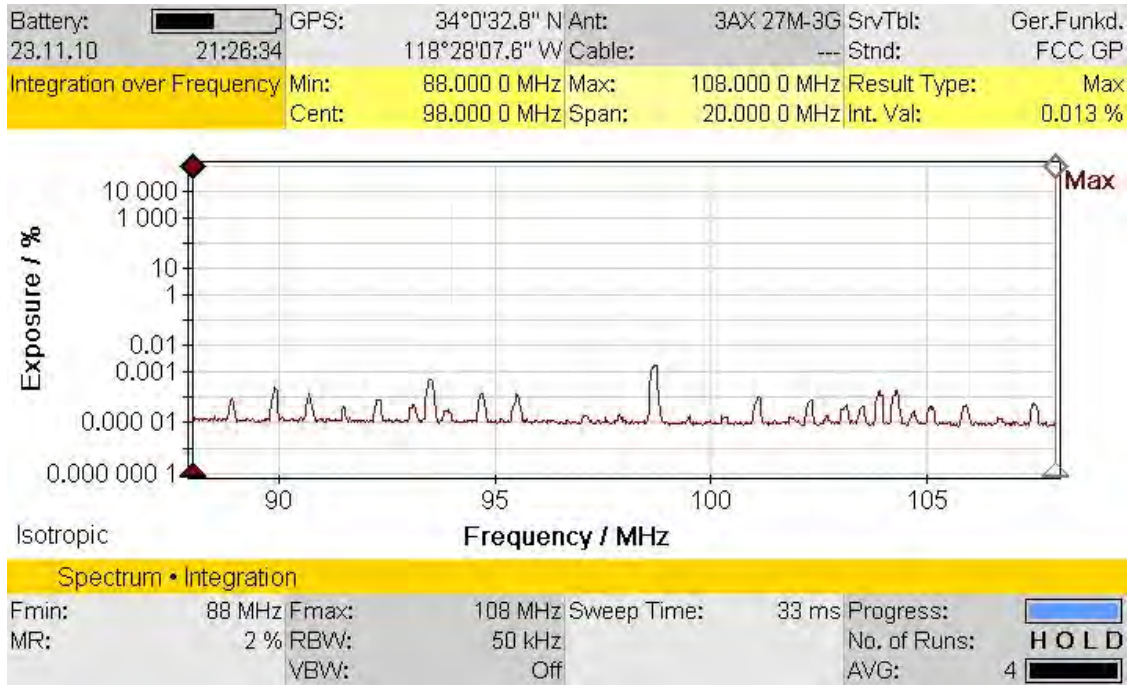


Figure 9-32
Spectrum scan of the FM radio broadcast band in Santa Monica, CA with a band integrated RF field equivalent to 0.013% of the FCC MPE for the public.

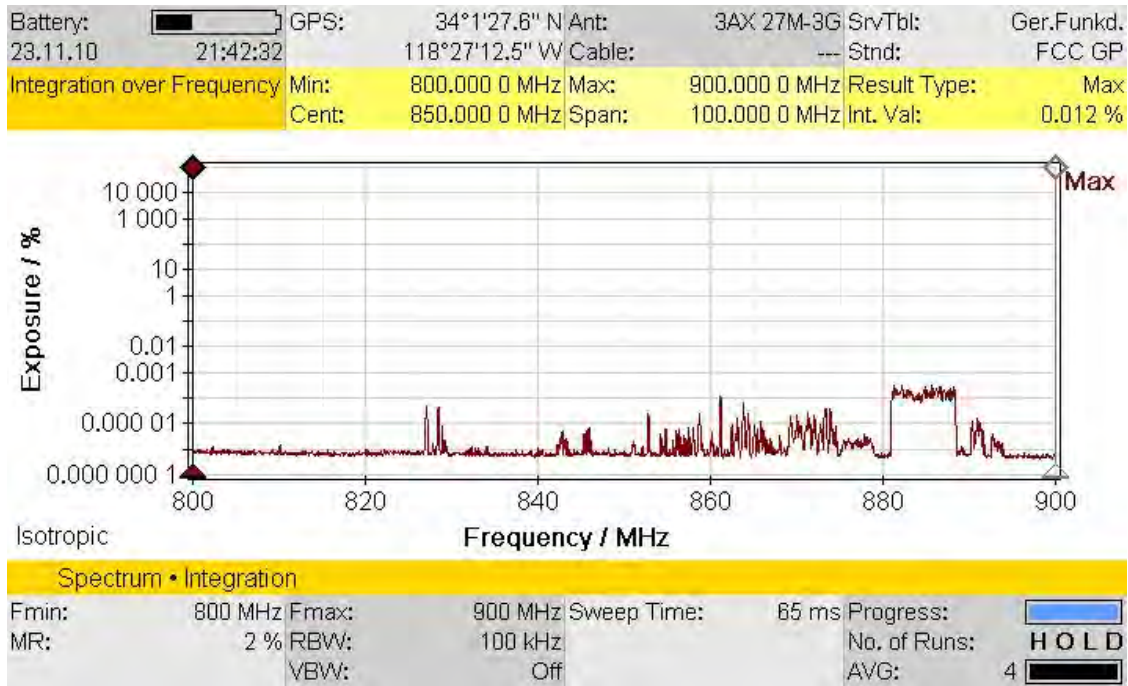


Figure 9-33
Spectrum scan of the 800 MHz to 900 MHz band in Santa Monica, CA, with a band integrated RF field equivalent to 0.012% of the FCC MPE for the public.

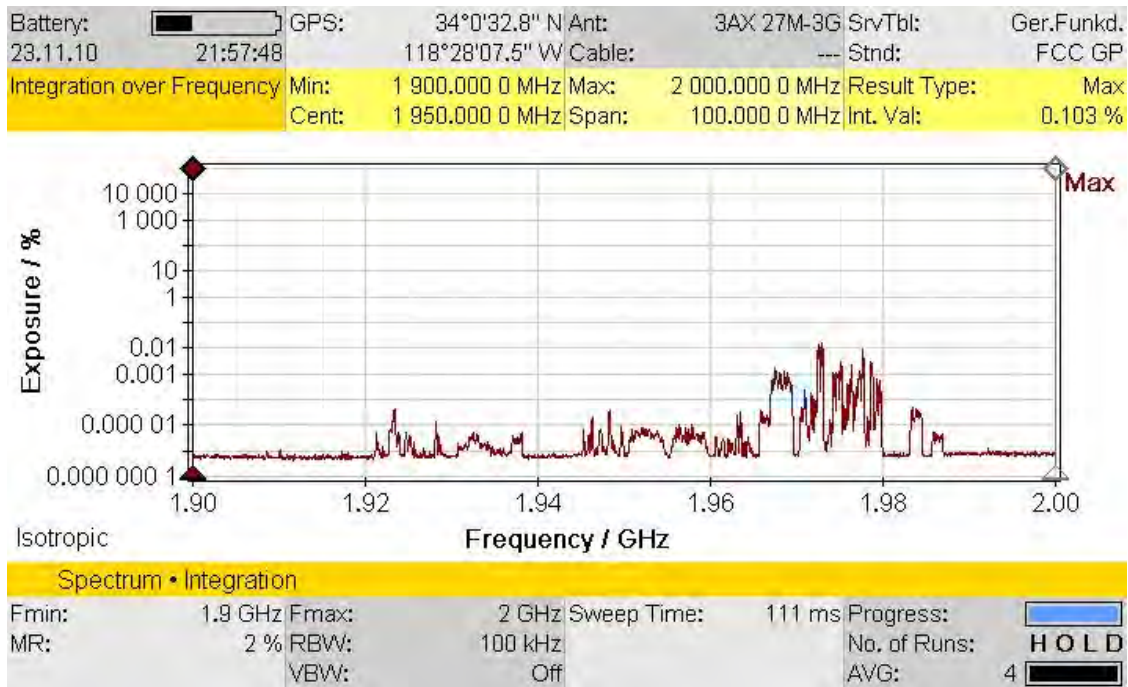


Figure 9-34
Spectrum scan of the 1.9 GHz to 2.0 GHz band in Santa Monica, CA, with a band integrated RF field equivalent to 0.103% of the FCC MPE for the public.

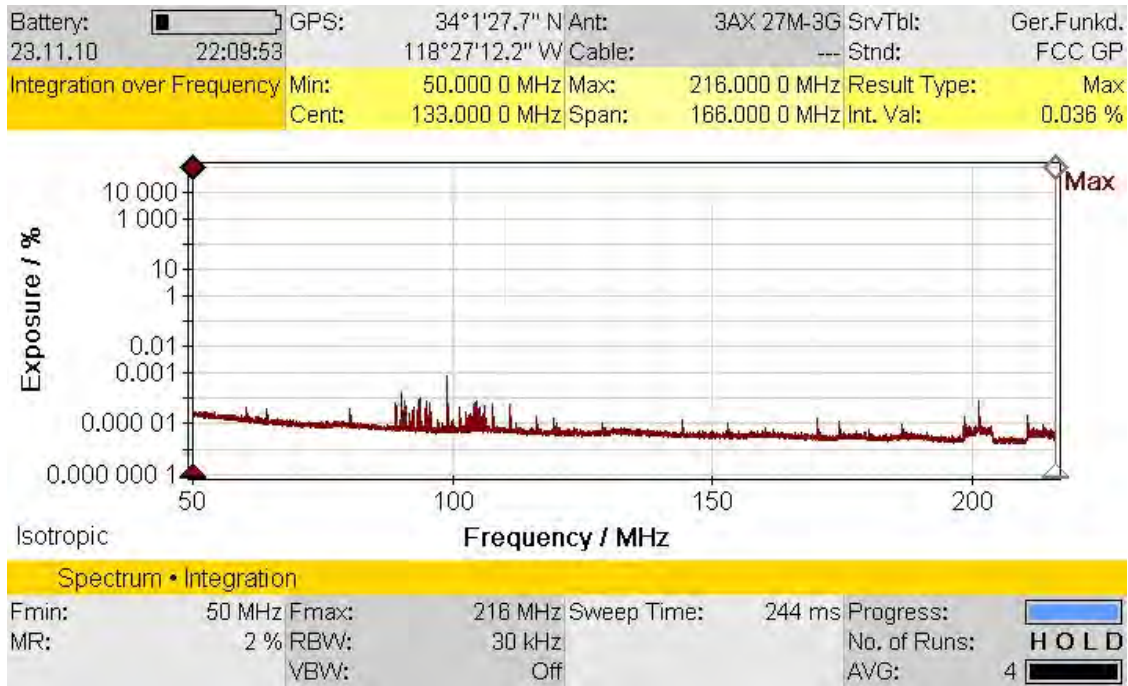


Figure 9-35
Spectrum scan of the 50 MHz to 216 MHz band in Santa Monica, CA, with a band integrated RF field equivalent to 0.036% of the FCC MPE for the public.

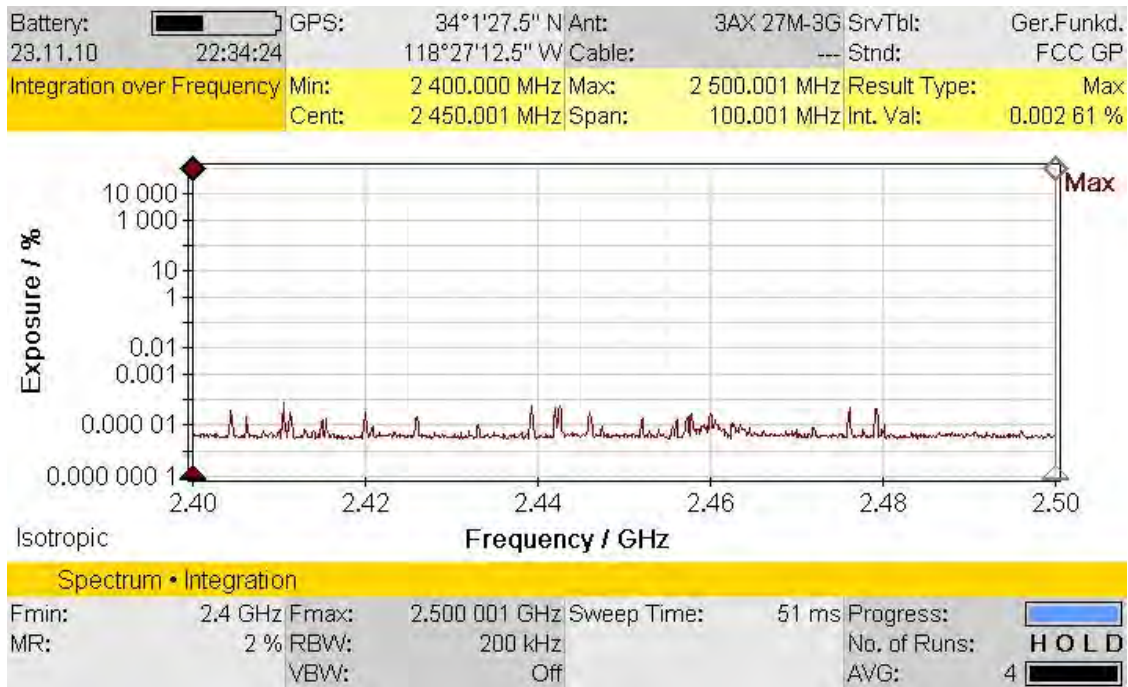


Figure 9-36
Spectrum scan of the 2.4 GHz to 2.5 GHz band in Santa Monica, CA, with a band integrated RF field equivalent to 0.0026% of the FCC MPE for the public.

The spectrum measurements represented in Figures 9-32-9-36 provide some perspective on environmental levels of RF from sources other than Smart Meters. The FM radio broadcast band has, historically, been determined to be a primary contributor to ambient RF fields¹⁵. Because most of the FM broadcasting within the LA region originates from atop Mt. Wilson, a considerable distance from many parts of the metropolitan area, median RF fields, in 1980, were found to be somewhat lower than in some other large

cities. However, with the introduction of cellular telephone base stations, ambient RF fields have likely increased somewhat simply due to the density of cellular and PCS base stations and their distribution among the population. Interestingly, Figure 9-34, which illustrates activity in the PCS band (cellular telephones), indicated the greatest value of peak RF field contribution of the several bands measured in this neighborhood set of measurements with a value equivalent to 0.1% of the FCC MPE.

¹⁵ Tell, R. A. and E. D. Mantiplly (1980). Population exposure to VHF and UHF broadcast radiation in the United States. *Proceedings of the IEEE*, Vol. 68, No. 1, January, pp. 6-12.

Section 10: Shielding Effectiveness Measurements

RF fields can be reduced in strength by introducing conductive materials between the field source and the area to be shielding from the emissions. For example, the metallic meter box within which all electric power meters are installed will attenuate RF fields that may be directed to the back of the meter. This is partially responsible for the reduction in radiated power directly behind Smart Meters tested found in this investigation. While performing the measurements of RF fields associated with Smart Meters in California, a series of measurements of insertion loss afforded by three different types of metal lath was conducted. Metal lath is commonly used in construction of stucco homes, typical of southern California and it was of interest to examine what influence such material might have on Smart Meter RF fields.

Shielding effectiveness of different metal meshes

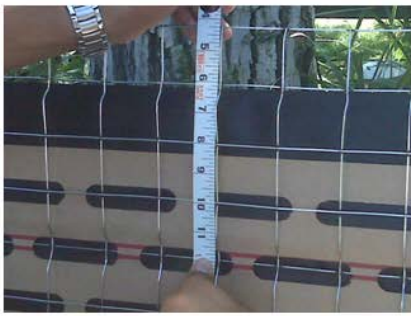
An impromptu measurement of three different metallic meshes was conducted by setting up the specially programmed Smart Meters, one for the 900 MHz band and the other for the 2.4 GHz Zigbee band, measuring the RF field with the SRM-3006 instrument and then placing a sheet of the different meshes between the

Smart Meter and the measurement probe. Figure 10-1 shows this process where the Smart Meter is installed in a specially designed socket to allow convenient operation of the meter in different locations.

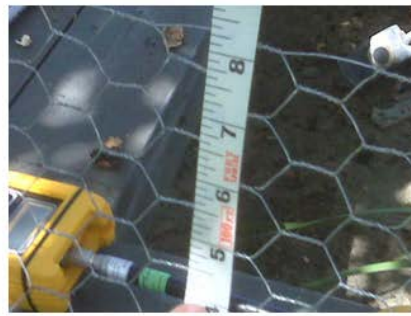
Three different forms of metal lath (mesh/netting) were evaluated at both the 900 MHz and 2.4 GHz frequencies associated with the Smart Meter emissions. Figure 10-2 shows these lath samples. The lath shown in panel A consisted of a square shape, measuring 2 inches on a side. The lath in panel B is what is commonly known as “chicken wire” consisting of hexagonal shaped openings approximately one inch by one inch. The lath in panel C was comparatively, significantly smaller in dimension, measuring approximately one-quarter inch by one-half inch for the openings. The lath in panel C is more commonly used in plaster work as opposed to exterior stucco application but is also used in application of exterior rock surfacing in some areas of the country. Insertion loss measurement results for the different types of metal lath are given in Table 10-1. Insertion loss is expressed in linear units as a reduction factor and logarithmically as decibels (dB). These data are presented graphically in Figure 10-3.



Figure 10-1
Measurement setup to determine the insertion loss presented by a conductive mesh (chicken wire in this case).



2" x 2"



1" x 1"



0.25" x 0.5"

Figure 10-2

Measurement setup to determine the insertion loss presented by a conductive mesh (chicken wire in this case).

Table 10-1

Insertion loss measurement results for three different types of metal lath expressed as a reduction factor (F) and in decibels (dB).

Frequency band	Panel A lath		Panel B lath		Panel C lath	
	F	dB	F	dB	F	dB
900 MHz	2.5	4.1	8.9	9.5	82	19.1
2.4 GHz	1.3	1.2	2.6	4.2	14	11.4

RF Insertion Loss of Different Mesh Sizes

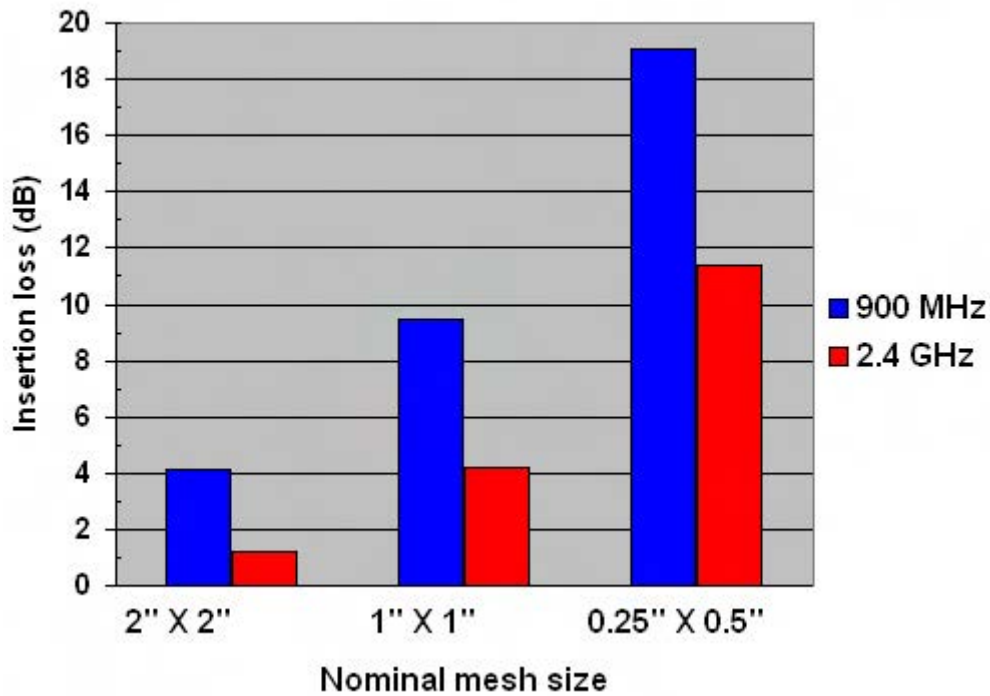


Figure 10-3

Insertion loss of three different metal mesh sizes.

The data given in Table 10-1 and shown in Figure 10-3 show an expected increase in insertion loss (attenuation) of RF fields with decreasing mesh size and a decrease in insertion loss with the higher frequency band. With the relatively large 2" by 2" mesh, the least insertion loss was associated with the 2.4 GHz band. The greatest insertion loss was for the longer wavelength emission in the 900 MHz band and the finest mesh size. The data suggest that the chicken-wire type netting commonly used in stucco home construction can afford significant reductions in RF fields that may enter the home ranging from 4.2 dB to 9.5 dB. This range corresponds to mesh transmissions of 38% in the 2.4 GHz band and 11% in the 900 MHz band.

Shielding effectiveness of a simulated stucco wall

To more completely evaluate the attenuation exhibited by a typical stucco wall, as might be found in southern California homes, a simulated wall section was constructed in Colville, WA. The wall was built as a 4 feet wide by 8 feet tall section on a support with casters to allow mobility. The wall was constructed with 2x4 dimensional lumber with studs on 16 inch centers with the "outside" wall sheathed with 7/16" OSB (oriented strand board). This sheathing was then covered with one layer of underlayment paper (Davis Wire All Purpose Super Kraft Asphalt Sheathing Paper) followed with the "chicken wire" lath being stapled onto the wall section (Davis Wire "self-furr" stucco netting, woven 17 gauge, 1.5 inch by 2.25 inch mesh opening). Two coats of stucco (Spec Mix® Scratch & Brown Preblended Stucco), including a base scratch coat followed with a brown coat, were applied to the lath. Each coat was allowed to set for several days. R-13 fiberglass insulation (Owens Corning with Kraft facing) was placed between the studs and the "interior" side of the wall was then covered with half-inch sheetrock (dry wall). Appendix F shows the wall during construction and Figures 10-4 and 10-5 show it set up with a Smart Meter positioned on a shelf on the "outside" wall surface with the two different measurement antennas supported on a tripod.

Measurements were conducted using the Wi-Spy spectrum analyzer device described earlier. The Wi-Spy unit was evaluated prior to its use by injecting swept signals from a communications monitor (IFR Model 2975) and using the Wi-Spy to acquire a large number of scans of the 900 MHz and 2.4 GHz bands. The Wi-Spy was determined to exhibit a response across each band that was within the range of ± 0.5 dB. A yagi antenna was established on a support and directed toward a Smart Meter programmed for continuous operation without the wall in place. The Smart Meters¹⁶ were positioned approximately 1 inch from the stucco surface of the wall to the rear surface of the meter and 58 inches from the ground to the center of the meter. RF field strength was then measured without the wall and with the wall in place to assess insertion loss. The measurement antenna and the Smart Meter was not moved during this process; only the wall was removed and replaced for the measurements with and without the wall. For the 900 MHz band, the five element yagi antenna was an M² Antenna Systems, Inc. Model 911-ISP (with 11 dBi gain) set 37 inches from the backside of the simulated wall to the end of the antenna boom and at the same height as the center of the Smart Meter. For the 2.4 GHz band, the yagi antenna was an Air802, LLC Model ANYA2412 (with 12 dBi gain) set 47 inches from the backside of the simulated wall to the end of the antenna boom. Figure 10-4 shows the 900 MHz yagi antenna in place for measuring the RF field behind the simulated wall. The 2.4 GHz yagi is shown during measurements of the attenuation of the wall in the higher frequency band in Figure 10-5.

For each frequency band, a series of five repeated measurements were performed of the received signal strength, measured in dBm, for horizontal and vertical polarizations. Table 10-5 summarizes the measurement data from which insertion loss values for the 900 MHz band and 2.4 GHz bands were determined. A representative view of the Wi-Spy spectrum analyzer display is seen in Figure 10-6.

¹⁶ Model CL200, 902.25 MHz, SCE# 222010-273722. Model CL200, 2405 MHz, SCE# 222010-273720.



Figure 10-4
Measurement setup for determining insertion loss of simulate stucco wall shown with the 900 MHz yagi antenna.

The data in Table 10-2 show that, under the measurement conditions used, the simulated stucco wall offered an overall average insertion loss (attenuation) of the Smart Meter RF fields of 6.1 dB in the 900 MHz RF LAN band and 2.5 dB in the 2.4 GHz Zigbee band. These data are consistent with the earlier measurements of insertion loss of different dimension metallic lath materials using the isotropic probe of the SRM-3006 instrument. Differences between the two sets of measurements are likely due to the different dimensions of the wire netting (1.5 inches in this case), inclusion of the wall building materials and the different measurement distances used. In the case of the earlier

described measurements, the measurement probe was located 6 inches from the various mesh materials compared to between 37 and 47 inches in the simulated wall measurements. Further, the isotropic measurements were made with the Smart Meter source placed 6 inches from the mesh and directed toward the mesh; some degree of interaction with the RF transmitters could be expected that could also contribute to differences in measured values of insertion loss. In the simulated wall measurements, the back of the meter was placed within 1 inch of the stucco with its underlying metallic netting.



Figure 10-5
Measurement setup for determining insertion loss of simulate stucco wall shown with the 2.4 GHz yagi antenna.

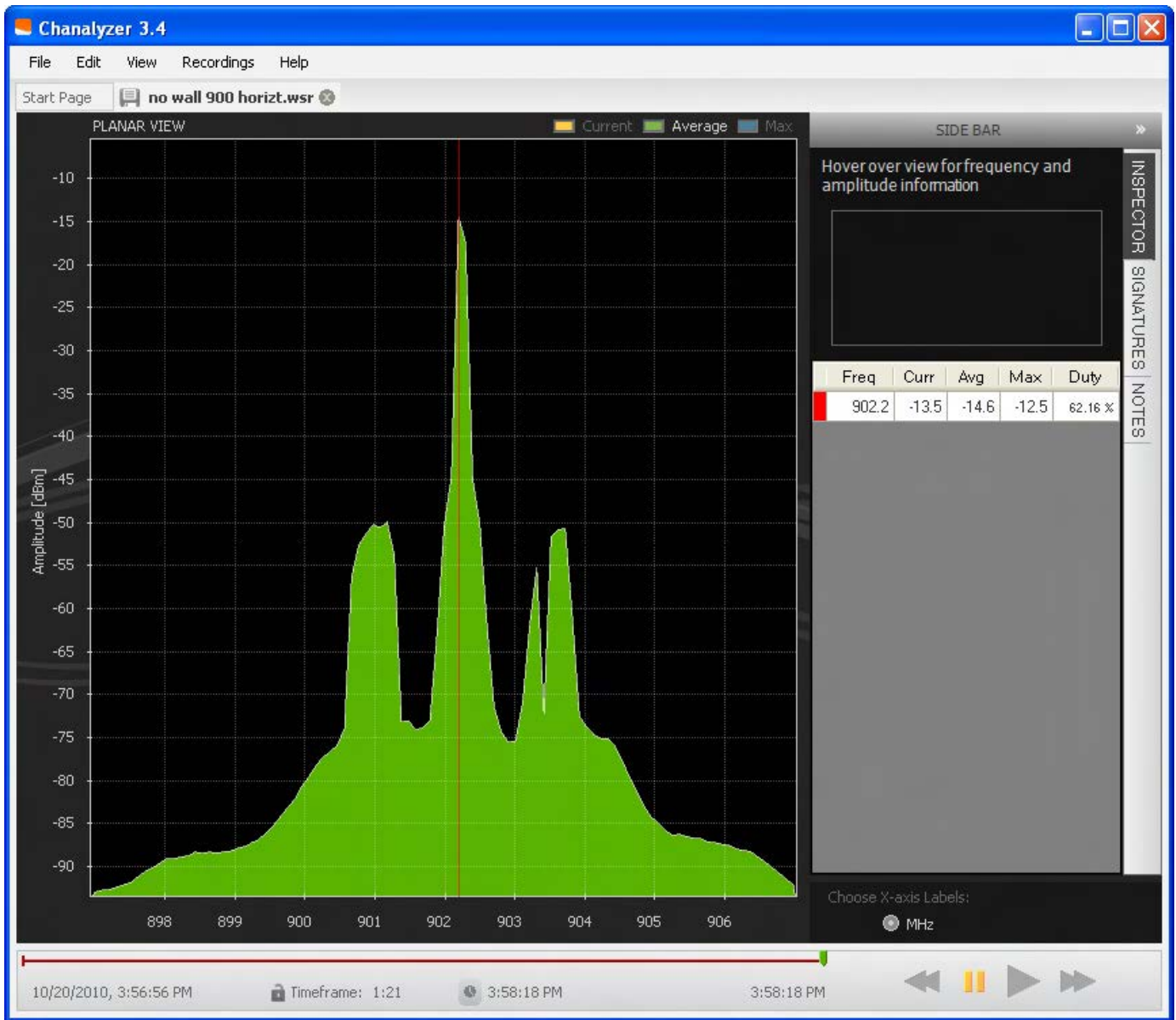


Figure 10-6
 Illustrative display of the Wi-Spy spectrum analyzer display showing the captured average signal measured over a period of 81 seconds from a 900 MHz RF LAN Smart Meter transmitter. In this measurement, the simulated wall was not present. Marker readout data are shown on the right side of the display.

Table 10-2

Insertion loss measurement data for simulated wall in 900 MHz and 2.4 GHz bands.

Frequency (MHz)	Trial	Signal level (dBm)				Insertion loss (dB)
		No wall		With wall		
		Horizontal	Vertical	Horizontal	Vertical	
902.25	1	-14.5	-18.2	-22.5	-21.8	6.2
902.25	2	-14.5	-18.0	-22.5	-21.5	6.1
902.25	3	-14.5	-18.3	-22.6	-21.4	6.0
902.25	4	-14.5	-18.0	-22.5	-21.6	6.1
902.25	5	-14.5	-18.1	-22.5	-21.6	6.1
					Mean±SD	6.1±0.1
2405	1	-30.7	-34.7	-34.7	-35.6	2.9
2405	2	-30.5	-35.0	-34.8	-35.2	2.8
2405	3	-30.7	-35.3	-34.5	-34.5	2.1
2405	4	-30.3	-35.2	-34.6	-33.8	2.1
2405	5	-30.3	-35.2	-34.4	-34.6	2.4
					Mean±SD	2.5±0.4

Section 11: Spatial Variation of RF Fields

During the time that the simulated wall was being constructed, the variation of RF field along a vertical line adjacent to a Smart Meter was determined for the 900 MHz RF LAN and the 2.4 GHz Zigbee transmitters. This measurement was to provide practical insight to the spatial distribution of exposure for someone standing near a Smart Meter. Such is relevant since RF exposure limits are in terms of not only time averaged values of fields but the spatial average over the dimensions of the body. In practice, to evaluate the spatial average for purposes of demonstrating

compliance with the IEEE exposure limits, an average of the RF field power density along a vertical line is recommended in IEEE C95.1-2005.

The SRM-3006 was used to measure the RF fields and log repetitive values as the SRM-3006 probe was moved slowly from the floor to a height of six feet above the floor with the Smart Meter positioned on a nonconductive table at a height of three feet. Figures 11-1 and 11-2 illustrate the measured results for this evaluation for the 900 MHz RF LAN and 2.4 GHz Zigbee bands.

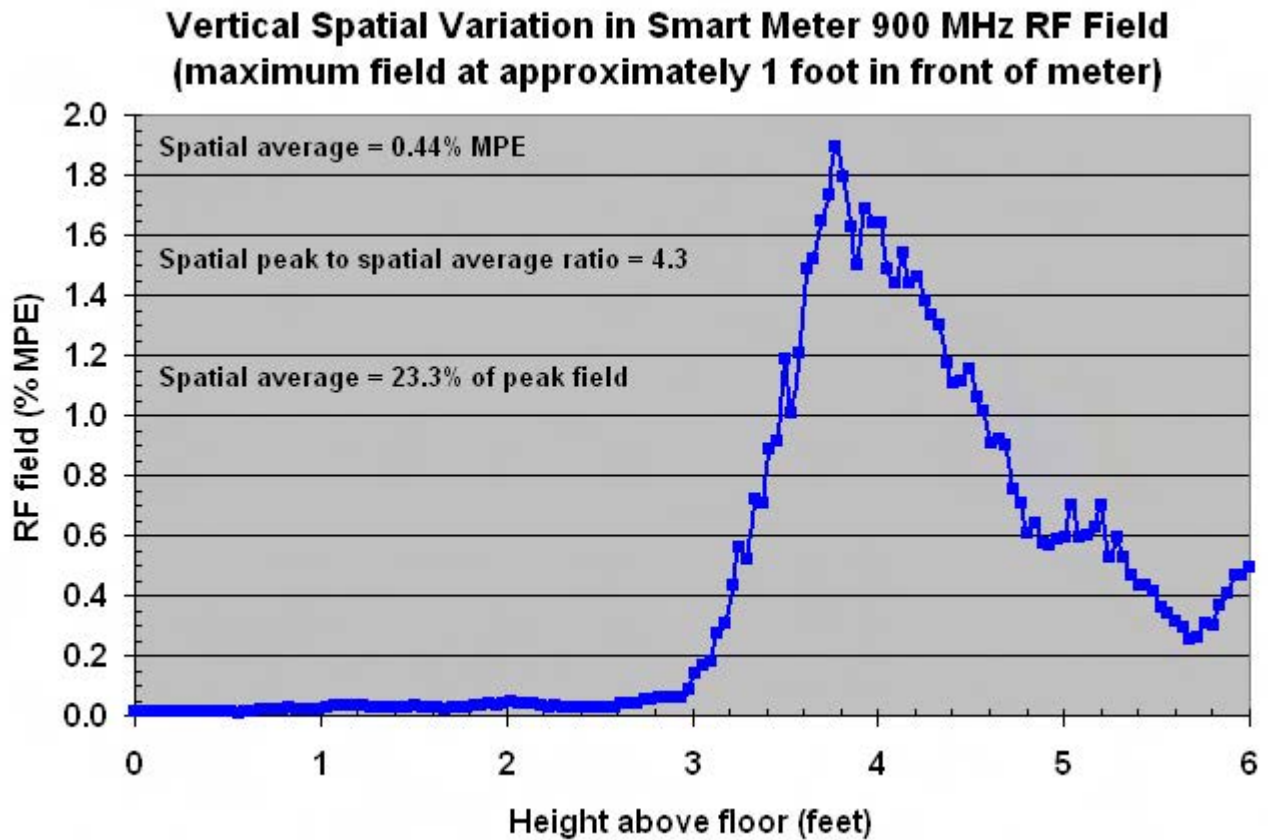


Figure 11-1
Vertical spatial variation in Smart Meter 900 MHz RF LAN field from 0 to 6 feet above the floor at a lateral distance from the Smart Meter of approximately 1 foot.

When the 252 readings obtained for the 900 MHz band over the six foot vertical height were analyzed, a spatial average equivalent to 0.44% of the MPE was obtained. The peak value was equivalent to 1.9% of the MPE. Hence, the six-foot spatial average was 23.3% of the overall peak value.

The result of similar measurements for the 2.4 GHz Zigbee transmitter with the Smart Meter at the same

height is shown in Figure 11-2. A total of 136 measurements were made along the vertical span of six feet. Analysis of the values resulted in a peak value equivalent to 1.3% of the public MPE with a spatial average of 0.24% making the spatial average 17.8% of the overall peak value. These results provide insight to how the spatially averaged exposure is related to the maximum (peak) value of field for someone standing immediately near a Smart Meter.

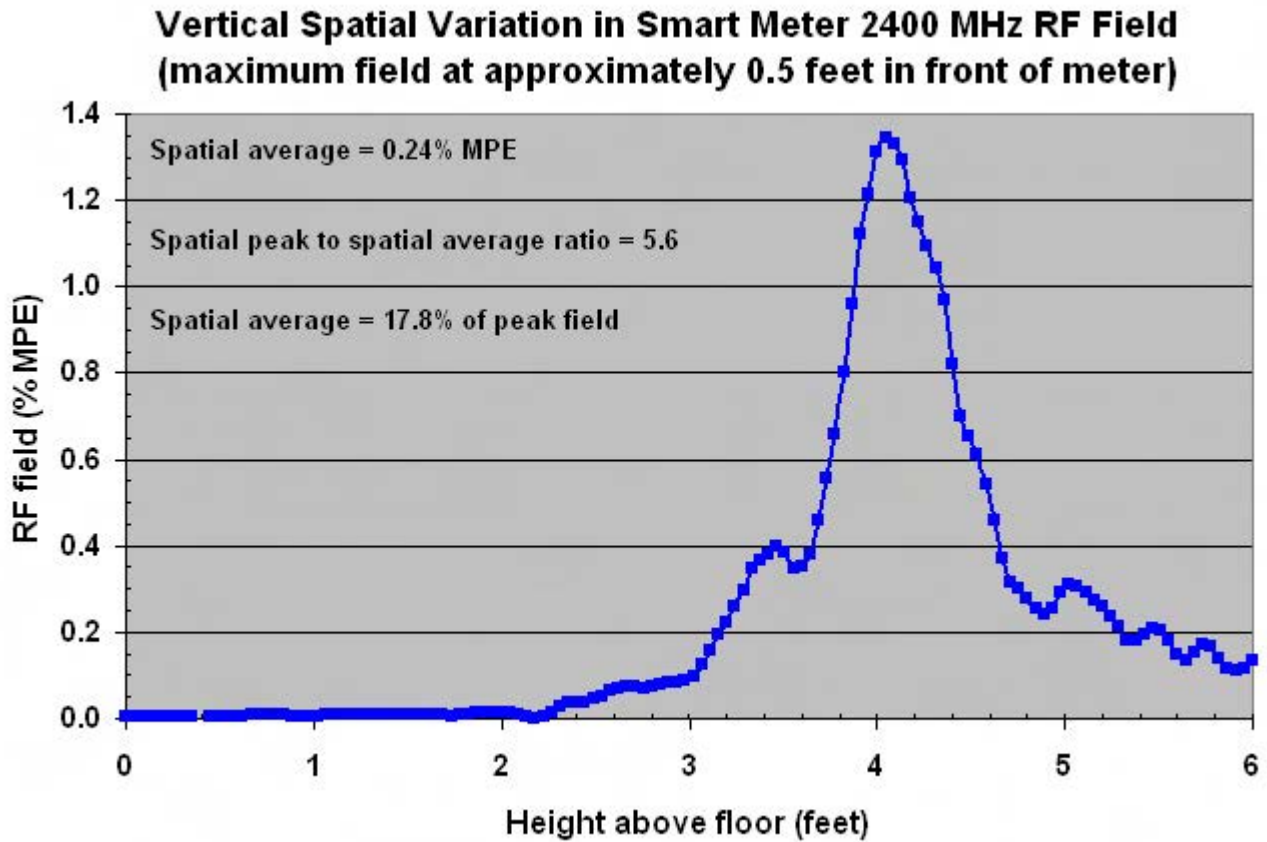


Figure 11-2
Vertical spatial variation in Smart Meter 2.4 GHz Zigbee transmitter field from 0 to 6 feet above the floor at a lateral distance from the Smart Meter of approximately 0.5 feet.

Section 12: Operational Duty Cycle of Meter Transmitters

While the utility of using continuous transmissions for performing measurements to characterize the magnitude of RF fields from Smart Meters has been described in this report, all of the scientifically based human exposure standards for RF exposure are in terms of time-averaged values of the RF fields, typically expressed in power density units. Attempting to make measurements of the actual time-averaged field magnitude, however, can be very difficult and time consuming. Further, the transmitter activity of a given Smart Meter is expected to vary from hour to hour and day to day. Hence, a single determination of duty cycle may provide insight to the likelihood of the value being rather large or very small but without much statistical power. Ideally, the duty cycle should be characterized over a sufficiently long time period to provide confidence in what the maximum expected duty cycle during any 30-minute period would be¹⁷. Clearly, making such determinations from on-site RF field measurements is fraught with significant challenge since an extended monitoring program would be needed. The limited measurements discussed below represent on a very preliminary approach to dealing with this challenge. A more comprehensive technical approach is warranted that is beyond the scope of what this project represented.

SRM-3006 measurements of peak and average values

Two different opportunities were pursued that provided limited insight to Smart Meter duty cycles. First, in the Itron meter farm, the SRM-3006 was taken on a stroll down two lanes of a part of the meter farm (western part), walking approximately mid-distance between the rows of meter racks (approximately 10-11 feet from either row of meter racks as shown in Figure 12-1. The instrument was set for measurement of both the peak field and average field. After completion of the walking survey, the recorded spectrum appeared as in Figure 12-2. When the peak and average spectra were integrated, the overall composite peak field was indicated as 0.114% of the MPE and the average value was indicated as 0.00023% of the MPE. These values may provide insight to what might be found in Smart Meter deployed neighborhoods and should represent conservative estimates of the magnitude of RF fields since it is difficult to envision a residential neighborhood with such a dense distribution of Smart Meters.

¹⁷ Thirty minutes is the averaging time for the FCC MPE for general public exposure.



*Figure 12-1
Measurements of aggregate maximum and average RF fields found along two rows of Smart Meters in the Itron meter farm during normal operation of the meters.*

Battery: 07/29/10 03:14:01 PM	GPS: 34°46'05.0" N 83°2'22.7" W	Ant: 3AX 50M-3G	SrvTbl: ---	Ger.Funkd. FCC GP
Integration over Frequency	Min: 902.000 0 MHz	Max: 928.000 0 MHz	Result Type: Avg	
	Cent: 915.000 0 MHz	Span: 26.000 0 MHz	Int. Val: 0.000 23 %	

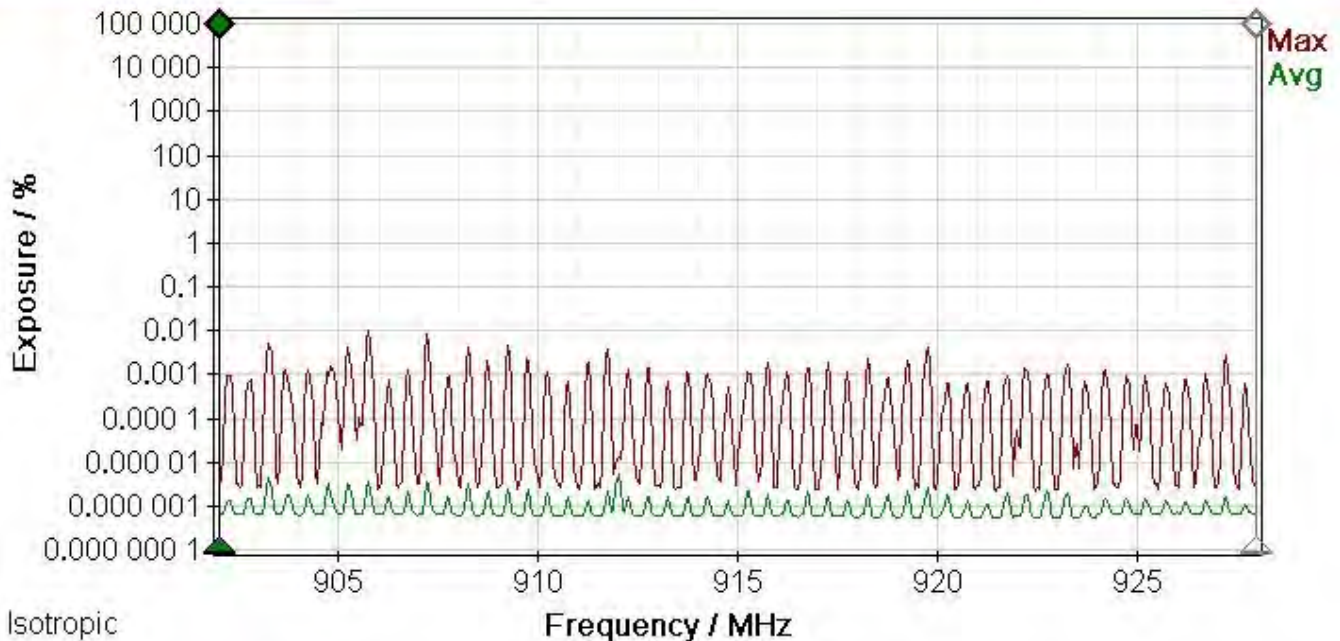


Figure 12-2
Spectrum analysis measurement of RF fields during walk through section of the Itron meter farm in which both the maximum (peak) field and the average field was measured.

An estimate of the duty cycle associated with operation of multiple Smart Meters is provided by the ratio of the average to peak integrated values. In this case, the ratio was equivalent to an approximate duty cycle of 0.2%. This singular value provides no insight to what the duty cycle might be of an individual, residential meter since measurements over a much longer period would be required.

Secondly, measurements taken at two apartment buildings in Downey, California during which measurements were performed over five-minute periods in front of banks of nine and eleven Smart Meters. The ratio of the integrated average to integrated peak spectra yielded apparent duty cycles of approximately 0.023% at the nine meter bank and 0.025% at the eleven meter bank. These values are substantially less than that found in the vicinity of thousands of meters at the Itron meter farm despite that fact that transmitter activity was easily noticeable during even the short duration of measurement.

Wi-Spy spectrum analyzer measurements

A Wi-Spy spectrum analyzer, described earlier in the instrumentation section, was applied to the measurement of the momentary emissions of a residential Smart Meter. A Wi-Spy feature that records the result of each spectrum scan by the analyzer was exploited to evaluate whether such a low cost instrument could be effective in revealing Smart Meter duty cycles. The device was placed close to a residential Smart Meter and allowed to acquire scans of the 902-928 MHz spectrum over a period of an hour. Each scan took approximately 0.37 seconds so during one hour of monitoring, approximately 10,657 scans of the spectrum were accumulated and stored to the hard disc drive of the laptop computer. This measurement was made during a time when the mesh network was being queried and the meter was expected to be transmitting. In essence, the frequency spectrum is captured as 255 signal amplitude values uniformly distributed over the frequency band. The resolution bandwidth of the Wi-Spy analyzer was 125 kHz. The stored data file was opened and converted to a spreadsheet compatible format to allow inspection of the individual signal levels

at each frequency for each of the 10,657 scans to provide insight about transmitter activity during the monitoring period. Hence, a spreadsheet containing a number of rows equal to the number of scans accomplished by the Wi-Spy analyzer with 255 columns resulted. A primary objective was to determine whether the recorded data in the Wi-Spy file could be interpreted in terms of transmitter activity.

The strategy used in inspecting the data was to count how many rows of data contained at least one instance of a signal being present on any frequency within the spectrum. This would signify that an emission from the meter was captured by the analyzer. Since the analyzer can only record the amplitude of a given frequency once every 0.37 seconds, it cannot accurately indicate how

long any particular emission lasted, only that one occurred during a scan. Thus, the analysis method applied in this case was that if an emission was detected during any one scan, it was assumed to last for the duration of the scan. In this way, a count of the total number of scans in which a signal was detected when multiplied by the scan time was assumed to conservatively represent (over estimate) the total amount of time that the transmitter was active. Duty cycle was then obtained by simply dividing the total transmit time by the total observation time.

Figure 12-3 shows the appearance of one of the measured “max hold” spectra of signals observed at a residential Smart Meter during an approximately 66 minute monitoring period.

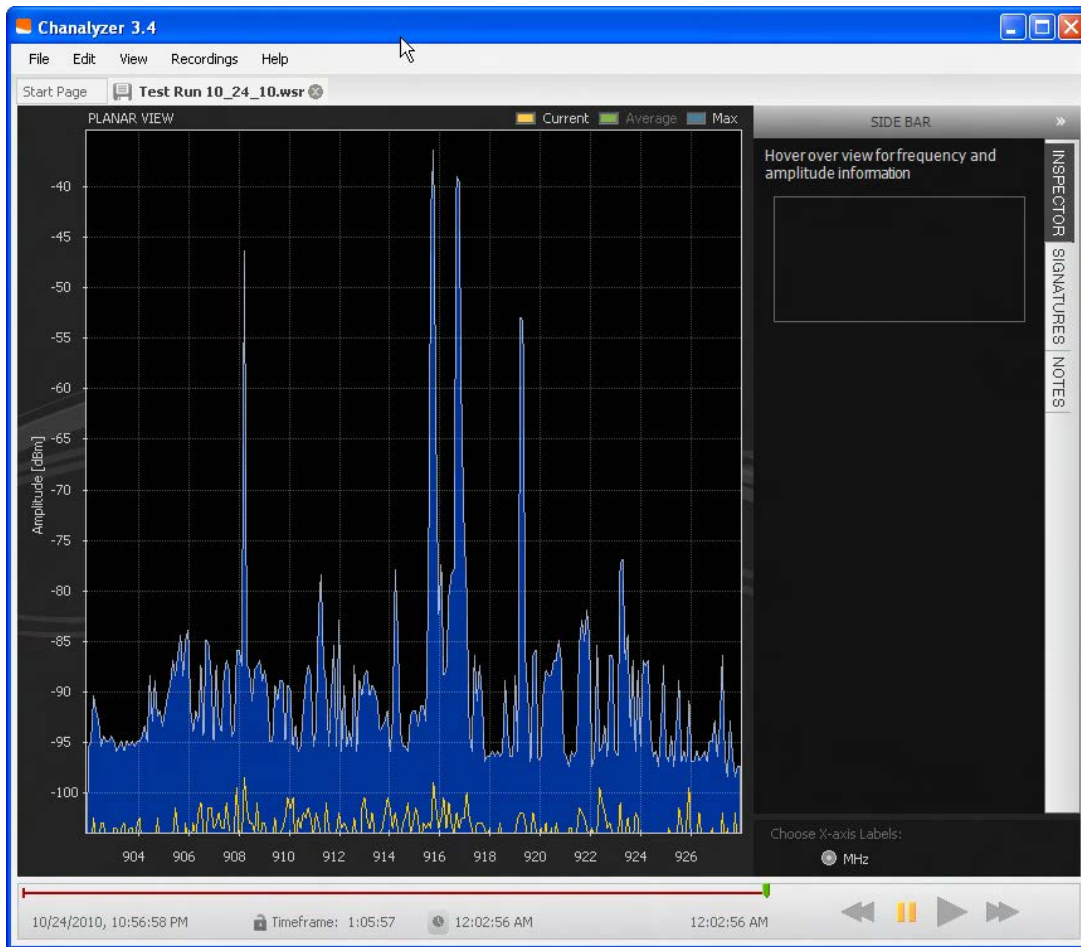


Figure 12-3
Wi-Spy display of Smart Meter RF fields observed during 66 minute monitoring period beginning at 10:56 P.M. local time. The blue spectrum is the “max hold” spectrum showing the maximum received signal power detected during the entire monitoring period. The four peaks that stand out from all of the rest of the detected signals, because of close proximity of the Wi-Spy to the meter, represent the momentary emissions detected from the Smart Meter being studied. Lower level signal peaks (typically 20 to 30 dB lower) are from other smart meters in the neighborhood.

Upon examination of the data file, it was found that four emission events occurred during the approximately one hour observation period that were apparently associated with the Smart Meter of interest. This means that the four major peaks shown in Figure 12-3 corresponded to those four events with no prior or subsequent signals occurring on or near the frequencies of the peaks. Following the conservative assumption that the detected emissions lasted for the duration of a

single scan, i.e., 0.37 seconds, a total transmission time of 4×0.37 seconds or 1.48 seconds. This total emission duration corresponds to a duty cycle, during the nominal one hour monitoring period, of 0.037%.

A subsequent Wi-Spy measurement was performed near the same residential Smart Meter on the next evening, this time almost two hours (1:55:25) between 9:25 P.M. and 11:20 P.M. as shown in Figure 12-4.

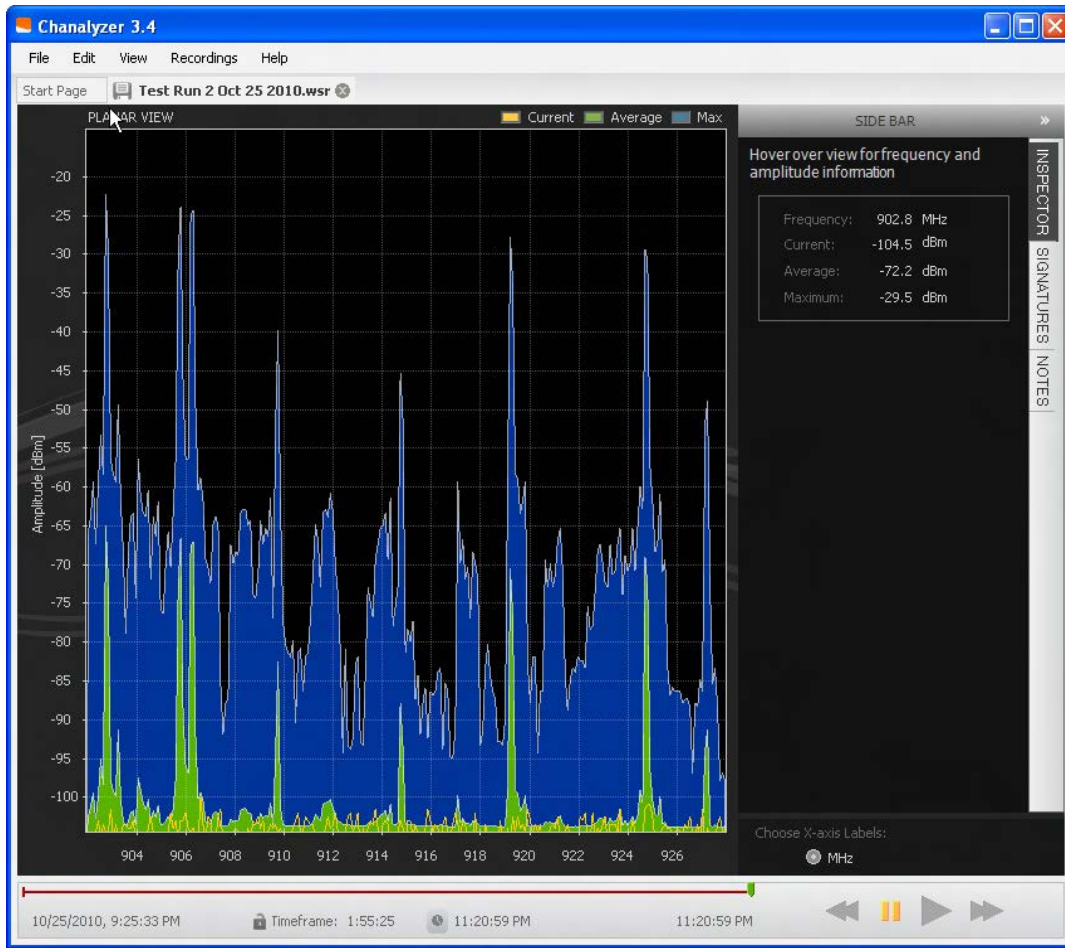


Figure 12-4
Wi-Spy display of Smart Meter RF fields observed during 115 minute monitoring period beginning at 9:25 P.M. local time.

Using the same analysis method, the measurement results were contained in 18632 scans of the band and suggested at least eight emission events were captured during the monitoring period from the meter of interest. Assuming that this represented the actual number of transmissions, with the same sweep time as in Figure 12-3, the apparent duty cycle would have been

0.0427%. This value is not significantly different from the first measurement on the previous day during approximately the same time.

On November 4, 2010, a Wi-Spy unit was set up at a fixed location in the Itron meter farm to capture a sample of RF fields in which the peak signal power and

average signal power values were measured over a 63 minute period. During this period, the Wi-Spy acquired a total of 15879 scans of the 902 - 928 MHz band emissions. This corresponds to a sweep period of 238 ms. Signal level measurements were made every 157 kHz across the 26 MHz of the band resulting in a total of 166 power values representing the spectrum. The result showed two clearly defined spectra, one of the peak signal level and the other of the average signal

level. No attempt was made to translate these measured signal power values into equivalent field strength or power density of the RF fields. A small, omnidirectional antenna was attached to the Wi-Spy analyzer at the time. The data file captured by the Wi-Spy software was separately analyzed to find the mean values of the peak and average power spectra. This result is shown in Figure 12-5.

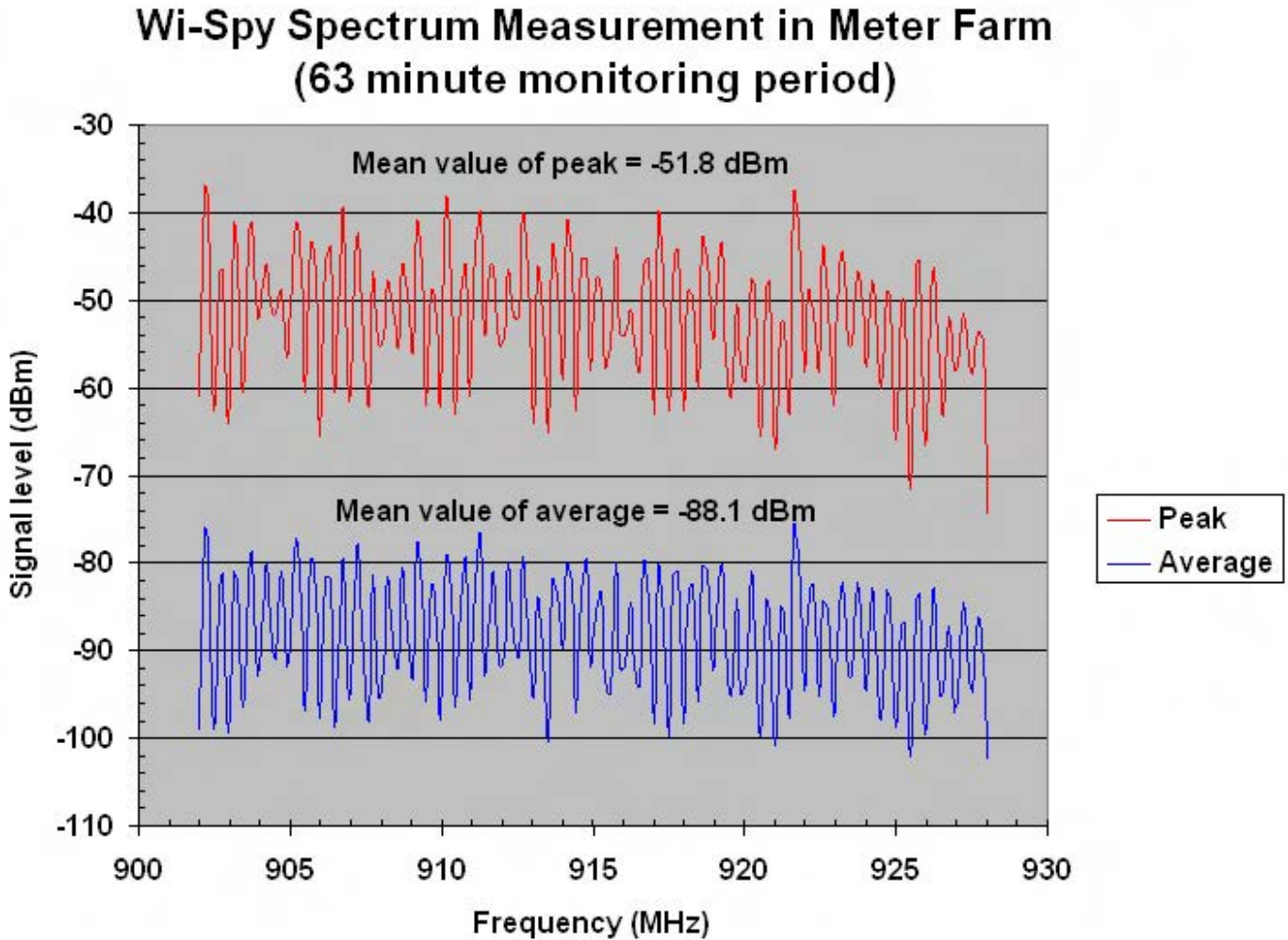


Figure 12-5

Processed signal power values obtained with the Wi-Spy spectrum analyzer on November 4, 2010, in the Itron meter farm. The average values of the peak and average spectra were -51.8 dBm and the -88.1 dBm respectively.

The difference between the mean values of the average and peak power spectra corresponds to 36.3 dB or an apparent duty cycle of 0.023%.

These exercises clearly indicate that the Wi-Spy unit is capable of detecting the Smart Meter emissions in terms

of sensitivity. However, it is not clear that all transmissions from the meter are captured due to the sweep time and display update produced by the Chanalyzer software. The analyzer sweep time as set up for the 902 MHz to 928 MHz frequency band is 370 ms. Hence, any specific frequency within the band is

observed once every 370 ms. This suggests that for emissions lasting less than 370 ms, the probability of detection is decreased but will also depend on when during a particular scan that the emission occurs.

SCE Smart Meter Network Management System

A preliminary investigation was made to examine the potential utility of the SCE Smart Meter Network Management software for remotely determining the operational duty cycle of specific Smart Meters. Acquiring measurement data at specific meters from which an assessment of transmitter duty cycle can be made is technically demanding because of the highly intermittent nature of the Smart Meter signals, the pseudorandom frequencies of the signals across the spectrum and the general variability of Smart Meter mesh network activity throughout a day, week, month or year. Because of the self-healing character of mesh networks, wherein alternative data transmission paths can be invoked on a moment-to-moment basis, Smart Meter transmitter activity is more meaningfully defined through a statistical description. A Smart Meter's transmitter activity on one day may not be the same as on another day despite the periodic transmission of beacon signals to alert other meters of its presence in the network or of regularly scheduled data dumps of electric energy consumption; activity during a particular hour of the day may not be replicated during the same hour on another day. Further, depending on the topology of the mesh network, the duty cycle of more distant meters within a given network could be expected to be less than that of meters closer to the associated cell relay meter. Smart Meter duty cycles are, therefore, not fixed and can be dissimilar from one another and vary over time. Consequently, a full characterization of a particular Smart Meter duty cycle requires collection of transmitter activity over a prolonged period of days if not weeks and months. Added to this complexity is the fact that the network consists of a large number of

meters and a full understanding of duty cycle means that a relatively long term data collection effort across many meters is necessary. The advantages of exploiting automated software based methods for obtaining such data are obvious. Finally, once the HAN function is implemented, the cumulative RF field caused by both the RF LAN and HAN transmitters and their effective duty cycles for a particular Smart Meter location may change.

During the period July 30 through October 26, 2010, SCE collected information pertaining to the number of data packets associated with either downlink or uplink communications from approximately 47,000 Smart Meters in part of SCE's territory. Downlink activity relates to data being propagated away from a cell relay meter while uplink activity is related to the transmission of data toward a cell relay meter. A presumption was made that both downlink and uplink traffic resulted in activity of the 900 MHz RF LAN transmitters in the meters. Using an estimate for packet length provided by Itron of 150 bytes for end point meters, with 8 bits per byte, and a data transmission rate for the 900 MHz RF LAN radio of 19.2 kbps (kilobits per second), the amount of transmitter activity was estimated for each of the meters on a daily basis for a total of 89 consecutive days. These transmitter duration data represented a total of 4,156,164 values. Each value of time (seconds per day) was then expressed as an estimated, average daily duty cycle. During the 89 days of data acquisition, some meters were found to not respond for various reasons or the data was corrupted resulting in an average number of meters from which valid data were obtained of 46,698 meters. Ultimately, these daily average duty cycles were then evaluated by examining their distribution in a percentile analysis. Figure 12-6 illustrates the result of this analysis where the average daily duty cycles are plotted across a range of percentiles.

SCE Smart Meter RF LAN Duty Cycles

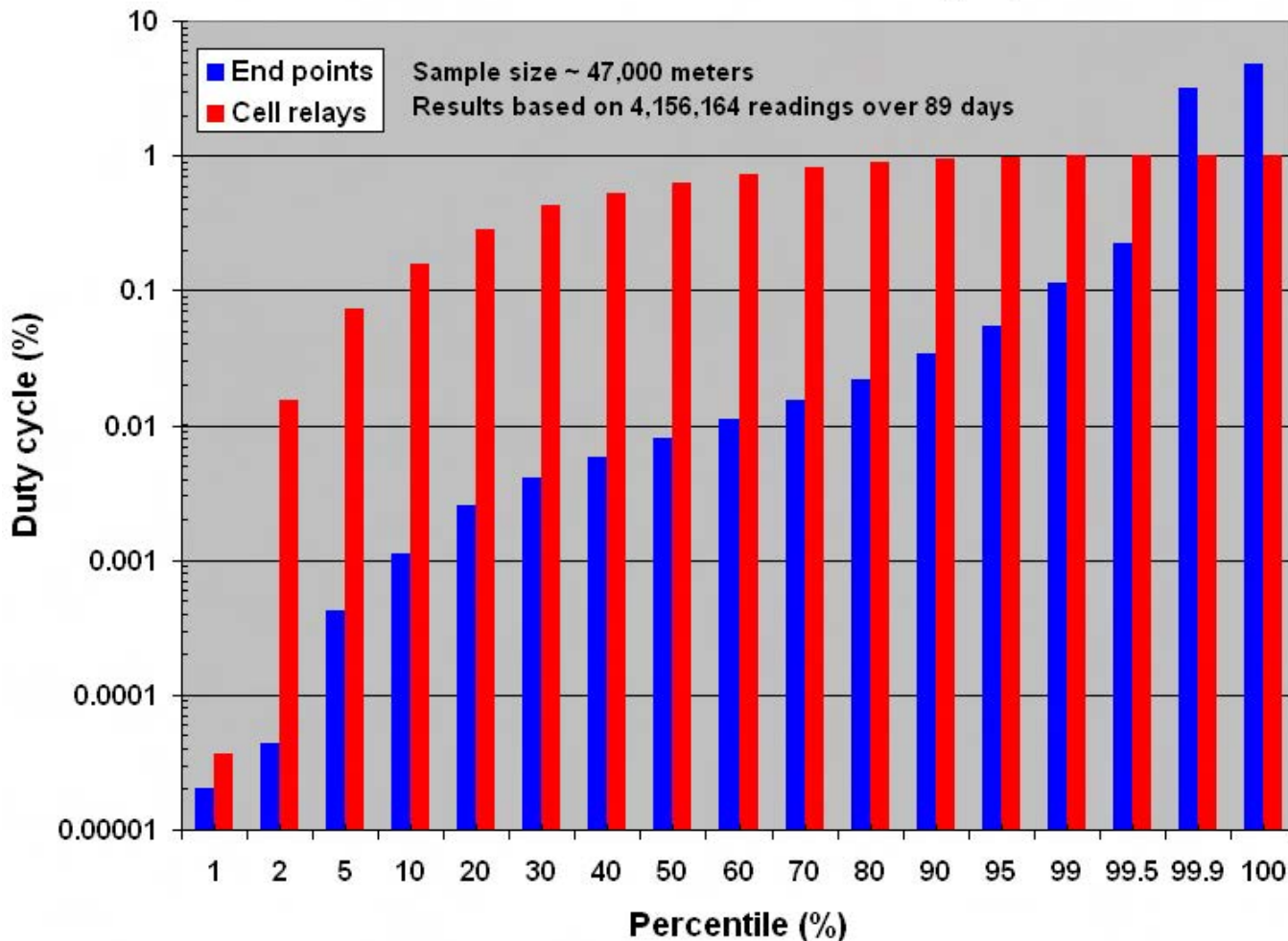


Figure 12-6
Analysis of SCE daily average duty cycle distribution for different percentiles based on 4,156,164 readings of transmitter activity from an average of 46,698 Itron Smart Meters over a period of 89 consecutive days. Analysis based on estimated transmitter activity during a day (see text).

RF LAN duty cycle data are presented in Figure 12-6 for both end point meters as well as cell relay meters. It was found that the sample size included some 111 cell relays. Based on information from Itron, the nominal packet size for data being transmitted down to the mesh network by a cell relay meter is 32 bytes. Using this figure for cell relays only, their estimated duty cycles were also determined and are shown in the figure.

Figure 12-6 tends to support the generally conservative estimate of approximately 5% for the duty cycle of some

meters within a mesh network stated by Itron.¹⁸ The maximum duty cycle obtained in the study was 4.74%. These data show that the upper duty cycle values pertain to only a very small percentage of meters; for example, while the duty cycle at the 99.9th percentile level (i.e., 99.9% of meters have smaller duty cycles) is 4.62%, dropping to the 99th percentile results in an average duty cycle of only 0.11%. Across the range of the 10th to 99th percentile, the duty cycle ranges from approximately 0.001% up to 0.1%. Figure 12-6 indicates

¹⁸ Analysis of Radio Frequency Exposure Associated with Itron OpenWay Communications Equipment. Itron publication, undated.

that most meters, most of the time operate with very small duty cycles. The data presented in Figure 12-6 must be recognized as what is likely a conservative approach insofar as the total data packets (up link and down link) passing through a Smart Meter were tallied by the SCE data collection effort with the same assumed packet size assigned to each (i.e., 150 bytes).

Using results from the SCE duty cycle study relative to uplink data for the cell relay meters, an estimate of the maximum cellular transmitter activity was made. In this analysis, the greatest uplink data passing through the cell relay was assumed to be transmitted to the WWAN by the cellular transceiver in the cell relay with a throughput of 1.536 Mbps¹⁹ with a 1/3 encoding overhead. Under this condition, an average duty cycle for the cellular transceiver in a cell relay is estimated to be approximately 0.088%. This very small value is due to the high data rate provided by the CDMA EVDO technology. This very low duty cycle for the CDMA EVDO implemented cell relays means that the time-averaged RF fields produced by cell relays will be correspondingly low. So, while the cellular transmitter is

rated at a power near one watt, the effective duty cycle will reduce time-averaged RF fields to small values.

SDG&E Smart Meter Network Management System

Similar efforts to characterize typical Smart Meter duty cycles were made by SDG&E, with support from Itron,

that provide additional insight to Smart Meter transmitter activity²⁰. In the SDG&E study, 6,865 end point and cell relay meters were monitored for the number of bytes of data transmitted over an observation period of one day ending December 2, 2010. The data is for meters distributed across ten cells of approximately 600 meters per cell. In this study, while substantially smaller in size than the SCE study, a more accurate and direct assessment of the transmitter activity was made by interrogating the number of bytes of data transmitted by the transmitter. This approach does not rely on any assumption of the data packet size as was done in the SCE data collection and, hence, minimizes uncertainty in the assessment of duty cycles. Figure 12-7 illustrates an analysis of the distribution of Smart Meter RF LAN activity for the SDG&E data.

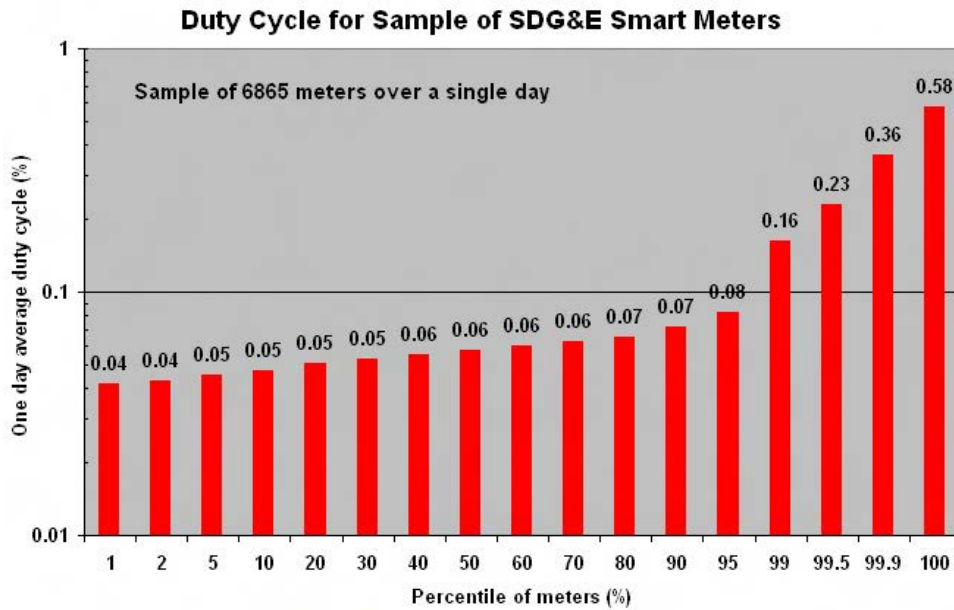


Figure 12-7 Results of an analysis of duty cycles for a sample of 6865 Itron Smart Meters deployed by SDG&E based on transmit duration during a single day of observation.

¹⁹Data rate for the CDMA EVDO Rev A cell relay modems ranges from 1536 kbps to 3072 kbps.

²⁰ Provided by Jim Turman, Safety and Emergency Services, San Diego Gas and Electric.

Figure 12-7 reveals a lower maximum duty cycle for the highest activity meters than observed from the SCE data but when the vast majority of meters are considered as a whole, the duty cycles are roughly in the same range. For instance, half of the SDG&E meters exhibited duty cycles of approximately 0.06%. From the SCE data, the 50th percentile of duty cycles was found to be approximately 0.01% rising to a value of about 0.06% at the 95th percentile. The differences in these two data sets is confounded by the fact that the data were collected in different ways, using different parameters for assessing transmitter activity, and represent substantially different sample sizes and sample collection periods. Nonetheless, because of uncertainties associated with data packet sizes in the down link and up link streams within the Itron mesh network, the SDG&E approach should yield more accurate values for meter duty cycles. Of further relevance, during this data collection period, a day light savings time update was performed as well as a meter firmware download (which

would require a large number of up link acknowledgements). These factors would tend to drive the apparent duty cycle of meters upward when compared to other times of the year. Importantly, any differences between these preliminary studies of Itron Smart Meter duty cycles should not be viewed as differences in how the two networks, one deployed by SCE and the other by SDG&E, are designed to operate but, rather, as the result of the differences in how data were collected. In the case of SCE, only indirect measures of transmitter activity were obtained that require an assumption as to data packet sizes whereas in the case of SDG&E, a direct assessment of data traffic through the meters was obtained. Future software based studies of duty cycles of Smart Meters should include measures of both data packet counts as well as the number of bytes of data transmitted; such studies can provide insight to average packet sizes should other studies be performed in a similar fashion.

Section 13: Ancillary Measurements

Microwave Oven

During the residential surveys, when a microwave oven was encountered in the kitchen, measurements were made with a cup of water placed inside the oven. Leakage fields, as documented in Table 9-8, were detected at two feet from the oven as great as 22% of the public MPE. Subsequently, additional measurements were performed at the author's home using the SRM-3006. These data for a measurement at 1 foot from the oven are shown in Figure 13-1. The

spectral distribution of the detected signal in Figure 13-1 is characteristic of microwave ovens; the frequency of the microwave oven drifts across a part of the spectrum and is essentially continuous in nature. Loading on the microwave oven due to temperature increases in the material being heated will cause the frequency to vary. Measurements taken at additional distances from the oven demonstrate a rapid decrease in signal with increasing distance as shown in Figure 13-2.

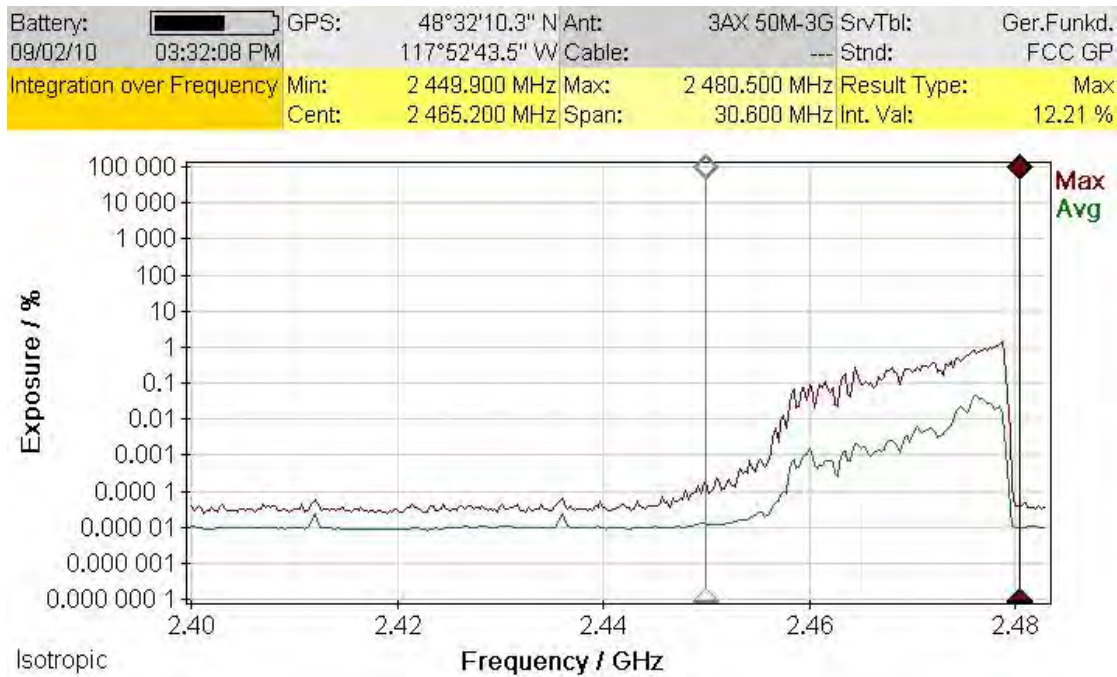


Figure 13-1
Measurement of microwave oven leakage at 1 foot from oven door seal.

Microwave Oven Leakage Fields (2.45 GHz)



Figure 13-2
Microwave oven leakage vs. distance.

Microwave ovens must comply with regulations promulgated by the Food and Drug Administration (FDA) on leakage levels.²¹ These regulations specify that the maximum leakage from a new oven, at the time of manufacture, shall not exceed a power density of 1 mW/cm². Once put into operation, the limit is set at a maximum leakage value of 5 mW/cm² at 5 cm from the oven surface. This is a product performance standard, not an exposure standard.²² In practice, modern microwave ovens typically comply easily with the regulations by a wide margin. Since the FCC MPE for whole body exposure at the microwave oven frequency, 2.45 GHz, is 1 mW/cm², a measurement value of 12% of the MPE corresponds to only 1/5 of 12%, or about 2.4% of the 5 mW/cm² product performance standard.

²¹ Performance Standards for Microwave and Radio Frequency Emitting Products, 21CFR1030.10. Food and Drug Administration, Department of Health and Human Services.

Cordless telephone

Cordless telephones operate in a number of different frequency bands including 49 MHz, 900 MHz, 2.4 GHz and 5.8 GHz. Figure 13-3 shows a spectrum obtained from a 900 MHz band cordless phone with the base unit emitting signals near the upper end of the spectrum and the portable receiver unit emitting near the bottom of the spectrum. This figure is applicable to a measurement at one foot from the base unit and receiver.

²² It should be noted that the local RF field leakage limit of 5 mW/cm² is five-fold greater than the MPE for whole body exposure applied by the FCC.

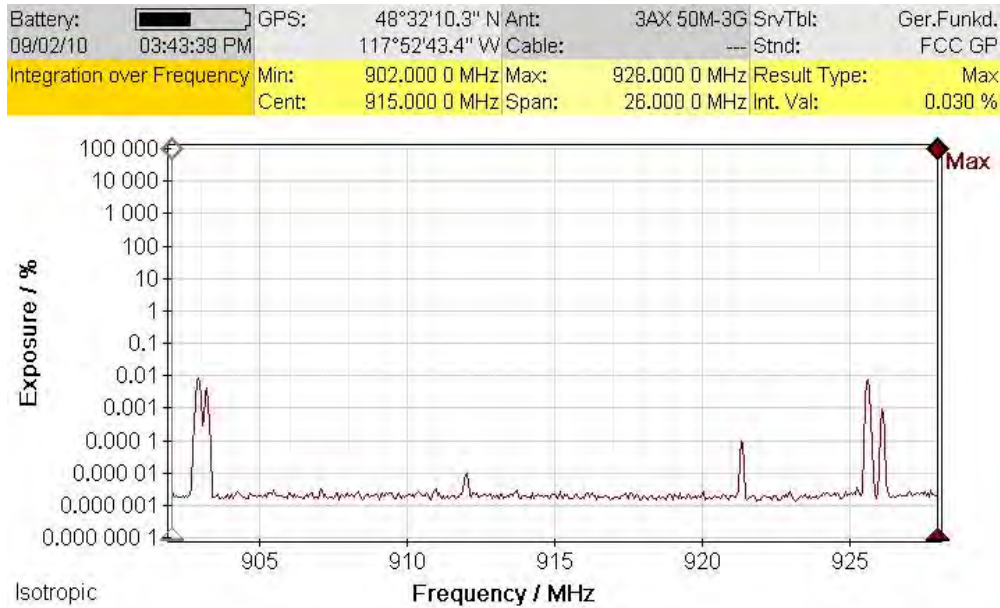


Figure 13-3

900 MHz cordless telephone RF fields from the base unit near the upper end of the spectrum and from the portable receiver unit near the lower end of the spectrum, measured at 1 foot from the base and receiver.

Wireless router

An observation also made during the residential measurements was the presence of a wireless router in a home office operating in the 2.4 GHz band. Figure 13-

4 illustrates a measurement of the RF field produced by a wireless router in the author's office at approximately one foot from the router. A maximum field of 0.24% of the MPE was measured.

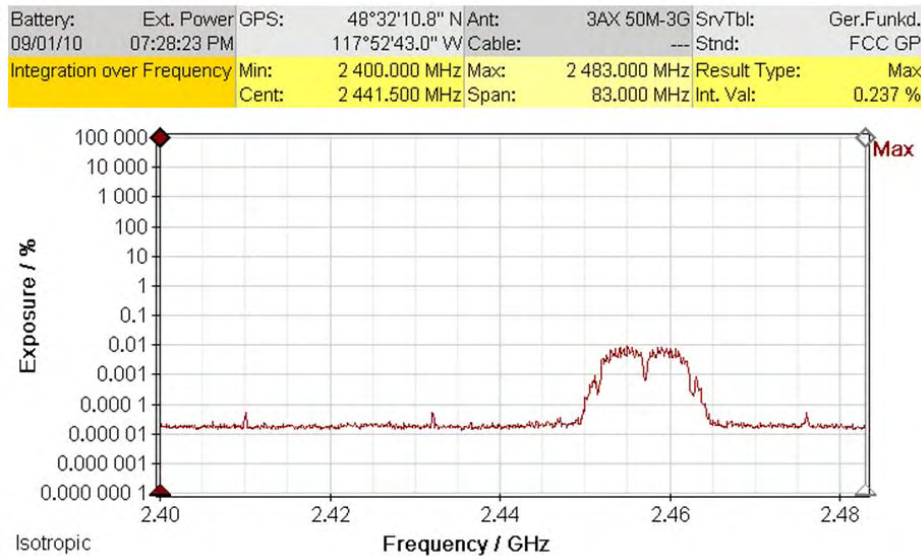


Figure 13-4

Measured RF emission spectrum of a wireless router at one foot from the router. The router was set to operate on Wi-Fi channel 10.

Measurement comparison (Model B8742D probe and SRM-3006)

Using the two specially programmed Smart Meters previously employed in the simulated stucco wall attenuation measurements, a comparison was made between the response of the broadband probe and the SRM meter. RF fields were measured by placing either

of the two probes with their centers at 20 cm from the face of either Smart Meter and recording the readings. Each broadband probe reading was multiplied by the factory determined correction factor for the appropriate frequency (0.67 at 915 MHz and 0.97 at 2450 MHz). The results are presented below.

*Table 13-1
Comparison of RF field probe readings at 902.25 MHz and 2405 MHz (%MPE)*

Probe	Frequency (MHz)	
	902.25	2405
B8742D	2.01	1.21
SRM-3006	2.29	1.37
Percentage difference (%)	13.0	12.3
Difference (±dB)	+0.53, -0.57	+0.54, -0.54

These data indicate that the two instruments yielded readings of the RF fields that were within the manufacturer’s specified uncertainties of calibration.

Section 14: Theoretical Analysis of RF Fields

Assessing RF fields associated with Smart Meters through theoretical analysis is an expedient approach to evaluating potential exposure of individuals who may be near the meters. This section describes the method used to obtain theoretical estimates of RF fields in the vicinity of the Itron Smart Meters studied in this project.

RF fields that might be associated with emissions from the various transmitting components of the Itron system, consisting of the Model CL200 end point meter and the Model C2SORD cell relay meter, were calculated following the methodology described here. This method includes a conservative approach of accounting for the possibility of ground reflections that can enhance the local RF field strength at any given location. The intensities of RF fields (expressed as power density) are calculated using conventional field calculation methods but with the inclusion of a ground reflection factor as recommended by the FCC²³. Power densities were calculated according to the following relationship:

$$S(W/m^2) = \frac{P_t \times G_{\max} \times \delta \times \Gamma}{4\pi R^2} \quad \text{Equation 14-1}$$

Where,

S is plane-wave equivalent power density (W/m²)

P_t is maximum transmitter output power (W)

G_{max} is the maximum possible antenna power gain (a dimensionless factor)

δ is the duty cycle of the transmitter (percentage of time that the transmitter actually transmits over time). More specifically, δ is the maximum duty cycle as found over any 30 minute period. This is because the averaging

time for the MPE in the FCC rules and the IEEE standard (C95.1-2005) for the general public and applicable to the frequencies used by the Itron Smart Meters is 30 minutes. Determining the value of δ is challenging as described above. In most cases, estimates of δ are used based on understanding of the mesh network characteristics. In any event, δ is generally a very small value since the Smart Meters do not transmit most of the time.

R is the radial distance between the transmitter and the point of interest (meters)

Γ is a factor that accounts for possible in-phase ground reflections that could enhance the resultant power density. Under ideal reflective conditions, such as with a metallic ground plane, a field reflected from the ground could add constructively (in phase) with the field directly incident from the source to cause a maximum two-fold increase of the field strength at the reception point. Were this to happen, the phenomenon could lead to an increase of (2)² or 4 fold in the power density since the electric field is proportional to the square of field strength. In this case, the value of Γ in equation 1 would be 4. Under more realistic environmental conditions, where perfectly reflective surfaces are rare, an electric field strength enhancement of 60% has been recommended by the FCC. This corresponds to an enhanced electric field strength of 1.6 times the field arriving from the source without reflection or a power density enhancement factor of (1.6)² or 2.56 for use in equation 1. Application of a ground reflection factor in exposure assessment calculations becomes less meaningful at locations that are very close to the Smart Meter for two reasons. Since the emissions are directional in the elevation plane with generally relatively a smaller magnitude of RF energy being propagated downward at steep angles, the RF field strength striking the a reflective ground will be small. The reflected magnitude will be similarly small. Further, for close exposure conditions, within a few feet of the Smart Meter, the difference in propagation path length between that of the directly incident field and the reflected field usually be substantial. Hence, any reflected field component at the location of a person

²³ FCC (1997). *Evaluating Compliance with FCC Guidelines for Human Exposure to Radiofrequency Electromagnetic Fields*. Federal Communications Commission, Office of Engineering & Technology, OET Bulletin 65, Edition 97-01, August.

standing immediately next to a Smart Meter will be a very small fraction of the directly incident RF field leading to, essentially, no material enhancement of the field. For this reason, calculation of RF fields for the situation of very close proximity to the meter, wherein the greatest intensity of the field will exist, will more accurately estimate the actual field if the value of Γ is set to unity (1). As the distance from the Smart Meter increases beyond some value such that the body may be more uniformly illuminated by the incident fields, ground reflected fields have the potential of much more significant enhancement of the radiated field but at such

distances, the magnitude of the field has become extremely small in comparison with that exhibited within a few feet of the meter.

For exposure distances of 1 to 3 feet in front of a meter mounted at 5 feet above the ground, the elevation angles to the ground that would result in an in-phase field addition range between nominally 78 degrees and 60 degrees. An examination of the elevation plane radiation patterns presented above reveals the following approximate values in Table 10-1 for the reduction in field for elevation angles of 60 to 90 degrees below the horizontal to the meter.

Table 14-1

Approximate RF field reductions (dB) caused by Smart Meter elevation plane patterns in the 60° to 90° range below a horizontal to the meter.

Angle (°)	Field reduction (dB)					
	900 MHz RF LAN end point meter	900 MHz RF LAN cell relay meter	2.4 GHz Zigbee end point meter	2.4 GHz Zigbee cell relay	850 MHz cellular cell relay	1880 PCS cell relay
60	-8	-7	-3	-11	-7	0
75	-10	-8	-4	-8	-10	-4
90	-11	-8	-8	-8	-10	-7

These data show that the typical range of RF field reduction is in the range of -3 to -10 dB with one exception associated with the 1880 MHz PCS transmitter in a cell relay meter at an angle of 60°. This range is equivalent to between 50% and 10% of the field power density at the same distance but within the main beam of the transmitter. The maximum possible combined RF field occurs if both the directly incident plus ground reflected waves add in phase with one another; the contribution provided by the ground reflected component suffers degradation simply due to

the weaker field directed toward the ground and the greater distance from the source to the point of interest. Through examination of the detailed pattern data represented by, for example, Figure 8-11 for the elevation plane pattern of a 900 MHz RF LAN end point transmitter, the relative EIRP along a vertical line located 1 foot adjacent to the Smart Meter from ground level to a height of 6 feet would be expected to be similar to Figure 14-2. Note the approximate qualitative similarity to the measured pattern shown in Figure 11-2 for the same type of transmitter.

Relative EIRP Along Vertical Six Foot Path One Foot Adjacent to Smart Meter

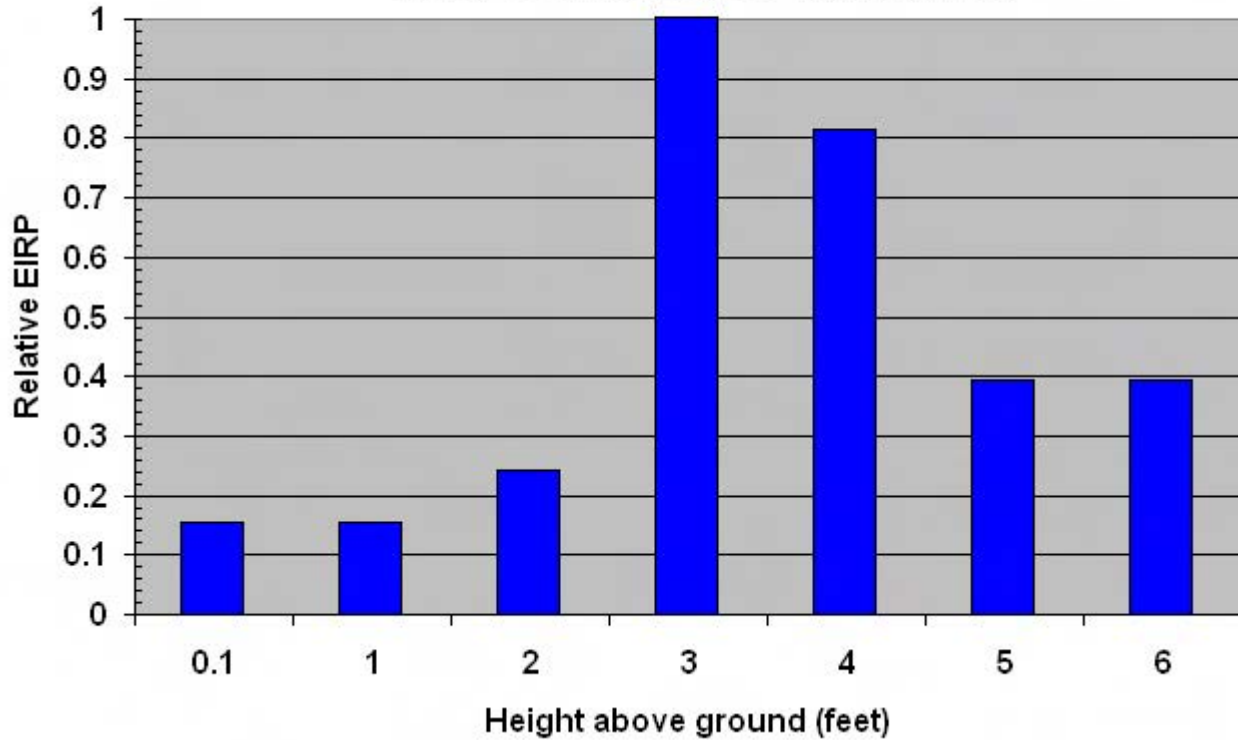


Figure 14-1
Relative EIRP of a 900 MHz RF LAN transmitter as observed along a six foot vertical line located one foot adjacent to the Smart Meter.

To illustrate the results of applying equation 1, calculations were performed for distances from 1 foot to 100 feet from each of the Smart Meter transmitters included in this study with the results shown in Figure 14-3. For the initial set of calculations, the duty cycle was assumed to be 100%, the same as the unique conditions under which RF fields were measured in this project. Such a value of duty cycle is not possible under normal operation of the mesh network. In fact, the mesh network is incapable of operation once the duty cycle were to reach approximately 30%²⁴. As discussed above, realistic duty cycle values are in the range of a few percent at most with typical values well less than

one percent. The results displayed may be adjusted by multiplying the indicated value by the duty cycle. Thus, the displayed field values are in terms of the instantaneous peak values of RF field. The calculated values also are for the maximum possible field based on the detailed pattern measurement data presented earlier; i.e., the calculated field magnitude is relevant only to that specific direction away from the meter at which the greatest RF field exists as represented by the transmitter powers summarized in Table 10-2. Further, the calculations plotted in Figures 14-3 and 14-4 include a value of 1.00 for Γ , i.e., no ground reflection enhancement.

²⁴ Personal communication from Itron.

RF Field from Smart Meter Transmitters (Each transmitter operating at specified power, 100% duty cycle and no ground reflections)

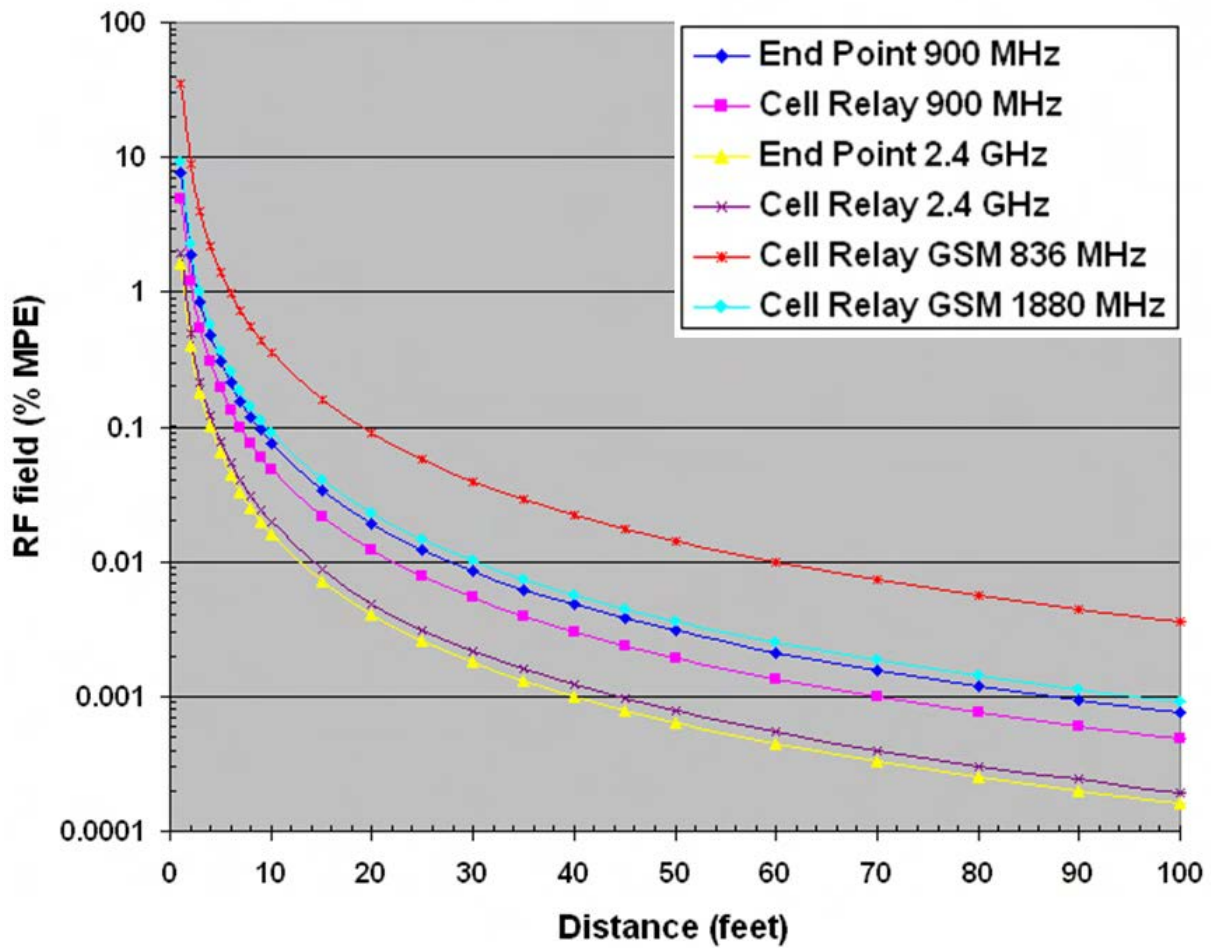


Figure 14-2
 Calculated RF fields up to 100 feet at point of maximum intensity in main beam expressed as percentage of FCC general public MPE as function of distance in maximum beam for Itron Smart Meter components investigated in this study. No ground reflections have been included in this analysis, the field values are relevant to the peak value of field during the time that the transmitter is actually transmitting (no duty cycle correction) and spatial averaging has not been applied to the values. Normal operation of the Smart Meter will significantly reduce the actual field found in practice near operating meters.

RF Field from Smart Meter Transmitters (Each transmitter operating at specified power, 100% duty cycle and no ground reflections)

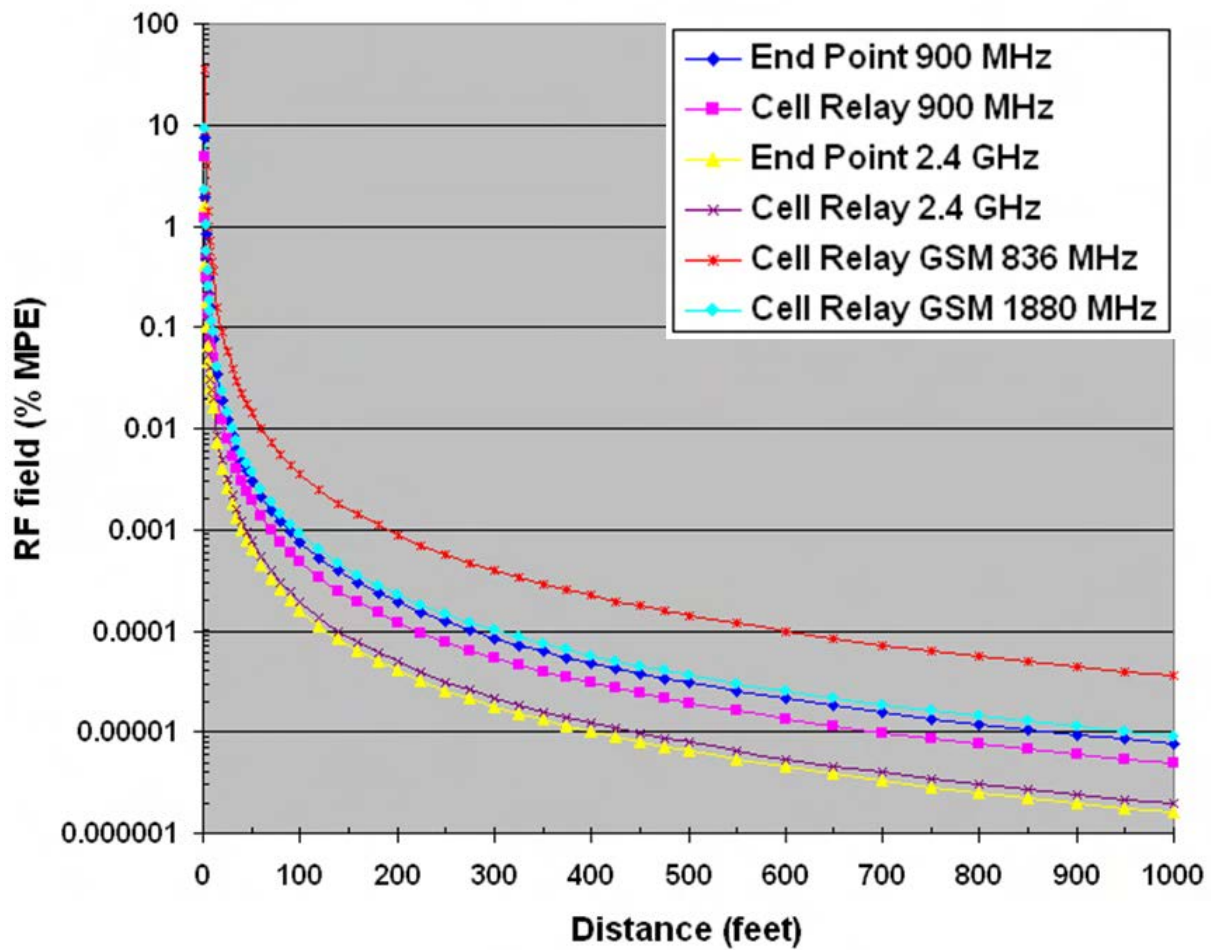


Figure 14-3
 Calculated RF fields up to 1000 feet associated with Smart Meters included in this study with the assumption that the transmitters operate continuously (not possible in actual operation in a mesh network) and no ground reflections occur that might add constructively to enhance the field at the point of interest.

Table 14-2

Summary of nominal transmitter peak powers and 99th percentile powers for Itron Smart Meters studied in this investigation.^o

Transmitter/ Meter	Frequency (MHz)	Gain (dBi)	Power gain	Most likely power (dBm)	99 th percentile power (dBm)
RF LAN end point	914.8	2.85	1.93	24.5	26.0
RF LAN cell relay	914.8	0.88	1.22	24.5	26.0
Zigbee end point	2440	4.24	2.65	18.5	20.6
Zigbee cell relay	2440	5.08	3.22	18.5	20.6
Cell relay GSM	836.6	1.85	1.53	31.8	
Cell relay GSM	1880	1.56	1.43	28.7	

^oUnder FCC rules at 47 CFR 15.247, the peak output power of frequency hopping (using more than 50 channels) and direct sequence spread spectrum transmitters is limited to 1 watt.

Figure 14-2 shows the calculated peak value of RF field for the most likely transmitter powers without the presumed presence of possible ground reflections for distances up to 100 feet. To emphasize, the values shown do not account for typical transmitter duty cycles or spatial averaging. And, it's relevant to recognize that the peak calculated field applies to a single point in space that corresponds to the specific direction in space occupied by the main beam emerging from the Smart Meter. This is not necessarily a direction perpendicular to the case of the meter. Hence, measured values of field taken along directions geometrically normal to the meter surface will not represent the maximum possible field value. Figure 14-3 is a similar plot of calculated field values over a distance up to 1000 feet.

Figures 14-2 and 14-3 illustrate the most likely maximum RF field adjacent to the Itron Smart Meter components evaluated in this study, before adjustment for transmitter duty cycles. To provide conservative estimates of maximum possible peak RF fields, calculations were prepared using the 99th percentile values of transmitter powers discussed earlier and listed in Table 10-2. These results are shown in Figures 14-4

and 98 for distances up to 30 feet from the meter for a 900 MHz RF LAN end point transmitter and a 2.4 GHz Zigbee cell relay transmitter, respectively, these two transmitters yielding the greatest measured gain as listed in Table 10-2. In each of the figures, the solid curve represents the most likely transmitter power and the assumption of no ground reflections with the upper bars showing the RF field value is the 99th percentile transmitter power with the worst case ground reflections. For the upper bars, an assumption was made that ground reflections could exist that would enhance the RF field at the calculation point following procedures outlined in FCC OET Bulletin 65 ($\Gamma = 2.56$). Such an assumption of ground reflections, however, is not realistic since the point of maximum field magnitude near the Smart Meter may not correspond to the point in space at which any ground reflected wave happens to add constructively to the directly incident wave (in phase field addition). RF field values comprising the plotted values in Figures 14-4 and 98 and a similar maximum possible value for the 836 MHz cellular transmitter of the cell relay are given in Table 14-3 for the distance range up to 30 feet.

RF Field from 900 MHz Smart Meter Transmitter
 (Transmitter operating at typical and 99th percentile power,
 100% duty cycle and maximum ground reflections)

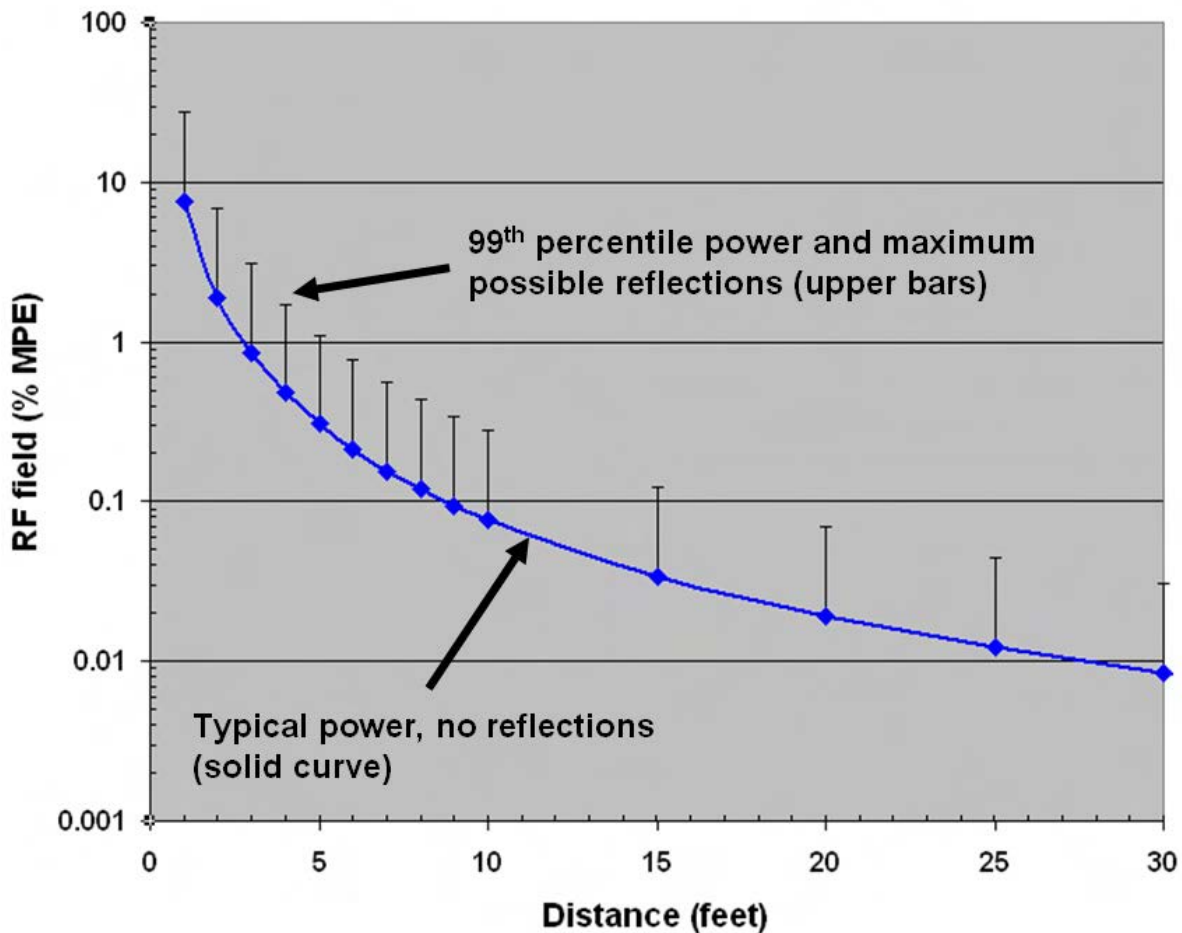


Figure 14-4

Calculated RF field produced by Smart Meter 900 MHz RF LAN transmitter using most likely transmitter power (solid curve) and 99th percentile transmitter power (bars above solid curve). Calculated maximum possible values are based on the 99th percentile transmitter power but assume the possibility of ground reflections ($\rho = 2.56$) that would enhance the RF field at the calculation point (point of maximum RF field emission near the meter). Such ground reflections are not realistic but follow guidance in FCC OET 65.

**RF Field from 2.4 GHz Zigbee Smart Meter Transmitter
(Transmitter operating at typical and 99th percentile power,
100% duty cycle and maximum ground reflections)**

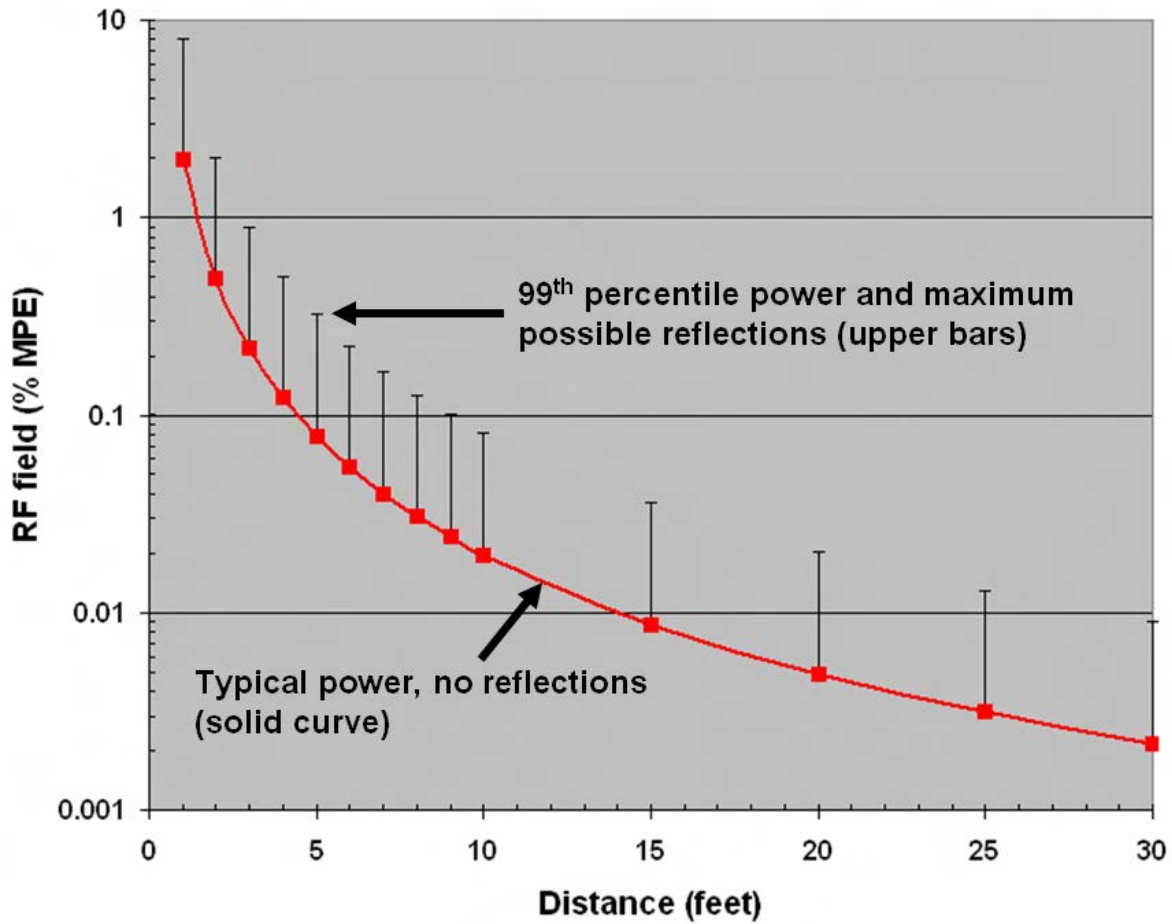


Figure 14-5
 Calculated RF field produced by Smart Meter 2.4 GHz Zigbee transmitter using most likely transmitter power (solid curve) and 99th percentile transmitter power (bars above solid curve). Calculated maximum possible values are based on the 99th percentile transmitter power but assume the possibility of ground reflections ($\Gamma = 2.56$) that would enhance the RF field at the calculation point (point of maximum RF field emission near the meter). Such ground reflections are not realistic but follow guidance in FCC OET 65.

Table 14-3

Calculated upper range of possible RF fields associated with the 900 MHz RF LAN, 2.4 GHz Zigbee and cellular cell relay Smart Meter transmitters. The 99th percentile powers for the RF LAN and Zigbee transmitters, main beam exposure, 100% duty cycle and presence of ground reflections (using a ground reflection factor of 2.56) to enhance fields were assumed. However, no spatial averaging was assumed.

Distance(ft)	RF field (% public MPE)			Cumulative value of peak fields ^a
	900 MHz end point	2.4 GHz cell relay	836 MHz cellular (cell relay)	
1	27.6	8.11	91.1	126.8
2	6.91	2.03	22.8	31.7
3	3.07	0.901	10.1	14.1
4	1.73	0.507	5.69	7.93
5	1.11	0.324	3.64	5.07
6	0.767	0.225	2.53	3.52
7	0.564	0.165	1.86	2.59
8	0.432	0.127	1.42	1.98
9	0.341	0.100	1.12	1.57
10	0.276	0.081	0.911	1.27
15	0.123	0.036	0.405	0.564
20	0.069	0.020	0.228	0.317
25	0.044	0.013	0.146	0.203
30	0.031	0.009	0.101	0.141

^aThis column represents a highly conservative estimate of the single point in space RF field and is the simple sum of values of maximum calculated fields from the three transmitters in the Smart Meter. Because of the difference in wavelengths of the three RF emissions, it is not possible for the three ground reflected field components to be a maximum at the exact same point in space. Hence, the values in this column are highly conservative estimates (over estimates) of the actual fields that would exist near the meter. Further, this analysis presumes that each transmitter is transmitting continuously; this is not realistic nor would the mesh network function if the 900 MHz RF LAN transmitter were to transmit continuously.

The matter of including a factor to account for ground reflections in Equation 1 was examined by applying a method of moments computation²⁵ to model the field produced by a horizontally oriented 900 MHz half-wave dipole antenna located five feet above the ground. RF field strengths were computed along a vertical line path of six feet, at one foot adjacent to the dipole antenna, with a vertical distance increment of one inch. Electric field strengths were converted to plane wave equivalent power density at each of 73 points and

normalized to the greatest value along the vertical line. The model was run for realistic ground constants²⁶ and assuming free space conditions with no ground reflections. Figure 14-6 presents the results of this analysis.

Values of spatially averaged power densities were computed for both cases, free space and ground reflections possible. The ratio of the spatially averaged resultant field with ground reflected field components

²⁵ EZNEC+ version 5.0.36 developed by Roy W. Lewallen
www.eznec.com

²⁶ Ground conductivity of 0.005 siemens per meter and dielectric constant of 13.

to the spatially averaged free space field was found to be 1.032 meaning that inclusions of possible ground reflections resulted in a spatially averaged field that was 3.2% greater than under free space assumptions (no reflections accounted for). At the point of maximum field, near the height of the dipole, the ratio of power densities was 1.127 showing that the ground reflections enhanced the local field, at that specific point, by 12.7% over the free space value. While this does represent a slight enhancement, it is substantially less than if an assumption of a ground reflection factor of 2.56 were to be used. Such an assumption would imply that the RF

field (power density) all along the vertical line would be 256% greater than the free space modeled value (no reflections). For this specific comparison (mounting height, ground conditions, lateral distance to the antenna, etc.), inclusion of a ground reflection factor of 2.56 for Γ in Equation 1 would result in RF fields being as much as 20 fold greater (227%) than the actual value with ground reflections. The magnitude of Γ affects the magnitude of the RF field at all points along the vertical line, resulting in spatially averaged values that are also 227% greater than that produced by the actual resultant field caused by ground reflections.

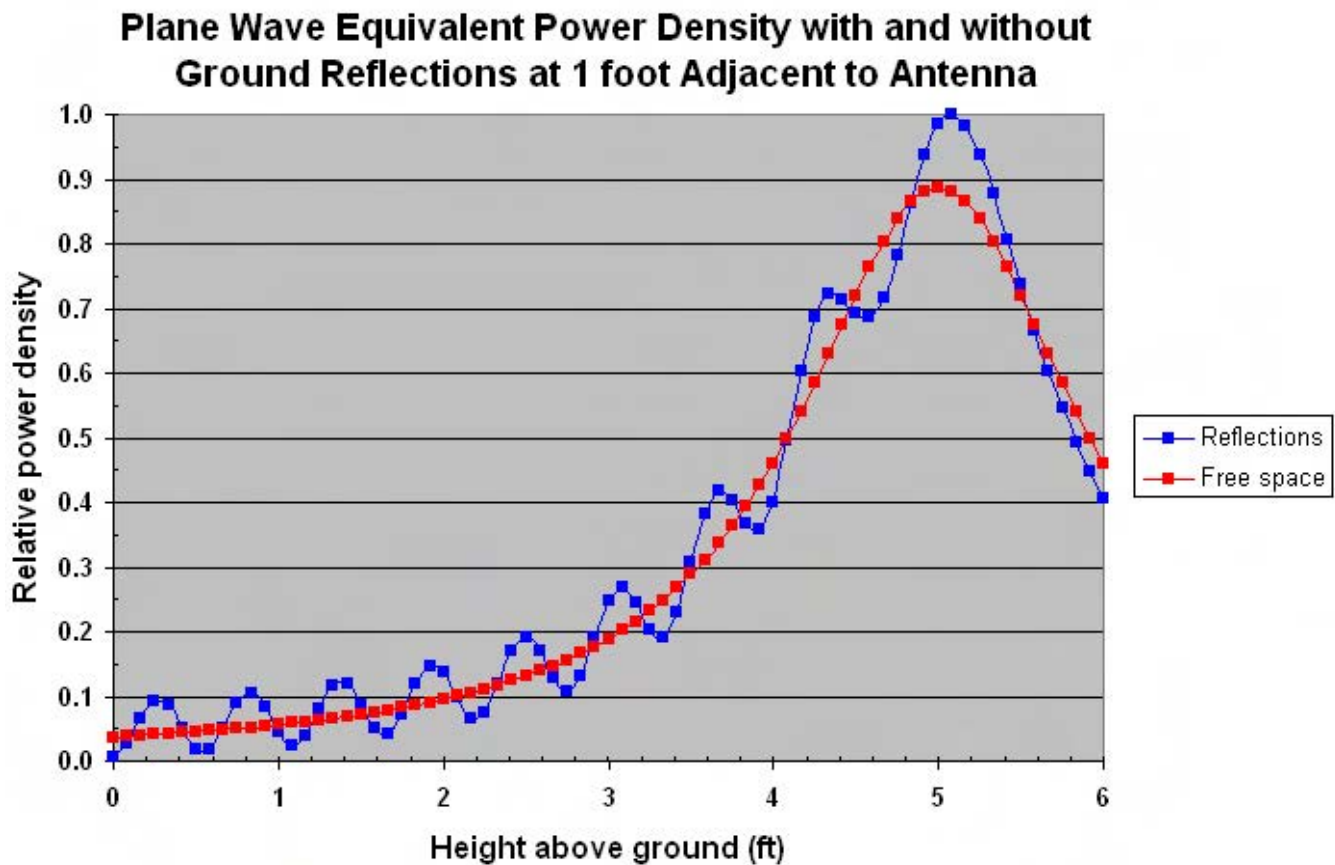


Figure 14-6
Relative calculated plane wave equivalent power density along a six-foot vertical path, one foot adjacent from a 900 MHz half-wave dipole positioned at five feet above the ground. Power density values are compared with and without ground reflections.

Similar calculated values of spatially averaged power densities, with and without the presence of ground reflections, are illustrated in Appendix G for vertical paths displaced 1 foot, 3 feet, 6 feet, 10 feet, 15 feet and 20 feet from a horizontally oriented 900 MHz dipole

mounted five feet above the ground. These results are summarized in Figure 14-7 which displays the impact of ground reflections on calculated six-foot spatially averaged values of exposure to RF fields.

Impact of Ground Reflections on Six-foot Spatially Averaged Values of Power Density

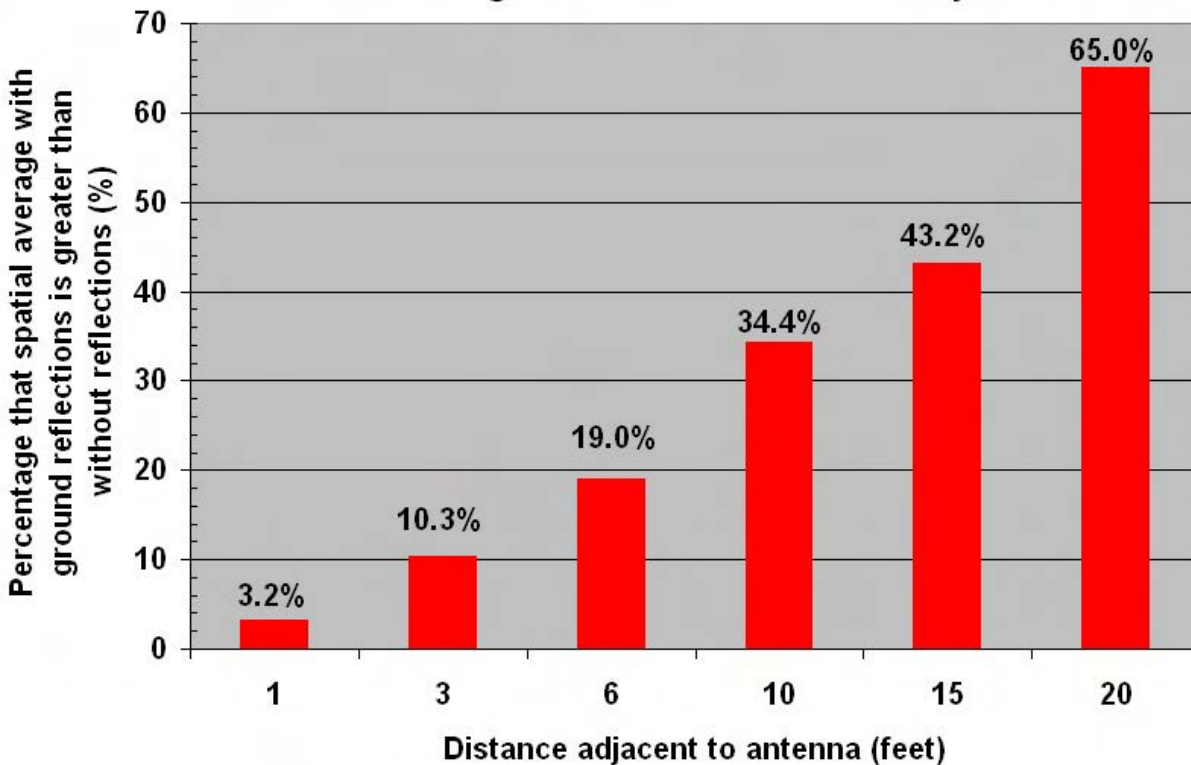


Figure 14-7

Impact of ground reflections on six-foot spatial average of power density for different distances lateral to a 900 MHz dipole antenna mounted at five feet above ground. Vertical axis is represents the percentage that the spatially averaged power density that includes any ground reflected fields is greater than the spatially averaged power density in free space (without any ground reflected fields).

The significance of the above analysis is that use of a fixed value for Γ can significantly over estimate spatially averaged values of RF fields in an attempt to account for possible ground reflection enhancement of the resultant field. Figure 14-7 illustrates that very close to the Smart Meter, ground reflections only account for approximately a 3.2% increase in the spatially averaged value of power density compared to assuming that reflections cannot occur. The contribution of constructive interference between the ground reflected field and that directly incident from the source results in greater values of spatial averages as the distance from the antenna increases. However, even at 20 feet from the source, the enhanced value comparable to being 65% greater than that without inclusion of ground reflections is still substantially less than that obtained from application of a Γ value of 2.56, i.e., a 256% increase in apparent power density! It is also significant to note that

at the closest distances, where the RF field will be greatest simply due to proximity, theoretical estimates of RF power density will have the greatest error due to over estimation if the ground reflection factor is more than a few percent. This finding suggests that theoretical estimates of Smart Meter RF fields very near the meters will be most accurate if Γ is approximately unity in value.

Calculated RF fields can often be greater than the actual fields that might be measured when occupying areas near the Smart Meters evaluated in this study. This can, among other things, be a result of not identifying the precise point in space wherein the maximum EIRP exists from the meter during measurements. This situation can also manifest itself when attempting to measure the composite RF fields associated with a large number of Smart Meters that are located close to one

another. For example, when positioned very close to a group of meters, such as represented by the meter racks in the Itron meter farm or adjacent to apartment houses with banks of meters, it is not possible to find any specific point that will be subject to the main beam of transmission from all of the collective meters simply due to geometric considerations. The close measurement may capture the main beam of one of the meters in the group but cannot capture the main beams of all of the meters. This can result in a lower field strength at points very close to the group of meters than might be anticipated. However, as the distance from the group of meters increases, there is a greater likelihood that the patterns of each meter will overlap in such a way as to make each meter a more equal contributor to the overall combined RF field. Simply increasing distance results in

a less spatially critical relationship between RF fields emitted by a given meter and specific location in the vicinity of the group of meters. Conceivably, with sufficient distance, albeit the combined RF fields will be very weak, the various meters will become essentially equal contributors to exposure.

This phenomenon is evident when the calculated maximum possible RF field of a single meter is compared to the measured composite field of many meters. In Figure 14-8, the measured values of the collective RF field of meters in the Itron meter farm were compared to the theoretical calculation of maximum possible field of a single 900 MHz RF LAN transmitter. In this figure, the ratio of the measured collective field to the single meter calculated field is plotted.

Ratio of Measured Group Collective Fields to Single Meter Calculated Fields

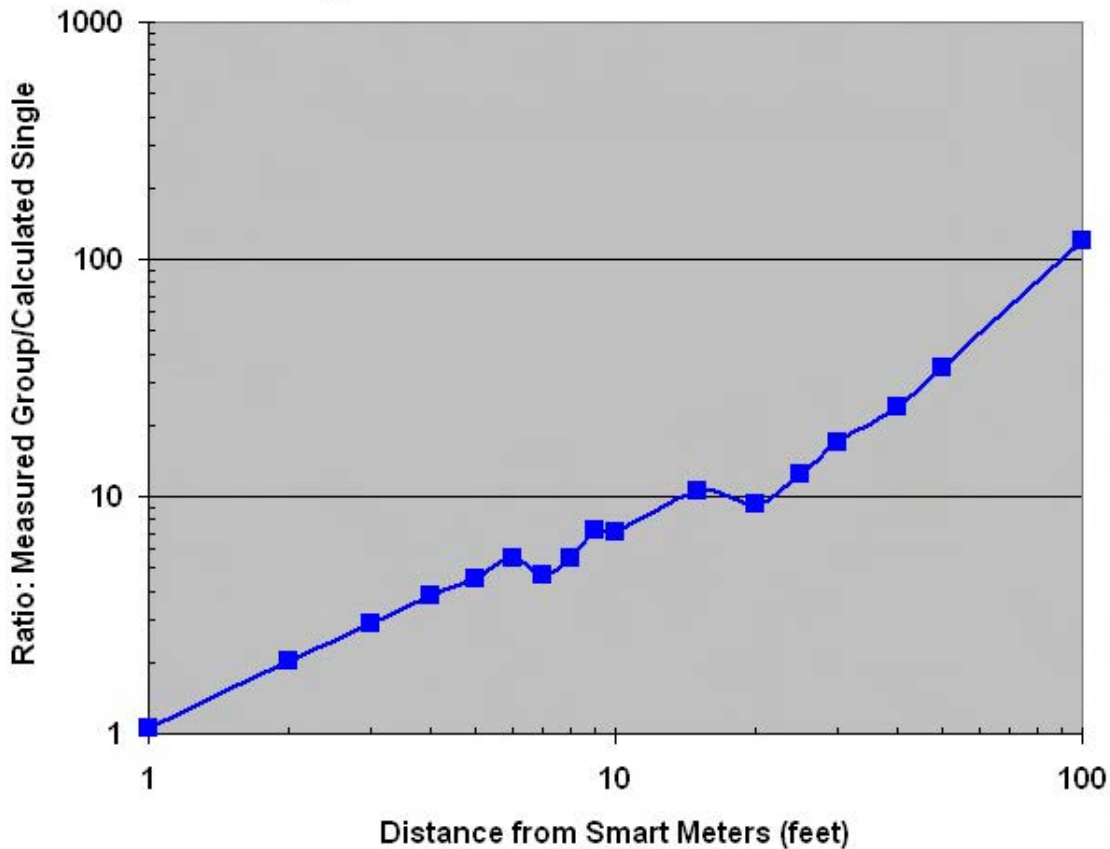


Figure 14-8
 Ratio of magnitude of measured RF fields of group of ten meters in the meter farm to magnitude of calculated RF field of a single meter from 1 to 100 feet. At greater distances from the group of ten meters, the contribution of RF fields from other meters within the meter farm become proportionally more significant.

In this figure, it is evident that near the group of multiple meters (ten meters in a rack) the measured value of the group is similar to that calculated for a single meter. However, as the distance from the group of meters increases, the ratio becomes greater, reflecting the capture of more energy from multiple meters. This supports the contention that when located very near a large group of meters, exposure is not necessarily simply additive due to the number of meters present. However, at large distances from the collection of meters, it is expected that exposure becomes more a result of the collective transmissions of all of the meters. Nonetheless, while this phenomenon is evident, the actual magnitude of the aggregate field becomes

significantly less than when located near the meters such that the resulting field may be irrelevant when assessing compliance with applicable RF exposure limits. The contributions of the many Smart Meters in the Itron meter farm likely impact the rate of field reduction with distance such that the decrease is not simply a function proportional to of the inverse square of distance.²⁷ One additional factor that relates to the observed decrease in measured field with distance from the rack of meters is that the measurement also included the contribution provided by the some 7000 meters operating within the meter farm; these signals were a part of the ambient field being measured since the detection probe of the SRM-3006 has an isotropic response.

²⁷ It is relevant to note that measurements made very close to a group of Smart Meters is somewhat similar to measurements in the near field of a large aperture antenna; when close to the group, the source does not appear as a point source but, rather, a spatially distributed source.

GHz. The FCC MPEs are in terms of 30-minute time averaged values as averaged over the body dimensions. It is important to note, from an FCC compliance perspective, that the use of the time averaging provision of the regulations relying on a particular behavior or action of an exposed person to achieve the necessary averaging of exposure is not acceptable. However, “source based” time-averaging based on an inherent property or duty-cycle of a device is allowed.^{28,29} Hence, the intermittent but routine transmissions of Smart Meters means that the time averaged value of exposure during any 30-minute period is to be used for assessing compliance with the FCC rules. To properly evaluate exposure relative to the FCC rules, the spatially averaged value of field is to be determined for comparison to the MPEs.

The above described FCC rules on RF exposure apply to FCC licensees. Electric utilities who may deploy many Smart Meters are not FCC licensees in respect to their use of Smart Meters with internal transmitters operating in the license free bands. However, besides the FCC rules applicable to its licensees, the FCC’s equipment authorization program oversees authorization of equipment using the radio frequency spectrum. These devices may not be imported and/or marketed until they have shown compliance with the technical standards which have been specified by the Commission. For many of the devices subject to the equipment authorization program, including those covered by Part 15 of the FCC’s rules, the FCC has included a requirement that the device manufacturer determine and represent that it meets the RF rules on exposure. This includes Smart Meters. In fact, the low power transmitters used in the Itron Smart Meters must be tested for compliance with the FCC RF rules before the Commission can issue a certification allowing the device to be marketed and used in commerce. An examination of the FCC’s equipment authorization database of certification reports reveals the application

of the FCC MPEs for assessing compliance with the FCC RF exposure rules³⁰. Smart Meters have been designated as mobile or fixed mount devices for which proximity to humans, once the device is installed, is specified as being 20 cm or greater. The FCC applies a 20 cm distance criterion to the intended use of a transmitting device relative to the body surface for determining whether the exposure must be evaluated through specific absorption rate (SAR) measurements. Because of the way that Smart Meters are intended to be used, SAR measurements are not called for, simply an assessment of RF fields in comparison to the MPEs.³¹

IEEE

The Institute of Electrical and Electronics Engineers (IEEE) in their IEEE Standard C95.1-2005 recommend maximum permissible exposure (MPE) values across the 3 kHz to 300 GHz spectrum that are frequency dependent. This frequency dependency feature is common to virtually all of the present standards or guidelines on RF exposure, taking into account the variation in RF energy absorption rates within the human body due to dimensional aspects of the body relative to wavelength. Figure 15-2 illustrates this frequency dependence for the IEEE standard for members of the general public. In the IEEE standard, these values are recommended as action levels. If the ambient RF field exceeds the action level, an RF safety program should be implemented to insure that exposures do not exceed the upper tier of the standard, or the MPE. When no RF safety program exists, the action levels may be used as MPEs for the general public. The MPEs are those values of RF field strength, or power density, that have been averaged over any 30-minute period (time averaging) and averaged over the dimensions of the body (spatial averaging).

²⁸ IEEE Standard C95.1-1991.

²⁹ Evaluating Compliance with FCC Guidelines for Human Exposure to Radiofrequency Electromagnetic Fields (1997). Office of Engineering and Technology Bulletin 65, Edition 97-01, Federal Communications Commission, August, p. 76. See also: 47 CFR 2.1093 (d)(5).

³⁰ See for example: <http://www.fcc.gov/oet/ea/fccid/> with an FCC device ID of SK9AMI-4.

³¹ When SAR is required, for devices intended to be used within 20 cm (about 8 inches) of the body, the localized SAR limit is 1.6 watts per kilogram of tissue, as averaged over any one gram of tissue.

Frequency range (MHz)	RMS electric field strength (E) ^a (V/m)	RMS magnetic field strength (H) ^a (A/m)	RMS power density (S) E-field, H-field (W/m ²)	Averaging time ^b E ² , H ² or S (min)	
0.1–1.34	614	16.3/f _M	(1000, 100 000/f _M ²) ^c	6	6
1.34–3	823.8/f _M	16.3/f _M	(1800/f _M ² , 100 000/f _M ²)	f _M ² /0.3	6
3–30	823.8/f _M	16.3/f _M	(1800/f _M ² , 100 000/f _M ²)	30	6
30–100	27.5	158.3/f _M ^{1.668}	(2, 9 400 000/f _M ^{3.336})	30	0.0636 f _M ^{1.337}
100–400	27.5	0.0729	2	30	30
400–2000	–	–	f _M /200	30	
2000–5000	–	–	10	30	
5000–30 000	–	–	10	150/f _G	
30 000–100 000	–	–	10	25.24/f _G ^{0.476}	
100 000–300 000	–	–	(90f _G –7000)/200	5048/[(9f _G –700)f _G ^{0.476}]	

NOTE—f_M is the frequency in MHz, f_G is the frequency in GHz.

^aFor exposures that are uniform over the dimensions of the body, such as certain far-field plane-wave exposures, the exposure field strengths and power densities are compared with the MPEs in the Table. For non-uniform exposures, the mean values of the exposure fields, as obtained by spatially averaging the squares of the field strengths or averaging the power densities over an area equivalent to the vertical cross section of the human body (projected area) or a smaller area depending on the frequency (see NOTES to Table 8 and Table 9 below), are compared with the MPEs in the Table.

^bThe left column is the averaging time for |E|², the right column is the averaging time for |H|². For frequencies greater than 400 MHz, the averaging time is for power density S

^cThese plane-wave equivalent power density values are commonly used as a convenient comparison with MPEs at higher frequencies and are displayed on some instruments in use.

Figure 15-2
Summary of the IEEE C95.1-2005 action levels or MPEs for the lower tier (applicable to members of the general public if uninformed about RF exposure and not able to reduce their exposure if necessary).

For the 902-928 MHz RF LAN emissions, the IEEE standard specifies an action level (MPE) of 0.451 mW/cm² or 451 μW/cm². This value is applicable at 902 MHz with a slightly greater value (0.464 mW/cm² or 464 μW/cm²) at the upper end of the band. At the mid-band frequency of 915 MHz, the MPE is 0.458 mW/cm² or 458 μW/cm². For the 2.4 GHz Zigbee transmitter emissions, the IEEE standard calls for a limit of 1 mW/cm² or 1,000 μW/cm² which applies across the frequency range of 2 GHz to 100 GHz.

ICNIRP

Internationally, the most widely recognized recommendations on RF exposure are guidelines of the International Commission on Non-Ionizing Radiation

Protection (ICNIRP)³². The guidelines for public exposure, reproduced in Figure 15-3 (Table 9-6 from the ICNIRP guidelines), are similar to the MPEs of the FCC. A difference, however, is in the averaging time (see footnote 3). The ICNIRP specifies an averaging time of six-minutes for assessing compliance with the “reference levels” for general public exposure to RF fields. This contrasts with the half-hour period stated in both the FCC rules and IEEE limits.

³² Guidelines for limiting exposure to time-varying electric, magnetic, and electromagnetic fields (up to 300 GHz). Health Physics, Vol. 74, No. 4, April 1998, pp. 494-522.

Table 7 Reference levels for general public exposure to time-varying electric and magnetic fields (unperturbed rms values)

Frequency range	E-field strength (V m ⁻¹)	H-field strength (A m ⁻¹)	B-field (μT)	Equivalent plane wave power density S_{eq} (W m ⁻²)
up to 1 Hz	—	3.2×10^4	4×10^4	—
1–8 Hz	10,000	$3.2 \times 10^4/f^2$	$4 \times 10^4/f^2$	—
8–25 Hz	10,000	$4,000/f$	$5,000/f$	—
0.025–0.8 kHz	$250/f$	$4/f$	$5/f$	—
0.8–3 kHz	$250/f$	5	6.25	—
3–150 kHz	87	5	6.25	—
0.15–1 MHz	87	$0.73/f$	$0.92/f$	—
1–10 MHz	$87/f^{0.2}$	$0.73/f$	$0.92/f$	—
10–400 MHz	28	0.073	0.092	2
400–2000 MHz	$1.375f^{0.2}$	$0.0037f^{0.2}$	$0.0046f^{0.2}$	$f/200$
2–300 GHz	61	0.16	0.20	10

Notes:

1. f as indicated in the frequency range column.
2. Provided that basic restrictions are met and adverse indirect effects can be excluded, field strength values can be exceeded.
3. For frequencies between 100 kHz and 10 GHz, S_{eq} , E^2 , H^2 , and B^2 are to be averaged over any 6-minute period.
4. For peak values at frequencies up to 100 kHz see Table 4, note 3.
5. For peak values at frequencies exceeding 100 kHz see Figures 1 and 2. Between 100 kHz and 10 MHz, peak values for the field strengths are obtained by interpolation from the 1.5-fold peak at 100 kHz to the 32-fold peak at 10 MHz. For frequencies exceeding 10 MHz it is suggested that the peak equivalent plane wave power density, as averaged over the pulse width, does not exceed 1000 times the S_{eq} restrictions, or that the field strength does not exceed 32 times the field strength exposure levels given in the table.
6. For frequencies exceeding 10 GHz, S_{eq} , E^2 , H^2 , and B^2 are to be averaged over any $68/f^{0.05}$ -minute period (f in GHz).
7. No E-field value is provided for frequencies <1 Hz, which are effectively static electric fields. For most people the annoying perception of surface electric charges will not occur at field strengths less than 25 kV m^{-1} . Spark discharges causing stress or annoyance should be avoided.

Figure 15-3

Summary of ICNIRP guidelines on RF exposure limits for the general public.

With regard to the Smart Meter fields associated with the transmitters evaluated in this study, i.e., in the 900 MHz and 2.4 GHz bands), the ICNIRP guidelines are identical to those of the FCC in terms of incident power densities except for averaging time.

Section 16: Discussion of Results and Insights

The issue of potential Smart Meter RF exposure of individuals can be addressed through an exposure assessment based on either direct measurements or theoretical calculations. This investigation sought to do both by collecting information on the physical transmitting characteristics of Itron Smart Meters at Itron's facility in South Carolina and at residential locations in southern California supplemented with some measurements in Colville, Washington. From detailed measurements of the transmitting pattern of the different RF sources within the meters, RF fields can be modeled through knowledge of the transmitter powers. A comprehensive exposure assessment for Smart Meters includes an evaluation of the maximum magnitude of the instantaneous peak field strength or power density in the area of interest and, then, adjustment of this value to account for the duty cycle of RF emissions from the meter and spatial averaging over typical body dimensions. Because the Smart Meters investigated in this study must meet certain technical specifications required by the FCC, application of the FCC MPE rules are most appropriate for such exposure assessments and, in fact, have become a requirement of the FCC as part of their equipment authorization program.

The low power nature of Smart Meter transmitters, typically less than one watt, means that any RF fields produced by them will be relatively weak. For example, even when the peak value of transmitter output power is assumed to apply continuously, which it does not and cannot when used in the mesh networks of Smart Meter deployed regions, the resulting RF fields are well below the applicable MPE limits. But, when typical transmitter duty cycles are applied, the resulting RF fields are reduced, commonly, by a hundred times or more to even lower values. Finally, if the potential exposure is interpreted as a spatially averaged value over the body, the final result is yet further reduced. Ultimately, indoor exposures will be even further reduced due to the RF field attenuation characteristics of common building materials.

Smart Meters are devices that are significantly different from portable radio transmitters, such as cellular

telephones and handi-talkies that are held against the head. In the latter case, RF exposure can be significantly greater simply due to the influence of device proximity relative to the body. Smart Meters are mounted in fixed locations and are not designed to be held against the body for proper use. Rather, typical exposure to Smart Meter fields will generally always be at some considerable distance as opposed to the use of devices like cell phones, cordless telephones, microwave ovens, wireless routers, etc. Nonetheless, for an exposure assessment that might be deemed a "worst case" scenario, it could be assumed that under relatively rare conditions, Smart Meters might be viewed from a close distance rather than from afar. For a person who may have a desire to approach the meter for a close-up view, while it would likely be a rare event, RF exposure will be near a maximum value. Such an exposure will be characterized by considerable spatial variability with the greatest RF fields near the surface of the meter.

Table 14-3 presents the results of an analysis that includes an upper range potential exposure scenario. The conservative estimates of duty cycle from the SCE data were used to convert peak values of RF fields to appropriate time-averaged values. A time-averaged duty cycle of 5% (maximum for end point meter RF LAN radios from the SCE data) has been applied to the calculated upper range values of fields for the 900 MHz RF LAN component of end point meters in Table 14-2. Consideration of ground reflections was included by application of a ground reflection factor of 1.344 at all distances, this being a conservative estimate of the actual value for distances up to ten feet from the meter (a ground reflection factor applicable at the closest analysis distance of one foot from the meter is actually smaller, being 1.032). An assumed upper range duty cycle of 1% has been applied to the 2.4 GHz Zigbee radio based on Itron information³³. In the case of cell relay meters, a duty cycle of 1% (based on the 99.9th percentile value of duty cycles) has been applied to the

³³ Analysis of Radio Frequency Exposure Associated with Itron OpenWay Communications Equipment. Itron publication, undated.

900 MHz RF LAN radio. An assumed duty cycle of 0.1% (based on uplink data traffic and the cellular modem data transmission rate) was applied to the cellular transmitter emissions of the cell relay meter. Table 14-3 provides values of RF fields expressed as a percentage of the MPE for two conditions: an assumption that each transmitter could operate at its maximum possible peak power (100% duty cycle) and the maximum expected operational duty cycle as given above. These values represent the estimated maximum

likely time-averaged total RF field that could exist near the Itron end point and cell relay Smart Meters studied in this report. The data tabulated in Table 14-3 for the maximum operational duty cycles are illustrated graphically in Figure 16-1. These results should be viewed as highly conservative estimates with actual RF fields being, in some cases, substantially less based on actual duty cycles.

Table 16-1

Estimated upper range of RF fields as a percentage of the FCC MPE for the public associated with Itron end point meters and cell relay meters including all RF components (900 MHz RF LAN, 2.4 GHz Zigbee and 850 MHz cellular transmitters). The 99th percentile powers for the RF LAN and Zigbee transmitters, main beam exposure and possibility of ground reflections to enhance fields was assumed.

	End point Smart Meter						Cell relay Smart Meter							
	RF LAN		HAN		Total		RF LAN		HAN		Cellular		Total	
DC (%)	100	5	100	1	100	Max	100	1	100	1	100	0.1	100	Max
Distance (ft)														
1	14.5	0.724	3.51	0.0351	18.0	0.759	9.20	0.092	4.26	0.0426	47.8	0.0478	61.3	0.182
2	3.62	0.181	0.876	0.00876	4.50	0.19	2.30	0.023	1.06	0.0106	12.0	0.012	15.4	0.0456
3	1.61	0.0805	0.389	0.00389	2.00	0.0844	1.02	0.0102	0.473	0.00473	5.31	0.00531	6.80	0.0202
4	0.906	0.0453	0.219	0.00219	1.12	0.0475	0.575	0.00575	0.266	0.00266	2.99	0.00299	3.83	0.0114
5	0.580	0.029	0.140	0.0014	0.72	0.0304	0.368	0.00368	0.170	0.0017	1.91	0.00191	2.45	0.00729
6	0.402	0.0201	0.0974	0.000974	0.499	0.0211	0.256	0.00256	0.118	0.00118	1.33	0.00133	1.70	0.00507
7	0.296	0.0148	0.0715	0.000715	0.368	0.0155	0.188	0.00188	0.0869	0.000869	0.976	0.000976	1.25	0.00372
8	0.226	0.0113	0.0548	0.000548	0.281	0.0118	0.144	0.00144	0.0665	0.000665	0.747	0.000747	0.958	0.00285
9	0.179	0.00894	0.0433	0.000433	0.222	0.00937	0.114	0.00114	0.0526	0.000526	0.590	0.00059	0.757	0.00226
10	0.145	0.00724	0.0351	0.000351	0.18	0.00759	0.092	0.00092	0.0426	0.000426	0.478	0.000478	0.613	0.00182
15	0.0644	0.00322	0.0156	0.000156	0.08	0.00338	0.0409	0.000409	0.0189	0.000189	0.212	0.000212	0.272	0.00081
20	0.0362	0.00181	0.00876	8.76E-05	0.045	0.0019	0.023	0.00023	0.0106	0.000106	0.120	0.00012	0.154	0.000456
25	0.0232	0.00116	0.00561	5.61E-05	0.0288	0.00122	0.0147	0.000147	0.00681	6.81E-05	0.0765	0.0000765	0.098	0.000292
30	0.0161	0.000805	0.00389	3.89E-05	0.02	0.000844	0.0102	0.000102	0.00473	4.73E-05	0.0531	0.0000531	0.068	0.000202

Estimated Maximum Likely Time-Averaged RF Field Near an Itron Smart Meter (Not including spatial averaging)

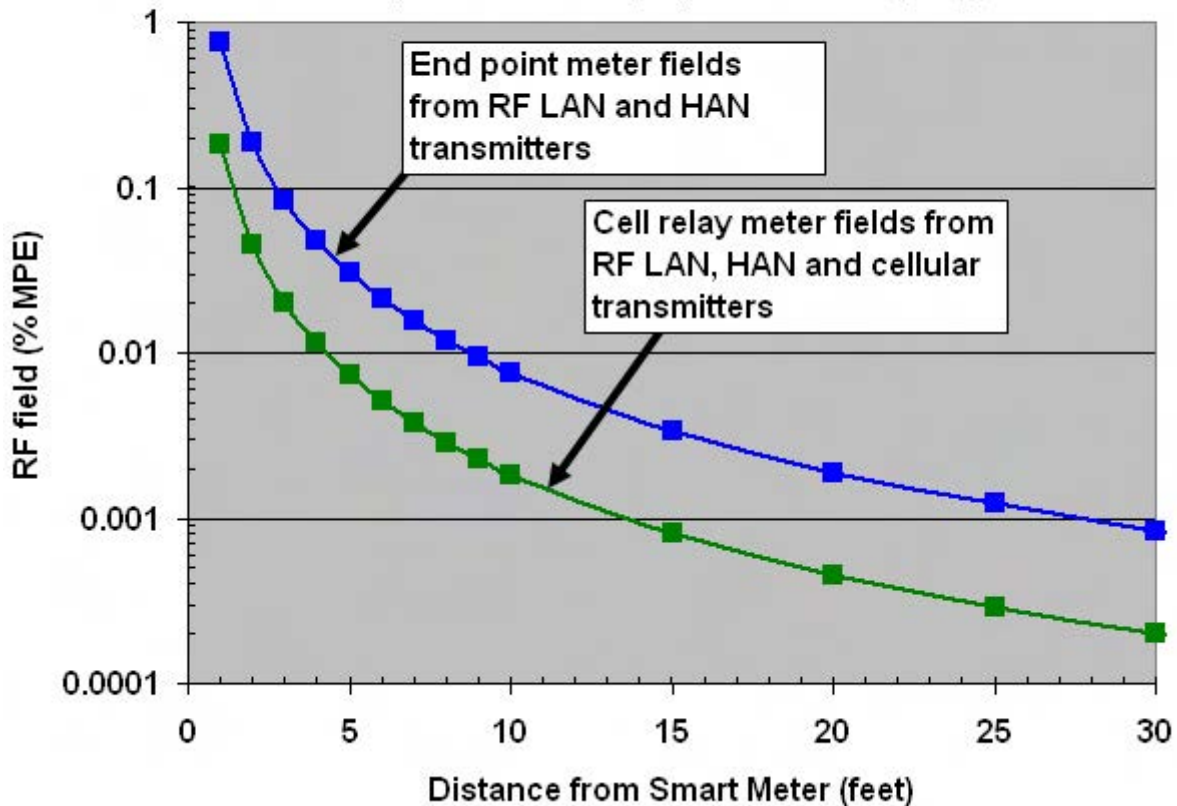


Figure 16-1
Estimated maximum likely time-averaged RF fields near Itron end point and cell relay Smart Meters included in this study. The plotted values are based on the 99th percentile values of transmitter powers, duty cycles given in Table 14-3 based on the conservative estimates from SCE data, main beam exposure and inclusion of realistic ground reflected fields ($\Gamma = 1.344$) that might add constructively to the resultant field. An assumption is made that the maximum RF field from all transmitters occurs at the same point in space. The graph pertains to a single end point meter and a single cell relay meter.

The RF field values shown in Figure 16-1 do not account for spatial averaging. Spatial averaging will be most significant when an individual is close to the meter such that there is considerable variation in the field over the body dimensions. As illustrated in Figures 11-2 and 11-3, when very close to a Smart Meter, the spatially averaged field will be substantially less than the spatial maximum value. For an end point meter, with exposure at approximately one foot from the meter, spatial averaging would be expected to reduce the maximum value shown in Figure 16-1 of about 0.8% of MPE to approximately 0.2% of MPE. For a cell relay, spatial averaging would result in reducing a spatial peak value

of about an exposure of 0.2% of MPE to about 0.06% of MPE.

When the exposure assessment is for locations within a residence, generally the point of maximum RF field produced by Smart Meters is very close to where the meter is mounted on the outside of the house. For those interior areas located behind the meter, the antenna patterns obtained during this study show that relatively significant reductions in RF energy exist toward the back side of the meter as compared to the frontal region, outside the house. Inspection of the various antenna patterns discussed earlier reveals, in most cases,

very significant reduction of the RF field directly behind the meters, some times less than one percent of the forward directed value (more than 20 dB down from the forward value). Although significant notches in the pattern can exist behind the meters, these pattern notches are in some cases not very broad. In a more conservative view, however, the pattern data support a practical field reduction of nominally 10 dB, i.e., a factor of ten reduction in the field relative to the forward directed value. This factor means that the RF

fields behind a Smart Meter mounted on the exterior wall of a house that are directed toward the house, will be about 1/10th of the RF field intensity at the same distance but in front of the meter, not taking into account any attenuation afforded by the wall construction itself. Peak values of Smart Meter RF fields found inside two residences equipped with continuously transmitting Smart Meters (to facilitate the measurements) are summarized in Table 16-1.

*Table 16-2
Summary of interior residential RF field measurements on two residences equipped with Smart Meters operating in continuous transmit mode.*

	Percent FCC MPE for the general public			
	Residence A		Residence B	
	900 MHz	2.4 GHz	900 MHz	2.4 GHz
Home maximum	0.0100	0.0288	0.00872	0.0150
Home average	0.00237	0.00825	0.00144	0.00779
Home minimum	0.00014	0.00588	0.00052	0.00596

These data pertain only to the interior room measurements but are exclusive of specific microwave oven measurements taken in residence A. The highest values in the 2.4 GHz band were both associated with the use of a wireless router within the room.

The effect that the structure of homes can have on Smart Meter fields inside the home is also significant. Based on the measurements reported here, RF fields directly behind a Smart Meter mounted on the exterior wall of a stucco home, but inside the house, would be expected to be attenuated by at least 6.1 dB in the 900 MHz RF LAN band and 2.5 dB in the 2.4 GHz Zigbee frequency band (these values represent the most conservative values of insertion loss found in the measurements conducted in California and Washington). For locations immediately near the surface of the wall, greater wall attenuation effects would be expected, similar to the values reported above in Table 10-1. Hence, it is expected that, for stucco type homes that have typical stucco netting on the outside, RF fields will be attenuated by a factor of 4 for the 900 MHz RF LAN transmitter and a factor of about 1.7 for the 2.4 GHz Zigbee transmitter. In the case of an end point meter, this would translate to a maximum indoor RF field of about 0.55% of the MPE, assuming that both the RF LAN and Zigbee transmitters are

continuously active and the distance from the meter to the inside surface of the wall is 12 inches. With only the RF LAN transmitter active, as was the case during the residential measurements in California, a maximum value of 0.36% of the MPE would be expected. These values do not assume application of spatial averaging or time averaging. During the measurements in actual residences, a maximum interior field from the RF LAN transmitter of 0.01% was measured (residence A). Interestingly, the measured RF field in the home office of this residence was 0.03% of the MPE due to the presence of a wireless router located in the office.

Acquiring measurement data on the very intermittent emissions of Smart Meters that can accurately yield the duty cycle of the meters is challenging. Even measuring the number of times that a Smart Meter emits a signal over a 24-hour day is problematic. The measurements documented here show that in no case did the RF fields, even with continuous transmission (100% duty cycle), approach the FCC MPE for the general public - calculated exposure at one foot for 100% duty cycle when spatially averaged (61.3% MPE × 0.233 = 14.3% MPE). Generally, maximum measured values were small fractions of the MPE. Limited measurement data taken in the Itron meter farm, with thousands of Smart Meters operating, suggested very low duty cycles of

about 0.2%. This measurement involved contributions of many meter emissions so that the meter farm likely represents a much more dense Smart Meter environment than most U.S. neighborhoods wherein Smart Meters have been deployed.

An alternative view of the RF field data presented in Table 14-3 is to note that at a distance of one foot directly in front of the meter, even if all transmitter components in the end point meters or cell relays were to operate in a continuous mode which is unrealistic and which would inhibit the mesh network from performing, and no adjustment for spatial averaging of the fields were to take place, the resulting RF fields are still less than the FCC MPE for public exposure.

The Wi-Spy measurements taken at a single residence and in the Itron meter farm also suggested that the duty cycle of Smart Meters, during the observation time, was very small, in the range of less than one percent.

Likely, the most accurate assessment of Smart Meter duty cycles can be through use of the meter data management system associated with operation of an electric utility company network of meters. Determining the amount of data transferred across the mesh network by a given meter can be one approach to “remotely” determining the activity of the Smart Meter. Through such analyses of meter activity, duty cycles applicable over specific time periods can be ascertained. For example, the variation of duty cycle throughout a day could be examined given collection of meter data over sufficiently long times. In this way, maximum 30-minute duty cycles can be determined and applied to calculated peak field values to obtain time-averaged values for direct comparison to the FCC MPEs.

Section 17: Conclusions

The radio transmitters inside the Itron Smart Meters studied in this project typically produce RF fields substantially below the FCC limit at 900 MHz in their vicinity. Because of the low power, low antenna gains and highly intermittent emissions, time-averaged RF fields to which someone standing immediately next to the meter could be exposed are substantially below any of the current scientifically based human exposure limits.

RF exposure produced by Smart Meters is dependent on transmitter powers, frequencies (exposure limits are frequency dependent), meter installation details such as mounting height, the construction details of the structure on which the meter is installed (building materials attenuate the RF signals of the Smart Meters) and the activity of the wireless mesh network itself. The transmitters emit intermittent signals having instantaneous peak field strengths, or power densities, that are already generally low by comparison with exposure limits but any resulting spatial averaging over the body and temporal averaging, for determining compliance with FCC MPEs, further reduces the exposure magnitude.

The Itron end point Smart Meters included in this study contained two transmitters, one operating in the 900 MHz license free band (for the RF LAN function) and the other in the 2.4 GHz license free band (for the home area network, HAN, function). These transmitters operate with nominal powers of 24.5 dBm (282 mW) and 18.5 dBm (70.8 mW) respectively. The more rare cell relay meters contain the same two transmitters described above and an additional cellular transmitter that operates at a nominal output power of between 25.1 dBm and 31.8 dBm depending on whether it uses GSM or CDMA technology and the particular frequency band used.

Antenna pattern measurements show that the Smart Meters generally radiate RF signals preferentially away from the meter but with relatively broad patterns, producing a very rough approximation to an omnidirectional emitter. However, behind the meter, the RF field is nominally a factor of 10 less than at the

same distance in front of the meter. Even with the broad pattern, RF exposure of a person standing immediately adjacent to a Smart Meter will be predominately of the portion of the body nearest the meter. Spatial averaging of the RF fields shows that the spatially averaged value of exposure, in terms of a percentage of the MPE, is on the order of one-fourth of the maximum value at any location on the body.

Measurements of Smart Meter fields present a challenge due to their highly intermittent nature and frequency hopping characteristic. The most effective approach to evaluating the magnitude of RF fields produced by Smart Meters with field measuring equipment is to cause the transmitters to operate in continuous mode, some times referred to as FCC mode, since this allows for much easier measurements. Such an approach results in determination of the instantaneous peak value of RF field to which must be applied appropriate duty cycle values to obtain time-averaged values for exposure. A valid and readily expedient approach to estimating potential exposure of Smart Meters is via calculation based on knowledge of the transmitting characteristics of the meter transmitters. The most common method of calculation is to invoke the maximum gain of the antennas in arriving at a conservative (typically an over estimate) value for the emitted field in the vicinity of the meter.

Both measurements and calculations of RF fields associated with the Itron meters included in this study were pursued in an effort to develop a solid basis for determining the peak fields that can exist near the meters. Both of these approaches yielded similar findings, namely that the RF fields produced by the Itron Smart Meters are compliant with applicable human exposure. Typical RF exposure near (at one foot) the Smart Meters evaluated are most likely less than 20% of the MPE in terms of instantaneous peak RF fields of an end point meter and less than 1% of the MPE in terms of time-averaged values (see Table 7-6). RF fields that occur as close as 1 foot from the cell relays (which occur in one in 500 to 750 residences) are less than 61% of the MPE in terms of instantaneous peak RF fields and less than 0.2% of the MPE in terms

of time-averaged values. At ten feet from an end point or cell relay meter, RF fields are likely less than 0.2% and 0.6% of the MPE in terms of instantaneous peak RF fields, respectively, and less than 0.01% and 0.002% of the MPE in terms of typical time-averaged RF fields, respectively.

To put these estimates into some practical perspective, spatially averaged values of fields will be substantially less (typically between 18%-24% of the peak values) and, for indoor locations such inside a residence, any resulting exposure will also be significantly reduced because of attenuation to the Smart Meter emissions caused by the construction materials of the wall separating the meter from the inside of the house. House attenuation effects could easily account for between 75%-89% reduction of the 900 MHz RF LAN emissions and between 44%-64% reduction of the 2.4 GHz Zigbee radio emissions indicated above.

Accurately determining time-averaged RF fields represents the most uncertainty in exposure assessments for the Smart Meters evaluated in this study. This is due to the dynamic signal transmissions of Smart Meters of varying length and the associated frequency hopping nature of the 900 MHz RF LAN transmitter making it difficult to properly capture every emission with “off the shelf” instrumentation. In reality, the transmitter activity of Smart Meters is best described in a statistical fashion since it is not possible to exactly define if and when a given Smart Meter will transmit and how often, with absolute accuracy. Given the nature of mesh networks, hundreds of meters are interacting with one another in a way to form connections between the various meters and, ultimately, a cell relay meter. The activity of this interaction leads to variability in the activity of each of the RF LAN transmitters and, hence, measurements at any particular time are not expected to

necessarily be indicative of the same transmitter’s activity during another time of day or on another day. Such measurements, even if properly made, can provide insight to a Smart Meter’s transmitting characteristics but, unless conducted over an extended period, are unlikely to yield meaningful measures of maximum average duty cycles. The most meaningful determination of Smart Meter duty cycles over the long term so that maximum 30-minute values can be ascertained is most likely based on exploiting software approaches. Through examining meter data throughputs, over many meters within a Smart Meter deployed region, and over an extended period of time, good statistical representation of meter RF activity should be achievable. Future work to develop comprehensive statistical descriptions of Smart Meter transmissions remains to be done but, in any event, the real duty cycles of Smart Meters would appear to be very small percentages. Ambient RF fields associated with operation of cellular base stations, radio and TV broadcasting and the emissions produced by a variety of everyday activities that involve the use of electronic devices can be comparable to or even exceed common exposures resulting from the operation of Smart Meters.

Regardless of duty cycle values for end point and cell relay meters, common exposures of individuals that are likely to result from the operation of the Itron Smart Meters evaluated in this study are very low and comply with scientifically based human exposure limits by a wide margin.

Appendix A: Instrument Calibration Certificates



Figure A-1
Calibration certificate for the Narda Model 8715 digital meter for use with the Model B8742D probe.



Certificate of Calibration

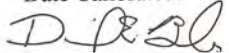
L-3 Communications, Narda Microwave-East, hereby certifies that the referenced instrument has been calibrated by qualified personnel to Narda's approved test procedures.

Furthermore, the instrument meets, or exceeds, all published specifications and the calibration has been performed with test instrumentation that, where applicable, is traceable to the National Institute of Standards and Technology.

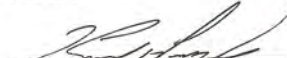
Narda's calibration measurements are traceable to the National Institute of Standards and Technology to the extent allowed by the bureau's calibration facilities.

Customer: RICHARD TELL ASSOCIATES INC Certificate #: 99298 2
COLVILLE, WA 99114

Model #: B8742D Serial #: 03002
Description: PROBE PO #: AMEX - TELL
Date Calibrated: 10/07/2009 R.O. #: 99298



Dan Beach
Manufacturing



Ken Peck
Quality Assurance

This certificate shall not be reproduced, except in full, without written approval from L-3 Communications, Narda Microwave-East
L-3 COMMUNICATIONS, NARDA MICROWAVE-EAST, 435 MORELAND ROAD, HAUPPAUGE, NEW YORK 11788, TEL: 631-231-1700, FAX: 631-231-1711

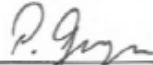
Figure A-2
Calibration certificate for the Narda Model B8742D broadband probe.

Calibration Certificate

Narda Safety Test Solutions hereby certifies that the object referred to in this certificate has been calibrated by qualified personnel using Narda's approved procedures. The calibration was carried out in accordance with a certified quality management system which conforms to ISO 9001

OBJECT	Selective Radiation Meter, Basic Unit, SRM-3006
MANUFACTURER	Narda Safety Test Solutions GmbH
PART NUMBER (P/N)	3006/01
SERIAL NUMBER (S/N)	A-0077
CUSTOMER	
CALIBRATION DATE	2009-11-06
RESULT ASSESSMENT	within specifications
AMBIENT CONDITIONS	Temperature: (23 ± 3)°C Relative humidity: (25 to 75)%
CALIBRATION PROCEDURE	3006-8701-00A

ISSUE DATE: 2009-12-10


 CALIBRATED BY:
 Paul Geyer


 AUTHORIZED SIGNATORY:
 Norbert Moll

MANAGEMENT
SYSTEM



Certified by DQS against
 DIN EN ISO 9001:2000
 (Reg.-No. 099379)

This calibration certificate may not be reproduced other than in full except with the permission of the issuing laboratory. Calibration certificates without signature are not valid.

CERTIFICATE 300601-A0077-20091106-62

PAGE 1 OF 6

Figure A-3
 Calibration certificate sheet 1 for the Narda Model SRM-3006 SN A-0077.

OBJECT

The spectrum analyzer is based on digital signal processing. Small frequency spans were measured at fixed local oscillator (1st LO) settings using discrete Fourier transformation (DFT). The LO was also swept for larger frequency spans.

A memory chip contains correction values for various frequencies and object settings. The stored values were taken into account automatically during the measurement.

METHOD OF MEASUREMENT

Calibration using the reference standard. The output power level of the synthesized CW generator was adjusted and calibrated using power sensors as reference standards.

The frequency of the generator was calibrated using a frequency counter.

The reflection of the object was measured directly using a vector network analyzer (VNA) calibrated by means of a calibration kit. The measuring equipment and the associated uncertainty were verified using a reference standard (traceability kit).

CALIBRATION PROCEDURE

The object was connected to the signal source instead of the power sensors in order to calibrate it.

Measurement of the RF frequency response was made with different settings of the measurement range. As a result, the measured values also include the effects due to the "input attenuator" and the "reference level accuracy".

The calibration factor was calculated for various frequencies and settings from a comparison between the "actual level" and the "indicated level".

All the selection filters are digital filters. No calibration of the filters is necessary.

TRACEABILITY

The calibration results are traceable to the International System of Units (SI) in accordance with ISO/IEC 17025. The measuring equipment used for calibration is traceable through the reference standards listed below.

STANDARD	MANUFACTURER	MODEL	SERIAL NUMBER	ID	CERTIFICATE	NEXT CAL. DATE	TRACE
HF-MILLIVOLTMETER	R&S	URV55	100143	913	0124 DKD-K-16101 2008-04	2010-04	DKD
DIODE POWER SENSOR	R&S	NRV Z4	100122	912	0171 DKD-K-16101 2008-11	2010-11	DKD
THERMAL POWER SENSOR	R&S	NRV Z51	101777	1635	0264 DKD-K-16101 2008-11	2010-11	DKD
MISMATCH VSWR 1,2 (f)	Rosenberger	--	01237	552-3	12996 DKD-K-00201 2008-05	2010-05	DKD
FREQUENCY COUNTER	Advantest	R5362	120700137	923	15137 DKD-K-00201 2009-09	2011-09	DKD

Figure A-3 (continued)

Calibration certificate sheet 2 for the Narda Model SRM-3006 SN A-0077.

UNCERTAINTY

The reported expanded uncertainty U is based on a standard uncertainty multiplied by a coverage factor $k = 1.96$, providing a level of confidence of approximately 95 %. The uncertainty evaluation has been carried out in accordance with the "Guide to the Expression of Uncertainty in Measurement" (GUM). The reported measurement uncertainty is derived from the uncertainty of the calibration procedure and the object during calibration, and makes no allowance for drift or operation under other environmental conditions.

MEASURING CONDITIONS

The following results were obtained after adjustment of the object under calibration. These values are within the setting ranges defined by the manufacturer.

RESULTS

1	FREQUENCY RESPONSE (IF):	passed
2	FREQUENCY RESPONSE (RF):	passed
3	OUT-OF-BAND RESPONSE:	passed
4	FREQUENCY ACCURACY	passed
5	NOISE SIDEBAND (SSB):	passed
6	SPURIOUS (input related)	passed
7	SPURIOUS (residual)	passed
8	NOISE FLOOR:	passed
9	INTERMODULATION REJECTION (2 nd and 3 rd order):	passed
10	INPUT RETURN LOSS:	passed

Figure A-3 (continued)

Calibration certificate sheet 3 for the Narda Model SRM-3006 SN A-0077.

APPENDIX

FREQUENCY RESPONSE (RF)

The generator was set to the *Fgen*. The object settings were *Fspan*, *RBW*, and *Fcent*.

The measurements were made at different settings of the measurement range *MR*. The nominal level of the generator was -7 dBm for $-32\text{dBm} \leq MR \leq -5\text{dBm}$ and -32 dBm for the remaining measurement ranges.

The frequency response *G* was calculated as the difference of the actual generator level L_{actual} and the indicated level $L_{indicated}$ according to the following equation:
 $G/\text{dB} = (L_{indicated} - L_{actual})/\text{dBm}$

Frequency in MHz	Fspan in MHz	RBW in kHz	Fcent in MHz	MR												U
				-30	-28	-25	-20	-15	-10	-5	0	5	10	15	20	
0.00901	0.002	0.01	0.01	0.04	0.03	0.02	0.01	0.01	0.04	0.02	0.02	0.01	0.01	0	0	0.2
0.012	0.006	0.5	0.012	0.04	0.03	0.02	0.01	0.01	0.04	0.02	0.02	0.01	0.01	0	-0.01	0.2
0.02	0.02	2	0.02	0.04	0.03	0.02	0.01	0.01	0.04	0.02	0.02	0.01	0.01	0	-0.01	0.2
0.04	0.02	2	0.04	0.04	0.03	0.02	0.01	0.01	0.04	0.02	0.02	0	0.01	0	-0.01	0.2
0.1	0.02	2	0.1	0.04	0.03	0.02	0.01	0.01	0.03	0.02	0.01	0	0.01	0	-0.01	0.2
0.5	0.02	2	0.5	0.04	0.03	0.02	0.01	0.01	0.04	0.02	0.02	0.01	0.01	0	-0.01	0.2
2	0.02	2	2	0.04	0.03	0.02	0.02	0.01	0.04	0.02	0.02	0.01	0.01	0	-0.01	0.2
10	0.02	2	10	0.05	0.05	0.04	0.03	0.02	0.05	0.04	0.03	0.02	0.02	0.01	0.01	0.2
20	0.02	2	20	0.05	0.05	0.04	0.03	0.02	0.06	0.04	0.04	0.03	0.03	0.02	0.02	0.2
30	0.02	2	30	0.05	0.04	0.04	0.03	0.02	0.04	0.04	0.03	0.02	0.02	0.01	-0.01	0.2
31.233	26.75	30	44.578	-0.28	-0.36	-0.27	-0.36	0.01	-0.23	-0.26	-0.36	0.01	-0.22	-0.25	-0.36	0.2
36.1	26.75	30	44.578	-0.13	-0.21	-0.16	-0.22	-0.04	-0.12	-0.16	-0.21	-0.03	-0.13	-0.16	-0.22	0.2
40	0.02	2	40	0.05	0.04	0.04	0.03	0.03	0.07	0.04	0.03	0.03	0.02	0.03	0.05	0.2
44.1	26.75	30	44.578	-0.01	-0.03	-0.03	-0.04	-0.05	-0.01	-0.04	-0.03	-0.06	-0.04	-0.03	-0.02	0.2
50	0.02	2	50	0.05	0.04	0.03	0.02	0.01	0.02	0.03	0.02	0.01	0.01	-0.01	-0.05	0.2
52.1	26.75	30	44.578	0.04	0.03	0.01	0.01	-0.1	0.05	-0.01	0.02	-0.1	-0.02	-0.02	0.06	0.2
57.9948	0.02	2	57.9868	0.04	0.03	0.03	0.02	0.01	0.07	0.03	0.02	0.01	0.01	0.02	0.05	0.2
58.344	26.75	30	44.999	0.03	0.03	-0.02	-0.01	-0.17	0.03	-0.04	0	-0.17	-0.07	-0.04	0.02	0.2
60.1	26.75	30	60.1	-0.01	-0.02	-0.02	-0.02	-0.02	0	-0.02	-0.02	-0.03	-0.02	-0.03	0	0.2
100.1	26.75	30	100.1	-0.02	-0.01	-0.01	-0.02	-0.03	-0.01	-0.02	-0.02	-0.03	-0.03	-0.03	-0.02	0.2
200.1	26.75	30	200.1	-0.02	-0.02	-0.02	-0.02	-0.03	0	-0.02	-0.03	-0.03	-0.03	-0.04	-0.01	0.2
300.1	26.75	30	300.1	-0.05	-0.05	-0.05	-0.05	-0.06	-0.05	-0.06	-0.06	-0.07	-0.07	-0.07	-0.06	0.2

Figure A-3 (continued)
 Calibration certificate sheet 4 for the Narda Model SRM-3006 SN A-0077.

Frequency in MHz	Fspan in MHz	RBW in kHz	Fcent in MHz	MR												U	
				-30	-28	-25	-20	-15	-10	-5	0	5	10	15	20		
400.1	26.75	30	400.1	0.02	0.02	0.01	0.02	0.01	0.02	0	0	-0.01	0	0	0	0.2	
500.1	26.75	30	500.1	0.02	0.02	0.01	0.02	0.01	0.02	0	0	-0.01	-0.01	-0.01	0	0.2	
600.1	26.75	30	600.1	-0.01	-0.01	-0.02	-0.02	-0.02	-0.02	-0.04	-0.03	-0.05	-0.05	-0.04	-0.01	0.2	
700.1	26.75	30	700.1	-0.02	-0.03	-0.03	-0.03	-0.03	-0.03	-0.04	-0.04	-0.05	-0.05	-0.05	-0.03	0.2	
800.1	26.75	30	800.1	-0.02	-0.02	-0.02	-0.03	-0.03	-0.03	-0.04	-0.04	-0.06	-0.06	-0.05	-0.04	0.2	
900.1	26.75	30	900.1	0	0	0	0	-0.01	-0.01	-0.02	-0.03	-0.04	-0.04	-0.03	-0.02	0.2	
1000.1	26.75	30	1000.1	-0.01	-0.01	-0.01	-0.01	-0.02	-0.02	-0.03	-0.04	-0.04	-0.04	-0.04	-0.03	0.2	
1100.1	26.75	30	1100.1	0	0	-0.01	0	-0.01	0	-0.03	-0.03	-0.03	-0.04	-0.04	0	0.2	
1200.1	26.75	30	1200.1	-0.01	-0.01	-0.02	-0.02	-0.02	-0.02	-0.04	-0.05	-0.04	-0.04	-0.05	-0.03	0.2	
1300.1	26.75	30	1300.1	-0.03	-0.03	-0.03	-0.04	-0.05	-0.05	-0.06	-0.07	-0.07	-0.07	-0.07	-0.06	0.2	
1400.1	26.75	30	1400.1	0.02	0.01	0.01	0.01	0	0.01	-0.02	-0.02	-0.02	-0.03	-0.02	-0.02	0.2	
1500.1	26.75	30	1500.1	0.07	0.07	0.06	0.06	0.06	0.05	0.03	0.02	0.03	0.02	0.01	0.03	0.2	
1600.1	26.75	30	1600.1	0.05	0.03	0.03	0.04	0.03	0.03	0	0	0.01	-0.01	0	0.01	0.2	
1700.1	26.75	30	1700.1	0.03	0.02	0.03	0.02	0.01	0.02	-0.01	-0.02	-0.01	-0.03	-0.02	-0.01	0.2	
1800.1	26.75	30	1800.1	0.03	0.02	0.02	0.01	0.01	0.01	-0.02	-0.02	-0.01	-0.02	-0.02	-0.01	0.2	
1900.1	26.75	30	1900.1	0.02	0.02	0.03	0.02	0.01	0.01	-0.02	-0.02	-0.01	-0.04	-0.04	-0.02	0.2	
2000.1	26.75	30	2000.1	0.05	0.04	0.04	0.03	0.02	0.03	-0.01	-0.01	0	-0.02	-0.02	-0.01	0.2	
2100.1	26.75	30	2100.1	0.04	0.04	0.04	0.04	0.03	0.03	-0.01	-0.02	-0.01	-0.03	-0.01	-0.02	0.2	
2200.1	26.75	30	2200.1	0.05	0.05	0.05	0.05	0.03	0.03	-0.02	-0.01	-0.01	-0.03	-0.01	-0.02	0.2	
2300.1	26.75	30	2300.1	0.05	0.05	0.05	0.05	0.03	0.02	0	-0.01	-0.02	-0.02	-0.02	0.01	0.2	
2400.1	26.75	30	2400.1	0.02	0.02	0.02	0.01	0.02	-0.01	-0.03	-0.03	-0.06	-0.06	-0.03	-0.02	0.2	
2500.1	26.75	30	2500.1	0.03	0.03	0.02	0.03	0.03	0	-0.03	-0.03	-0.05	-0.05	-0.04	-0.01	0.2	
2600.1	26.75	30	2600.1	0.05	0.04	0.04	0.05	0.04	-0.02	-0.02	-0.01	-0.05	-0.02	-0.03	-0.01	0.2	
2700.1	26.75	30	2700.1	0.06	0.06	0.05	0.05	0.04	-0.02	-0.02	-0.02	-0.04	-0.04	-0.04	-0.02	0.2	
2800.1	26.75	30	2800.1	0.06	0.05	0.05	0.05	0.04	-0.01	-0.02	-0.01	-0.04	-0.05	-0.03	-0.01	0.2	
2900.1	26.75	30	2900.1	0.06	0.06	0.03	0.06	0.06	-0.03	-0.02	-0.01	-0.05	-0.06	-0.03	0	0.2	
2999.9	26.75	30	2999.9	0.08	0.06	0.08	0.05	0.05	-0.02	-0.02	-0.02	-0.06	-0.04	-0.04	0.01	0.2	
3002.1	26.75	30	3002.1	0.01	0.01	0	0	0.02	-0.01	0.07	0.07	0.07	0.07	0.08	0.1	0.2	
3100.1	26.75	30	3100.1	-0.02	-0.02	-0.02	-0.01	-0.03	-0.02	0.05	0.06	0.06	0.06	0.07	0.1	0.2	
3200.1	26.75	30	3200.1	0.01	0.01	0	0.01	0.01	0.03	0.08	0.1	0.11	0.1	0.11	0.12	0.2	
3300.1	26.75	30	3300.1	0.03	0.03	0.04	0.03	0.04	0.08	0.11	0.11	0.12	0.12	0.13	0.13	0.2	
3400.1	26.75	30	3400.1	0.01	0.01	0.01	0.01	0.01	-0.02	0.1	0.09	0.1	0.11	0.1	0.11	0.12	0.2

Figure A-3 (continued)
 Calibration certificate sheet 5 for the Narda Model SRM-3006 SN A-0077.

Frequency in MHz	Fspan in MHz	RBW in kHz	Fcent in MHz	MR												U
				-30	-28	-25	-20	-15	-10	-5	0	5	10	15	20	
3500.1	26.75	30	3500.1	0.02	0.01	0.01	0.01	0	0.12	0.12	0.11	0.13	0.13	0.13	0.13	0.2
3600.1	26.75	30	3600.1	0.02	0.02	0.01	0	0.03	0.14	0.13	0.12	0.15	0.14	0.13	0.13	0.2
3700.1	26.75	30	3700.1	0.02	0.02	0.03	0.03	0.02	0.16	0.13	0.13	0.17	0.14	0.15	0.17	0.2
3800.1	26.75	30	3800.1	0.01	0.02	0.01	0.01	0.01	0.16	0.14	0.13	0.16	0.14	0.18	0.16	0.2
3900.1	26.75	30	3900.1	0.01	0.01	0.01	0	-0.01	0.17	0.14	0.14	0.16	0.16	0.17	0.15	0.2
4000.1	26.75	30	4000.1	0	0.01	0	-0.02	-0.01	0.18	0.15	0.14	0.16	0.17	0.16	0.14	0.2
4100.1	26.75	30	4100.1	0.04	0.03	0.04	0.03	0.02	0.19	0.19	0.19	0.2	0.2	0.2	0.21	0.2
4200.1	26.75	30	4200.1	0.06	0.05	0.05	0.05	0.03	0.2	0.22	0.21	0.22	0.22	0.22	0.24	0.2
4300.1	26.75	30	4300.1	0.05	0.07	0.05	0.05	0.04	0.24	0.23	0.23	0.24	0.24	0.24	0.26	0.2
4400.1	26.75	30	4400.1	0.04	0.04	0.04	0.04	0.02	0.23	0.24	0.23	0.22	0.24	0.26	0.26	0.2
4500.1	26.75	30	4500.1	0.02	0.02	0.03	0.03	0.02	0.23	0.24	0.25	0.23	0.24	0.25	0.26	0.2
4600.1	26.75	30	4600.1	0.06	0.06	0.05	0.04	0.04	0.29	0.27	0.29	0.25	0.27	0.3	0.31	0.2
4700.1	26.75	30	4700.1	0.07	0.07	0.06	0.06	0.06	0.33	0.32	0.32	0.27	0.29	0.31	0.33	0.2
4800.1	26.75	30	4800.1	0.05	0.03	0.04	0.03	0.03	0.34	0.3	0.3	0.24	0.28	0.29	0.31	0.2
4900.1	26.75	30	4900.1	0.02	0.02	0.02	0.01	0.01	0.33	0.3	0.3	0.24	0.29	0.29	0.3	0.2
5000.1	26.75	30	5000.1	0.03	0.03	0.02	0.03	0.02	0.37	0.3	0.3	0.27	0.28	0.29	0.32	0.2
5100.1	26.75	30	5100.1	0.05	0.04	0.04	0.05	0.05	0.37	0.34	0.33	0.3	0.32	0.33	0.35	0.2
5200.1	26.75	30	5200.1	0.05	0.07	0.07	0.04	0.05	0.39	0.33	0.33	0.3	0.32	0.34	0.33	0.2
5300.1	26.75	30	5300.1	0.09	0.09	0.09	0.09	0.07	0.42	0.36	0.36	0.33	0.34	0.34	0.33	0.2
5400.1	26.75	30	5400.1	0.09	0.1	0.08	0.07	0.1	0.4	0.34	0.34	0.35	0.35	0.34	0.32	0.2
5500.1	26.75	30	5500.1	0.07	0.08	0.08	0.07	0.08	0.35	0.29	0.3	0.32	0.31	0.32	0.31	0.2
5600.1	26.75	30	5600.1	0.1	0.12	0.11	0.13	0.1	0.32	0.3	0.31	0.35	0.31	0.33	0.32	0.2
5700.1	26.75	30	5700.1	0.13	0.12	0.11	0.1	0.12	0.29	0.3	0.29	0.32	0.3	0.29	0.28	0.2
5800.1	26.75	30	5800.1	0.16	0.13	0.13	0.13	0.12	0.33	0.3	0.25	0.32	0.3	0.28	0.26	0.2
5900.1	26.75	30	5900.1	0.13	0.16	0.17	0.16	0.16	0.35	0.3	0.26	0.3	0.29	0.29	0.25	0.2
5986.1	26.75	30	5986.625	0.16	0.17	0.15	0.16	0.16	0.33	0.27	0.24	0.28	0.28	0.28	0.25	0.2

Frequency Response G and Uncertainty U in dB

® Names and Logo are registered trademarks of Narda Safety Test Solutions GmbH and L-3 Communications Holdings, Inc. – Trade names are trademarks of the owners.

Figure A-3 (continued)
 Calibration certificate sheet 6 for the Narda Model SRM-3006 SN A-0077.

Calibration Certificate

Narda Safety Test Solutions hereby certifies that the referenced equipment has been calibrated by qualified personnel to Narda's approved procedures. The calibration was carried out within a certified quality management system conforming to ISO 9001:2000.

The metrological confirmation system for test equipment complies with ISO 10012-1.

Object	Three-Axis-Antenna, E-Field, 50 MHz to 3 GHz
Type	P/N 3501/02
Serial Number	H-0100
Manufacturer	Narda Safety Test Solutions
Customer	
Date of Calibration	21-Nov-2008
Results of Calibration	Test results within specifications
Confirmation interval recommended	24 Months
Ambient conditions	23°C +/-3°C (20...60)% rel. humidity
Calibration procedure	3000-8702-00A

Pfullingen, 22-Nov-2006

Person in charge
Yeter

Quality management representative
W. Kumbier



Certified by DQS according to
DIN EN ISO 9001:2000
(Reg.-No. 99379-QM)

Certificate No. 350102-H0100-061121

Date of issue: 22-Nov-2006

Page 1 of 5

Figure A-4
Calibration certificate sheet 1 for the Narda Model SRM-3006 SN H-0100.

Measurements

The calibration of RF field strength probes involves the generation of a calculable linearly polarized electromagnetic field, approximating to a plane wave, into which the device is placed. The RSS value of three axis is used.

At each test frequency, the probe is orientated in the analytic angle (54.74 degrees between probe axis and electric field vector) and rotated 360 degrees. The noted indicated output voltage is calculated from the geometric mean of the minimum and maximum readings during rotation. The antenna factor is calculated from the ratio of the applied field strength to the output voltage (nominal impedance 50 Ohm). The minimum and maximum readings during rotation are further used to calculate the ellipse ratio.

A power meter head is connected by means of an ferrite beaded 50 Ohm coaxial cable.

A Crawford TEM cell is used to generate the known field at frequencies up to 100 MHz. The field strength is derived from the TEM cell's properties and from the output power of the cell.

Over the frequency range from 200 MHz to 1.6 GHz, the probe is positioned in front of a double balanced ridge horn antenna. The field strength is set to a known value by means of a calibrated E-field reference probe.

Above 1.7GHz the probe is positioned with the boresight of a linearly polarized horn antenna. The field strength is derived from the mechanical dimensions and the input power of the antenna.

The antenna factor is permanently stored in the antenna connector memory. When combined with the SRM basic unit (BN 3001 series) the frequency response of the antenna is automatically compensated.

Uncertainties

The measurement uncertainty stated in this document is the expanded uncertainty with a coverage factor of 2 (corresponding, in the case of normal distribution, to a confidence probability of 95%).

The uncertainty analysis for this calibration was done in accordance with the ISO-Guide (Guide to the expression of Uncertainty in Measurement). The measurement uncertainties are derived from contributions from the measurement of power, impedance, attenuation, mismatch, length, frequency, stability of instrumentation, repeatability of handling and field uniformity in the field generators (TEM cell and anechoic chamber).

This statement of uncertainty applies to the measured values only and does not make any implementation or include any estimation as to the long-term stability of the calibrated device.

Traceability of Measuring Equipment

The calibration results are traceable to National Standards, which are consistent with the recommendations of the General Conference on Weights and Measure (CGPM), or to standards derived from natural constants. Physical units, which are not included in the list of accredited measured quantities such as field strength or power density, are traced to the basic units via approved measurement and computational methods.

The equipment used for this calibration is traceable to the reference listed above and the traceability is guaranteed by ISO 9001 Narda internal procedure.

Ref. / Working Standard	Type	Serial Number	Certificate Number	Cal Due Date	Traced Property
Network Analyser	ZVC	100032	0063 DKD-K-16101 06-04	Apr-07	Reflection
Calibration Kit, 50 Ohm N	ZV-Z21	100072	86553 DKD-K-19401 06-04	Apr-07	Reflection
Power Meter	URV 55	100213	0065 DKD-K-16101 06-04	Apr-08	Voltage
Power Sensor DC - 6GHz	NRV Z4	100199	0010 DKD-K-16101 06-05	Mai-08	Power
N Thru, 50 Ohm	0659.4666.00	78008	0067 DKD-K-16101 06-04	Apr-08	Attenuation
Calliper Ø - 800mm	-	310121016	649724 DKD-K-12001 06-05	Mai-07	Length
Set-Up "D" (50 MHz to 100 MHz)					
TEM Cell, DC - 120MHz	2-2250	-	MM 2-2250	Apr-2007	Length
Power Sensor 4.2GHz	8482A	2652A13544	04D265 DKD-K-02201 04-11	Nov-2006	Power
Power Meter, Two Channel	438A	2741U00723	2-119508307-1B	Nov-2006	Voltage
Attenuator 30dB	49-30-33	KCC 116	2824 DKD-K-C0501 05-04	Apr-2007	Attenuation
Set-Up "B" (200 MHz to 1600 MHz)					
E-Field Reference Probe	Type 9.2	V-0017	601C1734 / 51200637E	Dez-07	Field Strength
Radiation Meter	EMR-300	AG-0099	22443100-AG00990347	Nov-2007	Voltage
Set-Up "A" (1800 MHz to 3 GHz)					
Power Sensor 18GHz	8481A	2702A57612	05D131 DKD-K-02201 05-07	Jul-2007	Power
Power Sensor 18GHz	8481A	2702A75991	05D130 DKD-K-02201 05-07	Jul-2007	Power
Power Meter, Two Channel	E4419B	GB43311917	2-170204386-1B	Dez-2006	Voltage
Coupler 1-4GHz & 6dB Att.	3022 & 777C-6	77861/34425	00 596	Okt-2008	Attenuation
Coupler 1-4GHz & 10dB Att.	3022 & 777C-10	77860/38334	00 595	Okt-2008	Attenuation

Figure A-4 (continued)
 Calibration certificate sheet 3 for the Narda Model SRM-3006 SN H-0100.

Results

Frequency Response			passed	
Frequency in MHz	E _{applied} in V/m	Output voltage in dB(μV)	Meas. Uncertainty in dB	Antenna Factor in dB(1/m)
50	10,0	75,47	1,0	64,53
75	10,0	78,67	1,0	61,33
100	10,0	80,61	1,0	59,39
200	10,0	84,88	1,0	55,12
300	10,0	87,66	1,0	52,34
433	10,0	88,68	1,5	51,32
600	10,0	90,60	1,5	49,40
750	10,0	90,36	1,5	49,64
900	10,0	92,09	1,5	47,91
1000	10,0	92,17	1,5	47,83
1200	10,0	92,25	1,5	47,75
1400	10,0	91,72	1,5	48,28
1600	10,0	91,41	1,5	48,59
1800	10,0	90,85	1,0	49,15
2000	10,0	88,77	1,0	51,23
2200	10,0	87,32	1,0	52,68
2450	10,0	85,01	1,0	54,99
2700	10,0	84,71	1,0	55,29
3000	10,0	83,13	1,0	56,87

Frequency Flatness (100 - 3000 MHz): 13,6 dB

The Antenna Factor data is permanently stored in the antenna connector memory.
 The SRM basic unit uses this correction data to correct the display.

Three-Axis E-Field Antenna SRM

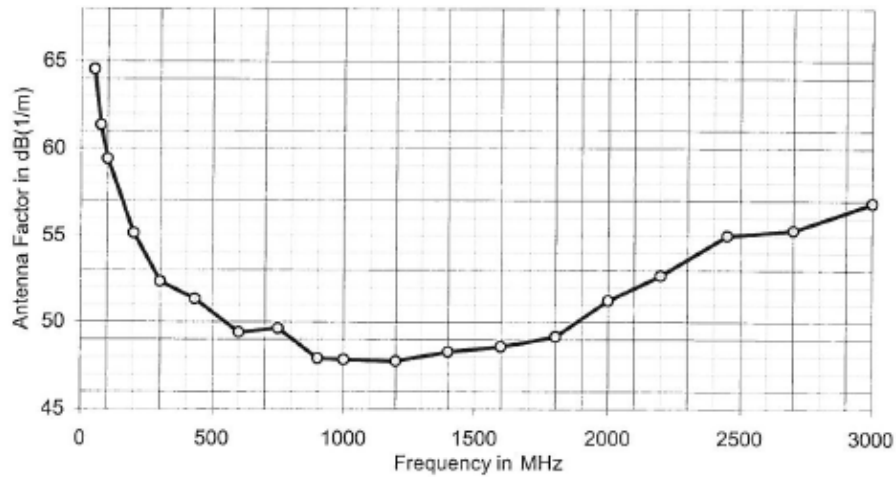


Figure A-4 (continued)
 Calibration certificate sheet 4 for the Narda Model SRM-3006 SN H-0100.

Rotational Ellipticity **passed**

Frequency in MHz	Ellipse Ratio in dB
50	+/-0,08
75	+/-0,05
100	+/-0,08
200	+/-0,08
300	+/-0,05
433	+/-0,13
600	+/-0,14
750	+/-0,20
900	+/-0,19
1000	+/-0,36
1200	+/-0,30
1400	+/-0,45
1600	+/-0,68
1800	+/-0,90
2000	+/-1,21
2200	+/-1,28
2450	+/-1,22
2700	+/-0,96
3000	+/-1,45

Output Return Loss **passed**

Figure A-4 (continued)
Calibration certificate sheet 5 for the Narda Model SRM-3006 SN H-0100.

Calibration Certificate

Narda Safety Test Solutions hereby certifies that the object referred to in this certificate has been calibrated by qualified personnel using Narda's approved procedures. The calibration was carried out in accordance with a certified quality management system which conforms to ISO 9001

OBJECT	Selective Radiation Meter, Basic Unit, SRM-3006
MANUFACTURER	Narda Safety Test Solutions GmbH
PART NUMBER (P/N)	3006/01
SERIAL NUMBER (S/N)	D-0070
CUSTOMER	
CALIBRATION DATE	2010-10-18
RESULT ASSESSMENT	within specifications
AMBIENT CONDITIONS	Temperature: (23 ± 3)°C Relative humidity: (25 to 75) %
CALIBRATION PROCEDURE	3006-8701-00A

ISSUE DATE: 2010-10-18


 CALIBRATED BY:
 Paul Geyer


 AUTHORIZED SIGNATORY:



Certified by DQS against
 ISO 9001:2008
 (Reg.-No. 099379 QM08)

This calibration certificate may not be reproduced other than in full except with the permission of the issuing laboratory. Calibration certificates without signature are not valid.

CERTIFICATE 300601-D0070-20101018-74

PAGE 1 OF 6

Figure A-5
 Calibration certificate sheet 1 for the Narda Model SRM-3006 SN H-0100.

OBJECT

The spectrum analyzer is based on digital signal processing. Small frequency spans were measured at fixed local oscillator (1st LO) settings using discrete Fourier transformation (DFT). The LO was also swept for larger frequency spans.

A memory chip contains correction values for various frequencies and object settings. The stored values were taken into account automatically during the measurement.

METHOD OF MEASUREMENT

Calibration using the reference standard. The output power level of the synthesized CW generator was adjusted and calibrated using power sensors as reference standards. The frequency of the generator was calibrated using a frequency counter.

The reflection of the object was measured directly using a vector network analyzer (VNA) calibrated by means of a calibration kit. The measuring equipment and the associated uncertainty were verified using a reference standard (verification kit).

CALIBRATION PROCEDURE

The object was connected to the signal source instead of the power sensors in order to calibrate it.

Measurement of the RF frequency response was made with different settings of the measurement range. As a result, the measured values also include the effects due to the "input attenuator" and the "reference level accuracy".

The calibration factor was calculated for various frequencies and settings from a comparison between the "actual level" and the "indicated level".

All the selection filters are digital filters. No calibration of the filters is necessary.

TRACEABILITY

The calibration results are traceable to the International System of Units (SI) in accordance with ISO/IEC 17025. The measuring equipment used for calibration is traceable through the reference standards listed below.

STANDARD	MANUFACTURER	MODEL	SERIAL NUMBER	ID	CERTIFICATE	NEXT CAL. DATE	TRACE
HF-MILLIVOLTMETER	R&S	URV 55	100143	913	0116 DKD-K-16101 2010-05	2012-05	DKD
DIODE POWER SENSOR	R&S	NRV Z4	100199	956	0104 DKD-K-16101 2010-05	2012-05	DKD
THERMAL POWER SENSOR	R&S	NRV Z51	101777	1635	0264 DKD-K-16101 2008-11	2010-11	DKD
MISMATCH VSWR 1,2 (f)	Rosenberger	--	01237	552-3	12996 DKD-K-00201 2008-05	#	DKD
FREQUENCY COUNTER	Advantest	R5362B	120700137	923	15137 DKD-K-00201 2009-09	#	DKD

Reference standard; not used for routine calibration

Figure A-5 (continued)

Calibration certificate sheet 2 for the Narda Model SRM-3006 SN H-0100.

UNCERTAINTY

The reported expanded uncertainty U is based on a standard uncertainty multiplied by a coverage factor $k = 1.96$, providing a level of confidence of approximately 95 %. The uncertainty evaluation has been carried out in accordance with the "Guide to the Expression of Uncertainty in Measurement" (GUM). The reported measurement uncertainty is derived from the uncertainty of the calibration procedure and the object during calibration, and makes no allowance for drift or operation under other environmental conditions.

MEASURING CONDITIONS

The following results were obtained after adjustment of the object under calibration. These values are within the setting ranges defined by the manufacturer.

RESULTS

1	FREQUENCY RESPONSE (IF):	passed
2	FREQUENCY RESPONSE (RF):	passed
3	OUT-OF-BAND RESPONSE:	passed
4	FREQUENCY ACCURACY	passed
5	NOISE SIDEBAND (SSB):	passed
6	SPURIOUS (input related)	passed
7	SPURIOUS (residual)	passed
8	NOISE FLOOR:	passed
9	INTERMODULATION REJECTION (2 nd and 3 rd order):	passed
10	INPUT RETURN LOSS:	passed

Figure A-5 (continued)

Calibration certificate sheet 3 for the Narda Model SRM-3006 SN H-0100.

APPENDIX

FREQUENCY RESPONSE (RF)

The generator was set to the *Fgen*. The object settings were *Fspan*, *RBW*, and *Fcent*.

The measurements were made at different settings of the measurement range *MR*. The nominal level of the generator was -32 dBm (for *MR* < -5 dBm) and -7 dBm (for *MR* ≥ -5 dBm), respectively. The frequency response *G* was calculated as the difference of the actual generator level *L_{actual}* and the indicated level *L_{indicated}* according to the following equation: $G/\text{dB} = (L_{\text{indicated}} - L_{\text{actual}}) / \text{dBm}$

Frequency in MHz	Fspan in MHz	RBW in kHz	Fcent in MHz	MR												U
				-30	-28	-25	-20	-15	-10	-5	0	5	10	15	20	
0.00901	0.002	0.01	0.01	-0.01	-0.01	-0.01	-0.01	-0.01	-0.01	-0.01	-0.01	-0.02	-0.02	-0.02	-0.02	0.2
0.012	0.006	0.5	0.012	0	-0.01	-0.01	-0.01	-0.01	-0.01	-0.01	-0.01	-0.01	-0.01	-0.01	-0.01	0.2
0.02	0.02	2	0.02	0	0	0	0	0	0	0	0	-0.01	-0.01	-0.01	-0.01	0.2
0.04	0.02	2	0.04	0	0	0	0	0	0	0	0	0	0	-0.01	-0.01	0.2
0.1	0.02	2	0.1	0.01	0.01	0.01	0	0	0.01	0	0	0	0	0	0	0.2
0.5	0.02	2	0.5	0.01	0.01	0.01	0	0	0.01	0	0	0	0	0	-0.01	0.2
2	0.02	2	2	0.01	0.01	0.01	0.01	0.01	0.01	0	0	0	0	0	-0.01	0.2
10	0.02	2	10	0.03	0.02	0.02	0.02	0.02	0.02	0.02	0.02	0.02	0.01	0.02	0.01	0.2
20	0.02	2	20	0.03	0.03	0.02	0.03	0.02	0.02	0.02	0.02	0.02	0.02	0.01	0.01	0.2
30	0.02	2	30	0.03	0.03	0.02	0.02	0.02	0.02	0.02	0.02	0.02	0.01	0.02	0.01	0.2
31.233	26.75	30	44.578	-0.06	-0.17	-0.13	-0.15	-0.27	-0.02	-0.15	-0.18	-0.28	0.02	-0.11	-0.13	0.2
36.1	26.75	30	44.578	0.03	-0.05	-0.03	-0.05	-0.09	0.09	-0.05	-0.06	-0.1	0.07	0.03	0.1	0.2
40	0.02	2	40	0.03	0.02	0.02	0.02	0.02	0.03	0.02	0.02	0.01	0.01	0	0.01	0.2
44.1	26.75	30	44.578	0.1	0.06	0.07	0.05	0.05	0.1	0.05	0.04	0.05	0.05	0.03	0.05	0.2
50	0.02	2	50	0.02	0.02	0.02	0.02	0.02	0.02	0.02	0.02	0.02	0.01	0.01	0.02	0.2
52.1	26.75	30	44.578	0.09	0.07	0.05	0.04	0.08	0.12	0.04	0.03	0.08	0	0.04	0.08	0.2
57.9948	0.02	2	57.9868	0.03	0.02	0.02	0.02	0.02	0.02	0.02	0.02	0.02	0.01	0.01	0.01	0.2
58.344	26.75	30	44.999	0.07	0.05	0.02	0	0.06	0.13	0.01	-0.01	0.05	-0.06	0.03	0.11	0.2
60.1	26.75	30	60.1	0.08	0.08	0.08	0.07	0.07	0.08	0.07	0.07	0.07	0.06	0.07	0.06	0.2
100.1	26.75	30	100.1	0.08	0.08	0.08	0.07	0.07	0.08	0.07	0.06	0.07	0.06	0.08	0.05	0.2
200.1	26.75	30	200.1	0.06	0.06	0.05	0.05	0.05	0.05	0.05	0.05	0.05	0.05	0.05	0.03	0.2
300.1	26.75	30	300.1	0.06	0.07	0.06	0.06	0.06	0.06	0.06	0.06	0.06	0.06	0.05	0.06	0.2
400.1	26.75	30	400.1	0.07	0.06	0.07	0.07	0.06	0.07	0.05	0.05	0.06	0.06	0.06	0.05	0.2

Figure A-5 (continued)
 Calibration certificate sheet 4 for the Narda Model SRM-3006 SN H-0100.

Frequency in MHz	Fspan in MHz	RBW in kHz	Fcent in MHz	MR												U
				-30	-28	-25	-20	-15	-10	-5	0	5	10	15	20	
500.1	26.75	30	500.1	0.06	0.06	0.06	0.07	0.06	0.07	0.06	0.06	0.05	0.05	0.05	0.06	0.2
600.1	26.75	30	600.1	0.08	0.08	0.08	0.08	0.08	0.07	0.08	0.07	0.07	0.07	0.06	0.07	0.2
700.1	26.75	30	700.1	0.08	0.08	0.08	0.07	0.07	0.08	0.07	0.08	0.07	0.07	0.07	0.06	0.2
800.1	26.75	30	800.1	0.07	0.07	0.07	0.07	0.07	0.06	0.06	0.07	0.07	0.06	0.06	0.06	0.2
900.1	26.75	30	900.1	0.06	0.06	0.06	0.06	0.06	0.06	0.06	0.05	0.06	0.05	0.05	0.04	0.2
1000.1	26.75	30	1000.1	0.06	0.06	0.07	0.05	0.05	0.05	0.06	0.06	0.06	0.06	0.05	0.04	0.2
1100.1	26.75	30	1100.1	0.07	0.07	0.07	0.07	0.06	0.07	0.07	0.06	0.06	0.06	0.06	0.05	0.2
1200.1	26.75	30	1200.1	0.07	0.06	0.06	0.06	0.06	0.07	0.06	0.06	0.06	0.06	0.06	0.06	0.2
1300.1	26.75	30	1300.1	0.06	0.06	0.06	0.06	0.06	0.06	0.05	0.05	0.05	0.05	0.05	0.04	0.2
1400.1	26.75	30	1400.1	0.09	0.09	0.08	0.08	0.08	0.08	0.08	0.08	0.07	0.08	0.08	0.07	0.2
1500.1	26.75	30	1500.1	0.11	0.1	0.11	0.1	0.1	0.1	0.09	0.1	0.09	0.1	0.09	0.1	0.2
1600.1	26.75	30	1600.1	0.08	0.09	0.08	0.09	0.08	0.08	0.07	0.08	0.07	0.08	0.06	0.07	0.2
1700.1	26.75	30	1700.1	0.12	0.12	0.12	0.13	0.12	0.12	0.12	0.12	0.12	0.11	0.11	0.12	0.2
1800.1	26.75	30	1800.1	0.08	0.08	0.08	0.08	0.08	0.08	0.08	0.08	0.07	0.06	0.07	0.05	0.2
1900.1	26.75	30	1900.1	0.07	0.07	0.07	0.07	0.06	0.06	0.06	0.05	0.06	0.06	0.06	0.07	0.2
2000.1	26.75	30	2000.1	0.08	0.08	0.08	0.06	0.07	0.07	0.06	0.06	0.06	0.07	0.06	0.06	0.2
2100.1	26.75	30	2100.1	0.09	0.09	0.08	0.09	0.07	0.1	0.09	0.09	0.08	0.07	0.08	0.07	0.2
2200.1	26.75	30	2200.1	0.1	0.08	0.08	0.09	0.08	0.08	0.09	0.08	0.08	0.08	0.08	0.07	0.2
2300.1	26.75	30	2300.1	0.09	0.08	0.09	0.08	0.08	0.1	0.09	0.08	0.08	0.08	0.06	0.07	0.2
2400.1	26.75	30	2400.1	0.09	0.08	0.08	0.1	0.09	0.09	0.1	0.08	0.08	0.09	0.07	0.06	0.2
2500.1	26.75	30	2500.1	0.07	0.05	0.05	0.05	0.04	0.05	0.06	0.04	0.04	0.05	0.04	0.04	0.2
2600.1	26.75	30	2600.1	0.08	0.07	0.07	0.08	0.07	0.06	0.07	0.07	0.06	0.07	0.07	0.06	0.2
2700.1	26.75	30	2700.1	0.11	0.11	0.12	0.12	0.11	0.12	0.12	0.11	0.12	0.1	0.1	0.1	0.2
2800.1	26.75	30	2800.1	0.11	0.12	0.1	0.09	0.09	0.09	0.09	0.09	0.09	0.1	0.09	0.08	0.2
2900.1	26.75	30	2900.1	0.08	0.08	0.1	0.09	0.08	0.08	0.09	0.1	0.08	0.08	0.08	0.08	0.2
2999.9	26.75	30	2999.9	0.07	0.09	0.06	0.07	0.08	0.07	0.09	0.08	0.07	0.09	0.07	0.07	0.2
3002.1	26.75	30	3002.1	0.06	0.07	0.07	0.06	0.07	0.06	0.07	0.07	0.06	0.07	0.05	0.05	0.2
3100.1	26.75	30	3100.1	0.08	0.07	0.07	0.06	0.07	0.07	0.06	0.05	0.06	0.06	0.05	0.06	0.2
3200.1	26.75	30	3200.1	0.08	0.09	0.08	0.08	0.08	0.09	0.09	0.09	0.09	0.08	0.08	0.08	0.2
3300.1	26.75	30	3300.1	0.09	0.09	0.1	0.09	0.09	0.08	0.09	0.09	0.08	0.08	0.09	0.08	0.2
3400.1	26.75	30	3400.1	0.1	0.08	0.09	0.09	0.08	0.09	0.09	0.09	0.09	0.09	0.09	0.09	0.2
3500.1	26.75	30	3500.1	0.11	0.1	0.1	0.09	0.08	0.1	0.1	0.1	0.09	0.1	0.09	0.1	0.2

Figure A-5 (continued)
 Calibration certificate sheet 5 for the Narda Model SRM-3006 SN H-0100.

Frequency in MHz	Fspan in MHz	RBW in kHz	Fcent in MHz	MR												U	
				-30	-28	-25	-20	-15	-10	-5	0	5	10	15	20		
3600.1	26.75	30	3600.1	0.06	0.06	0.07	0.07	0.06	0.06	0.06	0.06	0.06	0.06	0.06	0.06	0.06	0.2
3700.1	26.75	30	3700.1	0.05	0.06	0.05	0.07	0.06	0.07	0.07	0.06	0.06	0.06	0.06	0.07	0.05	0.2
3800.1	26.75	30	3800.1	0.07	0.07	0.07	0.08	0.07	0.08	0.07	0.08	0.07	0.08	0.06	0.07	0.05	0.2
3900.1	26.75	30	3900.1	0.07	0.05	0.06	0.06	0.06	0.06	0.06	0.06	0.05	0.06	0.05	0.07	0.05	0.2
4000.1	26.75	30	4000.1	0.06	0.06	0.06	0.05	0.05	0.07	0.06	0.05	0.05	0.06	0.06	0.03	0.2	
4100.1	26.75	30	4100.1	0.09	0.07	0.09	0.09	0.09	0.08	0.08	0.07	0.07	0.07	0.06	0.08	0.2	
4200.1	26.75	30	4200.1	0.11	0.11	0.1	0.11	0.1	0.13	0.11	0.11	0.1	0.1	0.1	0.09	0.2	
4300.1	26.75	30	4300.1	0.1	0.1	0.1	0.1	0.1	0.12	0.1	0.1	0.11	0.1	0.11	0.1	0.2	
4400.1	26.75	30	4400.1	0.08	0.09	0.09	0.08	0.09	0.08	0.09	0.09	0.07	0.08	0.07	0.1	0.2	
4500.1	26.75	30	4500.1	0.05	0.06	0.05	0.05	0.06	0.05	0.05	0.06	0.05	0.05	0.04	0.03	0.2	
4600.1	26.75	30	4600.1	0.06	0.08	0.07	0.09	0.08	0.08	0.06	0.07	0.07	0.07	0.06	0.07	0.2	
4700.1	26.75	30	4700.1	0.09	0.09	0.1	0.09	0.1	0.09	0.1	0.09	0.09	0.08	0.08	0.08	0.2	
4800.1	26.75	30	4800.1	0.06	0.08	0.06	0.05	0.05	0.07	0.06	0.05	0.05	0.05	0.05	0.03	0.2	
4900.1	26.75	30	4900.1	0.04	0.04	0.04	0.04	0.04	0.05	0.05	0.05	0.04	0.04	0.04	0.03	0.2	
5000.1	26.75	30	5000.1	0.07	0.08	0.06	0.08	0.06	0.05	0.04	0.06	0.06	0.05	0.05	0.05	0.2	
5100.1	26.75	30	5100.1	0.09	0.08	0.09	0.08	0.06	0.07	0.08	0.09	0.08	0.08	0.07	0.07	0.2	
5200.1	26.75	30	5200.1	0.1	0.09	0.1	0.08	0.08	0.1	0.09	0.1	0.09	0.08	0.09	0.07	0.2	
5300.1	26.75	30	5300.1	0.12	0.1	0.11	0.09	0.09	0.11	0.09	0.11	0.09	0.09	0.09	0.1	0.2	
5400.1	26.75	30	5400.1	0.11	0.1	0.12	0.11	0.12	0.12	0.09	0.09	0.11	0.09	0.1	0.09	0.2	
5500.1	26.75	30	5500.1	0.09	0.1	0.1	0.1	0.09	0.08	0.12	0.1	0.1	0.09	0.1	0.1	0.2	
5600.1	26.75	30	5600.1	0.12	0.11	0.1	0.1	0.08	0.1	0.09	0.11	0.07	0.09	0.1	0.08	0.2	
5700.1	26.75	30	5700.1	0.11	0.11	0.11	0.08	0.08	0.09	0.11	0.09	0.1	0.11	0.09	0.08	0.2	
5800.1	26.75	30	5800.1	0.14	0.11	0.12	0.11	0.12	0.12	0.1	0.12	0.11	0.1	0.12	0.12	0.2	
5900.1	26.75	30	5900.1	0.13	0.15	0.12	0.12	0.13	0.16	0.15	0.14	0.12	0.14	0.14	0.11	0.2	
5986.1	26.75	30	5986.625	0.16	0.14	0.15	0.15	0.14	0.14	0.14	0.14	0.13	0.13	0.13	0.12	0.2	

Frequency Response G and Uncertainty U in dB

© Names and Logo are registered trademarks of Narda Safety Test Solutions GmbH and L-3 Communications Holdings, Inc. – Trade names are trademarks of the owners.

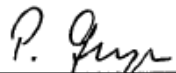
Figure A-5 (continued)
 Calibration certificate sheet 6 for the Narda Model SRM-3006 SN H-0100.

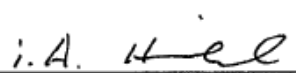
Calibration Certificate

Narda Safety Test Solutions hereby certifies that the referenced equipment has been calibrated by qualified personnel to Narda's approved procedures. The calibration was carried out within a certified quality management system conforming to ISO 9001.

Object	Antenna, Three-Axis, E-Field, 27 MHz to 3 GHz
Part Number (P/N)	3501/03
Serial Number (S/N)	K-0243
Manufacturer	Narda Safety Test Solutions GmbH
Customer	
Date of Calibration	07-Okt-2010
Results of Calibration	Test results within specifications
Confirmation interval recommended	24 Months
Ambient conditions	Temperature: (23 ± 3) °C Relative humidity: (20 to 60) %
Calibration procedure	3000-8702-00A

Pfullingen, 07-Okt-2010


 Person in charge
 Geyer


 Head of Laboratory
 J. v. Freeden



Certified by DQS according to
 ISO 9001:2008
 (Reg.-No. 099379 QM08)

This certificate may only be published in full, unless permission for the publication of an approved extract has been obtained in writing from the Managing Director.

Figure A-6
 Calibration certificate sheet 1 for the Narda Model SRM-3006 SN H-0100.

Measurements

The calibration of RF field strength probes involves the generation of a calculable linearly polarized electromagnetic field, approximating to a plane wave, into which the device is placed. The RSS value of three axis is used.

At each test frequency, the probe is orientated in the analytic angle (54.74 degrees between probe axis and electric field vector) and rotated 360 degrees. The noted indicated output voltage is calculated from the geometric mean of the minimum and maximum readings during rotation. The antenna factor is calculated from the ratio of the applied field strength to the output voltage (nominal impedance 50 Ohm). The minimum and maximum readings during rotation are further used to calculate the ellipse ratio.

A power meter head is connected by means of an ferrite beaded 50 Ohm coaxial cable.

A Crawford TEM cell is used to generate the known field at frequencies up to 100 MHz. The field strength is derived from the TEM cell's properties and from the output power of the cell. Over the frequency range from 200 MHz to 1.6 GHz, the probe is positioned in front of a double balanced ridge horn antenna. The field strength is set to a known value by means of a calibrated E-field reference probe.

Above 1.7GHz the probe is positioned with the boresight of a linearly polarized horn antenna. The field strength is derived from the mechanical dimensions and the input power of the antenna.

The antenna factor is permanently stored in the antenna connector memory. When combined with the SRM basic unit (BN 3001 series) the frequency response of the antenna is automatically compensated.

Uncertainties

The measurement uncertainty stated in this document is the expanded uncertainty with a coverage factor of 2 (corresponding, in the case of normal distribution, to a confidence probability of 95%).

The uncertainty analysis for this calibration was done in accordance with the ISO-Guide (Guide to the expression of Uncertainty in Measurement). The measurement uncertainties are derived from contributions from the measurement of power, impedance, attenuation, mismatch, length, frequency, stability of instrumentation, repeatability of handling and field uniformity in the field generators (TEM cell and anechoic chamber).

This statement of uncertainty applies to the measured values only and does not make any implementation or include any estimation as to the long-term stability of the calibrated device.

Figure A-6 (continued)
Calibration certificate sheet 2 for the Narda Model SRM-3006 SN H-0100.

Traceability of Measuring Equipment

The calibration results are traceable to National Standards, which are consistent with the recommendations of the General Conference on Weights and Measure (CGPM), or to standards derived from natural constants. Physical units, which are not included in the list of accredited measured quantities such as field strength or power density, are traced to the basic units via approved measurement and computational methods.

The equipment used for this calibration is traceable to the reference listed above and the traceability is guaranteed by ISO 9001 Narda internal procedure.

Reference- / Working- Standard	Manu- facturer	Model	Serial Number	Certificate Number	Cal Due Date	Trace
Power Sensor	R&S	NRV-Z4	100122	0171 DKD-K-16101 2008-11	2010-11	DKD
RF-Millivoltmeter	R&S	URV55	100213	0224 DKD-K-16101 2010-08	2012-08	DKD
Set-Up "A" (1800 MHz to 3 GHz)						
Calliper	Preisser	0-800mm	310121016	649724 DKD-K-12001 06-05	#	DKD
Power Sensor	agilent	8481A	US37299951	1-2217165994-1	2011-08	UKAS147
Power Sensor	agilent	8481A	US37299952	1-2217214152-1	2011-09	UKAS147
Power Meter	agilent	E4419A	MY40330449	1-2217141092-1A	2011-09	UKAS147
Set-Up "B" (200 MHz to 1600 MHz)						
E-Field Reference Probe	Narda	Type 9.2	V-0017	51200637E	#	SIT08
Power Sensor	agilent	8481A	US37299870	1-2217214643-1	2011-09	UKAS147
Power Sensor	agilent	8481A	2702A57611	1-2217165886-1	2011-09	UKAS147
Power Meter	agilent	E4419B	GB43311917	1-2295928041-1A	2011-11	UKAS147
Set-Up "D" (100 kHz to 100 MHz)						
Calliper	Preisser	0-800mm	310121016	649724 DKD-K-12001 06-05	#	DKD
Power Sensor	agilent	8482A	2652A13544	08D177 DKD-K-02201 2008-06	2010-12	DKD
Power Meter	agilent	438A	2741U00723	1-1321958613-1A	2010-12	UKAS147
Attenuator	Weinschel	49-30-33	KC115	3248 DKD-K-00501 2008-06	2011-06	DKD

Reference standard; not used for routine calibration

Figure A-6 (continued)
 Calibration certificate sheet 3 for the Narda Model SRM-3006 SN H-0100.

Results

Frequency Response				passed
Frequency in MHz	E_applied in V/m	Output voltage in dB(μ V)	Meas. Uncertainty in dB	Antenna Factor in dB(1/m)
26	10,0	70,85	1,0	69,15
45	10,0	74,77	1,0	65,23
75	10,0	78,97	1,0	61,03
100	10,0	80,73	1,0	59,27
200	10,0	85,08	1,0	54,92
300	10,0	87,79	1,0	52,21
433	10,0	88,28	1,5	51,72
600	10,0	90,61	1,5	49,39
750	10,0	90,39	1,5	49,61
900	10,0	92,56	1,5	47,44
1000	10,0	92,66	1,5	47,34
1200	10,0	92,17	1,5	47,83
1400	10,0	92,10	1,5	47,90
1600	10,0	91,48	1,5	48,52
1800	10,0	91,06	1,0	48,94
2000	10,0	88,57	1,0	51,43
2200	10,0	86,76	1,0	53,24
2450	10,0	84,91	1,0	55,09
2700	10,0	83,97	1,0	56,03
3000	10,0	82,07	1,0	57,93

Frequency Flatness (100 - 3000 MHz): 11,9 dB

The Antenna Factor data is permanently stored in the antenna connector memory.
The SRM basic unit uses this correction data to correct the display.

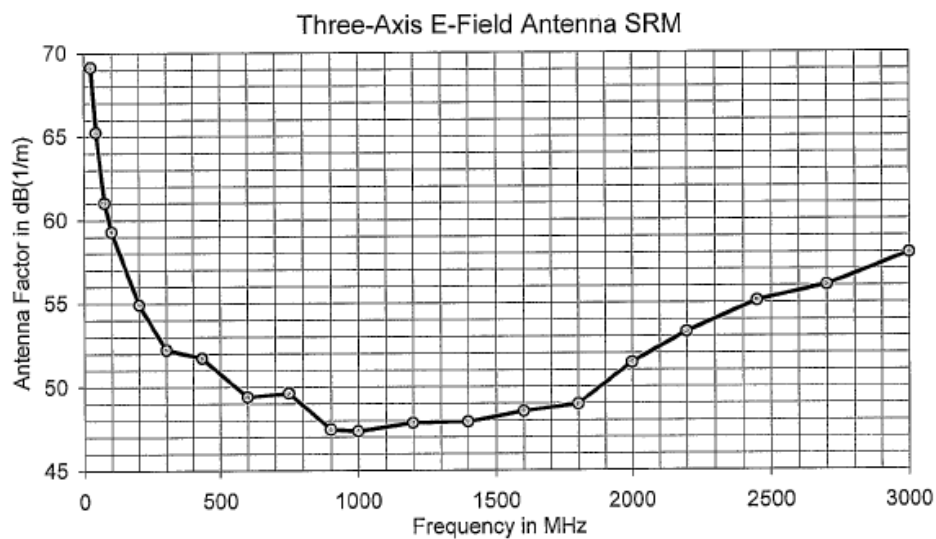


Figure A-6 (continued)
Calibration certificate sheet 4 for the Narda Model SRM-3006 SN H-0100.

Rotational Ellipticity **passed**

Frequency in MHz	Ellipse Ratio in dB
26	+/-0,14
45	+/-0,17
75	+/-0,14
100	+/-0,14
200	+/-0,09
300	+/-0,06
433	+/-0,04
600	+/-0,08
750	+/-0,19
900	+/-0,13
1000	+/-0,36
1200	+/-0,46
1400	+/-0,41
1600	+/-0,86
1800	+/-0,68
2000	+/-1,22
2200	+/-1,55
2450	+/-1,45
2700	+/-1,66
3000	+/-1,99

Output Return Loss **passed**

Figure A-6 (continued)
Calibration certificate sheet 5 for the Narda Model SRM-3006 SN H-0100.

Appendix B: SRM-3006 900 MHz Spectrum Measurement Scans (meter farm)

Battery: 07/29/10 12:51:12 PM	GPS: 34°46'01.7" N 83°2'20.7" W	Ant: 3AX 50M-3G Cable: ---	SrvTbl: Ger.Funkd. Std: FCC GP
Integration over Frequency	Min: 902.000 0 MHz Cent: 915.000 0 MHz	Max: 928.000 0 MHz Span: 26.000 0 MHz	Result Type: Max Int. Val: 8.098 %

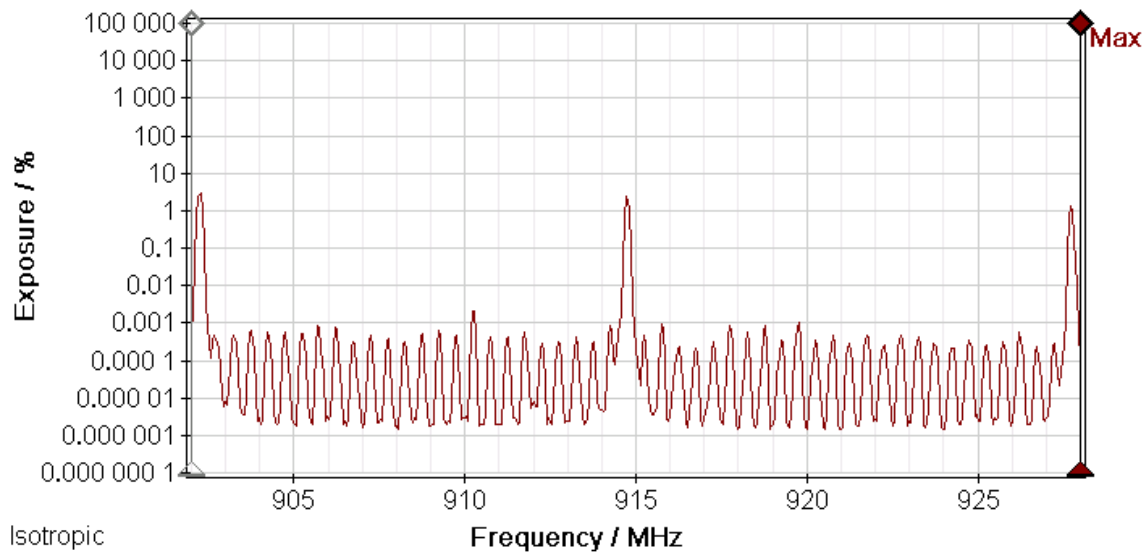


Figure B-1
900 MHz band composite RF field from rack of 10 SmartMeters at 1 foot.

Battery: 07/29/10	12:52:58 PM	GPS: 34°46'01.9" N 83°2'20.4" W	Ant: 3AX 50M-3G Cable: ---	SrvTbl: --- Stnd: ---	Ger.Funkd. FCC GP
Integration over Frequency		Min: 902.000 0 MHz Cent: 915.000 0 MHz	Max: 928.000 0 MHz Span: 26.000 0 MHz	Result Type: Max Int. Val: 3.898 %	

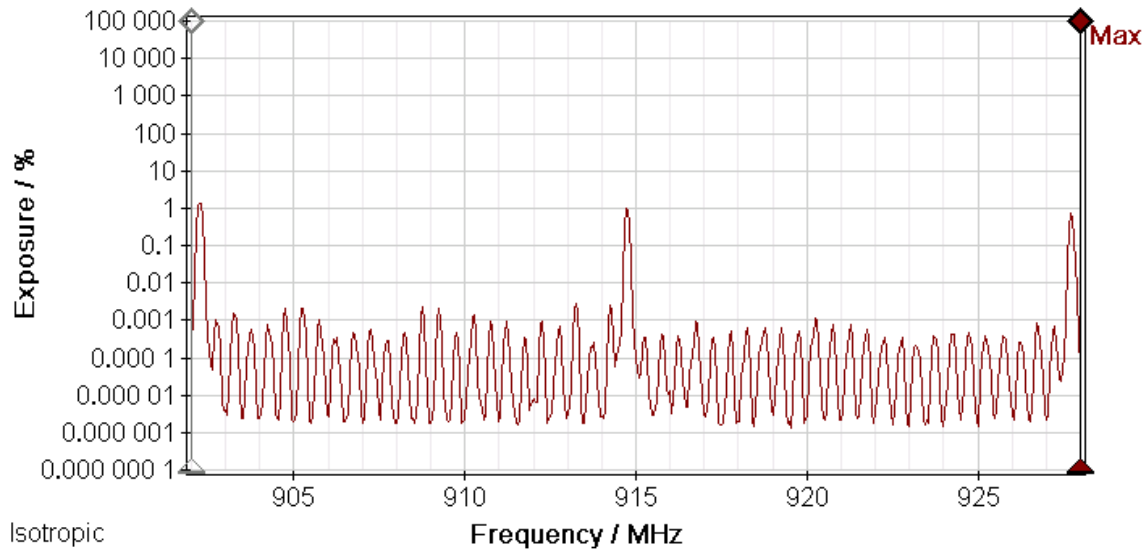


Figure B-2
900 MHz band composite RF field from rack of 10 SmartMeters at 2 feet.

Battery: 07/29/10	12:53:53 PM	GPS: 34°46'01.7" N 83°2'20.7" W	Ant: 3AX 50M-3G Cable: ---	SrvTbl: --- Stnd: ---	Ger.Funkd. FCC GP
Integration over Frequency		Min: 902.000 0 MHz Cent: 915.000 0 MHz	Max: 928.000 0 MHz Span: 26.000 0 MHz	Result Type: Max Int. Val: 2.471 %	

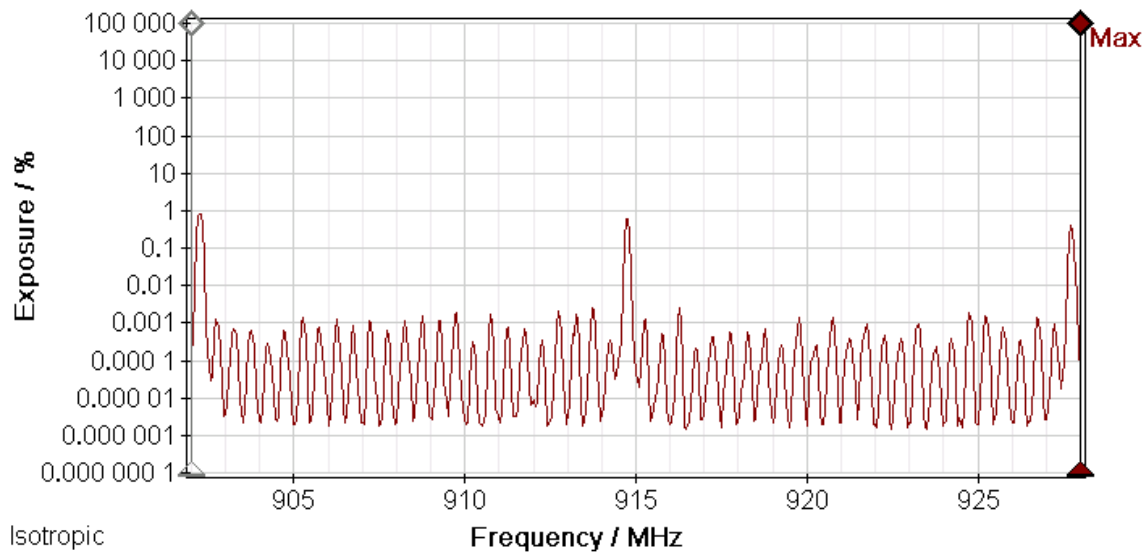


Figure B-3
900 MHz band composite RF field from rack of 10 SmartMeters at 3 feet.

Battery: 07/29/10 12:54:46 PM	GPS: 34°46'01.7" N 83°2'20.8" W	Ant: 3AX 50M-3G	Cable: ---	SrvTbl: ---	Ger.Funkd. FCC GP
Integration over Frequency		Min: 902.000 0 MHz	Max: 928.000 0 MHz	Result Type: Max	
		Cent: 915.000 0 MHz	Span: 26.000 0 MHz	Int. Val: 1.827 %	

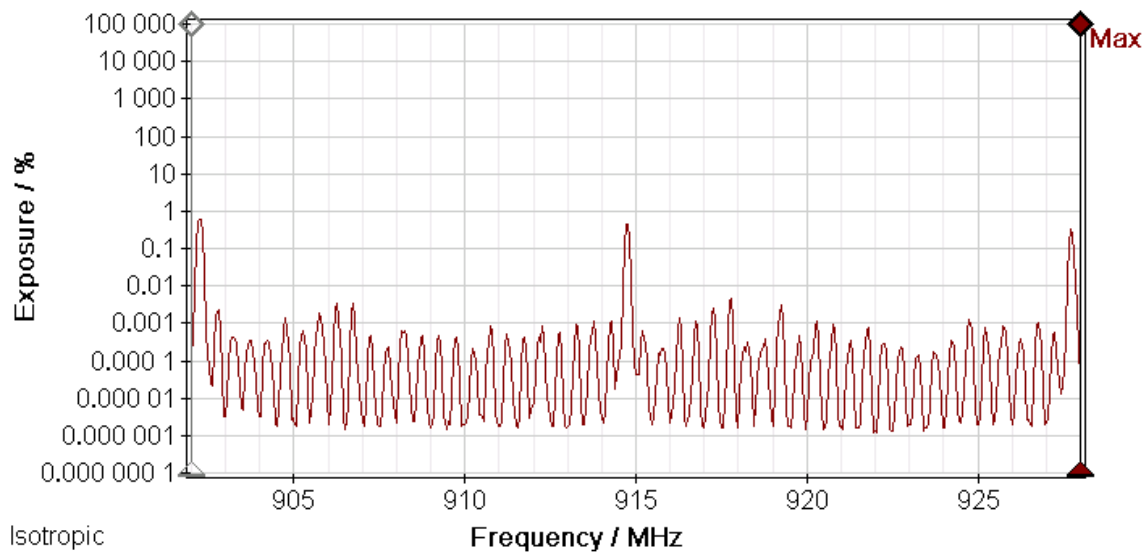


Figure B-4
900 MHz band composite RF field from rack of 10 SmartMeters at 4 feet.

Battery: 07/29/10 12:55:27 PM	GPS: 34°46'01.9" N 83°2'20.7" W	Ant: 3AX 50M-3G	Cable: ---	SrvTbl: ---	Ger.Funkd. FCC GP
Integration over Frequency		Min: 902.000 0 MHz	Max: 928.000 0 MHz	Result Type: Max	
		Cent: 915.000 0 MHz	Span: 26.000 0 MHz	Int. Val: 1.382 %	

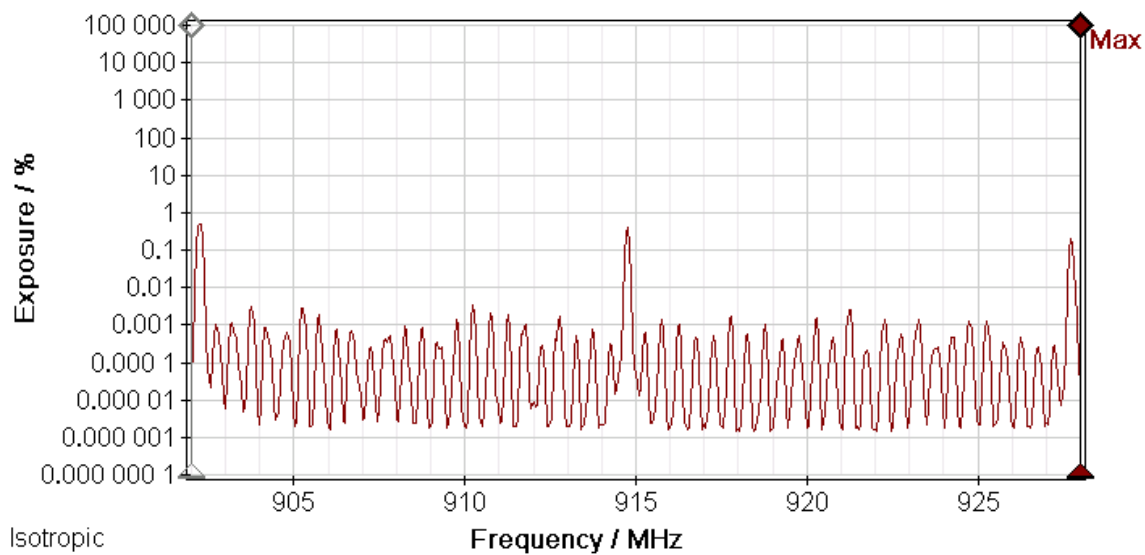


Figure B-5
900 MHz band composite RF field from rack of 10 SmartMeters at 5 feet.

Battery: 07/29/10 12:56:21 PM	GPS: 34°46'01.9" N 83°2'20.6" W	Ant: 3AX 50M-3G	Cable: ---	SrvTbl: ---	Ger.Funkd. FCC GP
Integration over Frequency		Min: 902.000 0 MHz	Max: 928.000 0 MHz	Result Type: Max	
		Cent: 915.000 0 MHz	Span: 26.000 0 MHz	Int. Val: 1.157 %	

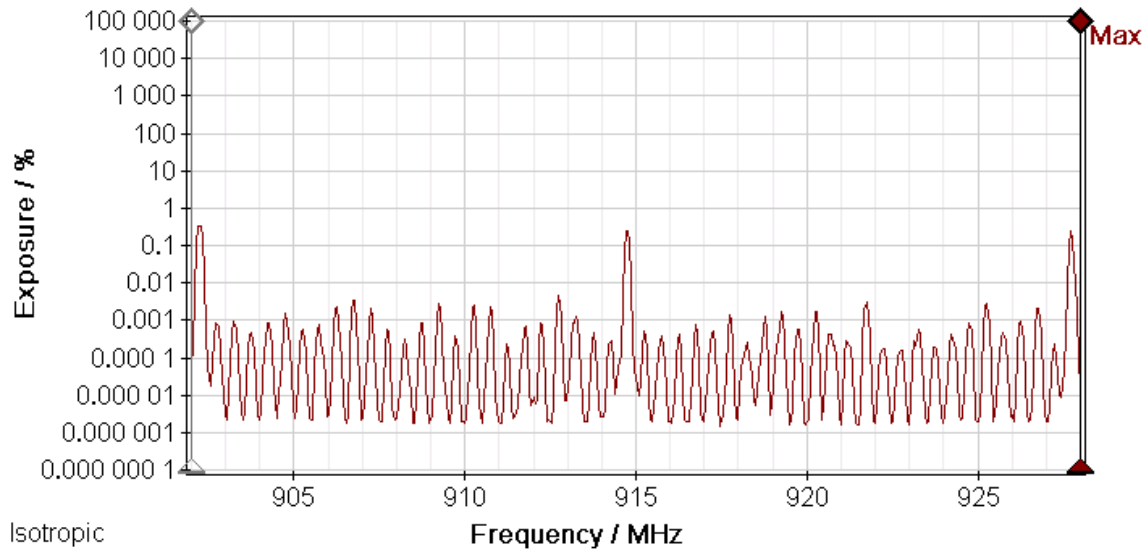


Figure B-6
900 MHz band composite RF field from rack of 10 SmartMeters at 6 feet.

Battery: 07/29/10 12:57:07 PM	GPS: 34°46'01.8" N 83°2'20.7" W	Ant: 3AX 50M-3G	Cable: ---	SrvTbl: ---	Ger.Funkd. FCC GP
Integration over Frequency		Min: 902.000 0 MHz	Max: 928.000 0 MHz	Result Type: Max	
		Cent: 915.000 0 MHz	Span: 26.000 0 MHz	Int. Val: 0.722 %	

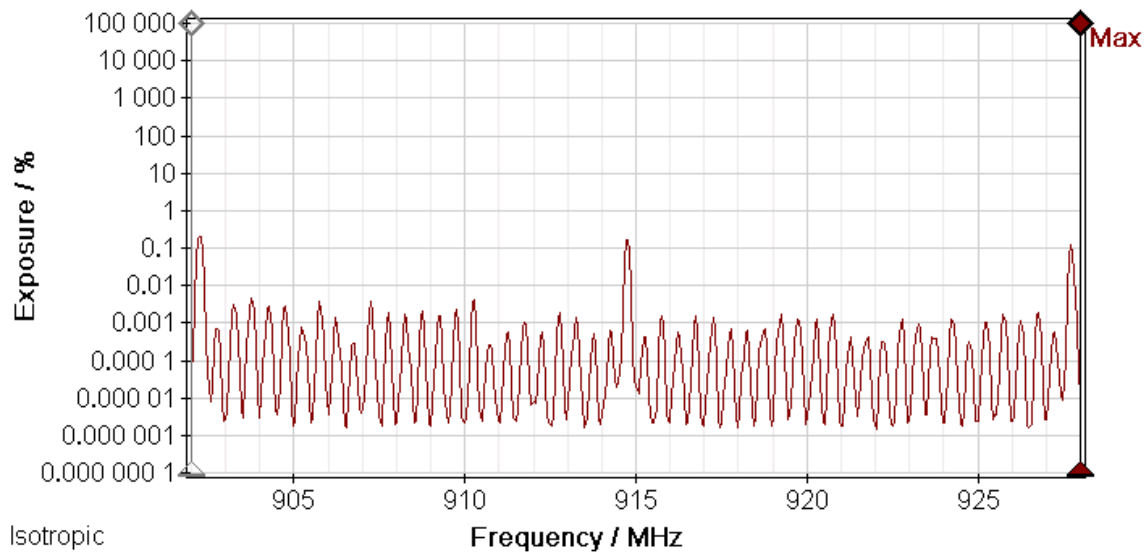


Figure B-7
900 MHz band composite RF field from rack of 10 SmartMeters at 7 feet.

Battery: 07/29/10	12:57:55 PM	GPS: 34°46'01.8" N 83°2'20.7" W	Ant: 3AX 50M-3G Cable: ---	SrvTbl: --- Stnd: ---	Ger.Funkd. FCC GP
Integration over Frequency		Min: 902.000 0 MHz Cent: 915.000 0 MHz	Max: 928.000 0 MHz Span: 26.000 0 MHz	Result Type: Max Int. Val: 0.655 %	

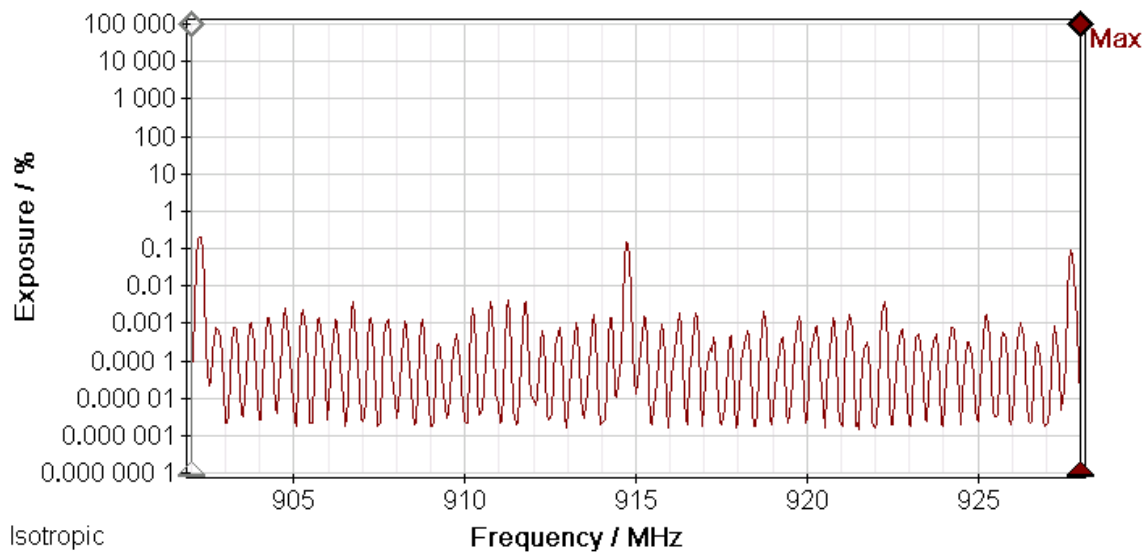


Figure B-8
900 MHz band composite RF field from rack of 10 SmartMeters at 8 feet.

Battery: 07/29/10	12:58:40 PM	GPS: 34°46'01.8" N 83°2'20.8" W	Ant: 3AX 50M-3G Cable: ---	SrvTbl: --- Stnd: ---	Ger.Funkd. FCC GP
Integration over Frequency		Min: 902.000 0 MHz Cent: 915.000 0 MHz	Max: 928.000 0 MHz Span: 26.000 0 MHz	Result Type: Max Int. Val: 0.681 %	

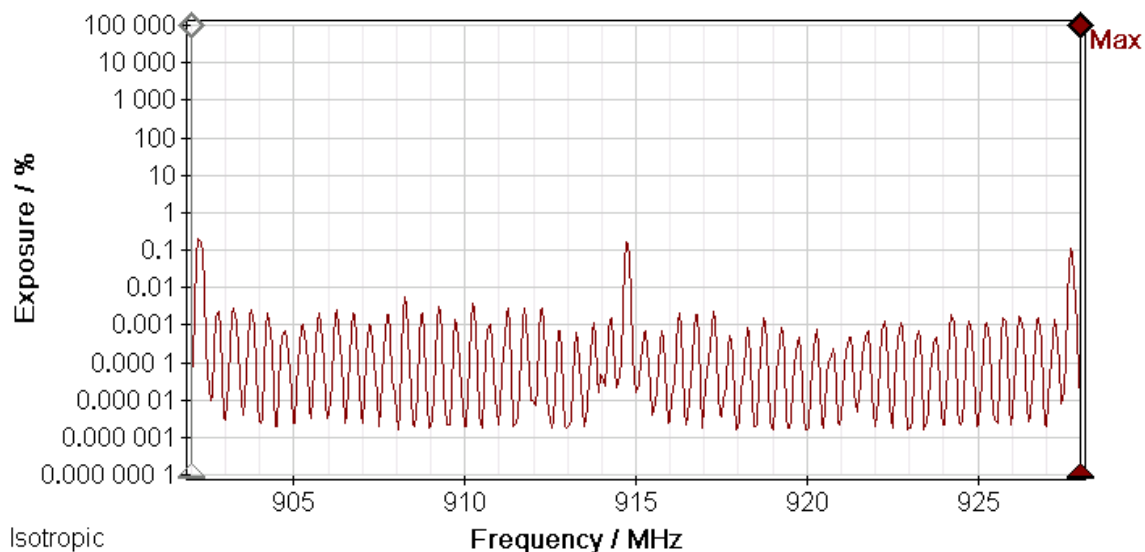


Figure B-9
900 MHz band composite RF field from rack of 10 SmartMeters at 9 feet.

Battery: 07/29/10 12:59:23 PM	GPS: 34°46'01.8" N 83°2'20.8" W	Ant: 3AX 50M-3G	Cable: ---	SrvTbl: ---	Ger.Funkd. FCC GP
Integration over Frequency		Min: 902.000 0 MHz	Max: 928.000 0 MHz	Result Type: Max	
		Cent: 915.000 0 MHz	Span: 26.000 0 MHz	Int. Val: 0.536 %	

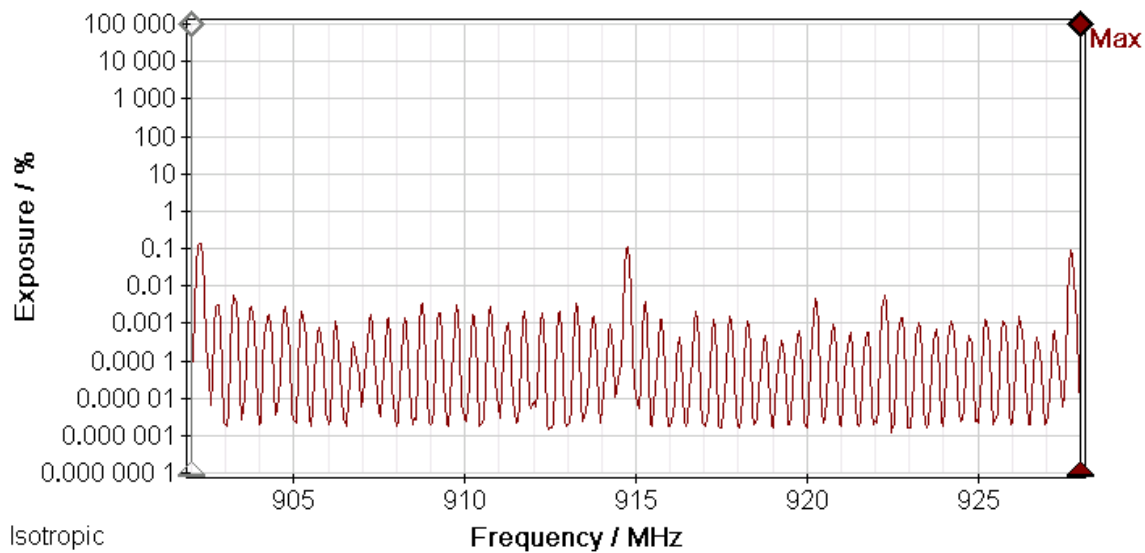


Figure B-10
900 MHz band composite RF field from rack of 10 SmartMeters at 10 feet.

Battery: 07/29/10 01:00:15 PM	GPS: 34°46'01.8" N 83°2'20.8" W	Ant: 3AX 50M-3G	Cable: ---	SrvTbl: ---	Ger.Funkd. FCC GP
Integration over Frequency		Min: 902.000 0 MHz	Max: 928.000 0 MHz	Result Type: Max	
		Cent: 915.000 0 MHz	Span: 26.000 0 MHz	Int. Val: 0.358 %	

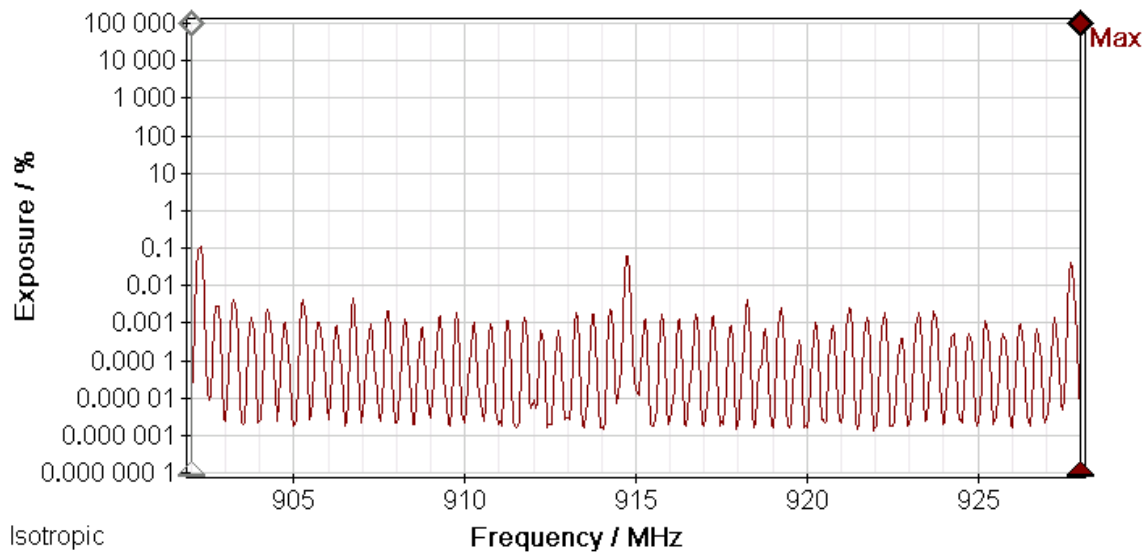


Figure B-11
900 MHz band composite RF field from rack of 10 SmartMeters at 15 feet.

Battery: 07/29/10 01:01:11 PM	GPS: 34°46'01.9" N 83°2'20.9" W	Ant: 3AX 50M-3G	SrvTbl: ---	Ger.Funkd. FCC GP
Integration over Frequency	Min: 902.000 0 MHz Cent: 915.000 0 MHz	Max: 928.000 0 MHz Span: 26.000 0 MHz	Result Type: Max	Int. Val: 0.177 %

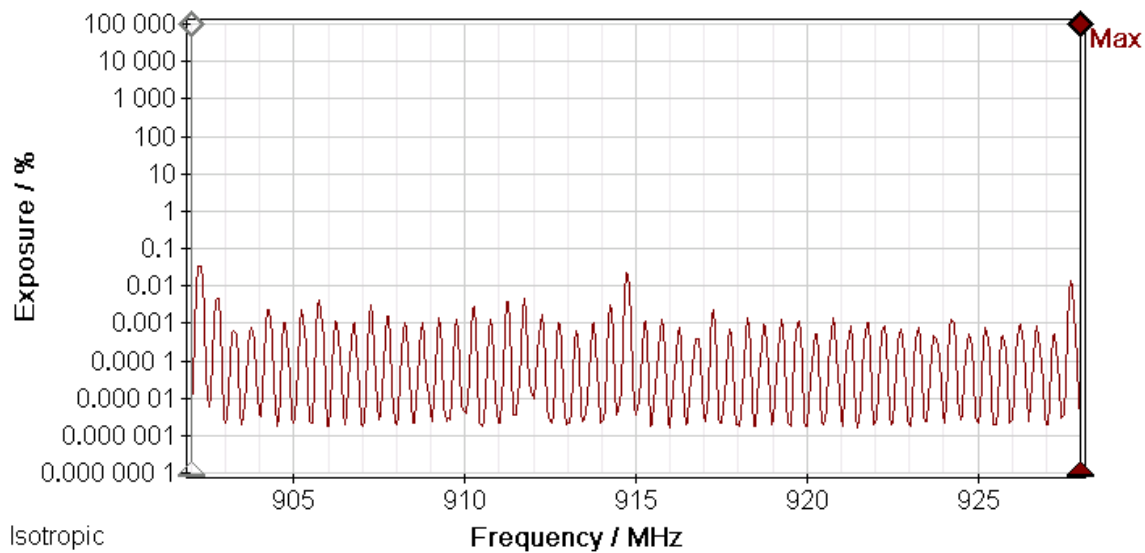


Figure B-12
900 MHz band composite RF field from rack of 10 SmartMeters at 20 feet.

Battery: 07/29/10 01:02:13 PM	GPS: 34°46'01.9" N 83°2'20.9" W	Ant: 3AX 50M-3G	SrvTbl: ---	Ger.Funkd. FCC GP
Integration over Frequency	Min: 902.000 0 MHz Cent: 915.000 0 MHz	Max: 928.000 0 MHz Span: 26.000 0 MHz	Result Type: Max	Int. Val: 0.152 %

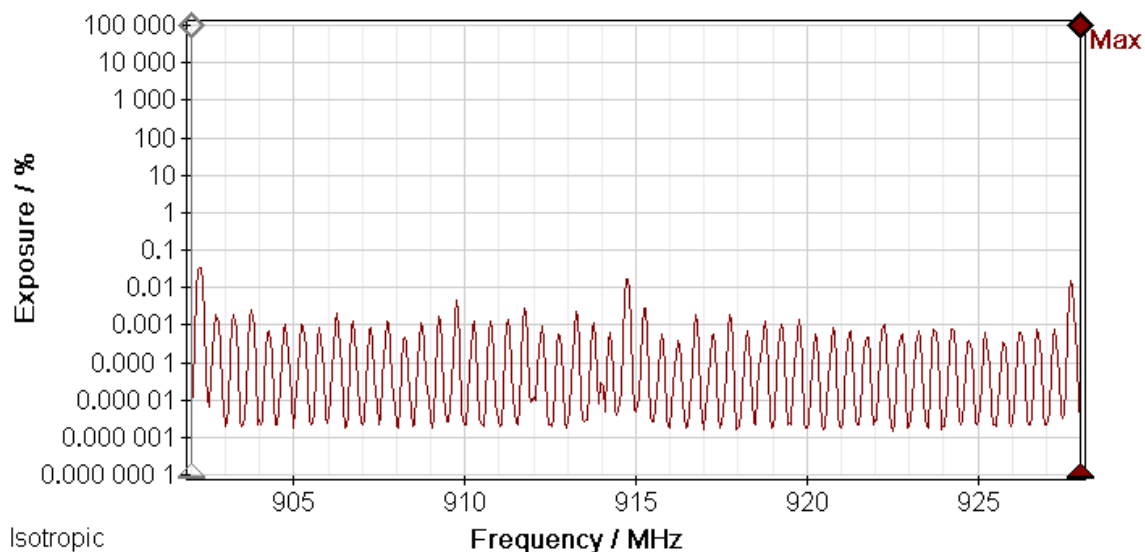


Figure B-13
900 MHz band composite RF field from rack of 10 SmartMeters at 25 feet.

Battery: 07/29/10 01:03:11 PM	GPS: 34°46'01.9" N 83°2'20.9" W	Ant: 3AX 50M-3G Cable: ---	SrvTbl: --- Stnd: ---	Ger.Funkd. FCC GP
Integration over Frequency	Min: 902.000 0 MHz Cent: 915.000 0 MHz	Max: 928.000 0 MHz Span: 26.000 0 MHz	Result Type: Max Int. Val: 0.144 %	

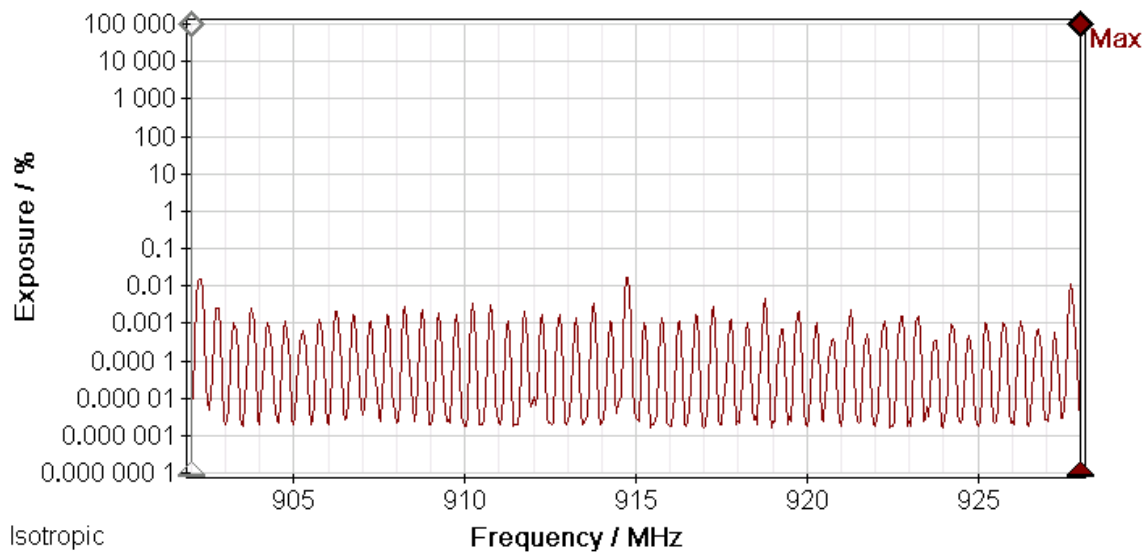


Figure B-14
900 MHz band composite RF field from rack of 10 SmartMeters at 30 feet.

Battery: 07/29/10 01:05:13 PM	GPS: 34°46'02.1" N 83°2'21.0" W	Ant: 3AX 50M-3G Cable: ---	SrvTbl: --- Stnd: ---	Ger.Funkd. FCC GP
Integration over Frequency	Min: 902.000 0 MHz Cent: 915.000 0 MHz	Max: 928.000 0 MHz Span: 26.000 0 MHz	Result Type: Max Int. Val: 0.113 %	

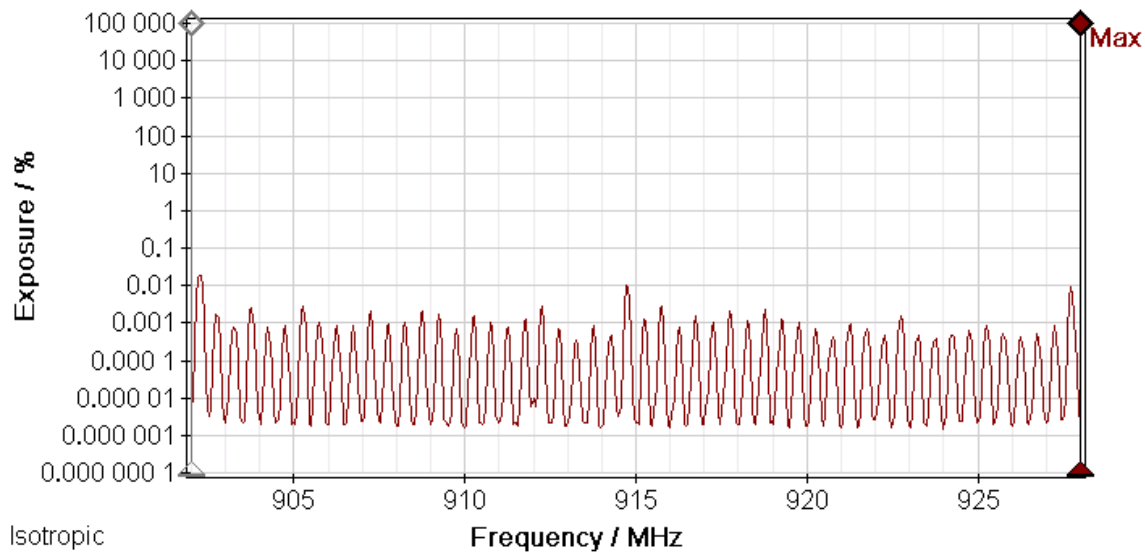


Figure B-15
900 MHz band composite RF field from rack of 10 SmartMeters at 40 feet.

Battery: 07/29/10 01:06:11 PM	GPS: 34°46'02.1" N 83°2'21.1" W	Ant: 3AX 50M-3G	Cable: ---	SrvTbl: ---	Ger.Funkd. FCC GP
Integration over Frequency		Min: 902.000 0 MHz	Max: 928.000 0 MHz	Result Type: Max	
		Cent: 915.000 0 MHz	Span: 26.000 0 MHz	Int. Val: 0.107 %	

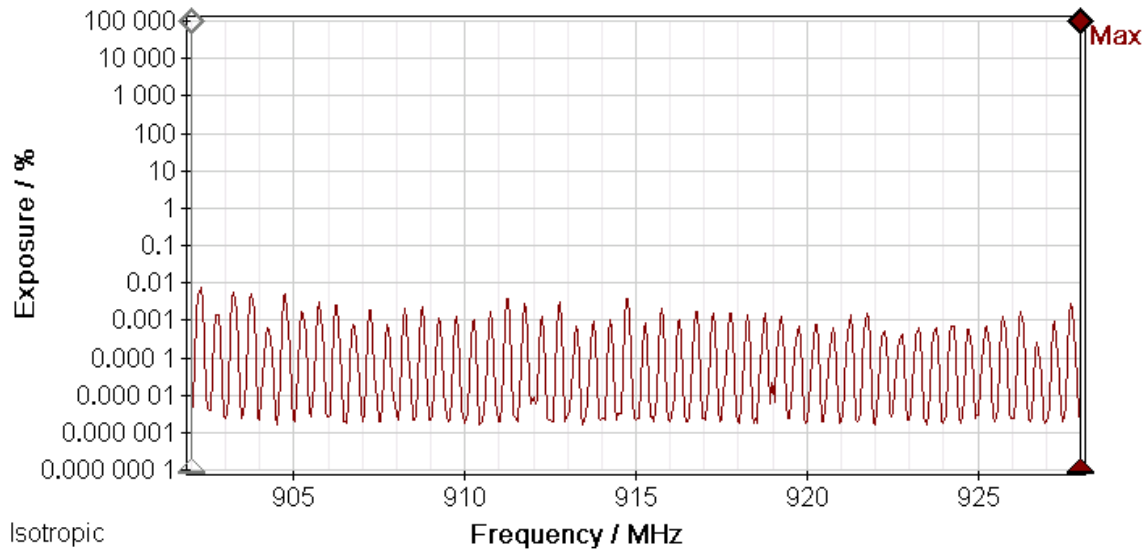


Figure B-16
900 MHz band composite RF field from rack of 10 SmartMeters at 50 feet.

Battery: 07/29/10 01:07:25 PM	GPS: 34°46'02.3" N 83°2'21.3" W	Ant: 3AX 50M-3G	Cable: ---	SrvTbl: ---	Ger.Funkd. FCC GP
Integration over Frequency		Min: 902.000 0 MHz	Max: 928.000 0 MHz	Result Type: Max	
		Cent: 915.000 0 MHz	Span: 26.000 0 MHz	Int. Val: 0.073 %	

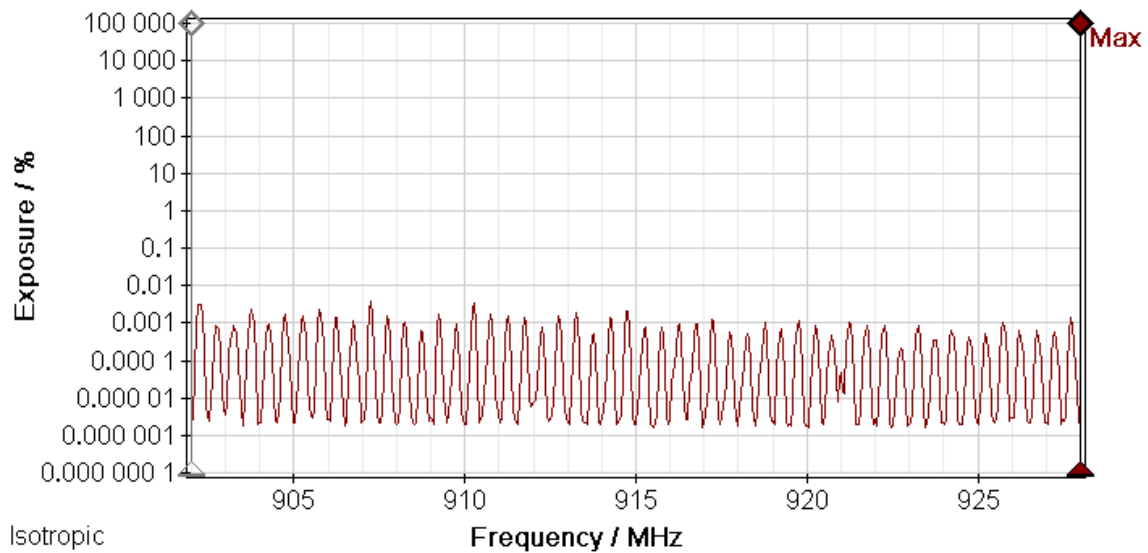


Figure B-17
900 MHz band composite RF field from rack of 10 SmartMeters at 75 feet.

Battery: 07/29/10 01:08:38 PM	GPS: 34°46'02.5" N 83°2'21.4" W	Ant: 3AX 50M-3G	Cable: ---	SrvTbl: ---	Ger.Funkd. FCC GP
Integration over Frequency		Min: 902.000 0 MHz	Max: 928.000 0 MHz	Result Type: Max	
		Cent: 915.000 0 MHz	Span: 26.000 0 MHz	Int. Val: 0.092 %	

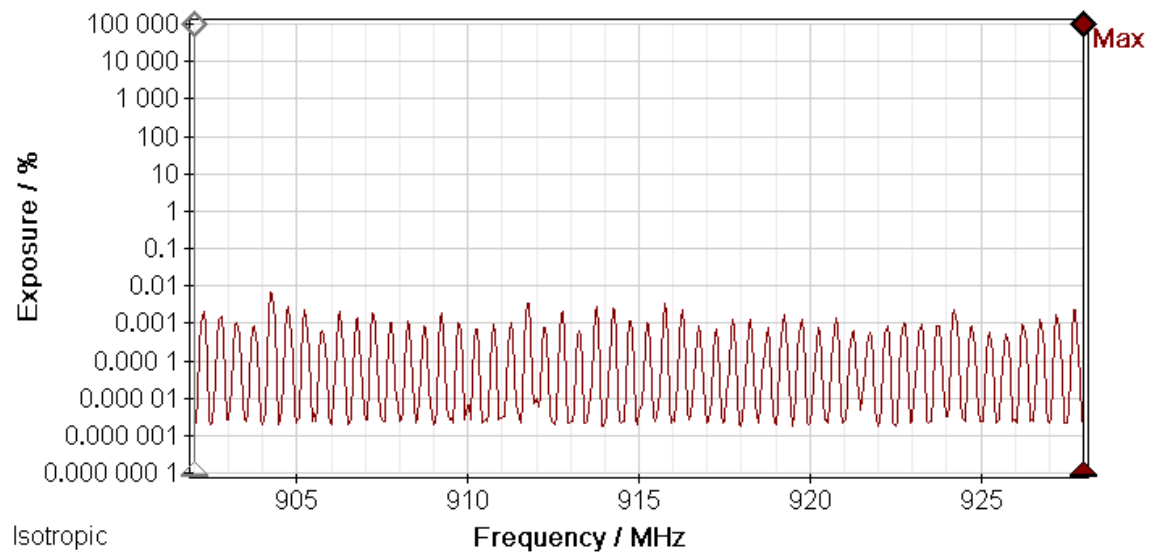


Figure B-18
900 MHz band composite RF field from rack of 10 SmartMeters at 100 feet.

Appendix C: SRM-3006 900 MHz Spectrum Measurements Scans (rear of meters)

Battery: 07/29/10 01:10:36 PM	GPS: 34°46'01.8" N 83°2'20.6" W	Ant: 3AX 50M-3G	SrvTbl: ---	Ger.Funkd. FCC GP
Integration over Frequency	Min: 902.000 0 MHz Cent: 915.000 0 MHz	Max: 928.000 0 MHz Span: 26.000 0 MHz	Result Type: Max	Int. Val: 0.571 %

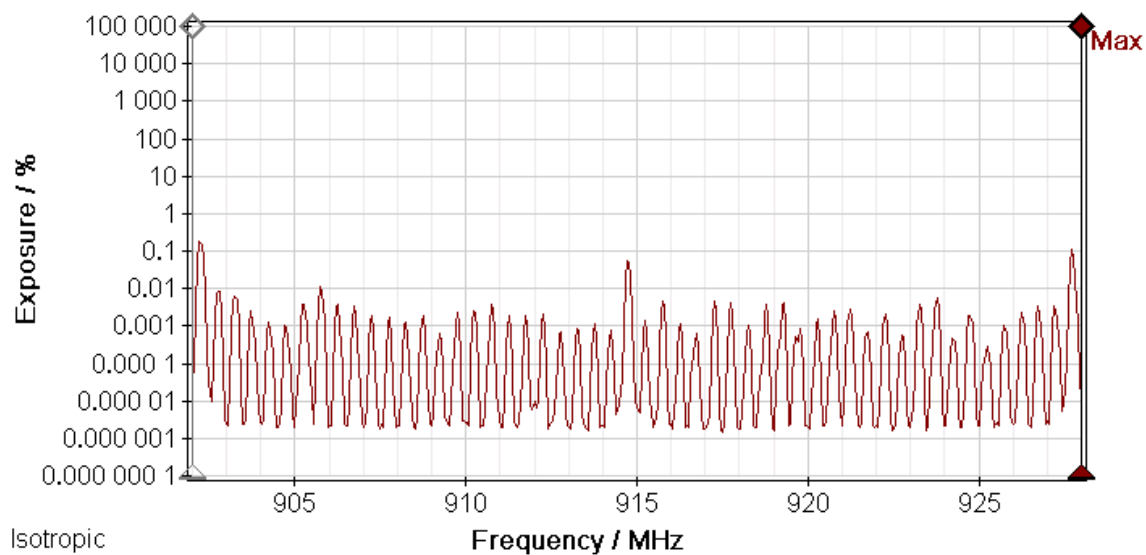


Figure C-1
900 MHz band composite RF field from rack of 10 SmartMeters at 20 cm behind meters.

Battery: 07/29/10 01:11:30 PM	GPS: 34°46'01.6" N 83°2'20.6" W	Ant: 3AX 50M-3G	Cable: ---	SrvTbl: ---	Ger.Funkd. FCC GP
Integration over Frequency		Min: 902.000 0 MHz	Max: 928.000 0 MHz	Result Type: Max	
		Cent: 915.000 0 MHz	Span: 26.000 0 MHz	Int. Val: 0.257 %	

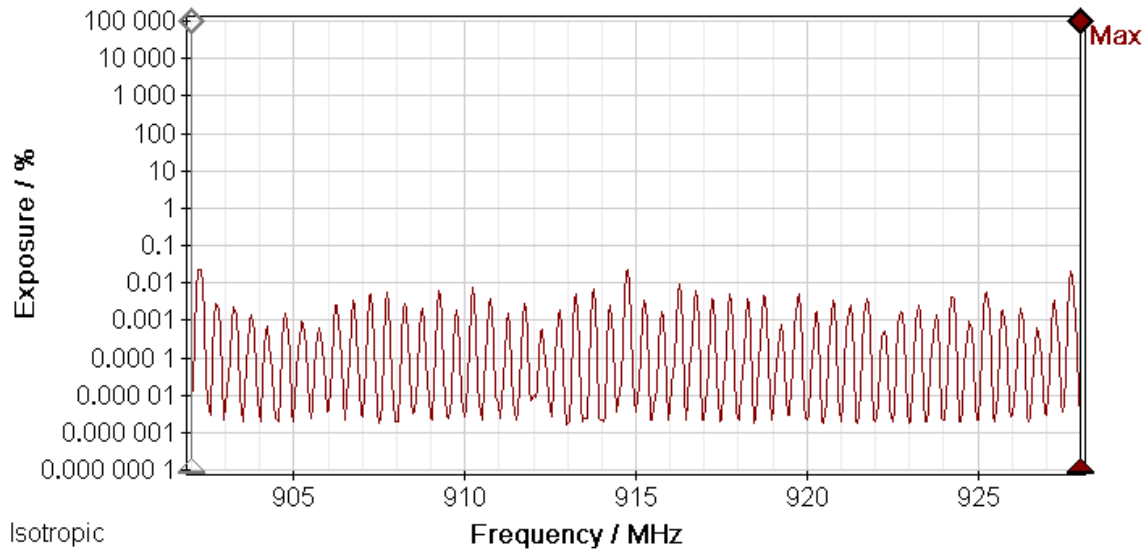


Figure C-2
900 MHz band composite RF field from rack of 10 SmartMeters at 5 feet behind meters.

Battery: 07/29/10 01:12:29 PM	GPS: 34°46'01.8" N 83°2'20.6" W	Ant: 3AX 50M-3G	Cable: ---	SrvTbl: ---	Ger.Funkd. FCC GP
Integration over Frequency		Min: 902.000 0 MHz	Max: 928.000 0 MHz	Result Type: Max	
		Cent: 915.000 0 MHz	Span: 26.000 0 MHz	Int. Val: 0.272 %	

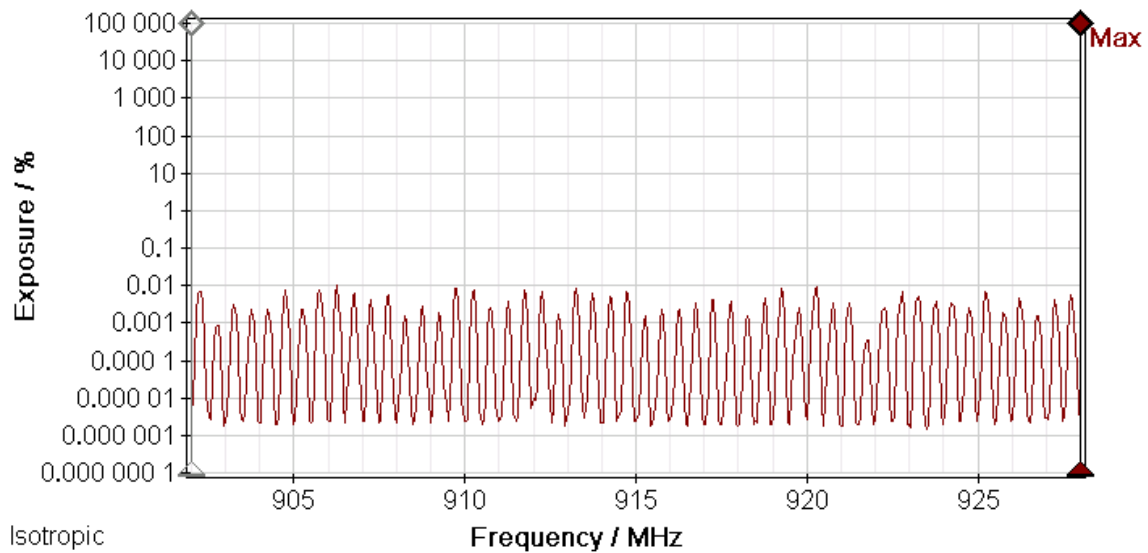


Figure C-3
900 MHz band composite RF field from rack of 10 SmartMeters at 10 feet behind meters.

Appendix D: SRM-3006 2.4 GHz Spectrum Measurement Scans (meter farm)

Battery: 07/29/10 02:29:42 PM	GPS: 34°46'01.2" N 83°2'20.3" W	Ant: 3AX 50M-3G	SrvTbl: ---	Ger.Funkd. FCC GP
Integration over Frequency	Min: 2 400.000 MHz Cent: 2 441.500 MHz	Max: 2 483.000 MHz Span: 83.000 MHz	Result Type: Max	Int. Val: 4.499 %

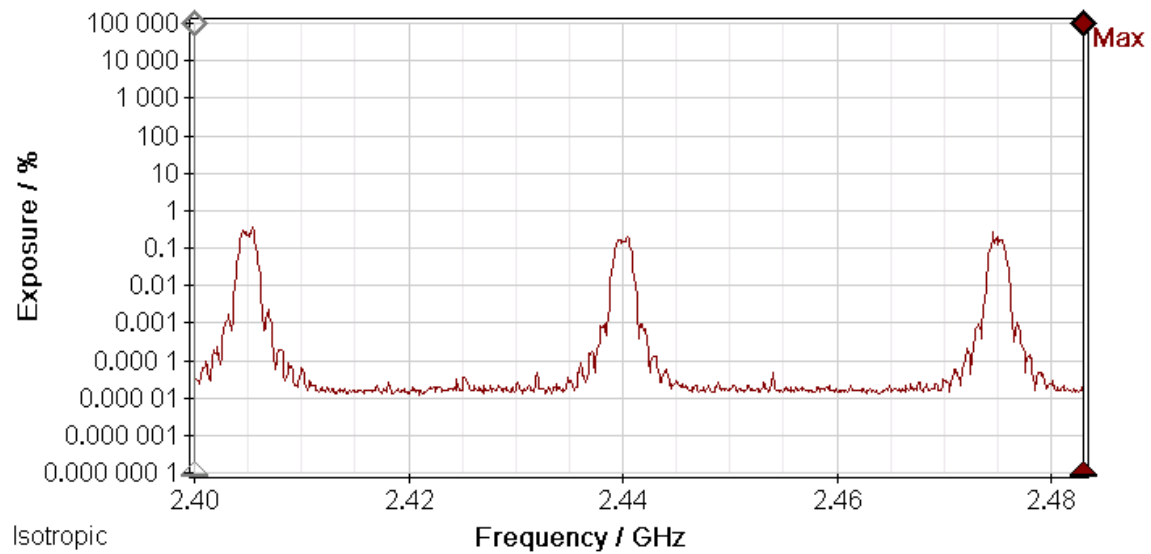


Figure D-1
2.4 GHz band composite RF field from rack of 10 SmartMeters at 1 foot.

Battery: 07/29/10 02:30:53 PM	GPS: 34°46'01.7" N 83°2'20.6" W	Ant: 3AX 50M-3G	Cable: ---	SrvTbl: ---	Ger.Funkd. FCC GP
Integration over Frequency		Min: 2 400.000 MHz	Max: 2 483.000 MHz	Result Type: Max	
		Cent: 2 441.500 MHz	Span: 83.000 MHz	Int. Val: 2.459 %	

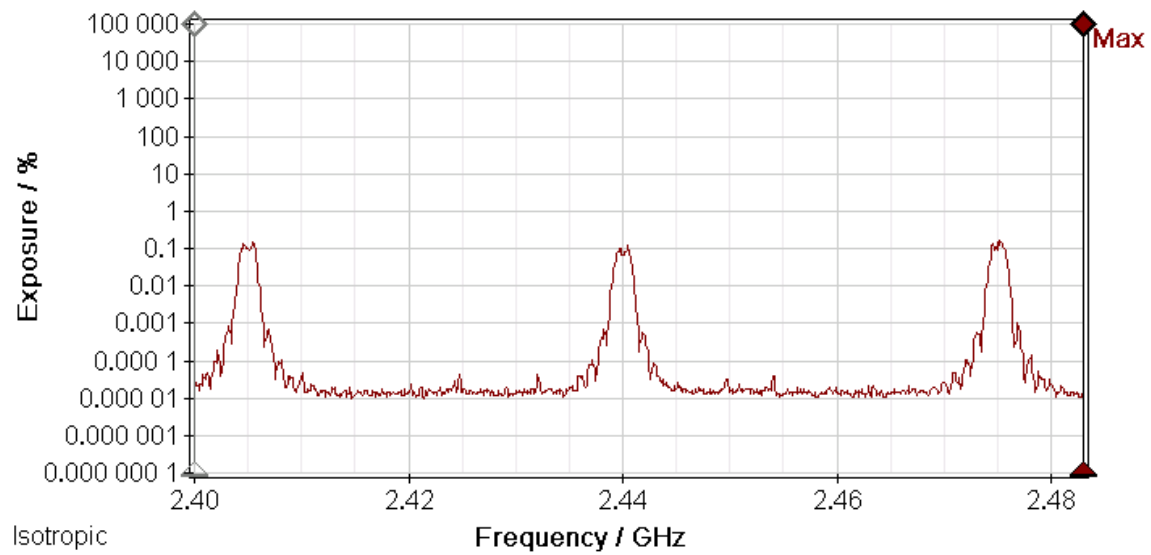


Figure D-2
2.4 GHz band composite RF field from rack of 10 SmartMeters at 2 feet.

Battery: 07/29/10 02:31:41 PM	GPS: 34°46'01.9" N 83°2'20.6" W	Ant: 3AX 50M-3G	Cable: ---	SrvTbl: ---	Ger.Funkd. FCC GP
Integration over Frequency		Min: 2 400.000 MHz	Max: 2 483.000 MHz	Result Type: Max	
		Cent: 2 441.500 MHz	Span: 83.000 MHz	Int. Val: 1.021 %	

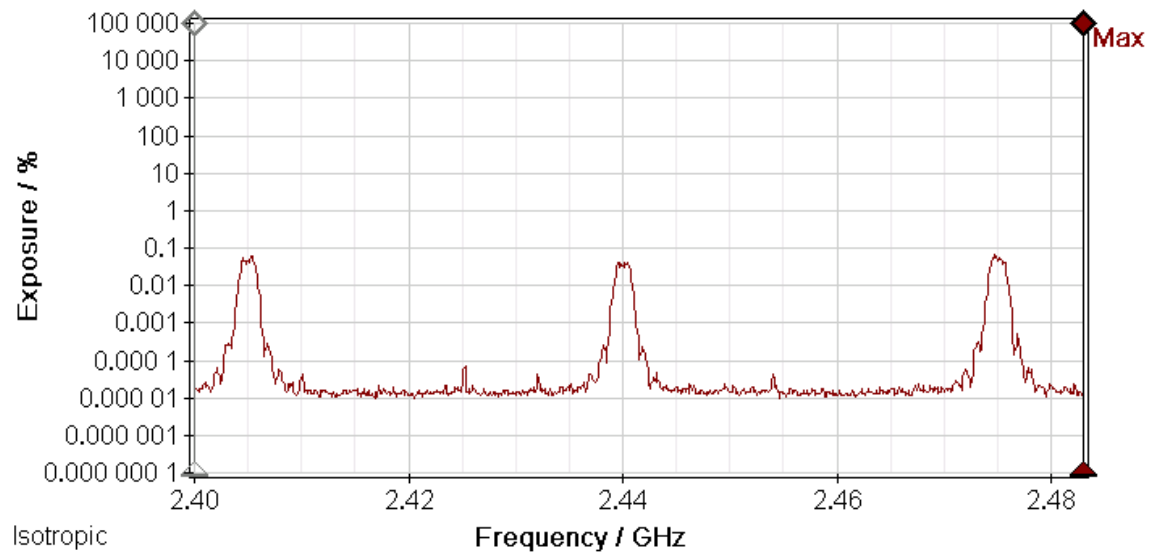


Figure D-3
2.4 GHz band composite RF field from rack of 10 SmartMeters at 3 feet.

Battery: 07/29/10 02:32:25 PM	GPS: 34°46'01.8" N 83°2'20.6" W	Ant: 3AX 50M-3G	SrvTbl: ---	Ger.Funkd. FCC GP
Integration over Frequency	Min: 2 400.000 MHz Cent: 2 441.500 MHz	Max: 2 483.000 MHz Span: 83.000 MHz	Result Type: Max	Int. Val: 0.567 %

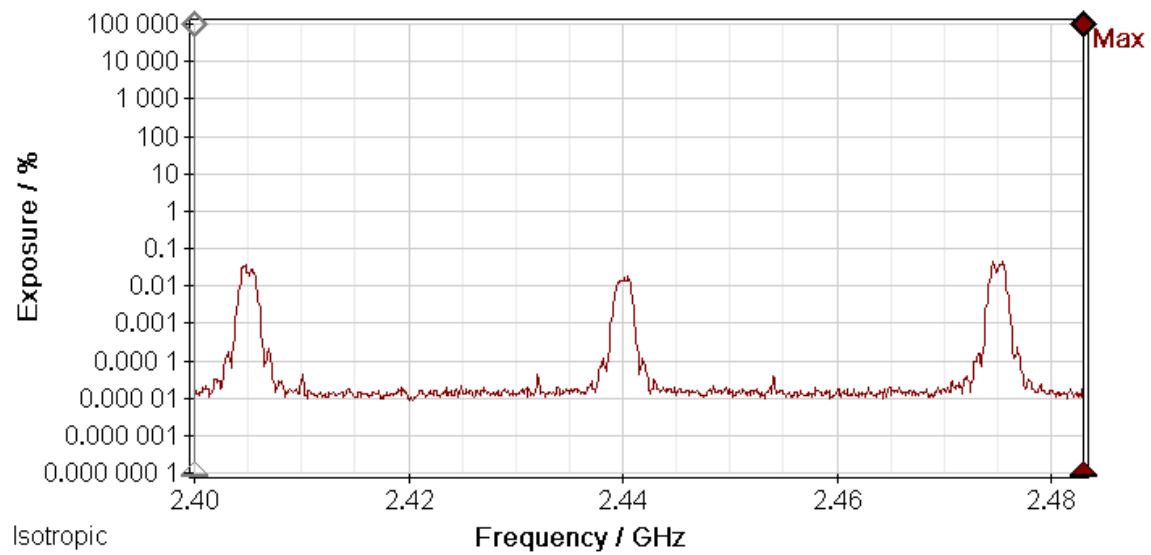


Figure D-4
2.4 GHz band composite RF field from rack of 10 SmartMeters at 4 feet.

Battery: 07/29/10 02:33:07 PM	GPS: 34°46'01.8" N 83°2'20.6" W	Ant: 3AX 50M-3G	SrvTbl: ---	Ger.Funkd. FCC GP
Integration over Frequency	Min: 2 400.000 MHz Cent: 2 441.500 MHz	Max: 2 483.000 MHz Span: 83.000 MHz	Result Type: Max	Int. Val: 0.457 %

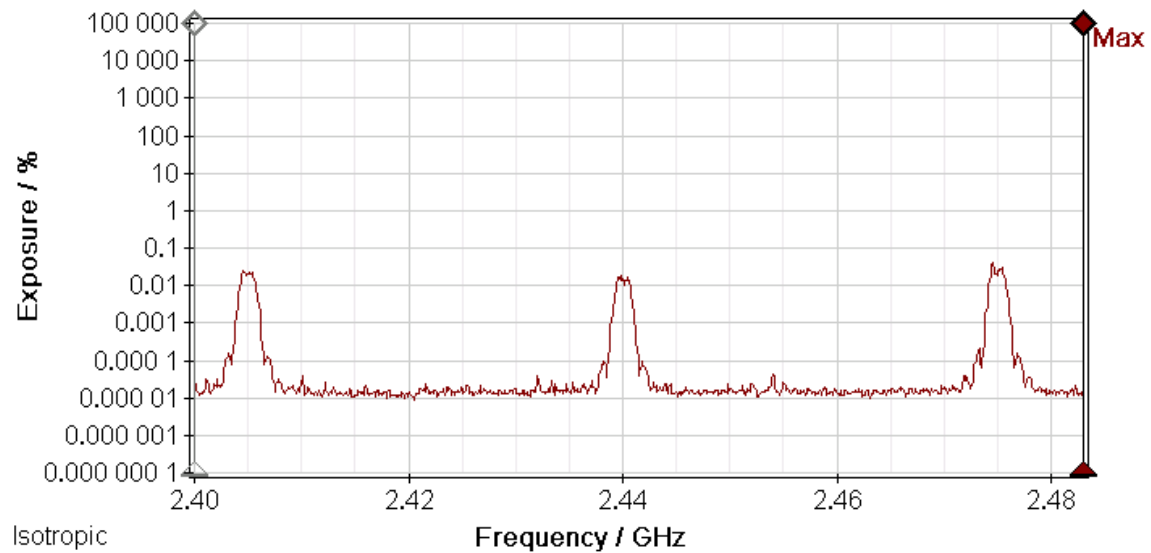


Figure D-5
2.4 GHz band composite RF field from rack of 10 SmartMeters at 5 feet.

Battery: 07/29/10 02:33:54 PM	GPS: 34°46'01.8" N 83°2'20.6" W	Ant: 3AX 50M-3G	Cable: ---	SrvTbl: ---	Ger.Funkd. FCC GP
Integration over Frequency		Min: 2 400.000 MHz	Max: 2 483.000 MHz	Result Type: Max	
		Cent: 2 441.500 MHz	Span: 83.000 MHz	Int. Val: 0.348 %	

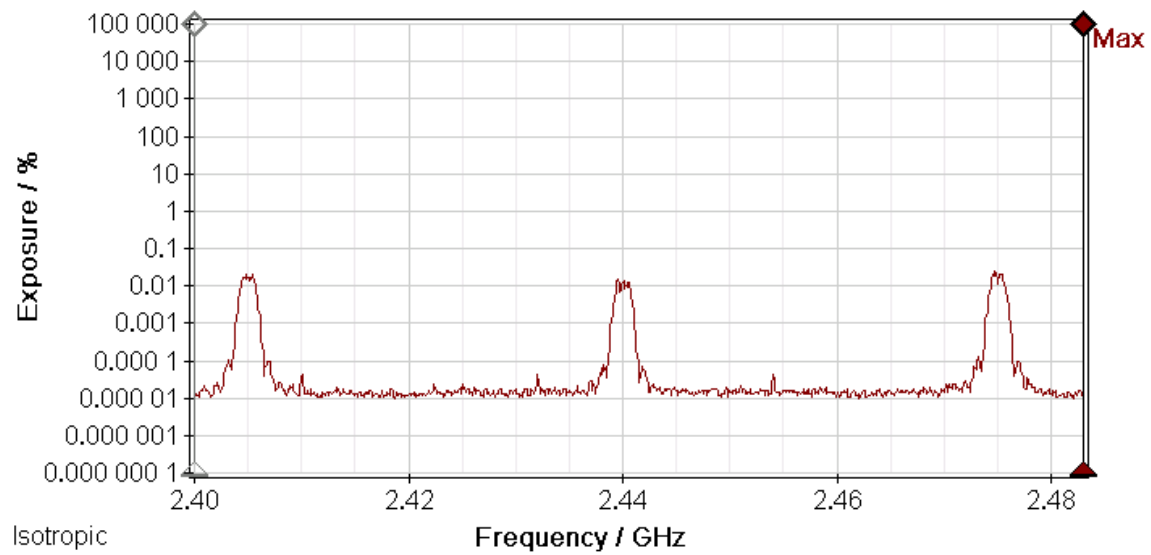


Figure D-6
2.4 GHz band composite RF field from rack of 10 SmartMeters at 6 feet.

Battery: 07/29/10 02:34:33 PM	GPS: 34°46'01.7" N 83°2'20.6" W	Ant: 3AX 50M-3G	Cable: ---	SrvTbl: ---	Ger.Funkd. FCC GP
Integration over Frequency		Min: 2 400.000 MHz	Max: 2 483.000 MHz	Result Type: Max	
		Cent: 2 441.500 MHz	Span: 83.000 MHz	Int. Val: 0.258 %	

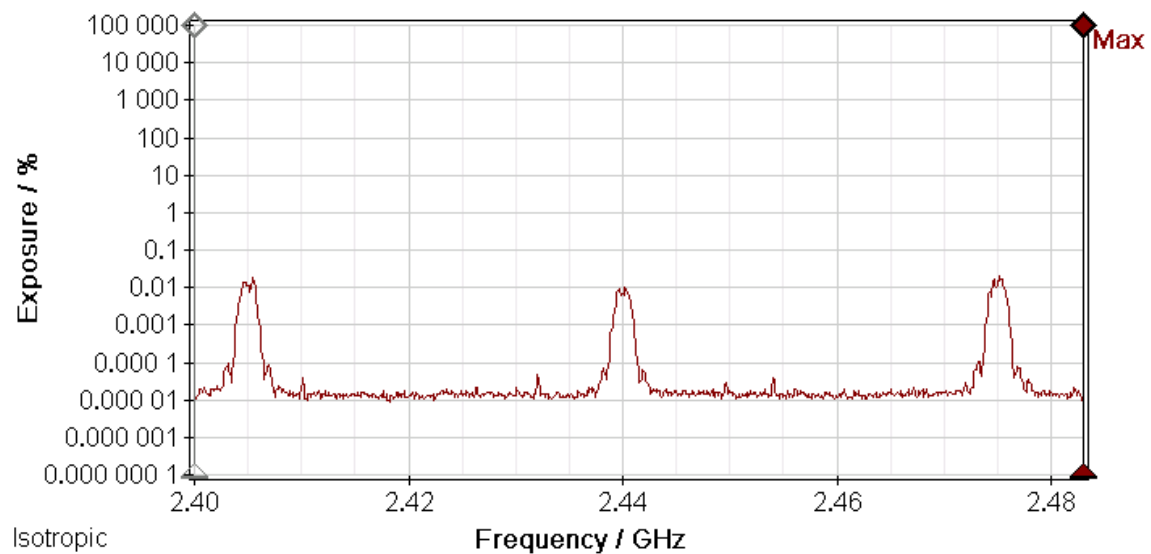


Figure D-7
2.4 GHz band composite RF field from rack of 10 SmartMeters at 7 feet.

Battery: 07/29/10 02:35:15 PM	GPS: 34°46'01.7" N 83°2'20.6" W	Ant: 3AX 50M-3G	Cable: ---	SrvTbl: ---	Ger.Funkd. FCC GP
Integration over Frequency	Min: 2 400.000 MHz Cent: 2 441.500 MHz	Max: 2 483.000 MHz Span: 83.000 MHz	Result Type: Max	Int. Val: 0.187 %	

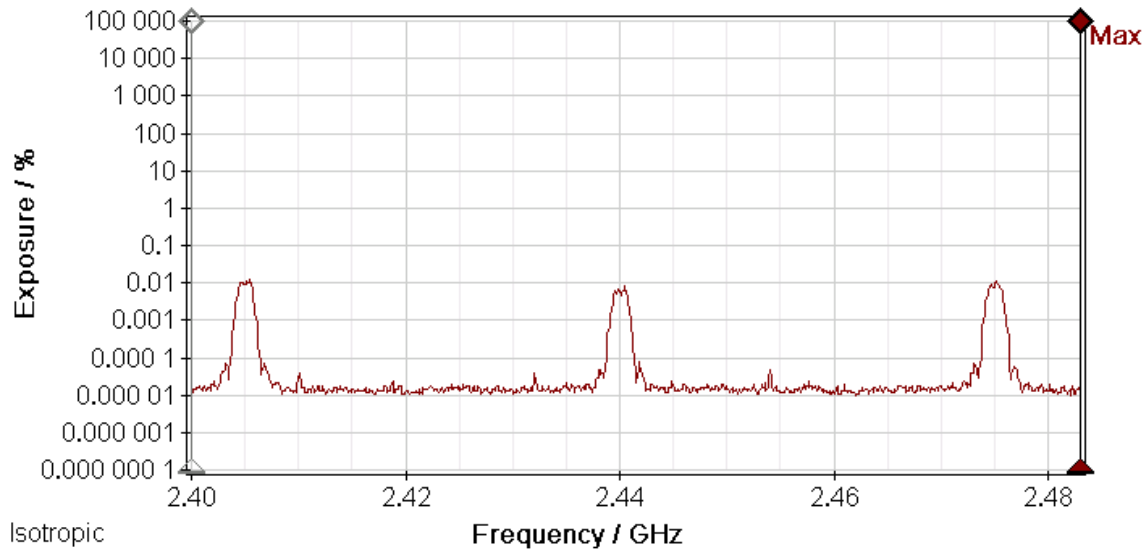


Figure D-8
2.4 GHz band composite RF field from rack of 10 SmartMeters at 8 feet.

Battery: 07/29/10 02:35:53 PM	GPS: 34°46'01.9" N 83°2'20.6" W	Ant: 3AX 50M-3G	Cable: ---	SrvTbl: ---	Ger.Funkd. FCC GP
Integration over Frequency	Min: 2 400.000 MHz Cent: 2 441.500 MHz	Max: 2 483.000 MHz Span: 83.000 MHz	Result Type: Max	Int. Val: 0.163 %	

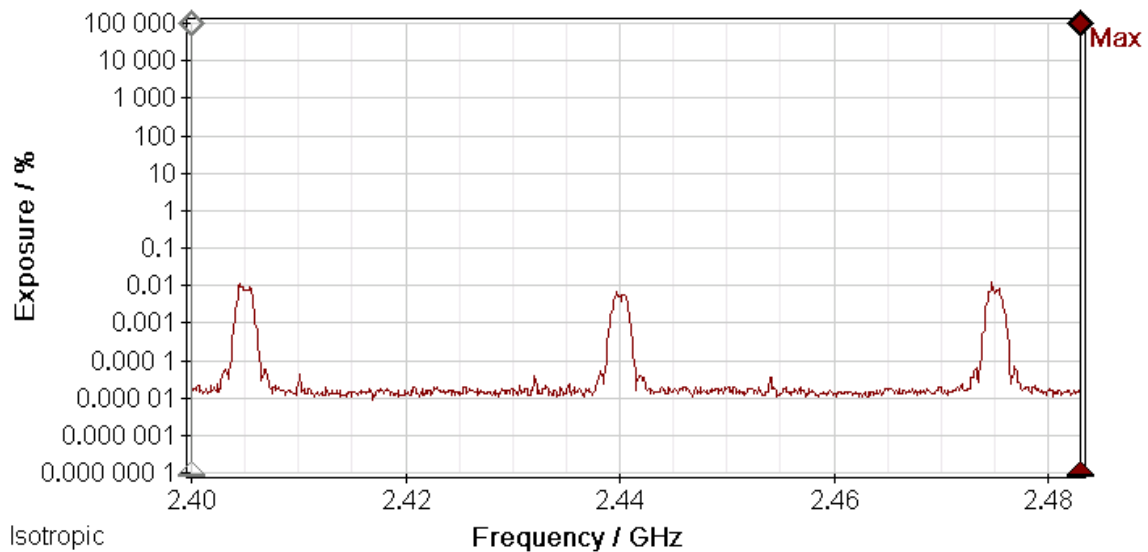


Figure D-9
2.4 GHz band composite RF field from rack of 10 SmartMeters at 9 feet.

Battery: 07/29/10 02:36:34 PM	GPS: 34°46'01.9" N 83°2'20.5" W	Ant: 3AX 50M-3G	Cable: ---	SrvTbl: ---	Ger.Funkd. FCC GP
Integration over Frequency	Min: 2 400.000 MHz Cent: 2 441.500 MHz	Max: 2 483.000 MHz Span: 83.000 MHz	Result Type: Max	Int. Val: 0.134 %	

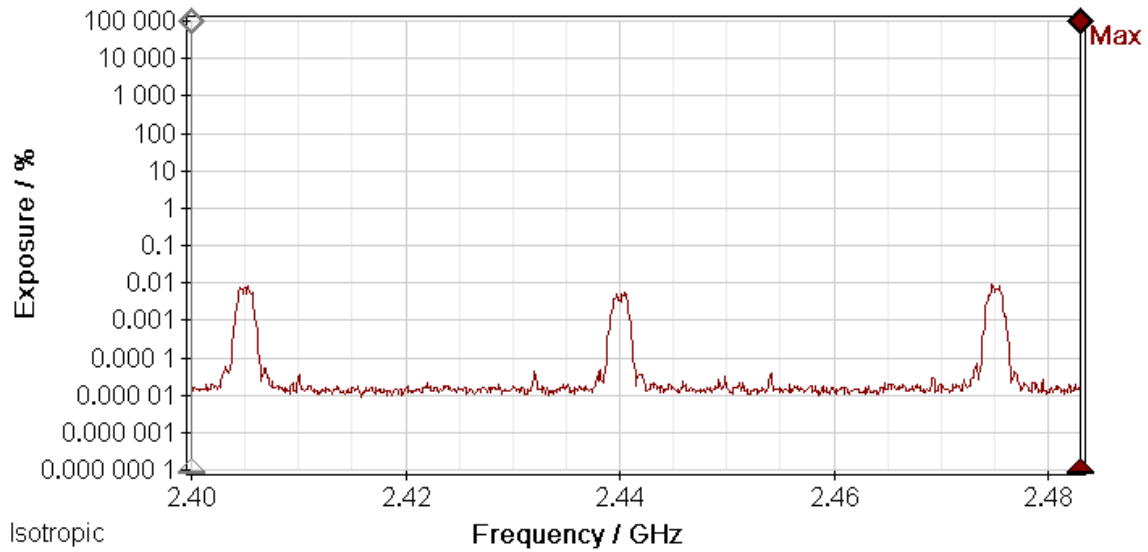


Figure D-10
2.4 GHz band composite RF field from rack of 10 SmartMeters at 10 feet.

Battery: 07/29/10 02:37:25 PM	GPS: 34°46'01.8" N 83°2'20.6" W	Ant: 3AX 50M-3G	Cable: ---	SrvTbl: ---	Ger.Funkd. FCC GP
Integration over Frequency	Min: 2 400.000 MHz Cent: 2 441.500 MHz	Max: 2 483.000 MHz Span: 83.000 MHz	Result Type: Max	Int. Val: 0.076 %	

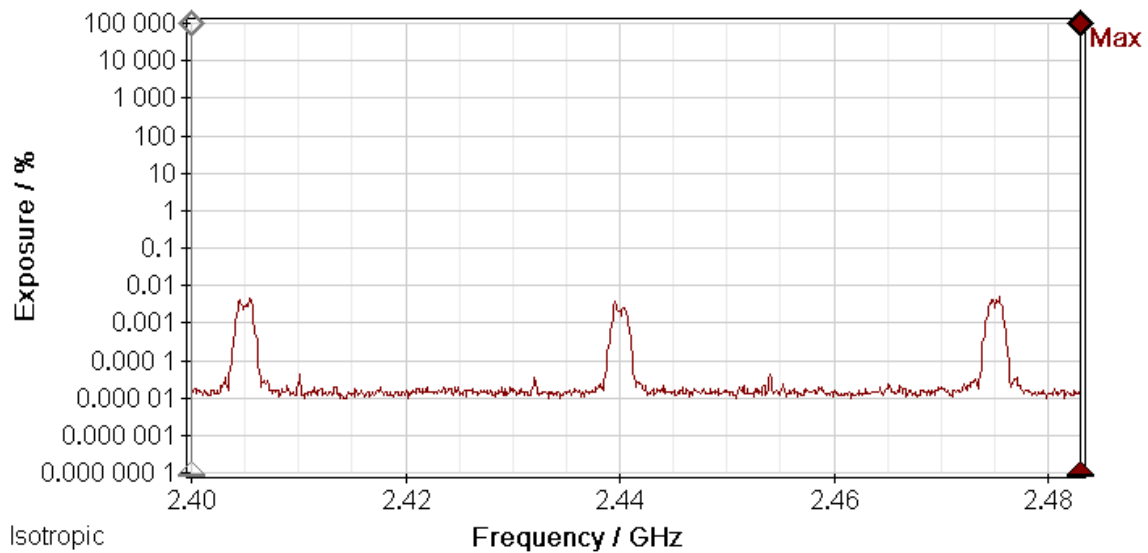


Figure D-11
2.4 GHz band composite RF field from rack of 10 SmartMeters at 15 feet.

Battery: 07/29/10 02:38:17 PM	GPS: 34°46'01.8" N 83°2'20.7" W	Ant: 3AX 50M-3G	SrvTbl: ---	Ger.Funkd. FCC GP
Integration over Frequency	Min: 2 400.000 MHz	Max: 2 483.000 MHz	Result Type: Max	
	Cent: 2 441.500 MHz	Span: 83.000 MHz	Int. Val: 0.044 %	

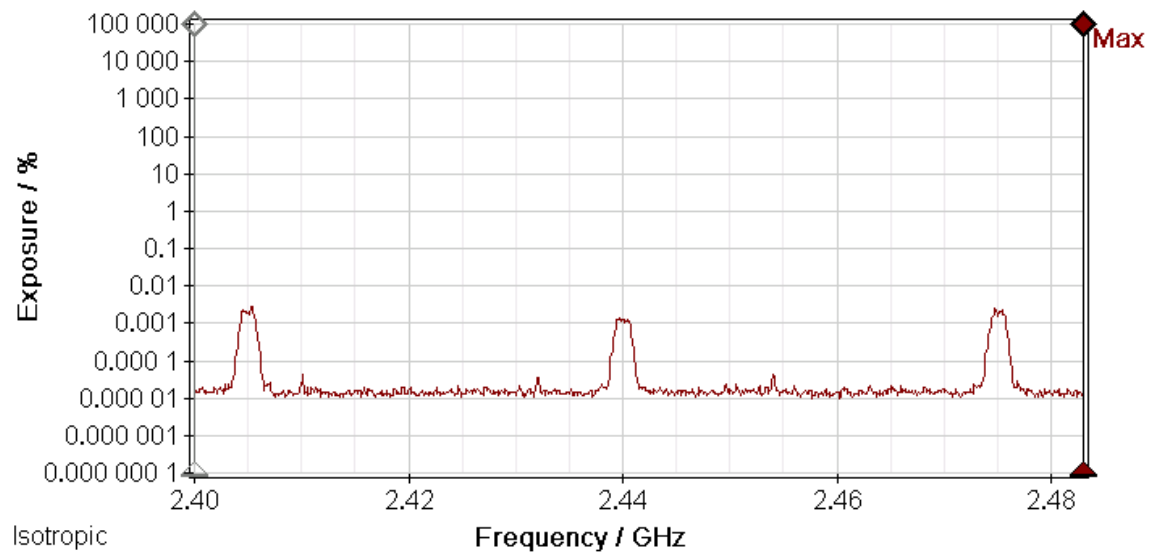


Figure D-12
2.4 GHz band composite RF field from rack of 10 SmartMeters at 20 feet.

Battery: 07/29/10 02:38:55 PM	GPS: 34°46'01.8" N 83°2'20.7" W	Ant: 3AX 50M-3G	SrvTbl: ---	Ger.Funkd. FCC GP
Integration over Frequency	Min: 2 400.000 MHz	Max: 2 483.000 MHz	Result Type: Max	
	Cent: 2 441.500 MHz	Span: 83.000 MHz	Int. Val: 0.033 %	

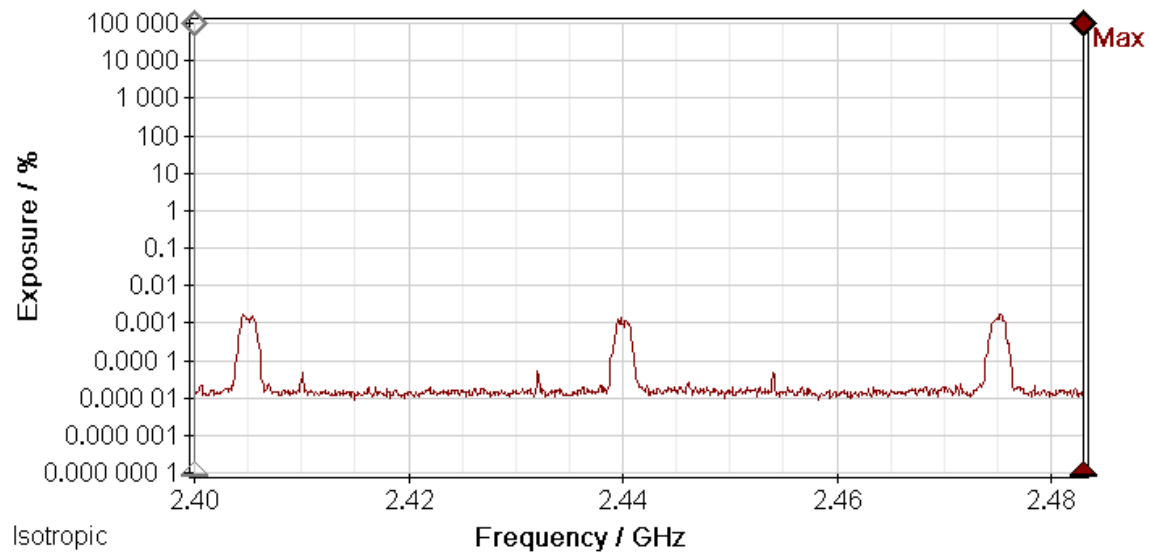


Figure D-13
2.4 GHz band composite RF field from rack of 10 SmartMeters at 25 feet.

Battery: 07/29/10 02:39:57 PM	GPS: 34°46'01.9" N 83°2'20.8" W	Ant: 3AX 50M-3G	SrvTbl: ---	Ger.Funkd. FCC GP
Integration over Frequency	Min: 2 400.000 MHz Cent: 2 441.500 MHz	Max: 2 483.000 MHz Span: 83.000 MHz	Result Type: Max	Int. Val: 0.020 %

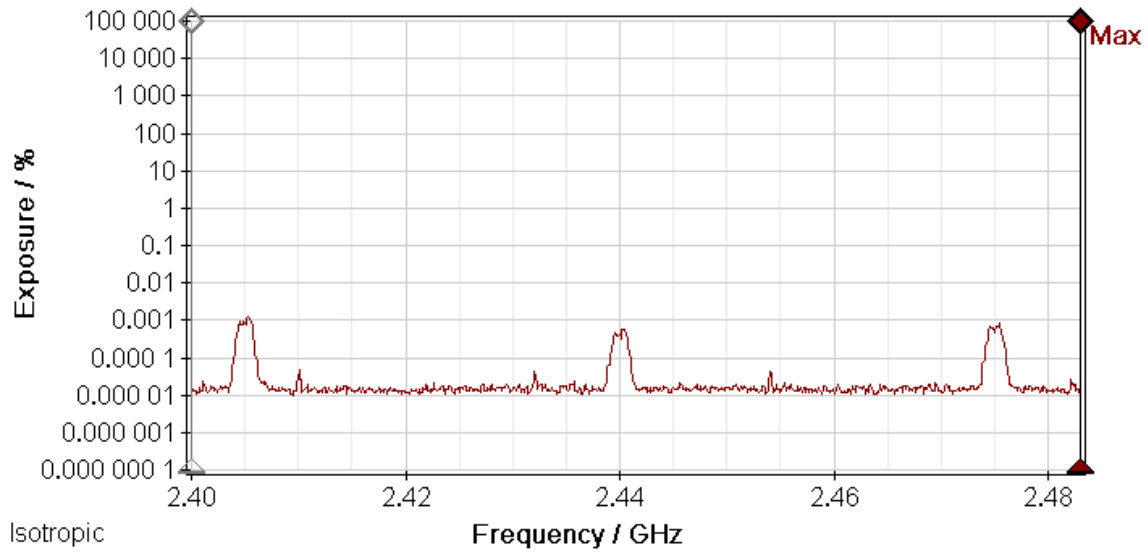


Figure D-14
2.4 GHz band composite RF field from rack of 10 SmartMeters at 30 feet.

Battery: 07/29/10 02:40:46 PM	GPS: 34°46'02.0" N 83°2'20.9" W	Ant: 3AX 50M-3G	SrvTbl: ---	Ger.Funkd. FCC GP
Integration over Frequency	Min: 2 400.000 MHz Cent: 2 441.500 MHz	Max: 2 483.000 MHz Span: 83.000 MHz	Result Type: Max	Int. Val: 0.014 %

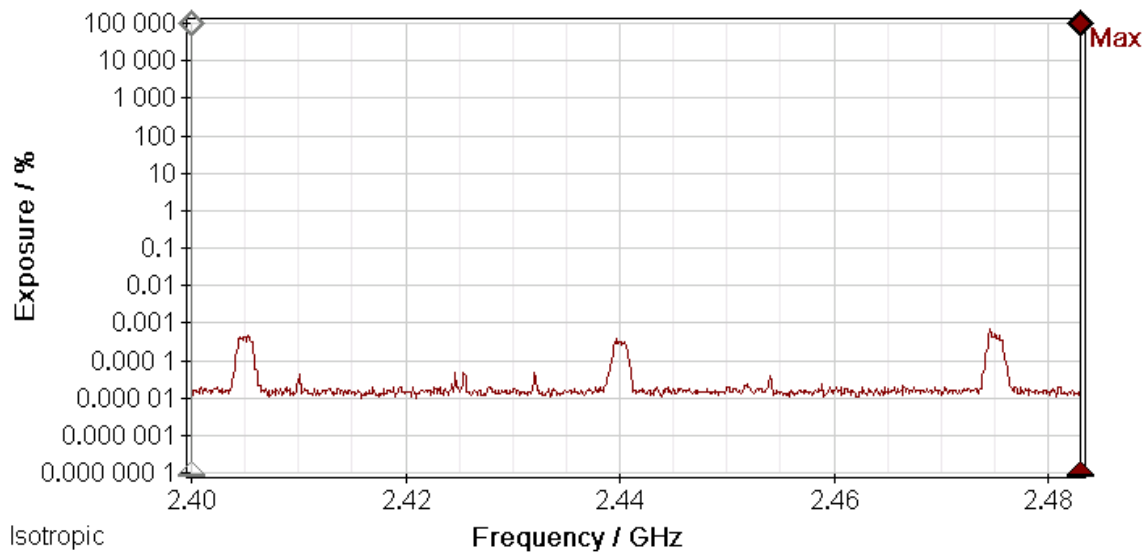


Figure D-15
2.4 GHz band composite RF field from rack of 10 SmartMeters at 40 feet.

Battery: 07/29/10 02:41:44 PM	GPS: 34°46'02.1" N 83°2'21.0" W	Ant: 3AX 50M-3G	Cable: ---	SrvTbl: ---	Ger.Funkd. FCC GP
Integration over Frequency		Min: 2 400.000 MHz	Max: 2 483.000 MHz	Result Type: Max	
		Cent: 2 441.500 MHz	Span: 83.000 MHz	Int. Val: 0.013 %	

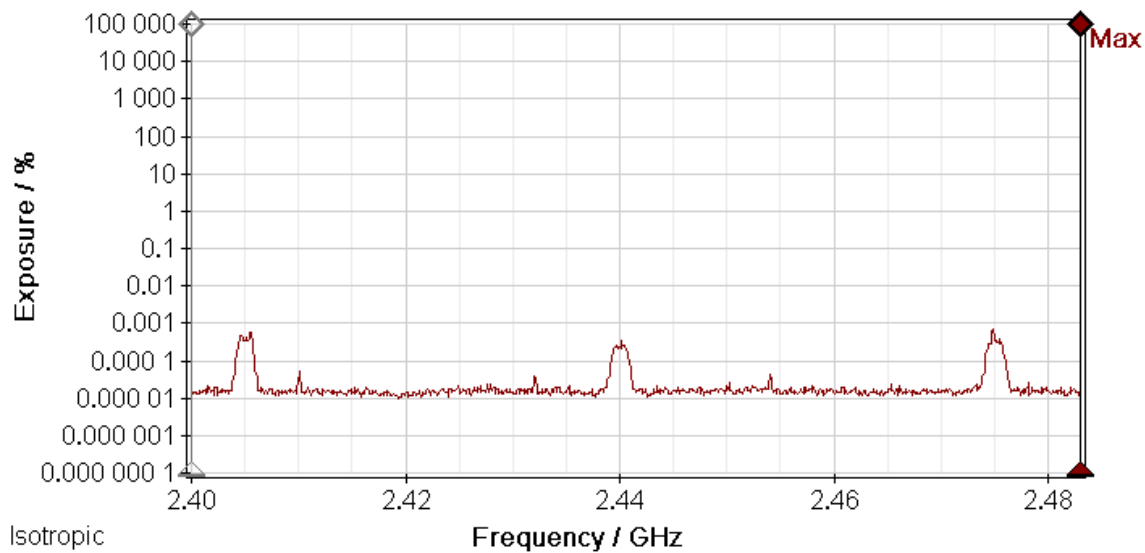


Figure D-16
2.4 GHz band composite RF field from rack of 10 SmartMeters at 50 feet.

Battery: 07/29/10 02:42:40 PM	GPS: 34°46'02.3" N 83°2'21.1" W	Ant: 3AX 50M-3G	Cable: ---	SrvTbl: ---	Ger.Funkd. FCC GP
Integration over Frequency		Min: 2 400.000 MHz	Max: 2 483.000 MHz	Result Type: Max	
		Cent: 2 441.500 MHz	Span: 83.000 MHz	Int. Val: 0.009 10 %	

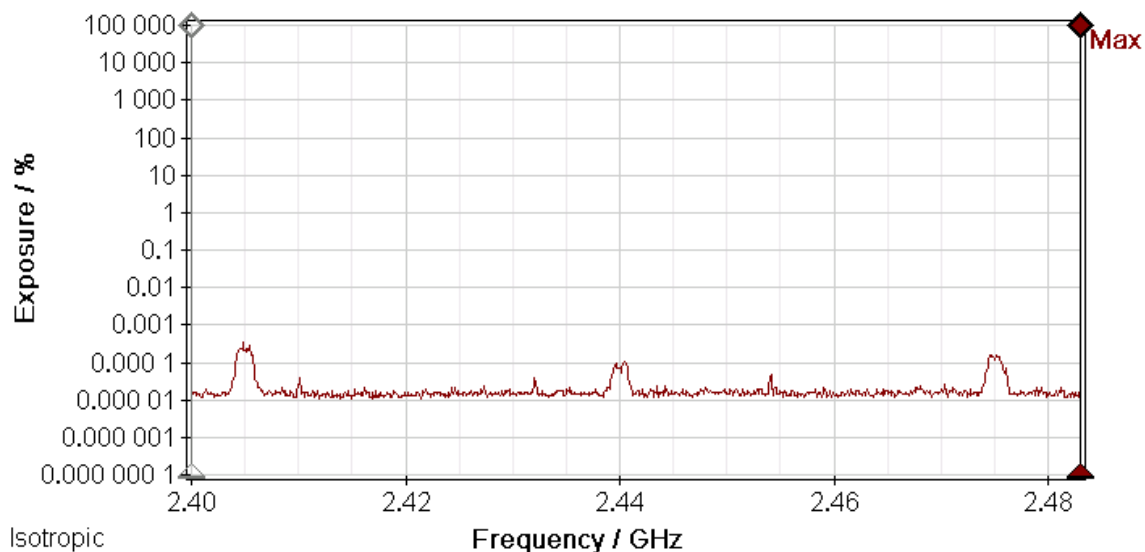


Figure D-17
2.4 GHz band composite RF field from rack of 10 SmartMeters at 75 feet.

Battery: 07/29/10 02:43:34 PM	GPS: 34°46'02.4" N 83°2'21.3" W	Ant: 3AX 50M-3G	Cable: ---	SrvTbl: ---	Ger.Funkd. FCC GP
Integration over Frequency		Min: 2 400.000 MHz	Max: 2 483.000 MHz	Result Type: Max	
		Cent: 2 441.500 MHz	Span: 83.000 MHz	Int. Val: 0.008 52 %	

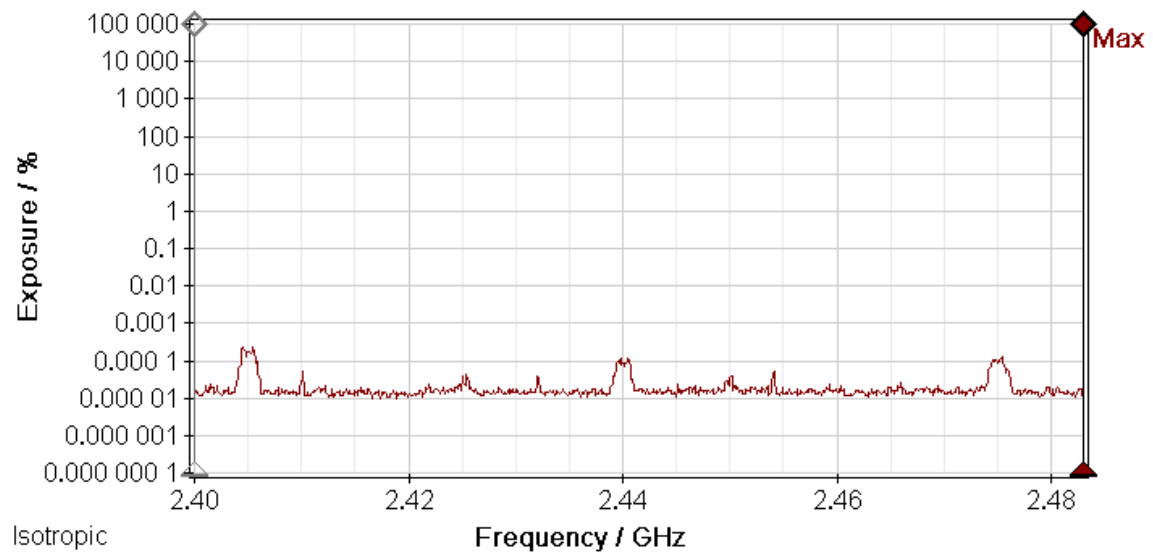


Figure D-18
2.4 GHz band composite RF field from rack of 10 SmartMeters at 100 feet.

Appendix E: SRM-3006 2.4 GHz Spectrum Measurement Scans (rear of meters)

Battery: 07/29/10 02:45:56 PM	GPS: 34°46'01.7" N 83°2'20.6" W	Ant: 3AX 50M-3G	SrvTbl: ---	Ger.Funkd. FCC GP
Integration over Frequency		Min: 2 400.000 MHz	Max: 2 483.000 MHz	Result Type: Max
		Cent: 2 441.500 MHz	Span: 83.000 MHz	Int. Val: 0.200 %

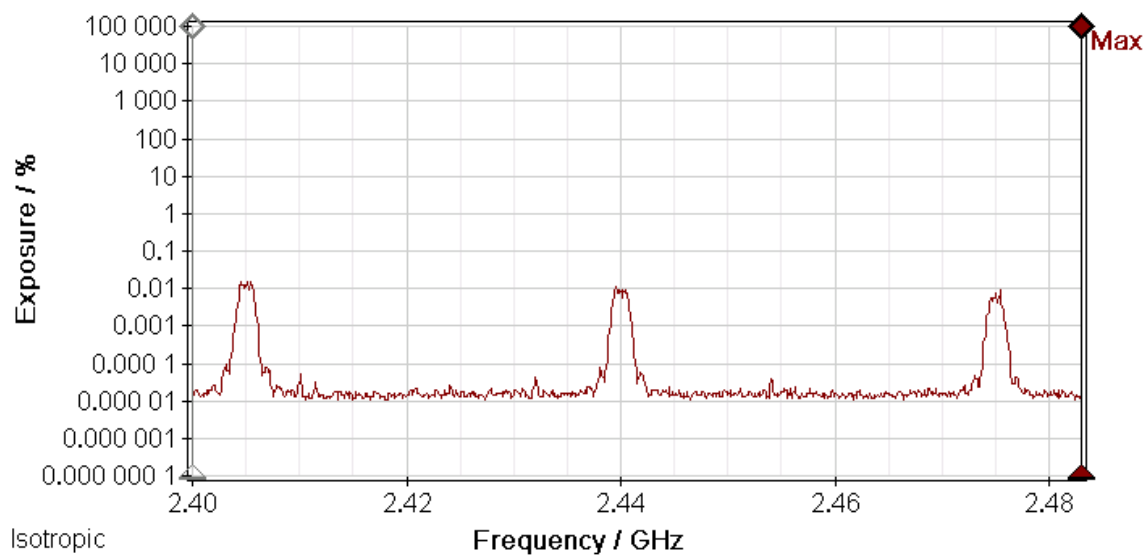


Figure E-1
2.4 GHz band composite RF field at 20 cm behind rack of 10 SmartMeters.

Battery: 07/29/10 02:46:58 PM	GPS: 34°46'01.5" N 83°2'20.6" W	Ant: 3AX 50M-3G	SrvTbl: ---	Ger.Funkd. FCC GP
Integration over Frequency	Min: 2 400.000 MHz Cent: 2 441.500 MHz	Max: 2 483.000 MHz Span: 83.000 MHz	Result Type: Max	Int. Val: 0.014 %

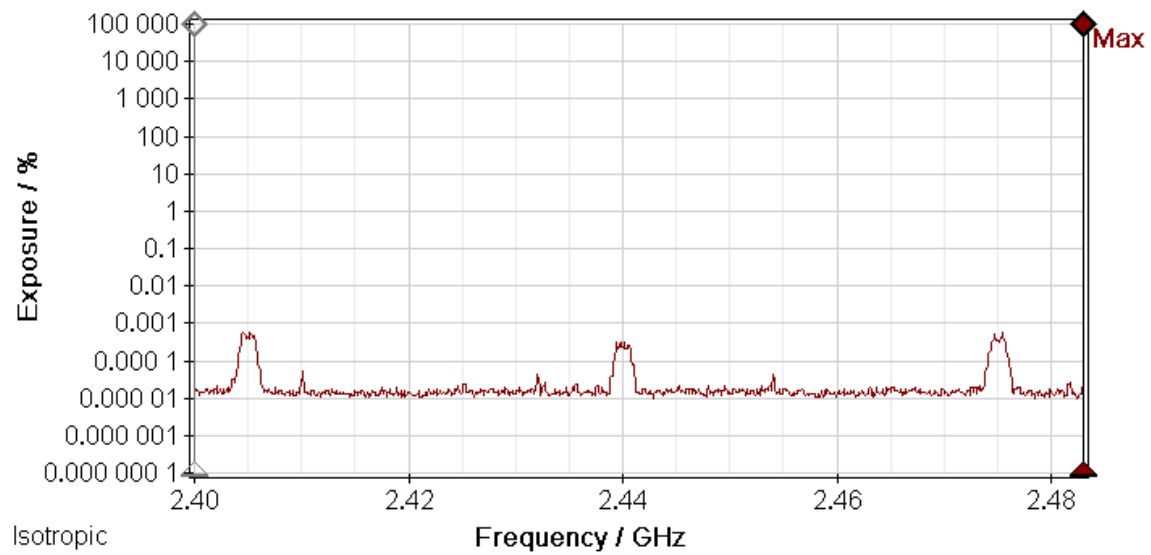


Figure E-2
2.4 GHz band composite RF field at 5 feet behind rack of 10 SmartMeters.

Battery: 07/29/10 02:47:46 PM	GPS: 34°46'01.6" N 83°2'20.6" W	Ant: 3AX 50M-3G	SrvTbl: ---	Ger.Funkd. FCC GP
Integration over Frequency	Min: 2 400.000 MHz Cent: 2 441.500 MHz	Max: 2 483.000 MHz Span: 83.000 MHz	Result Type: Max	Int. Val: 0.011 %

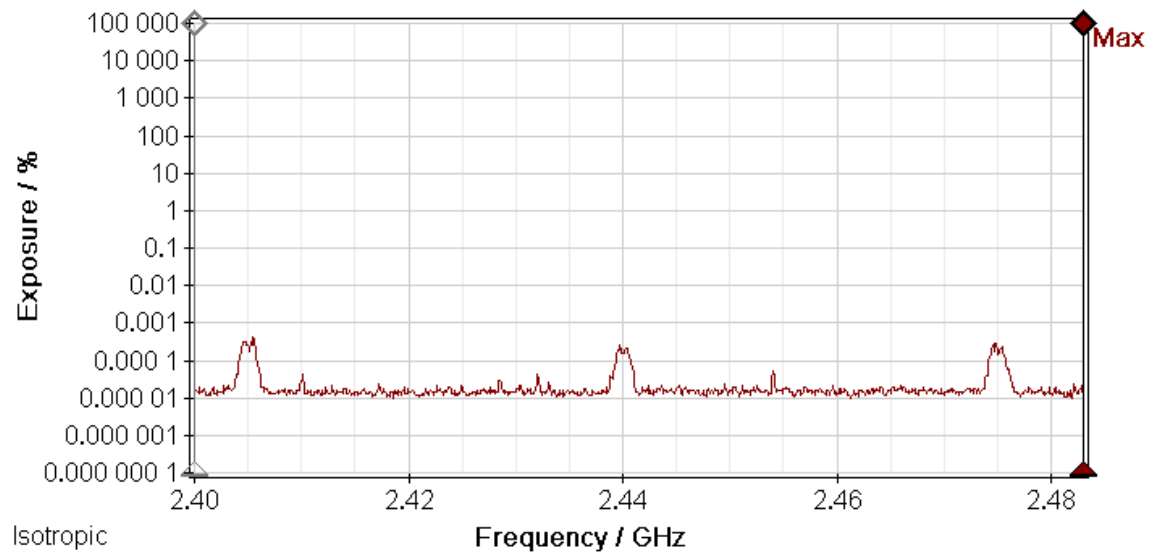


Figure E-3
2.4 GHz band composite RF field at 10 feet behind rack of 10 SmartMeters.

Battery: 07/29/10 02:44:55 PM	GPS: 34°46'01.7" N 83°2'20.5" W	Ant: 3AX 50M-3G	Cable: ---	SrvTbl: ---	Ger.Funkd. FCC GP
Integration over Frequency		Min: 2 400.000 MHz	Max: 2 483.000 MHz	Result Type: Max	
		Cent: 2 441.500 MHz	Span: 83.000 MHz	Int. Val: 1.193 %	

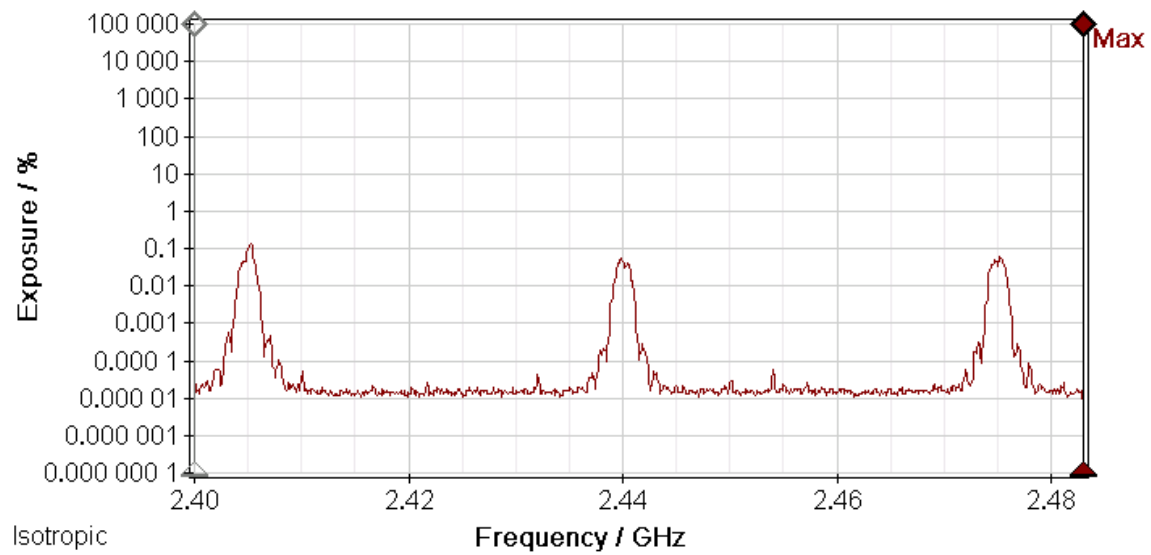


Figure E-4
 2.4 GHz band composite RF field obtained with lateral walk at 3 feet in front of rack of 10 SmartMeters from well beyond each side of rack.

Appendix F: Photos of Simulated Stucco Wall During Construction



Figure F-1
Simulated wall section prior to installation of insulation, sheetrock and stucco lath (netting).

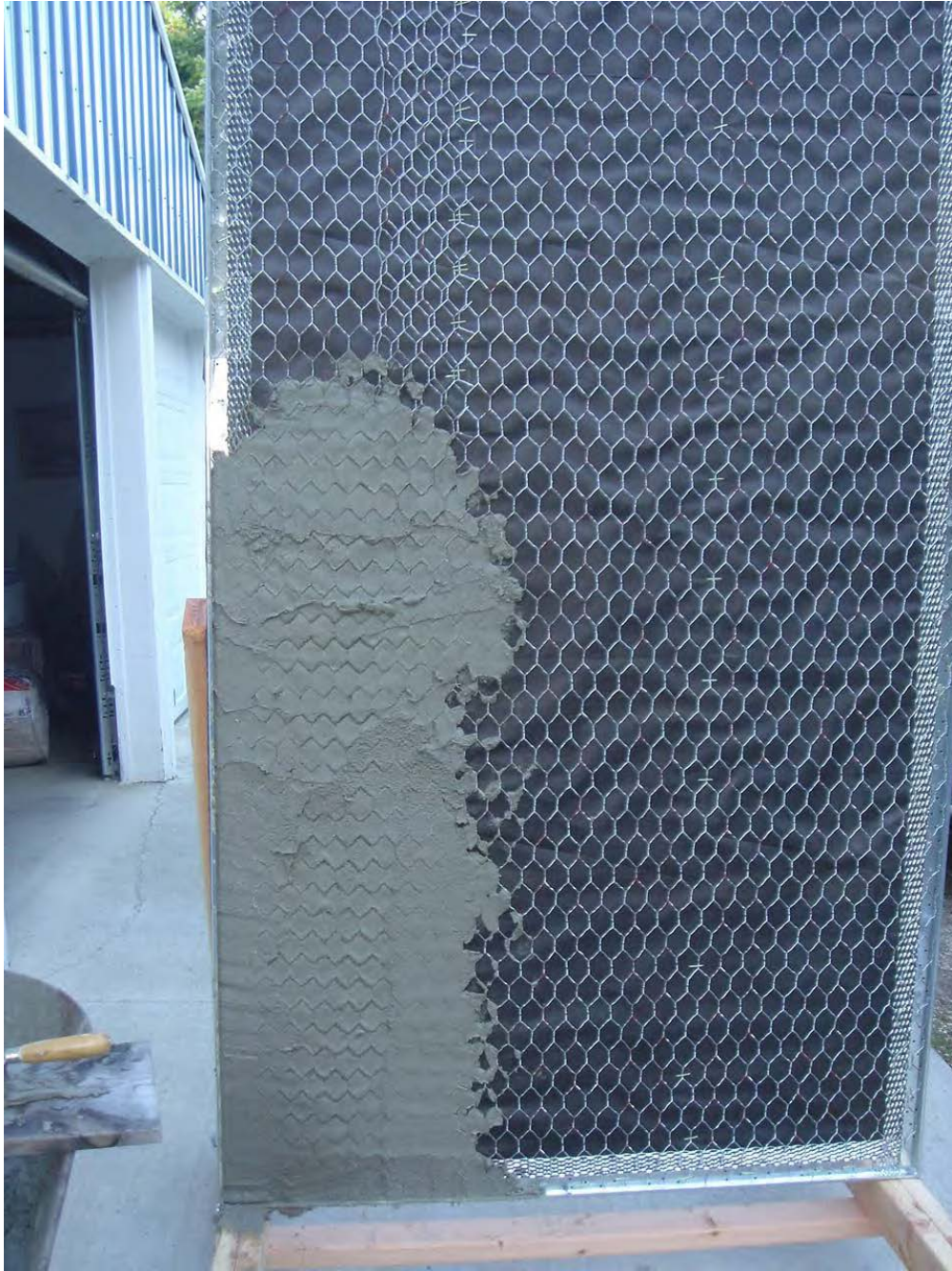


Figure F-2
Simulated wall section showing initial installation of stucco scratch coat of stucco during construction with underlying 1.5 inch stucco netting.

Appendix G: Modeling of RF fields of a 915 MHz Dipole for Spatial Averaging

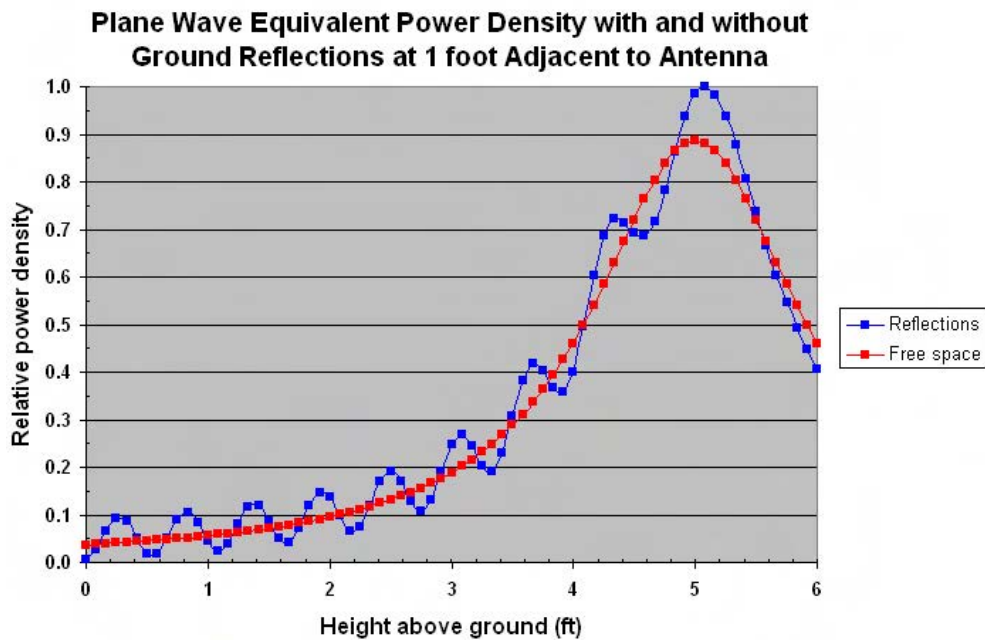


Figure G-1

Plane wave equivalent power density with and without ground reflections along a six-foot vertical line at 1 foot adjacent to a 900 MHz horizontally polarized dipole located at 5 feet above ground. Ratio of spatial average with reflections to spatial average without reflections is 1.032.

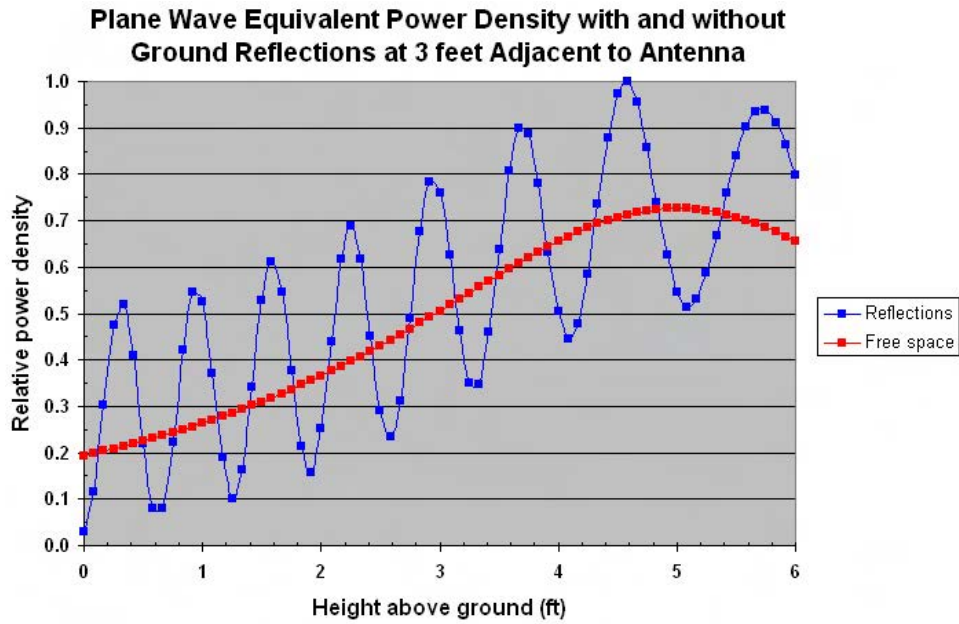


Figure G-2

Plane wave equivalent power density with and without ground reflections along a six-foot vertical line at 3 feet adjacent to a 900 MHz horizontally polarized dipole located at 5 feet above ground. Ratio of spatial average with reflections to spatial average without reflections is 1.103.

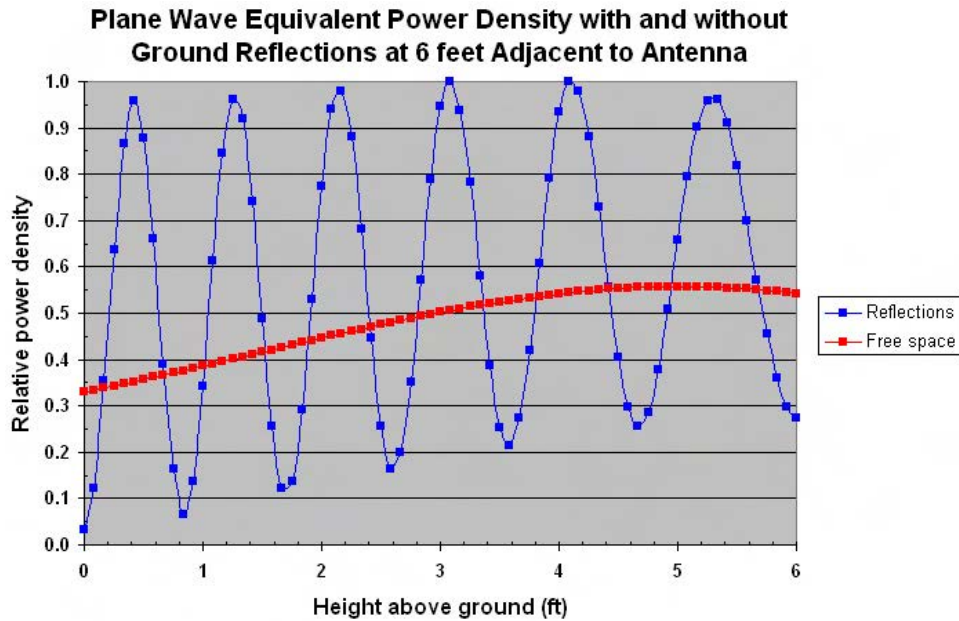


Figure G-3

Plane wave equivalent power density with and without ground reflections along a six-foot vertical line at 6 feet adjacent to a 900 MHz horizontally polarized dipole located at 5 feet above ground. Ratio of spatial average with reflections to spatial average without reflections is 1.190.

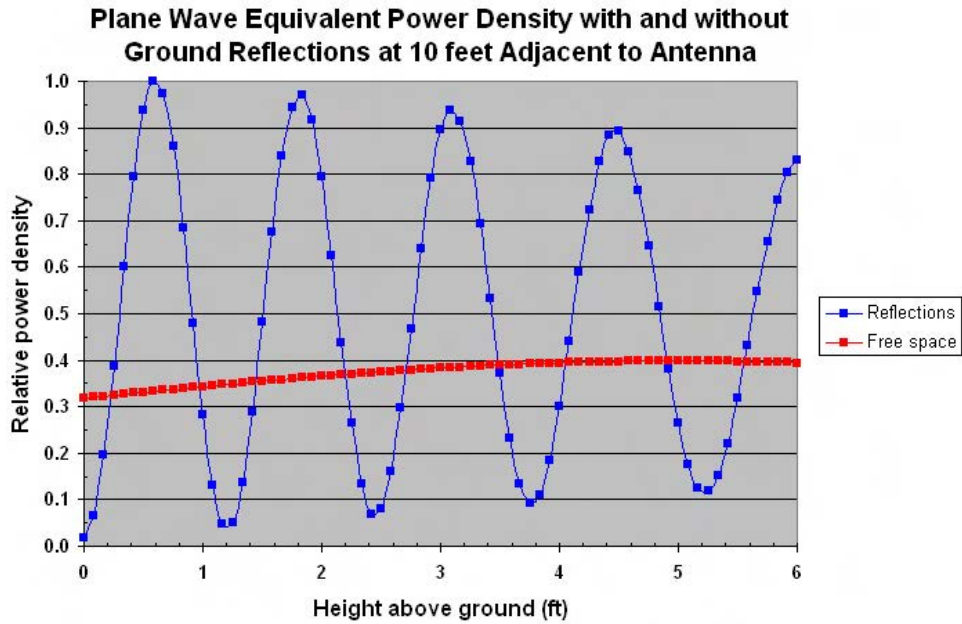


Figure G-4

Plane wave equivalent power density with and without ground reflections along a six-foot vertical line at 10 feet adjacent to a 900 MHz horizontally polarized dipole located at 5 feet above ground. Ratio of spatial average with reflections to spatial average without reflections is 1.344.

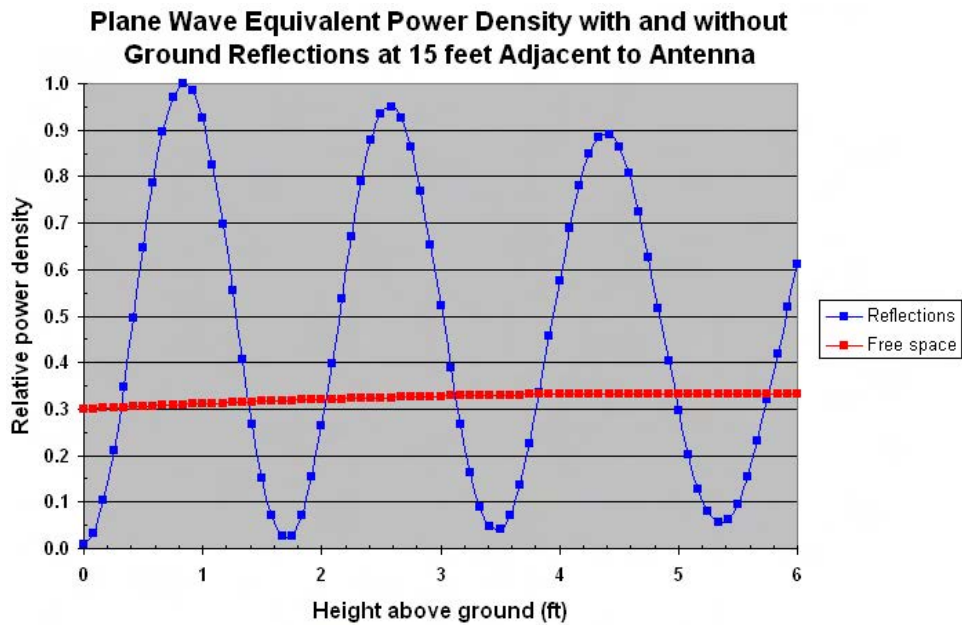


Figure G-5

Plane wave equivalent power density with and without ground reflections along a six-foot vertical line at 15 feet adjacent to a 900 MHz horizontally polarized dipole located at 5 feet above ground. Ratio of spatial average with reflections to spatial average without reflections is 1.432.

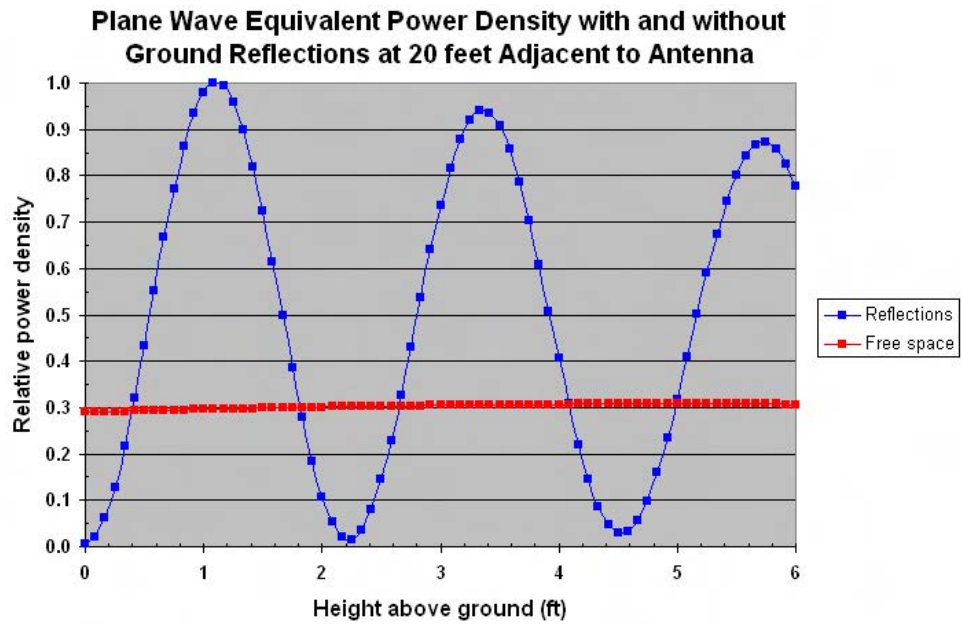


Figure G-6

Plane wave equivalent power density with and without ground reflections along a six-foot vertical line at 20 feet adjacent to a 900 MHz horizontally polarized dipole located at 5 feet above ground. Ratio of spatial average with reflections to spatial average without reflections is 1.650.

Appendix H: Glossary of Terms

AirCard- An AirCard is a device that, typically, is inserted into a laptop computer, that provides access to the Internet via a wireless wide area network (WWAN) normally operated by cellular telephone companies. This is to be distinguished from Wi-Fi wireless capability built into most modern laptop computers that allow communication with a so-called hot spot as in cyber cafes.

AMI- Advanced metering infrastructure.

AMR- Automatic meter reading.

ANSI- American National Standards Institute, issued first standard for protection against intense microwave exposure in 1966.

anechoic- A term meaning without echos or reflections. Anechoic chambers are often used for antenna pattern measurements to minimize any disturbance of the measurement data due to reflections from the local environment.

antenna- A device designed to efficiently convert conducted electrical energy into radiating electromagnetic waves in free space (or vice versa).

antenna pattern- Typically a graphical plot illustrating the directional nature of radiated fields produced by an antenna. The pattern also shows the directional nature of the antenna when used for receiving signals.

attenuation- The phenomenon by which the amplitude of an RF signal is reduced as it moves from one point in a system to another. It is often given in decibels.

averaging Time (T_{avg})- The appropriate time period over which exposure is averaged for purposes of determining compliance with the maximum permissible exposure (MPE). For exposure durations less than the averaging time, the maximum permissible exposure, MPE' , in any time interval, is found from:

$$MPE' = MPE \left(\frac{T_{avg}}{T_{exp}} \right)$$

where T_{exp} is the exposure duration in that interval expressed in the same units as T_{avg} . T_{exp} is limited by restriction on peak power density.

azimuth pattern- Commonly a term referring to an antenna pattern showing the distribution of radiated field from the antenna in the azimuth plane (horizontal plane).

bandwidth- A measure of the frequency range occupied by an electromagnetic signal. It is equal to the difference between the upper frequency and the lower frequency, usually expressed in Hertz.

beacon signal- A very short duration signal emitted by Smart Meters (7.5 milliseconds in the case of the Itron meters) to indicate their availability to connect to other meters within a mesh network. Beacon signals occur periodically at different time intervals depending on the state of connectivity with the mesh network and any requirements to transmit data. This interval can vary from approximately once every 3.5 seconds to once an hour but can be absent during times when the Smart Meter must transmit energy consumption data to the network (see text for more detail).

calibration correction factor- A numerical factor obtained through a calibration process that is used to multiply RF field meter readings by to obtain corrected readings to achieve the maximum accuracy possible.

carrier current- A term used to include the use of electric power lines for communication of voice or data signals by imposing a radiofrequency signal on the 60-Hz voltage waveform. The data signals are “received” at some distant point by a receiver connected to the power line, not by use of an antenna to detect a radiated RF fields.

CDMA- Code division multiple access. A method by which several signals can be sent simultaneously over the same channel by encoding each signal with a unique code that allows each signal to be extracted from the total. The other signals within the communications channel are considered noise.

cell relay- A form of Smart Meter that provides the normal function of an end point meter but also allows for data connectivity with the electric utility company via a wireless wide area network that functions in the cellular telephone or personal communications service (PCS) bands.

continuous exposure- Exposure for durations exceeding the corresponding averaging time (usually 6 minutes for occupational exposure and 30 minutes for the general public). Exposure for less than the averaging time is called short-term exposure.

controlled environment- Controlled environments are locations where there is exposure which may be incurred by persons who are aware of the potential for exposure associated with employment, by other cognizant persons or as the incidental result of transient passage through areas where analysis shows the exposure levels are below some standard level for this environment but above the level for uncontrolled environments.

controlled exposure- a term applied by the FCC to occupational human exposures to radio frequency fields when persons are exposed as a consequence of their employment and in which those persons who are exposed have been made fully aware of the potential for exposure and can exercise control over their exposure.

dB_i- decibel referenced to an isotropic antenna- a theoretical antenna which transmits (or receives) electromagnetic energy uniformly in all directions (i.e. there is no preferential direction).

dBm- A logarithmic expression for radiofrequency power where 0 dBm is defined as equal to 1 milliwatt (mW). Hence, +10 dBm is 10 mW, +20 dBm is 100 mW, etc., and -10 dBm is 0.1 mW.

decibel (dB)- a dimensionless quantity used to logarithmically compare some value to a reference level. For power levels (watts or watts/m²), it would be ten times the logarithm (to the base ten) of the given power level divided by a reference power level. For quantities like volts or volts per meter, a decibel is twenty times the logarithm (to the base ten) of the ratio of a level to a reference level.

direct sequence- As used in direct sequence spread spectrum radio transmission, a modulation technique wherein the resulting transmitted bandwidth of a

signal is spread over a much wider band and resembles white noise.

duty cycle- a measured of the percentage or fraction of time that an RF device is in operation. A duty cycle of 1.0, or 100%, corresponds to continuous operation. Also called duty factor. A duty cycle of 0.01 or 1% corresponds to a transmitter operating on average only 1% of the time.

effective isotropic radiated power (EIRP)- the apparent transmitted power from an isotropic antenna (i.e. a theoretical antenna that transmits uniformly in all possible directions as an expanding sphere).

effective radiated power (ERP)- the apparent transmitted power from an antenna, taking into account the effect of the antenna to concentrate the power in a given direction rather than emitting it in all directions, expressed in watts (W), and typically referenced to a half-wave dipole type of antenna.

electric field strength- a field vector (E) describing the force that electrical charges have on other electrical charges, often related to voltage differences, measured in volts per meter (V/m).

electromagnetic field- a composition of both an electric field and a magnetic field that are related in a fixed way that can convey electromagnetic energy. Antennas produce electromagnetic fields when they are used to transmit signals.

electromagnetic spectrum- the range of frequencies associated with electromagnetic fields. The spectrum ranges from extremely low frequencies beginning at zero hertz to the highest frequencies corresponding to cosmic radiation from space.

elevation pattern- Commonly a term referring to an antenna pattern showing the distribution of radiated field from the antenna in the elevation plane (vertical plane).

end point meter- A term used to designate a Smart Meter that is installed on a home or business to record and transmit electric energy consumption but that does not provide access point features such as those provided by a cell relay.

EPA- Environmental Protection Agency.

EVDO- Evolution-Data Optimized. A third generation telecommunications standard for wireless transmission of

data via radio signals. EVDO presents an advantage over other technologies since it uses the same transmission frequencies as existing CDMA networks, providing a cost advantage since additional, new spectrum is not required to implement this method of communication. The major EVDO deployments in the U.S. are by Verizon and Sprint.

exposure- exposure occurs whenever a person is subjected to electric, magnetic or electromagnetic fields or to contact currents other than those originating from physiological processes in the body and other natural phenomena.

far field- the far field is a term used to denote the region far from an antenna compared to the wavelength corresponding to the frequency of operation. It is a distance from an antenna beyond which the transmitted power densities decrease inversely with the square of the distance.

Federal Communications Commission (FCC)- the Federal Communications Commission (FCC) is an independent agency of the US Federal Government and is directly responsible to Congress. The FCC was established by the Communications Act of 1934 and is charged with regulating interstate and international communications by radio, television, wire, satellite, and cable. The FCC also allocates bands of frequencies for non-government communications services (the NTIA allocates government frequencies). The guidelines for human exposure to radio frequency electromagnetic fields as set by the FCC are contained in the Office of Engineering and Technology (OET) Bulletin 65, Edition 97-01 (August 1997). Additional information is contained in OET Bulletin 65 Supplement A (radio and television broadcast stations), Supplement B (amateur radio stations), and Supplement C (mobile and portable devices).

free space impedance- an expression of the apparent degree to which free space impedes the flow of electromagnetic energy expressed in ohms and equal to the ratio of the strength of the electric and magnetic fields (the impedance of free space is equal to 377 ohms).

frequency conformal- A term used to describe broadband RF field probes that have an inherent frequency shaped response that is tailored to a specific frequency dependent RF exposure standard. The

output of such a probe is normally expressed in percentage of the exposure standard.

gain, antenna- a measure of the ability of an antenna to concentrate the power delivered to it from a transmitter into a directional beam of energy. A search light exhibits a large gain since it can concentrate light energy into a very narrow beam while not radiating very much light in other directions. It is common for cellular antennas to exhibit gains of 10 dB or more in the elevation plane, i.e., concentrate the power delivered to the antenna from the transmitter by a factor of 10 times in the direction of the main beam giving rise to an effective radiated power greater than the actual transmitter output power. In other directions, for example, behind the antenna, the antenna will greatly decrease the emitted signals. Gain is often referenced to an isotropic antenna (given as dBi).

gigahertz (GHz)- one billion hertz.

ground reflection factor- A factor commonly used in calculations of RF field power densities that expresses the power reflection coefficient of the ground over which the RF field is being computed. The purpose of the factor is to account for the fact that ground reflected RF fields can add constructively in an enhanced (stronger) resultant RF field.

HAN- Home Area Network. In the context of Smart Meters, a local area network for communication between a personal computer and various electrical appliances, equipment or systems to accomplish optimized electric energy consumption at the home. Small sensors with low power radio transmitters are attached to the various electrical appliances for communication in the HAN.

hertz- the unit for expressing frequency, one Hertz (Hz) equals one cycle per second.

IEEE- Institute of Electrical and Electronics Engineers.

insertion loss- A measure of the reduction in transmitted radio frequency energy afforded by some material or structure. The materials used in home construction can attenuate the RF signals produced by Smart Meters such that RF field strengths inside a home will be less than at the same distance but outside the home in front of the meter.

ISM- Industrial, Scientific, and Medical. There are various ISM frequency bands designated by the FCC for

equipment or appliances designed to generate and use RF energy for industrial, scientific or medical purposes.

isotropic antenna- a theoretical antenna which transmits (or receives) electromagnetic energy uniformly in all directions (i.e. there is no preferential direction). The radiated wavefront is assumed to be an expanding sphere.

isotropic probe- Similar to isotropic antenna but normally related to RF measurement instruments designed to evaluate the magnitude of RF fields from a safety perspective. The isotropic character of the probe results in a measurement of the resultant RF field produced by all polarization components.

“license free”- a phrase meaning that an RF transmitter is operated at such low power and within an authorized frequency band that no formal license to operate is required by the FCC. There are restrictions placed on these devices, however, such as they shall not produce interference and/or may not create RF fields exceeding particular field strengths.

magnetic field strength- a field vector (H) that is equal to the magnetic flux density divided by the permeability of the medium. Magnetic field strength is expressed in units of amperes per meter (A/m).

max hold spectrum- A feature often present on instruments such as spectrum analyzers in which the instantaneous peak values of measured signals are captured and continuously displayed so that, over time, the absolute maximum signal values can be determined even if they were only present for a short period.

maximum permissible exposure (MPE)- the rms and peak electric and magnetic field strength, their squares, or the plane wave equivalent power densities associated with these fields and the induced and contact currents to which a person may be exposed without harmful effect and with an acceptable safety factor.

megahertz (MHz)- one million hertz.

mesh network- A term describing a network, typically wireless, in which multiple nodes communicate among themselves and data can be relayed via various nodes to some access point. Mesh networks are self

healing in that should a particular pathway become nonfunctional for some reason, alternative paths are automatically configured to carry the data. Mesh networks can expand beyond the normal range of any single node (Smart Meter) by relaying of data among the different meters.

microwatts- one-millionth of a watt, a microwatt (μW) or 10^{-6} watts.

microwatt per square centimeter ($\mu W/cm^2$)- a measure of the power density flowing through an area of space, one millionth of a watt passing through a square centimeter.

microwave- an electromagnetic wave at super high frequencies, typically above 300 MHz, the wavelength of which is very short (micro).

milliwatt per square centimeter (mW/cm^2)- a measure of the power density flowing through an area of space, one thousandth of a watt passing through a square centimeter. One milliwatt per square centimeter is equal to 1,000 microwatts per square centimeter.

mode- A statistical term referring to the most frequently observed value among many. It is distinguished from the mean or median of a distribution.

modem- In the context of Smart Meters, a term commonly used to describe a wireless transceiver capable of receiving and transmitting data over a wireless wide area network. An AirCard is a form of cellular modem. Cellular modems are used in Smart Meter access points to transmit data via the Internet to electric utility companies.

modulation- refers to the variation of either the frequency or amplitude of an electromagnetic field for purposes of conveying information such as voice, data or video programming.

near field- a region very near antennas in which the relationship between the electric and magnetic fields is complex and not fixed as in the far field, and in which the power density does not necessarily decrease inversely with the square of the distance. This region is sometimes defined as closer than about one-sixth of the wavelength. In the near field region the electric and magnetic fields can be determined, independently of each other, from the free-charge distribution and the free-current distribution respectively. The spatial variability of the near field can be large. The near field predominately contains reactive energy that enters space but returns to the antenna (this is

different from energy that is radiated away from the antenna and propagates through space).

nearfield coupling- A phenomenon that can occur when an RF measurement probe is placed within the reactive near field of an RF source such that the probe interacts strongly with the source in a way that typically draws power from the source than would not occur at greater distances. When nearfield coupling occurs, field probe readings are typically erroneously greater than the actual RF field magnitude.

omnidirectional antenna- an antenna that emits a signal of essentially constant strength in all directions, in contrast to a directional antenna.

PCS- Personal communications service. Typically used to designate a band of frequencies in the 1900 MHz range with similar features to cellular telephone base stations but, commonly, with added data transmission performance.

picowatts- picowatts or pW (10^{-12} watts).

planar scan- In the context of this study, a spatial scan over a plane in front of a Smart Meter or a group of Smart Meters at a fixed distance from the Smart Meters.

plane wave- wave with parallel planar (flat) surfaces of constant phase (See also Spherical wave). Note: The cover of this report shows an idealized spherical wave that expands outward- in an appropriate region that this spherical wave can be considered as a plane (flat) wave.

plane wave equivalent power density- the power density associated with an electromagnetic wave propagated in free space in which the front of the wave is flat (plane). Meters used for measuring power density are often calibrated in terms of the plane wave equivalent power density.

polarization- the orientation of the electric field component of an electromagnetic field relative to the earth's surface. Vertical polarization refers to the condition in which the electric field component is vertical, or perpendicular, with respect to the ground, horizontal polarization refers to the condition in which the electric field component is parallel to the ground.

power density- power density (S , sometimes called the Poynting vector) is the power per unit area normal to the direction of propagation, usually expressed in units of watts per square meter (W/m^2) or, for convenience, milliwatts per square centimeter (mw/cm^2) or microwatts per square centimeter ($\mu w/cm^2$). For plane waves, power density, electric field strength, E , and magnetic field strength, H , are related by the impedance of free space, i.e. 120π (377) ohms. In particular, $S = E^2/120\pi = 120\pi H^2$ (Where E and H are expressed in units of V/m and A/m , respectively, S is in units of W/m^2). Although many RF survey instruments indicate power density units, the actual quantities measured are E or E^2 or H or H^2 .

Poynting vector- a field vector quantity equal to the vector product (cross product) of the electric field and magnetic field of an electromagnetic wave. The Poynting vector (S , also called power density) is equal to $E \times H$, with units of W/m^2 .

product performance standard- Typically a numerical value defining a maximum allowed RF emission magnitude at or near the surface of an electronic device. For microwave ovens, the product performance standard specifies a maximum leakage of RF energy from the oven of 5 mW/cm^2 at any point 5 cm from the surface of the oven. A product performance standard is not the same as a whole body exposure standard. Compliance with the microwave oven leakage standard of 5 mW/cm^2 is not inconsistent with the whole body exposure limit of 1 mW/cm^2 since emission intensity decreases rapidly with distance from the oven and whole body exposure values will generally be substantially less than the whole body limit at such a distance that the whole body is exposed.

radiating field- the components of the total electromagnetic field produced by an antenna that contains all of the energy propagated away from the antenna. In the radiation field, both the electric and magnetic fields are codependent with an intensity that varies inversely with distance from the source.

radiation pattern- a description of the spatial distribution of RF energy emitted from an antenna. Two radiation patterns are required to completely describe the transmitting performance of an antenna, one for the azimuth plane and another for the elevation plane.

radio- a term used loosely to describe a radio transmitter or transceiver.

radio frequency (RF)- although the RF spectrum is formally defined in terms of frequency as extending from 0 to 3000 GHz, the frequency range of interest is 3 kHz to 300 GHz.

radio spectrum- the portion of the electromagnetic spectrum with wavelengths above the infrared region in which coherent waves can be generated and modulated to convey information- generally about 3 kHz to 300 GHz.

reflection- an electromagnetic wave (the “reflected” wave) caused by a change in the electrical properties of the environment in which an “incident” wave is propagating. This wave usually travels in a different direction than the incident wave. Generally, the larger and more abrupt the change in the electrical properties of the environment, the larger the reflected wave

resolution bandwidth- A specification for spectrum analyzers that denotes the ability of the analyzer to identify two signals on different frequencies.

resultant field- The combined result of all polarization components of an electromagnetic field found by determining the sum of three orthogonal components of power density or the root sum squared of three orthogonal components of electric or magnetic field strength.

RF - radiofrequency.

root-mean-square (RMS)- the effective value of, or the value associated with joule heating, of a periodic electromagnetic wave. The RMS value of a wave is obtained by taking the square root of the mean of the squared value of the wave.

router, wireless- A device commonly used in homes and offices for wireless distribution of Internet connectivity, most commonly operating in the 2.4 GHz license free band.

safety factor- additional safety is incorporated into MPE limits by the use of a safety factor (SF). A safe level exposure is divided by the safety factor to yield the allowable exposure limits or maximum permissible exposure (MPE). The FCC uses a SF of 5 for occupational and 50 for public exposure limits. This means the MPE for the general public is 50 times less than a level determined to be safe.

shielding effectiveness- A measure of the ability of a material or structure to attenuate RF fields, typically specified in decibels.

slot antenna- An antenna constructed from a metal substrate with a slot cut in the metal. When driven by a transmitter, the slot radiates like a wire dipole. The antenna pattern of the slot antenna is determined by its size and shape and the driving frequency. In the Itron Smart Meters studied in this project, slot antennas are represented by thick lines on printed circuit cards wherein the metal surface has been removed to create slots.

spatial average- For RF exposure limits, a determination of the average value of power density over the projected cross section area of the body. In practice, an average along a vertical line representing the height of a person.

specific absorption rate (SAR)- the time derivative of the incremental energy absorbed by (dissipated in) an incremental mass contained in a volume) of a given density. SAR is expressed in units of watts per kilogram (or milliwatts per gram, mW/g). Guidelines for human exposure to radio frequency fields are based on SAR thresholds where adverse biological effects may occur. When the human body is exposed to a radio frequency field, the SAR experienced is proportional to the squared value of the electric field strength induced in the body.

spectrum analyzer- An electronic instrument, similar to a receiver, that sweeps across a part of the RF spectrum and displays detected signals as peaks on a visual display screen. Spectrum analyzers normally continuously sweep repetitively over a given frequency band at a relatively high rate thereby allowing for the observation of intermittent signals.

spherical wave- a wave with concentric spherical surfaces of constant phase. Far from its source a spherical wave expands to approximate a flat surface or plane wave over discrete areas. Note: the cover of this report shows an idealized spherical wave generated by a rod antenna.

spread spectrum- Refers to a method by which an RF signal that is generated in a particular bandwidth is deliberately spread in the frequency domain resulting in a signal with a wider bandwidth. Such a technique is used to enhance secure communications, to reduce interference and to prevent detection.

time-averaged exposure- In the context of RF exposure limits, an average of the exposure value over a specified

time period. Commonly, for occupational exposures, the averaging time is six-minutes and for members of the general public 30-minutes. All scientifically based RF exposure limits are in terms of time-averaged values.

transceiver- A radio device that has both transmitting and receiving capability. Strictly, the radio devices in Smart Meters are transceivers since they can both transmit data and receive data. Commonly, in the context of evaluating RF fields, the term transmitter or radio is used to refer to the transmitting feature of the transceiver.

uncontrolled environment- uncontrolled environments are locations where there is the exposure of individuals who have no knowledge or control of their exposure. The exposures may occur in living quarters or workplaces where there are no expectations that the exposure levels may exceed some standard level limits for this environment

uncontrolled exposure- a term applied by the FCC to human exposures to radio frequency fields when the general public is exposed or in which persons who are exposed as a consequence of their employment may not be made fully aware of the potential for exposure or cannot exercise control over their exposure. Members of the general public always fall under this category when exposure is not employment-related.

USB- Universal serial bus commonly found on personal computers.

WWAN- wireless wide area network. WWANs are provided by several cellular telephone companies for wireless connectivity directly to the Internet for data transmission. WWANs are different from so-called wireless “hot spots” such as found in cyber cafes and operate in either the 850 MHz cellular or 1900 MHz PCS bands.

yagi antenna- A multi-element antenna composed of a number of dipole elements attached to a boom such that the combination of elements (a driven element and a reflector and possible director elements) and their spacing result in elevated values of gain. Design originally credited in 1926 to Shintaro Uda and Hidetsugu Yagi in Japan and sometimes called a Yagi-Uda antenna.

Zigbee- A specification for a data communications protocol used by small, low power digital radios commonly implemented in low-rate wireless personal area networks or HANs.

Export Control Restrictions

Access to and use of EPRI Intellectual Property is granted with the specific understanding and requirement that responsibility for ensuring full compliance with all applicable U.S. and foreign export laws and regulations is being undertaken by you and your company. This includes an obligation to ensure that any individual receiving access hereunder who is not a U.S. citizen or permanent U.S. resident is permitted access under applicable U.S. and foreign export laws and regulations. In the event you are uncertain whether you or your company may lawfully obtain access to this EPRI Intellectual Property, you acknowledge that it is your obligation to consult with your company's legal counsel to determine whether this access is lawful. Although EPRI may make available on a case-by-case basis an informal assessment of the applicable U.S. export classification for specific EPRI Intellectual Property, you and your company acknowledge that this assessment is solely for informational purposes and not for reliance purposes. You and your company acknowledge that it is still the obligation of you and your company to make your own assessment of the applicable U.S. export classification and ensure compliance accordingly. You and your company understand and acknowledge your obligations to make a prompt report to EPRI and the appropriate authorities regarding any access to or use of EPRI Intellectual Property hereunder that may be in violation of applicable U.S. or foreign export laws or regulations.

The Electric Power Research Institute Inc., (EPRI, www.epri.com) conducts research and development relating to the generation, delivery and use of electricity for the benefit of the public. An independent, nonprofit organization, EPRI brings together its scientists and engineers as well as experts from academia and industry to help address challenges in electricity, including reliability, efficiency, health, safety and the environment. EPRI also provides technology, policy and economic analyses to drive long-range research and development planning, and supports research in emerging technologies. EPRI's members represent more than 90 percent of the electricity generated and delivered in the United States, and international participation extends to 40 countries. EPRI's principal offices and laboratories are located in Palo Alto, Calif.; Charlotte, N.C.; Knoxville, Tenn.; and Lenox, Mass.

Together...Shaping the Future of Electricity

Program:

Electric and Magnetic Fields (EMF) Health Assessment and
Radio-Frequency Safety

© 2010 Electric Power Research Institute (EPRI), Inc. All rights reserved. Electric Power Research Institute, EPRI, and TOGETHER...SHAPING THE FUTURE OF ELECTRICITY are registered service marks of the Electric Power Research Institute, Inc.

1021126

Electric Power Research Institute

3420 Hillview Avenue, Palo Alto, California 94304-1338 • PO Box 10412, Palo Alto, California 94303-0813 USA
800.313.3774 • 650.855.2121 • askepri@epri.com • www.epri.com